

A thesis submitted to Cardiff  
University of the Degree of  
Doctor of Philosophy

**Cardiff School of Engineering**

**Integrated Water Losses  
Assessment and Water  
Balance Study over Arid and  
Semi-Arid Basins Located in  
Developing Countries**

**By**

**Ali Tuama Helu**  
September 2015

---

## DECLARATION

This work has not previously been accepted in substance for any degree and is not concurrently submitted in candidature for any other higher degree.

Signed: ..... (Ali Helu)                      Date: .....

### Statement 1:

This thesis is being submitted in partial fulfilment of the requirements for the degree of PhD.

Signed: ..... (Ali Helu)                      Date: .....

### Statement 2:

This thesis is the result of my own independent work/investigation, except where otherwise stated. Other sources are acknowledged by explicit references.

Signed: ..... (Ali Helu)                      Date: .....

### Statement 3:

I hereby give consent for my thesis, if accepted, to be available for photocopying, inter-library loan and for the title and summary to be made available to outside organisations.

Signed: ..... (Ali Helu)                      Date: .....

### Statement 4:

I hereby give consent for my thesis, if accepted, to be available for photocopying and for inter-library loans after expiry of a bar on access previously approved by the Academic Standards & Quality Committee.

Signed: ..... (Ali Helu)                      Date: .....

## NOTICE OF SUBMISSION OF THESIS: POSTGRADUATE RESEARCH DEGREES

Please TYPE or write in BLACK ink and use BLOCK capitals

CANDIDATE'S LAST NAME	<b>HELU</b>
CANDIDATE'S FIRST NAME(S)	<b>ALI TUAMA</b>
CANDIDATE'S ID NUMBER	<b>C1159769</b>
SCHOOL	<b>CARDIFF SCHOOL OF ENGINEERING</b>
TITLE OF DEGREE	Please circle appropriate degree title EdD, EngD, DSW, DClinPsy, DHS, MCh, MD, MPhil, MScD by Research, <b>PhD</b>
FULL TITLE OF THESIS	<b>Integrated Water Losses Assessment and Water Balance Study over Arid and Semi-Arid Basins Located in Developing Countries</b>  <b>Tigris River in Iraq</b>
IS THIS A RESUBMISSION?	<b>NO</b>
THESIS SUBMITTED FOR EXAMINATION IN	Permanent Binding <input type="checkbox"/> Temporary binding <input checked="" type="checkbox"/>
CANDIDATE SIGNATURE	DATE:

## **ACKNOWLEDGEMENTS**

Finishing this doctoral thesis has been a truly life-changing experience for me and it would not have been possible to undertake without the support and guidance that I received from many people.

My greatest thanks are to Dr. Bettina Bockelmann- Evans, the main supervisor of this PhD thesis, for her valuable encouragements and sympathies. Her support and guidance are highly appreciated. Special thanks are also due Dr. Michaela Bray, the second-supervisor, for her continued support and constructive comment on different aspects of the thesis. In addition, specific help on supporting ideas and editing technical works from Prof. Roger Falconer is highly appreciated.

Thanks also go to all HRC members, staff and postgraduate students, especially from whom I have great opportunities to make real friendship and to exchange knowledge, in Cardiff School of Engineering. Many thanks for the financial support from CH2M, CARA and PAC and also Cardiff University, which helped to finish this PhD study. Special appreciation is paid to the Iraqi Water Resources Ministry, Iraqi Environmental Ministry for their efforts to provide prerequisite data and information for this PhD.

Valuable support from the beloved family. My father Tuama, without his efforts, this work was impossible to be done. My mother, Taghreed and my mother in law, Ridhab for their prayers; my sister, Mai and here kids and my brothers Mohammed and Ayman, has encouraged me to overcome all the barriers; with your love, I believe I can do the best. It is never enough to just say 'Thank-you' but please accept my great and sincere appreciation for what you all have done for me.

Last but not least, a great love from my wife, Ban and 'little kids' – Mena, Sadeer and Aiya are the endless source of happiness and encouragements. They are the most important people in my world and I dedicate this thesis to them.



## **ABSTRACT**

Climate change, population growth, and water resources crossing political boundaries are the main issues threatening water allocation for agricultural, industrial and domestic uses in developing countries. Integrated water resources management developed in a sustainable manner is essential to allow future generations to meet their water needs. A lack of data in developing countries is the biggest problem that can hinder developing necessary understandings. The Tigris river basin is a prime example, not only because it is located in a developing country, but also due to its long history of armed conflicts and breakdown of law and care. Unstable situation makes data collection difficult, available data poor in quality and the measuring tools and methods rudimentary. The insufficient data lead to the impact of the climate change on water resources to be not conclusively determined.

This study shows the climate change impacts through investigate the evapotranspiration (ET) changes over the years. Five potential evapotranspiration models have been studied and classified according to the complexity in terms of the number of variables. Choosing the most suitable ET model helped to fill and reconstruct gaps in historical data sets. The statistical downscaling model SDSM was used to predict the evapotranspiration changes for the next 100 years.

Google Earth and 3DRoutBuilder helped to produce an entire river profile with a simple, good quality representation of river networks. That aid the run of the hydrodynamic model (ISIS -1D) which has been utilised to produce water levels and water flow information to establish a robust river losses and water balance assessment for a river.

Planning of alternative water resources schemes on river basins located in Arid-Semi Arid region needs an assessment of the hydrologic/hydraulic behaviours of that river. In view of this, the thesis further explores the sustainability of water quantities of rivers based on generated climate scenarios and population increases.

# CONTENTS

CHAPTER ONE: INTRODUCTION.....	1
1.1 Water Resources in Iraq .....	2
1.2 The Tigris River .....	5
1.3 Tigris Catchment Management.....	7
1.4 River Losses Assessment in Developing Countries .....	9
1.5 Research Aims and Objectives .....	11
1.6 Thesis Outline.....	13
CHAPTER TWO: LITERATURE REVIEW .....	15
2.1 Water Balance for Rivers .....	15
2.2 Climate Change Impacts on Water Resources.....	26
2.3 Evapo[transpi]ration .....	36
2.4 Evapo[transpi]ration Impacts on Rivers.....	45
2.5 Hydrodynamic Models.....	48
2.6 River Profile Development.....	50
2.7 Chapter Conclusion & Research Questions .....	61
CHAPTER THREE: AREA OF STUDY AND DATA AVAILABILITY .....	63
3.1 Location, Topography and Climate .....	63
3.2 Available Data for Tigris River.....	65
3.3 Data Management.....	75
CHAPTER FOUR: METHODOLOGY .....	76
4.1 Evapo[transpi]ration .....	77
4.2 SDSM.....	80
4.3 River Profile and Hydraulic Characteristics .....	83
4.4 Hydraulic Model (ISIS – 1D) .....	85

4.5	Water Balance/Water Losses Assessment .....	88
4.6	Summary .....	88
CHAPTER FIVE:  EVAPO[TRANSPI]RATION.....		91
5.1	Evapotranspiration Models .....	94
5.2	ET Models Comparison .....	100
5.3	Evapo[transpi]ration Losses Representation .....	105
5.4	Evapo[transpi]ration - Future Projections.....	107
5.5	Summary .....	117
CHAPTER SIX:  RIVER MODELLING.....		120
6.1	Boundary Conditions .....	121
6.2	Tigris Steady State Modelling Results .....	152
6.3	Tigris Un-Steady-State Modelling Results .....	154
6.4	Tigris Model: Validation.....	158
6.5	Summary .....	159
CHAPTER SEVEN:  RIVER LOSSES ASSESSMENT AND WATER BALANCE FOR TIGRIS .....		162
7.1	Tigris Northern Region Model.....	163
7.2	Tigris Middle Region Model .....	166
7.3	Tigris Southern Region Model.....	170
7.4	Tigris River – Water Balance .....	174
7.5	Summary .....	177
CHAPTER EIGHT:  CONCLUSIONS, LIMITATIONS AND RECOMMENDATIONS FOR FURTHER STUDY		179
8.1	Research Conclusions .....	179
8.2	Research Limitations .....	184
8.3	Recommendations for Further Research .....	185

# LIST of FIGURES

Figure 1-1: Freshwater Stress: Annual Renewable Supplies per Capita per River Basin. According to Population Action International, based upon the UN Medium Population Projections of 1998, more than 2.8 billion people in 48 countries will face water stress or scarcity conditions by 2025. This graph illustrates projected water stress and water scarcity for World nations in 2025. ....	1
Figure 1-2: A map of Iraq. The location of Iraq and all of its boarded countries are shown. Source: GICJ & Iraq .....	2
Figure 1-3: The Euphrates-Tigris river basin. ....	3
Figure 1-4: Annual water discharge of the Tigris and the Euphrates Rivers. Water discharges from 1940 to 2002 were measured at the closest input into the Mesopotamian marshlands. (AlMaarofi, 2012) .....	4
Figure 1-5: A potential scenario for Iraq Water system after splitting into smaller countries. ....	9
Figure 4-1: The general procedure to study the water losses of Tigris River.....	76
Figure 5-1: Thornthwaite relationship between soil type, moisture availability and the ratio between actual and potential evapotranspiration. The source: LEARNING HYDROLOGY, edited by the author.....	92
Figure 5-2: Evaporation Pans.....	93
Figure 5-3: Comparison of mean monthly potential evapotranspiration based on Pan-A method and five empirical methods over the Tigris Basin – Northern, Middle, Southern regions. ....	101
Figure 5-4: Performance of the selected ET models against ET observations over Tigris northern region. ....	104
Figure 5-5: Performance of the selected ET models against ET observations over Tigris middle region.....	104
Figure 5-6: Performance of the selected ET models against ET observations over Tigris southern region .....	104
Figure 5-7: Northern Region (Mosul) measured Evapo[transpi]ration – NCAR ET relationship. ....	107
Figure 5-8: Southern Region (Basra) measured Evapo[transpi]ration – NCAR ET relationship. ....	108
Figure 5-9: Visual Representation of how the generated daily ET values correspond the ‘modified’ observed ET over the Northern Region.....	112
Figure 5-10: Northern downscaled ET model representation for the period 1961 to 1970 (SDSM Default).....	112
Figure 5-11: Calibration of the downscaled model for the period 1961 to 1970 (after model setting changes) .....	112
Figure 5-12: Validation of the downscaled model for the period 1971 to 1980.....	113
Figure 5-13: Data missing values substitution/simulation using SDSM over the middle region (Baghdad). ....	115
Figure 5-14: Tigris northern region annual average ET for the period from 1961 to 2099 using downscaled HadCM3 A2 and B2 models .....	116
Figure 5-15: Tigris Middle region annual average ET for the period from 1961 to 2099 using downscaled HadCM3 A2 and B2 models .....	116
Figure 5-16: Tigris southern region annual average ET for the period from 1961 to 2099 using downscaled HadCM3 A2 and B2 models .....	117

Figure 6-1: 15 years' worth of monthly mean discharges at Mosul Dam streamflow-gaging station extracted from Saleh (2010) and edited by the author. ....	124
Figure 6-2: 15 years' worth of monthly mean discharges at GreatZab Tributary streamflow-gaging station extracted from Saleh (2010) and edited by the author. ....	124
Figure 6-3: 15 years' worth of monthly mean discharges at LeaserZab Tributary streamflow-gaging station extracted from Saleh (2010) and edited by the author. ....	125
Figure 6-4: 15 years' worth of monthly mean discharges at Adheem Tributary streamflow-gaging station extracted from Saleh (2010) and edited by the author. ....	125
Figure 6-5: 15 years' worth of monthly mean discharge at Diyala Tributary streamflow-gaging station extracted from Saleh (2010) and edited by the author. ....	126
Figure 6-6: Shows Mosul City Centre and Tigris River. The locations of the five cross sections are illustrated as red lines crossing the river. ....	130
Figure 6-7: Outline of RiverSurveyor system and transducer depth.....	133
Figure 6-8: The movement range of the SonTek River survey boat (refer to Table 6.2) within the channel width represented by the double sided arrow .....	135
Figure 6-9: A processed SRTM GL3 raster for Mosul City. Tigris River's centre line is represented in light blue line, the 5 cross sections locations are identified in red lines cross the river reach. ....	136
Figure 6-10: shows elevations of measured cross section (Obs.) at location – number 1 as identified in Table 6.2. This cross section is compered against one generated using SRTM GL3 raster (SGL3Danalyst) and another one generated using Google Earth DEM (GE3DRB).....	141
Figure 6-11: shows elevations of measured cross section (Obs.) at location – number S39 as identified in Table 6.2. This cross section is compered against one generated using SRTM GL3 raster (SGL3Danalyst) and another one generated using Google Earth DEM (GE3DRB). ....	141
Figure 6-12: Tigris River Hydraulic Characteristics.....	144
Figure 6-13: Tigris River Resulted Longitudinal Section from inserting the generated River Cross sections using 3DRoutBuilder and Google Earth.....	146
Figure 6-14: Population Growth Distribution from Seven Main Cities Located along Tigris River.....	149
Figure 6-15: Iraqi Marshes Map quoted from "UNEP Study Sounds Alarm about the Disappearance of the Mesopotamian Marshlands".....	151
Figure 6-16: Schematic of full ISIS-Tigris structure .....	151
Figure 6-17: Steady state river stages for four generated river profiles.....	153
Figure 6-18: The Generated Tigris model by Incorporating September 1972 event and GE3DRB. ....	154
Figure 6-19: Calibration – Simulated vs Measured Water Levels at the Downstream End of the Northern Region – at Cross Section 322.....	157
Figure 6-20: Simulated Water Level for the Study Period (1970-2000) at Cross Section 640.....	159
Figure 6-21: Validation of the Simulated Water Level for the Driest Period (from 1978 to 1980) of the Study at Cross Section 640. ....	159

Figure 7-1: The Tigris northern model reach – an image by Google Earth and model river and water elevations .....	163
<i>Figure 7-2: Tigris River, Water Losses_ Northern Region .....</i>	<i>164</i>
Figure 7-3: The Tigris middle model simulated by Google Earth and 3DRoutBuilder .....	167
<i>Figure 7-4: Tigris River, Water Losses_ Middle Region .....</i>	<i>168</i>
Figure 7-5: The Tigris southern model simulated by Google Earth and 3DRoutBuilder .....	171
<i>Figure 7-6: Tigris River, Water Losses_ Southern Region .....</i>	<i>172</i>
Figure 7-7: Tigris and Euphrates river basin and the annual average precipitation. Source: UVicSpace, edited by the author .....	174
Figure 7-8: Annual precipitation, Population Consumption rate, ET and the remaining river flow at the downstream point of Tigris Model .....	175
Figure 7-9: Statistical discharge prediction for the future of available water resources in Tigris.....	177
<i>Figure 0-1: shows elevation measured cross section (Obs.) compered against one generated using SRTM GL3 raster (SGL3Danalyst); one generated using Synthetic technique (Interpolated S) and another one generated using Google Earth DEM (GE3DRB). Its location is identified in Table 6.2. ....</i>	<i>198</i>
<i>Figure 0-2: shows elevation measured cross section (Obs.) compered against one generated using SRTM GL3 raster (SGL3Danalyst); one generated using Synthetic technique (Interpolated S) and another one generated using Google Earth DEM (GE3DRB). Its location is identified in Table 6.2. ....</i>	<i>198</i>
<i>Figure 0-3: shows elevation measured cross section (Obs.) compered against one generated using SRTM GL3 raster (SGL3Danalyst); one generated using Synthetic technique (Interpolated S) and another one generated using Google Earth DEM (GE3DRB). Its location is identified in Table 6.2. ....</i>	<i>199</i>
<i>Figure 0-4: shows elevation measured cross section (Obs.) compered against one generated using SRTM GL3 raster (SGL3Danalyst); one generated using Synthetic technique (Interpolated S) and another one generated using Google Earth DEM (GE3DRB). Its location is identified in Table 6.2. ....</i>	<i>199</i>
<i>Figure 0-5: shows elevations of measured cross section (Obs.) at location – number 2 as identified in Table 6.2. This cross section is compered against one generated using SRTM GL3 raster (SGL3Danalyst) and another one generated using Google Earth DEM (GE3DRB). ....</i>	<i>200</i>
<i>Figure 0-6: shows elevations of measured cross section (Obs.) at location – number 3 as identified in Table 6.2. This cross section is compered against one generated using SRTM GL3 raster (SGL3Danalyst) and another one generated using Google Earth DEM (GE3DRB). ....</i>	<i>200</i>
<i>Figure 0-8: shows elevations of measured cross section (Obs.) at location – number 4 as identified in Table 6.2. This cross section is compered against one generated using SRTM GL3 raster (SGL3Danalyst) and another one generated using Google Earth DEM (GE3DRB). ....</i>	<i>201</i>
<i>Figure 0-10: shows elevations of measured cross section (Obs.) at location – number 5 as identified in Table 6.2. This cross section is compered against one generated using SRTM GL3 raster (SGL3Danalyst) and another one generated using Google Earth DEM (GE3DRB). ....</i>	<i>201</i>
<i>Figure 0-12: shows elevations of measured cross section (Obs.) at location – number 6 as identified in Table 6.2. This cross section is compered against one generated using SRTM GL3 raster (SGL3Danalyst) and another one generated using Google Earth DEM (GE3DRB). ....</i>	<i>202</i>

*Figure 0-14: shows elevations of measured cross section (Obs.) at location – number 7 as identified in Table 6.2. This cross section is compared against one generated using SRTM GL3 raster (SGL3DAnalyst) and another one generated using Google Earth DEM (GE3DRB). .....202*

*Figure 0-16: shows elevations of measured cross section (Obs.) at location – number 8 as identified in Table 6.2. This cross section is compared against one generated using SRTM GL3 raster (SGL3DAnalyst) and another one generated using Google Earth DEM (GE3DRB). .....203*

*Figure 0-18: shows elevations of measured cross section (Obs.) at location – number 9 as identified in Table 6.2. This cross section is compared against one generated using SRTM GL3 raster (SGL3DAnalyst) and another one generated using Google Earth DEM (GE3DRB).....203*

## LIST OF TABLES

Table 1.1: A list of dams located on Tigris River, their capacity and purposes. Note: HP = hydropower; I = irrigation; FC = flood control; UC = under construction; BCM = billion cubic meters.....	7
Table 1.2: The main agreements between the Tigris River Transboundary Countries .....	8
Table 5.1: Comparison of the complexity of each model in terms of quantity of parameters required. ....	100
Table 5.2: Types of Predictor Variables .....	108
Table 5.3: Downscaling models and large scale atmospheric predictor variable used to downscale ET for the Tigris River Catchment .....	110
Table 6.1: Cross Section Spacing Recommendations in 1D Hydraulic Models.....	122
Table 6.2: observed cross sections' details obtained in different locations along Tigris River using the River Surveyor technique and provided exclusively to this research.....	132
Table 6.3: Five observed cross sections' obtained in relatively closed locations along Tigris River Reach in Mosul City using the River Surveyor technique and provided exclusively to this research.....	134
Table 6.4: River Cross Sections with interpolated River Bad .....	138
Table 6.5: Summary of the Cross sections Hydraulic Characteristics Averages.....	143
Table 6.6: National Periodical Census for Iraqi Governorates located along the study area.....	148
Table 7.1: Discharge values for the most downstream cross section (#340) of the Tigris northern model. ....	165
Table 7.2: Statistics obtained from the most downstream cross section (640) of the Tigris middle model.....	169
Table 7.3: Statistics obtained from the most downstream point, cross section #1170 of the Tigris southern region model.....	173
Table 7.4: Major terms in the water balance of the Tigris, 1970 - 2000. All flows are expressed as volumes of water of the basin per year. ....	176



## ABBREVIATIONS

ASTER	Advanced Spaceborne Thermal Emission and Reflection radiometer
BCM	Billions of cubic meters
DEM	Digital Elevation Model
DSM	Digital Surface Models
DTM	Digital Terrain Models
ECMWF	European Centre for Medium-range Weather Forecasting
FAO	Food and Agriculture Organisation of the United Nations
GCM	General Circulation model
GIS	Geographic Information Systems
HEC-RAS	Hydrologic Engineering Centre – River Analysis System
IMoWR	Iraqi Ministry of Water Resources
IPCC	Intergovernmental Panel on Climate Change
LiDAR	Light Detection and Ranging
NASA	National Aeronautics and Space Administration
NOAA	National Oceanic and Atmospheric Administration
R <sup>2</sup>	Coefficient of Determination
RCM	Regional climate model
SDSM	Statistical Down-Scaling Models
SRTM	Shuttle Radar Topography Mission
UN	United Nations
UNEP	United Nations Environment Programme
WMS	Watershed Modelling System
WRF	Weather Research and Forecasting
WSE	Water Surface Elevation

## Chapter One: Introduction

Water scarcity has become a major problem, particularly in arid regions such as Africa and Australia as well as parts of Asia. A growing population brings the need for additional food and industrial production and, thus, additional water (Sağlam, 2010). Climate change is likely to cause an increase in the frequency and severity of droughts, floods, heat-waves and storms world-wide (Figure 1.1). The water run-off from agricultural fertilisers containing nitrogen has already created more than 200 large "dead zones" in seas and near to river-mouths, where fish cannot live any longer (Dimov, B, 2013). Relatively cheap technology to pump water from underground resources and rivers with few control restrictions have led to over-use of scarce resources. Poor water resources management has resulted in a high risk of wasting the water needed for irrigation or industrial purposes. Better understanding and development, along with more widespread adoption, of sustainable water management strategies (WMS) and computer modelling tools to assess these losses, can help to inform better decision making.

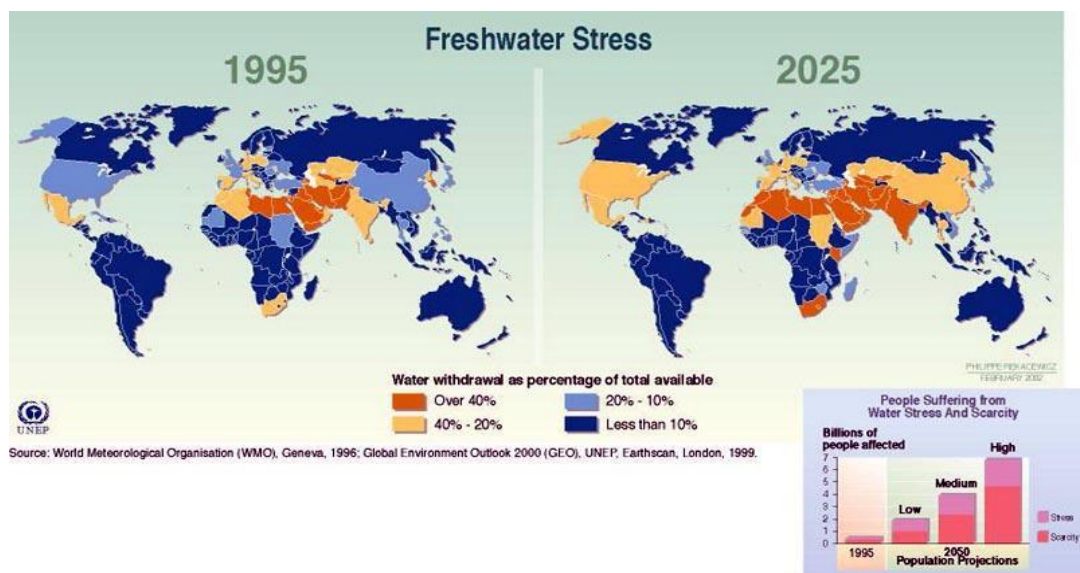


Figure 1-1: Freshwater Stress: Annual Renewable Supplies per Capita per River Basin. According to Population Action International, based upon the UN Medium Population Projections of 1998, more than 2.8 billion people in 48 countries will face water stress or scarcity conditions by 2025. This graph illustrates projected water stress and water scarcity for World nations in 2025.

*"There is a water crisis today. But the crisis is not about having too little water to satisfy our needs. It is a crisis of managing water so badly that billions of people - and the environment - suffer badly."* (World Water Council, 2000)

Water losses from rivers located in developing countries have not received much attention in global discussions of the sustainable use of natural resources. It has been examined even less in the context of population growth. Establishing an accurate estimation of river water losses due to climate change is urgently needed. However, carrying out such task is very complicated due to many reasons, the most important of which is the stage of development of the country in which the water budget study is to be done, and how much historical data are available. Data required including meteorological data, irrigation water use, crop size, and humidity conditions that dominate typical water use practices, in addition, the quality of data is also important.

## 1.1 Water Resources in Iraq

Iraq, a middle eastern – south west Asian country with a total area of 438,320km<sup>2</sup>, is bordered by Turkey to the north, the Islamic Republic of Iran to the east, the Persian Gulf to the southeast, Saudi Arabia and Kuwait to the south, and Jordan and the Syrian Arab Republic to the west, (Figure 1.2)



Figure 1-2: A map of Iraq. The location of Iraq and all of its boarded countries are shown. Source: GICJ &

Iraq

Iraq is fed by two major rivers, the Tigris and the Euphrates. Both of them originate outside of Iraq. The Tigris and the Euphrates account for 98% of Iraq's surface water supply. Their flow is very vulnerable to dams and water diversions in Turkey, Syria and Iran. The Tigris and Euphrates rivers together form the Tigris-Euphrates (TE) Basin. It is known as the second largest basin in the Middle East after the River Nile. Figure 1.3 shows a map of the TE river basin. Turkey, the upstream country in the basin, has embarked on comprehensive development of its part of the TE basin.



Figure 1-3: The Euphrates-Tigris river basin.

The Tigris-Euphrates Basin has been dramatically affected by several anthropogenic activities, mainly dam construction and desiccation as well as the significant increase in population. These changes have created new concerns about water needs for food production. These actions also influence the entire ecosystem of the area. The drying of Iraqi Marshes has had a significant influence on water availability and a potential effect upon the local climate. Fed by the great Tigris and Euphrates rivers, the marshes (the Mesopotamian Marshes or Iraqi Marshes) were once the largest and richest in wildlife in

the Middle East, and – at some 7,700 square miles – the third most extensive in the world.

*“They are thought to be the site of the Garden of Eden, but Saddam Hussein turned them into hell on earth.” G. Lean 2013*

In the early 1990s, the order was to drain the southern Iraq's great marshes. It was one of the biggest environmental disasters of the twentieth century, and with it, an ancient way of life - dating back thousands of years - was almost wiped out. Some national and international reports (e.g. Future Directions International and AQUASTAT) concluded that the annual water discharge of the Tigris and the Euphrates Rivers has been significantly reduced for the last 50 years. Figure 1.4 shows the annual water discharge of the two rivers into the Mesopotamian marshlands from 1940 to 2007. The red line (flow trend) shows the gradual reduction of the two rivers' water discharge during the recorded period. Generally, the figure indicates two periods of water discharge reduction. The first period was during the 1970's, in which many dams were constructed at the two rivers' upstream sections in Turkey. The second period is the late of 1990s when the Iraqi government started to drain the marshlands in the southern region.

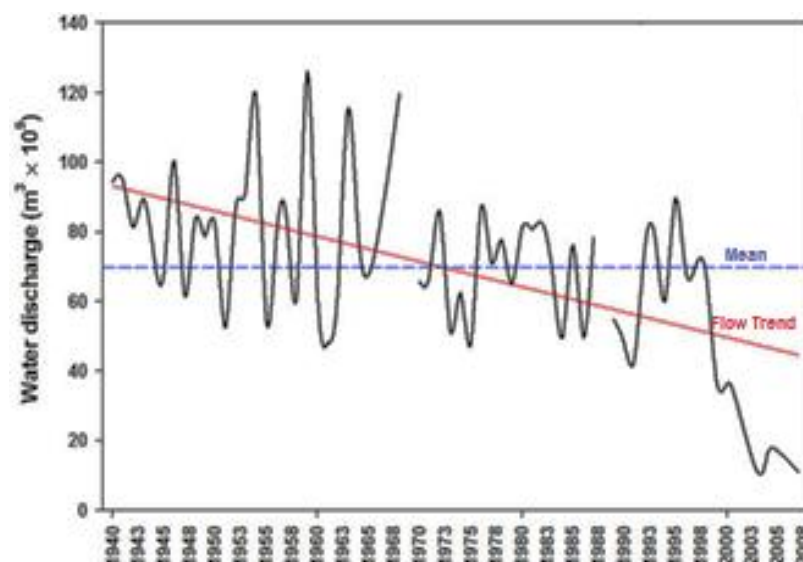


Figure 1-4: Annual water discharge of the Tigris and the Euphrates Rivers. Water discharges from 1940 to 2002 were measured at the closest input into the Mesopotamian marshlands. (AlMaarofi, 2012)

The period leading up to the 1990s, the Mesopotamian marshlands lost more than 30% of their annual water discharge. The situation of water shortage becomes more complicated over time. Unfortunately, the current annual water discharges of the two rivers are still decreasing, and their average discharge from early inundation in 2003 to 2007 was about  $13.8 \times 10^9 \text{ m}^3$  (AlMaarofi et al., 2012). This indicates that the Mesopotamian marshlands have lost more than 80% of their historical water input. This situation is dramatically affecting the current hydrological conditions of the re-flooded marshes. This also indicates that the existing quantity of water in the two rivers is not enough to recover the historical Mesopotamian's size.

A number of UN agencies including UNICEF, UNESCO, etc., in cooperation with the Iraqi Ministry of Water Resources, announced that the Tigris and Euphrates rivers could be completely dried up soon because of the compounded effect of climate change, reduced upstream supply, and increase in domestic and industrial use. That announcement was made on International World Water Day, 22/03/2011. Further investigations were subsequently made to get the truth of this issue, but the basis of this announcement was not discovered. Nevertheless, the announcement is the main motivation to carry out this study.

## 1.2 Tigris River

The Tigris is one of the largest rivers of the Middle East, with a length of 1,850km. It initially flows through Turkey for 432km, forms the eastern border of Syria for a stretch of only 44km before flowing downstream in Iraq for 1,418km. Its source is in southwestern Turkey by Lake Hazar and is joined by the rivers Khabour, Big (Greater or Upper) Zab, little (Lesser or Lower) Zab, Adhaim, Diyala, and Karun as well as several other lesser or seasonal rivers with a total catchment area of 221,000 km<sup>2</sup> (see Figure 1.3). Along its course, the Tigris passes through some of the major cities of Iraq including Mosul, Tikrit, Samarra, and the capital Baghdad. At Qurna, the Tigris joins with

the Euphrates and for the remaining 170 km to the outlet at the Persian Gulf, it is known as Shatt al-Arab.

Topographically, the Tigris basin plain is surrounded by mountains in the north and the east, which can reach altitudes of 3550m above sea level, and by desert areas in the south and west, which account for over 40 percent of the land area. The basin climate is mainly of the continental, subtropical semi-arid type, with the north and north-eastern mountainous regions having a Mediterranean climate. Rainfall is very seasonal and occurs in the winter from December to February, except in the north and northeast of the country, where the rainy season is from November to April.

Iraq has embarked on developing many hydraulic schemes and projects including dams of different sizes and types, weirs, and reservoirs for energy generation and irrigation purposes. Currently, Iraq has constructed 8 dams on the river with different uses and capacities (see Figure 1.3 and Table 1.1). The resulting reservoirs are used for hydropower production and to provide water irrigation, flood control, and flow regulation. Iraq has also constructed a canal linking the Tigris and Euphrates rivers through the Thartar reservoir for flood control and flow regulation. Iran is located to the east of Iraq, and only a small part of the Tigris watershed lies within its boundaries. However, the Iraq-Iran border region contains a mountainous area where the headwaters of certain Tigris tributaries provide more than half the annual flow of the Tigris River. Because Saudi Arabia occupies a portion of the watershed that consists of desert with intermittent streams, no significant water resource projects have been carried out in this country's proportion of the watershed.



Table 1.1: A list of dams located on Tigris River, their capacity and purposes.

<b>Major Reservoir</b>	<b>Use</b>	<b>Year Built</b>	<b>Gross Storage m<sup>3</sup> *10<sup>9</sup></b>	<b>Surface Area (km<sup>2</sup>)</b>	<b>HP (MW)</b>	<b>Height (m)</b>	<b>Elevation (m)</b>	<b>Irrigated Area (km<sup>2</sup>)</b>
<b>Mosul</b>	HP/I	1985	13.15	371	320	100	250	1,677
<b>Bekme</b>	HP/I	UC	8.3	56	1,500	230	400	8,700
<b>Dokan</b>	HP/I	1961	6.82	270	400	116	420	1,500
<b>Dibbis</b>	I	1965	3	32	—	15	306	1,500
<b>Therthar</b>	FC/I	1954	72.8	2,170	—	65	0	7559
<b>Adheem</b>	HP/I	1999	1.35	250	—	60	115	455
<b>Derbendikhan</b>	HP/I	1962	3	121	249	135	400	669
<b>Hamrin</b>	I	1980	3.95	440	—	40	74	1,944

Note: HP = hydropower; I = irrigation; FC = flood control; UC = under construction.

### 1.3 Tigris Catchment Management

Freshwater resources are becoming scarce in the Tigris River catchment and tensions among different users are rising, both at national and international levels. Political borders and boundaries rarely coincide with borders of watersheds, ensuring that politics inevitably intrude on water policy. Over 260 river basins and nearly 270 groundwater aquifers are shared by two or more nations (Wolf et al., 1999, UNESCO, 2009). Just as oil and gas create disputes between states, water has long played a role in international politics and conflicts. Inequalities in the distribution, allocation, and use of water have been a source of tension and dispute. In addition, water resources have long been used to achieve military and political goals, including the use of water systems and infrastructure, such as dams and supply canals, as military targets (Gleick, 1993). Changes within a basin can lead to transboundary tensions in the absence of strong institutions and agreements. When major projects proceed without regional collaboration, they can become a point of conflict, heightening regional instability. Parana La Plata, Aral Sea, Jordan and the Danube may serve as examples. Due to the pressure on the Aral Sea, half of its superficies has disappeared, representing two thirds of its



volume. 36,000 km<sup>2</sup> of marine grounds are now covered by salt. Most of the areas where water will soon be scarcest are in poor countries, which have little resilience to cope. Many are also in areas where there is already political instability, tension, or outright conflict, and the competition for water resources will heighten these problems.

Water use in Iraq for irrigation and hydropower production is constantly increasing, with numerous operational and planned projects along the river's main course and its tributaries placing pressure on flow regimes in the basin. Periodic droughts affect water supply and may impact water allocation to different sectors in the future. There is no basin-wide agreement and no common approach or consensus on how to manage the Euphrates and Tigris Rivers, i.e. whether the two rivers should be considered part of a single watercourse system or as separate basins. While the development of new infrastructure along the rivers has in general not sparked disputes among basin countries, the Ilisu Dam Project in Turkey remains controversial. Iran's damming of the Wand River has also caused tensions between Iran and Iraq (BGR, 2013). Table 1.2 summarises the main agreements between the transboundary counties in Tigris basin in terms of organisation and control of the usage of the river.

*Table 1.2: The main agreements between the Tigris River Transboundary Countries*

<b>Transboundary Countries</b>	<b>Year</b>	<b>Agreement's Summary</b>
<b>Iraq – Turkey</b>	1946	The Treaty of Friendship and Good Neighbourly Relations is the first legal instrument of cooperation on water between the two riparian countries. Among others, it addresses flow regulation on the Tigris and Euphrates and their tributaries and the monitoring of flow data. The parties also commit to the principle of prior notification with regards to water infrastructure projects.
<b>Iran – Iraq</b>	1975	Agreement on the use of shared watercourses in which the signatory parties agree on the division of a number of shared Tigris tributaries.
<b>Iraq – Syria</b>	2002	Agreement on the establishment of a pumping station on the Tigris River in Syria, specifying project area and volume of water extracted.
<b>Syria – Turkey</b>	2009	The Turkish-Syrian Strategic Cooperation Council Agreement covers water issues and can be regarded as the Turkish approval of Syria's pumping project on the Tigris River.

It should be noted that none of these agreements are officially recognised: when the related meetings took place, not all the involved counties attended, and they did not happen under international observation.

Iraq is close to being divided into very small countries based on a very complicated splitting regime. This dividing regime could be very unique and based on a combination of religious denominational and ethnic considerations at the same time. This could have important implications for the water sharing system situation more difficult, as each of these potential regions will claim their own right for the water (see Figure 1.5).



Figure 1-5: A potential scenario for Iraq Water system after splitting into smaller countries.

## 1.4 River Losses Assessment in Developing Countries

It has been shown that effective water resources assessment and management can be implemented through a decision making plan (Palmer et al., 2004). This plan should be based on reliable data and sufficient information of the status and trends of water sources including quantity, quality and statistical details of droughts or floods

events (WMO, 2009). To provide a comprehensive and accurate river losses assessment for rivers located in developing countries such as the Tigris, getting robust data needs to be considered carefully. In any scientific research based on gathering and analysing data, data sets can be intermediate results as well. In the UK for example, sometimes data sets for research purposes are published or easily accessible, but this is not the case in Iraq, which has a long history of armed conflicts, ignorance and lack of awareness, as well as poverty. Wind speed, wind direction, rainfall, temperature, river flow, etc. are essential parameters for water strategy applications, studies and development as well as for evaluating the quantity of water losses due to direct removal from the water surface (evaporation) and the quantities which are removed from the soil in Arid and Semi-Arid catchments (transpiration). Calculating the total amount of evapotranspiration is a complicated process. This process requires the use of complex models involving a large range of variables, as well as a wide range of observations for performance assessments. These kinds of data are subject to numerous types of errors, the most common of which are missing observations, unreasonable readings and spurious zeroes (Kotsiantis et al., 2006).

For the Tigris, missing data are expected. The author's investigations and efforts proved that there are gauging stations in the study area but these have poor facilities and primitive measuring tools (the issues are explained in detail in chapter 2). To fulfil the aims of this research, different types of numerical models are used. These models typically require a complete time series of meteorological inputs, thus reconstructing missing data is a key issue in the functionality of such physical models. The reconstruction of missing weather data is different from weather forecasting because both data collected before the gap and data collected after the gap can be used. Still, the dependencies between the missing and available weather variables are expected to be complex, and advanced data analysis tools are needed to find and to express these dependencies with sufficient accuracy (Kotsiantis et al., 2006).

## 1.5 Research Aims and Objectives

The aim of this research is to give a better understanding of the impact of climate change on arid and semi-arid basins located in a developing country.

Evapotranspiration (ET) is considered to represent the climate change impacts on these areas. The potential usage of Google Earth as a source of geometrical to obtain river profiles for rivers located in area with severe lack of data, was investigated in this study to aid research in developing countries.

Tigris River was selected to be the case study of this project. Although it is referred to as one of the largest rivers in the world, it has been historically undervalued and under-represented in terms of research. It has not been studied much in terms of water quantity, quality and climate change impact.

In order to meet the main aim of this research, the project process is divided into three main stages:

- Evaluate the water resources including precipitation, and quantify the total amount of water flows along the Tigris;
- Quantify the amount of water lost due to evapotranspiration accurately; and
- Develop an integrated water balance and water losses assessment study based on historical records, which can give a vision of the water sustainability in the future.

In the following, a summary of questions raised during the literature review (Chapter 2, 2.7) are listed as well as the objectives which were carried out to answer those question and consequently achieve the main aim of the research:

1. Which one of the well-known ET models best represents the evapotranspiration rates for rivers located in arid and semi-arid catchments with severe lack of data? (Addressed in chapter 2 & 5).
2. Is it possible to study the past, present and future ET trends for rivers located in arid and semi-arid catchments with severe lack of data? (Addressed in chapter 2 & 5).

3. Do the available weather simulation and forecast models such as SDSM have the ability to predict future ET trends for rivers located in arid and semi-arid catchments with severe lack of data? (Addressed in chapter 2 & 5).
4. Is Google Earth capable of generating accurate river cross sections in areas with severe lack of data? (Addressed in chapter 2 & 6).
5. Is ISIS-1D able to provide accurate river losses estimation for long rivers? (Addressed in chapter 6)
6. Are any of the available water balance models capable of adequately highlighting water losses for rivers located in arid and semi-arid catchments with severe lack of data? (Addressed in chapter 2 & 7)

The research objectives addressing these questions are as follows:

1. Implement a comprehensive literature review that shows the state of the art of techniques and technologies in river ET losses assessment and water balance studies. Through this review, all parameters, tools and models required to carry out water balance studies will be identified (Addressed in Chapter 2).
2. Data-sets (often in combination with models and parameters) are themselves becoming more important and can sometimes be seen as the primary intellectual output of a research study. Collect, retrieve and reconstruct existing data sets as much as possible in an effort to create a water balance data set for rivers located in developing countries which is as complete as possible, and make it more widely accessible (Addressed in Chapter 3).
3. Examine and analyse the accuracy of different interpolation techniques and data reconstruction methods for missing historical records for all of the relevant data (Addressed in Chapters 4 & 5).
4. Examine several evapotranspiration models to find the most suitable one to simulate river ET water losses (Addressed in Chapter 5).

5. Investigate the potential of using statistical downscaling models in terms of filling the gaps of the obtained data in semi-arid and arid catchments (Addressed in Chapter 5).
6. Implement a comprehensive water balance trend analysis based on observed data to study the current situation of the Tigris River in terms of available discharge (Addressed in Chapter 6).
7. Investigate how hydrodynamic models can simulate and highlight large-scale water quantity flow processes in open channels and determine the impact of evapotranspiration on river discharge (Addressed in Chapters 6 & 7).
8. Provide a better understanding of the future of the Tigris River in terms of how the water quantities in the river are affected by climate change and other factors (Addressed in Chapter 7).

Combining the main aim of this research with these stages will help in proposing new approaches and frameworks for evaluating possible implications for resources management, policy making, and other engineering applications not only for the Tigris, but for other rivers sharing similar conditions.

## 1.6 Thesis Outline

**Chapter 1: Introduction** gives a brief overview of the current global water situation globally as well as in Iraq, the status of the Tigris River, general information about evapotranspiration and a quick glance at the importance of robust data sets. The main aim and objectives of the research are also outlined.

**Chapter 2: Literature Review** will discuss the recent studies that have been conducted regarding river losses in addition to a thorough investigation and analysis of some of well-known ET models and their applications. Downscaling techniques are also mentioned in this chapter plus some hydrodynamic river models.

**Chapter 3: Data** describes the available observed river flow and metrological data and their sources, as well as reanalysed data which are prerequisite for reconstruction purposes. This chapter shows some trend analyses for the main variables as well as comparisons between the observed and reanalysed data.

**Chapter 4: Methodology** will discuss the theoretical framework adopted throughout this research.

**Chapter 5: Tigris River Basin & Evapo[transpi]ration presents** analysis of approximately 40 years of observed data to reveal pertinent ET trends. This chapter also will present comparisons between different ET models. The setup, preliminary testing and calibration of the SDSM, as well as final results obtained from the model, are also presented. This model constitutes a decision support tool for assessing local climate change impacts using the statistical downscaling technique.

**Chapter 6** includes, thorough explanation of the importance of incorporating **hydrodynamic models** in such a study, justification of employing ISIS-1D as a suitable model for the study. ISIS 1D setup is explained, including a suggestion to use a new methodology in **river profile generation**. Preliminary testing, calibration and final river losses predictions are also reported.

**Chapter 7:** describes the integrated water balance study developed for the Tigris river with the selected regains over the period of investigation (from 1970 – 2000).

**Chapter 8: Conclusion** summarises the main findings of this research project including opportunities, challenges, research limitations and recommendations for future research.

## Chapter Two: Literature Review

Large rivers crossing arid and semi-arid regions are vital life support elements for the survival of people who normally live alongside them. They help to provide regular water supply and fertile soils, to recharge underground aquifers and to lessen the impact of seasonal floods.

This chapter reviews studies that take into account understanding the impact of climate change on water resources alongside its well-known potential scenarios. Methods and tools for generating and re-constructing meteorological data are also presented, in addition to sources of model uncertainty, water balance elements trends at different levels and river water budget approaches.

Evapotranspiration impacts and evaluation methods are also reviewed because their components have a great influence on the water quantities in arid and semi-arid catchments. In addition to that, fundamentals and concepts pertaining to hydrodynamic models are considered. Developing the necessary understanding of these tools' mechanisms can be a great asset in the prediction of the required hydrological variables and the identification of the water losses distribution. This chapter also investigates the suitability of certain data sources to provide information for the generation of river profiles, alongside other details, to help develop a better understanding of rivers that are either ungauged or have a severe lack of data.

### 2.1 Water Balance for Rivers

This section reviews previously developed water balance studies for major rivers around the world. This will highlight information, recent findings, investigations and scientific results which may be beneficial in developing a consistent Tigris River balance study with stable long-term prospects. The development of a rigorous program of data quality assurance, management, archiving and unbiased surface water information that is readily accessible to all, is also discussed.



### 2.1.1 Water Balance Concept

A water balance can be simply a tool that quantifies the inputs and outputs of a hydraulic system. Any difference between inputs and outputs represents a change in the total water mass – or storage – of the system. A typical water balance study for a specific watershed might account for net precipitation inputs ( $P$ ) and outputs by stream flows ( $Q$ ) and evapotranspiration ( $ET$ ). When  $P > [Q + ET]$  water has been stored in the system as either soil moisture or a head increase within the saturated zone. Over longer durations, changes in storage go to zero and all  $P$  can be accounted for by flow,  $ET$  and in some cases, groundwater flow out of the basin.

Water balance assessment is a prerequisite to understand the key processes of the hydrologic cycle in a certain region. The challenge is more acute in developing countries, where climate and runoff data is often scarce, as in the case of the Tigris River, for example. In such cases, a water balance study can provide insights into the hydrological behaviour of a catchment and can identify changes in main hydrological processes. In order to understand water balances, complex hydrologic systems have always been simplified. Thornthwaite et al. (1957) conceptualised a catchment water balance model for long term monthly climatic conditions, which then led to many studies on water balance models for similar conditions at catchment, region or continent scale.

To provide better understanding of the impacts of climate change on water availability, trends pertaining to one or more of the water balance's elements have to be estimated because the different hydrological processes are related to each other and are governed by conservation of mass. Therefore, any trend displayed by one hydrological process is likely to be related to those displayed by other processes. Precipitation, evaporation, change in storage and runoff are the most fundamental processes in the water balance. All of these elements are linked together by conservation of mass (Reggiani et al., 2000).

$$\frac{ds}{dt} = P \pm E \pm R \quad (2-1)$$

where,

$\frac{ds}{dt}$  is change of storage,

P is the precipitation,

E is the is evaporation (-) or condensation (+)

R is runoff to (+) or away from (-) a control volume which includes both surface and subsurface components.

Quantifying these elements' time variant characteristics in response to climate change is foremost in current hydrological studies.

Studying river water balance is valuable because it provides an estimate of changes in water mass in the subsurface without direct measurements of soil moisture or changes in head which can be highly spatially and temporally heterogeneous, making accurate field sampling nearly impossible at large scales (Lundmark et al., 2006).

### **2.1.2 Water Balance Approaches**

There are several ways in which one may approach a water balance study. Essentially these are different ways to derive gridded discharge information. They include averaging the runoff from all stations within each grid cell, statistically interpolating runoff between gauges, using an empirical relationship that relates runoff to precipitation, potential evaporation, and temperature, using a soil-water balance type model, and overlaying grid cells onto catchment runoff maps to derive area-weighted runoff estimates. Given adequate data, the atmospheric water balance is a promising method for estimating regional evaporation, runoff, and changes in basin storage. However, significant uncertainties in runoff estimation using atmospheric data exist even at the continental scale (Reed et al, 1998), as poorly defined continental or basin boundaries may contribute to inaccuracies in runoff estimation. The commonly used surface water balance relies on the fact that, with the exception of coastal areas, the landscape can often be divided into watershed units from which there is only one surface water outflow point (Bahati, 2008).

Simulating streamflow for large river basins accurately is an important issue with regards to the prediction of the timing and magnitude of floods and droughts. Moreover, it helps to assess the hydrological impacts of climate change. Many studies have been implemented with the aim of quantify the impact of climate change on extreme value distributions of river streamflow.

Certain studies have the advantage of having access to a sufficient number of meteorological variables at a high enough spatial and temporal resolution to power more sophisticated models; often conceptual water balance models have been used to simulate future streamflow. Examples of water balance models for the Rhine include Rhineflow (Van Deursen et al., 1993) and STREAM (Spatial Tools for River basins and Environment and Analysis of Management options (Aerts et al., 1999). These statistical water balance models were developed with the aim of highlighting water quantity changes in large rivers. RhineFlow is the most popular water budget model, developed by Van Deursen et al. (1993) to assess the water balance situation for the Rhine River. This model is based on an approach devised by Thornthwaite and Mather [1957], which relies on daily temperature measurements. The streamflow is obtained from this model by adding the net water production from a particular catchment. Assuming that all water available for runoff leaves the catchment within one time step, the model produces month-to-month runoff for the water system including main tributaries. To get accurate simulated streamflow, it is essential to have a realistic description of all relevant land surface processes, including the partitioning of available energy. Errors in estimates of evaporation might propagate into similar errors in other terms of the energy and water balance and ultimately affect streamflow prediction.

Land surface models (LSMs) derive evapotranspiration from coupled water and energy balance simulations [Liang et al., 1994; Famiglietti and Wood, 1994], and are able to utilise additional information provided by regional climate model (RCM) output, such as solar radiation, wind speed, specific humidity and atmospheric pressure. Therefore, LSMs carry the potential to more accurately estimate hydrological partitioning

(evaporation, soil moisture, surface runoff and streamflow). Because of the complex model structure and the large number of parameters in LSMs, they are generally more difficult to parameterise. LSM intercomparison experiments have demonstrated large variability in simulated land surface-atmosphere fluxes and streamflow using different LSMs [e.g., Pitman et al., 1999; Wood et al., 1998; Lohmann et al., 2004b]. The original purpose of LSMs was to represent the land surface in (regional) climate simulations used for climate models and numerical weather prediction [e.g., Liang et al., 1994; Koster et al., 2000; Zeng et al., 2002; Dai et al., 2003]. Recently, LSMs have also been used for (experimental) streamflow forecasting [e.g., Wood et al., 2005]. However, many studies assessing climate change impacts use water balance models, as well as short-term flood forecasting systems (e.g., in the Netherlands [Sprokkereef, 2001a]).

### **2.1.3 Water Balance Studies**

Hydrological water balance models can be based on the interactions between the water, atmosphere, and land surface; which is a combination of the atmospheric water balance, surface water balance and the soil water balance. This section discusses typical examples that illustrate the usage of these models.

Cohen et al. (2001) undertook a water balance study for the Colorado River, aiming for more robust assessment of the sources and magnitudes of the river's discharge than what had previously been published. The main motivation behind the study arose from the fact that the delta, which is formed by the deposition of sediment from periodic Colorado River floods, has been altered by the construction of upstream impoundments and the conversion of wetlands to irrigated agriculture. In turn that has led to a reduction in the delta's extent from some 7,770 km<sup>2</sup> to only about 600 km<sup>2</sup>. The study relied on published records, including discharge and precipitation supplemented by other unpublished agricultural drainage records obtained from authorities. Evaporation and evapotranspiration (ET) were calculated using published reports of vegetation type,

extent and density, ET coefficients and pan evaporation rates. Their values were incorporated into the system as the main water loss sources.

The study used a mass balance to characterise discharge through the study area. The mass balance equation (Owen-Joyce et al., 1996) can be described as:

$$Q_{ds} = Q_{us} + Q_{rf} + P + T_r - E - ET - \Delta S_a - Q_{sb} \quad (2-2)$$

where,

$Q_{ds}$  = flow at downstream boundary,

$Q_{us}$  = flow at upstream boundary,

$Q_{rf}$  = return flow to the river (from outside the region),

P = rainfall

$T_r$  = tributary inflow (local runoff),

E = Evaporation,

ET = evapotranspiration,

$\Delta S_a$  = changes in aquifer storage,

$Q_{sb}$  = flow to sub-basin.

Groundwater as a distinct source was not assessed as part of this study. Presumably, it was applied as irrigation and delivered for municipal use, contributing to the water balance in the form of agricultural drainage and municipal effluent, because actual records of groundwater extraction and recharge for the study area were not available.

This study produced historical discharge records for several locations along the river, which is located on the boundary between the United States of America and Mexico. The estimated discharge for this study at the downstream boundary of the main-stem suggests that recorded discharge in the studied region may not be a reliable indicator of total discharge through the system. This study was limited to the calendar year period 1992 – 1998 because of data constraints.

In Central Europe, recent floods in the Rhine (1993 and 1995), Elbe (2002) and Danube (2002), as well as droughts (e.g., the summer of 2003) have caused billions of euros of

damage. Improving streamflow simulations in these densely populated large river basins is important for the accurate prediction of timing and magnitude of floods and droughts. Hurkmans et al. (2008) investigated and compared the accuracy of streamflow simulations of a water balance approach (Spatial Tools for River basins and Environment and Analysis of Management (STREAM)) and a land surface model (Variable Infiltration Capacity (VIC)) approach. Both models were applied to the Rhine River Basin using regional climate model output as atmospheric forcing, and were evaluated using observed streamflow and lysimeter data.

STREAM is a distributed grid based water-balance model (Aerts et al., 1999) which is in turn based on the integrated GIS water balance model for the River Rhine (Rhineflow) (Van Deursen et al., 1993). STREAM only needs precipitation and temperature as dynamic input variables and its application is relatively simple. Snow, soil moisture and groundwater are the main storage reservoirs of the model. It divides outflow into two components: the first one is affected by soil moisture and the second one is affected by ground water storage. Both behave as linear reservoirs. Potential evapotranspiration is derived from surface temperature, using the modified (Thornthwaite et al., 1957) model:

$$PE = 16 * \left[ \frac{10 * Tm}{H} \right]^A \quad (2-3)$$

where,

PE = Potential Evapotranspiration (mm/month)

Tm = mean monthly air temperature (°C)

$$H = \text{annual heat index} = \sum_{i=1}^{12} \left( \frac{Tmi}{5} \right)^{1.514}$$

$A = 0.49 + 0.01792 * H - 0.0000771 * H^2 + 0.000000675 * H^3$ , A is the Thornthwaite parameter.

Actual evapotranspiration is calculated using the soil moisture storage and the so-called 'accumulated potential water losses. It should be noted that in this model, the snow

accumulation is equal to precipitation when temperature is below zero degrees Celsius; snowmelt linearly depends on temperature.

The study also identified the Variable Infiltration Capacity (VIC) model which was developed by Liang et al. (1994), as a variable-layer soil-vegetation-atmosphere transfer (SVAT) scheme for general and regional circulation and weather prediction models. The study states that, when snow is present on the ground, the model is coupled with a two layer energy- and mass-balance model.

VIC can operate in two modes: the energy balance mode, in which the energy balance is solved iteratively to obtain the surface temperature, and the water balance mode, in which surface temperature is assumed equal to air temperature. In both modes, potential evapotranspiration is calculated using the Penman-Monteith equation. In the energy balance mode a time step of 3 hours is used, in correspondence with availability of forcing data, whereas in water balance mode the model is integrated at a daily time step. Therefore simulation times are drastically reduced compared to the full mode.

Routing of surface runoff and base flow from all models is done using the algorithm developed by Lohmann et al. (1996), which was subsequently applied in combination with VIC. The sum of base flow and runoff from the models is complicated by a normalized impulse response function, based on the St. Venant equation, assuming that water from each grid cell flows into the channel in the steepest direction to the next cell.

The study concluded that that VIC was more robust and less dependent on model calibration. Although STREAM performs better during the calibration period (Nash-Sutcliffe efficiency (E) of 0.47 versus E= 0.29 for VIC), VIC more accurately simulates discharge during the validation period, including peak flows (E= 0.31 versus E = 0.21 for STREAM). This was the case for most locations throughout the basin, except for the Alpine part where both models have difficulties due to the complex terrain and surface reservoirs. In addition, VIC simulates the annual evaporation cycle more realistically using lysimeters. The whole process covered the period between 1993 until 1998. It should be noted that water quantities in the river were not discussed in detail.

Tekleab (2011) published a study aiming to obtain better understanding of water balance dynamics in the upper Blue Nile catchments on annual and monthly time scales and on a spatial scale of mesoscale to large scale. This study is a good example of a study in which the understanding of the processes at sub-catchment level is generally lacking and a considerable gap in multi-objective calibration for optimal parameter sets towards different objective functions exists.

The author's intention was to use a water balance approach based on Budyko's hypotheses (Budyko, 1974) and incorporate the following information:

1. Monthly stream flow time series observations of 20 rivers covering the period 1995–2004 that have been collected from the Ministry of Water Resources Ethiopia,
2. Monthly meteorological data, including precipitation, for the same period, obtained from the Ethiopian National Meteorological Agency (ENMA).
3. Potential evaporation data, computed using Hargreaves method with minimum and maximum average monthly temperature as input data (Hargreaves and Samani, 1982).
4. The catchment boundary and the drainage pattern delineated using ArcGIS 9.3 with a 90 m resolution digital elevation model of the NASA Shuttle Radar Topographic Mission (SRTM) obtained from the Consortium for Spatial Information.

The Budyko (1974) equation can be written as follows:

$$\frac{E}{P} = \left[ \phi \tanh\left(\frac{1}{\phi}\right) (1 - \exp^{-\phi}) \right]^{0.5} \quad (2-4)$$

$\phi$ : Aridity index =  $E_p/P$

However the water balance analysis using a Budyko-type curve at annual scale reveals that the aridity index does not exert a first order control in most of the catchments. This implies a need to increase model complexity to monthly time scale to include the effects



of seasonal soil moisture dynamics. Thus, the model of Zhang et al. (2004) was used instead:

$$\frac{E}{P} = 1 + \frac{E_o}{P} - \left[ 1 + \left( \frac{E_o}{P} \right)^w \right]^{\frac{1}{w}} \quad (2-5)$$

w: Plant (available) Water coefficient

The dynamic water balance model used in this study predicted the direct runoff and other processes. The model was based on the limit concept; i.e. for dry environments, since the amount of rainfall is small, the aridity index approaches infinity or equivalently evaporation approaches rainfall. For wet environments, where the amount of rainfall is large, the aridity index approaches zero and the actual evaporation approaches the potential evaporation. However, the study suggested that on an annual time scale the reasons for poor model efficiencies in the majority of the catchments, which followed distinct Budyko-type curves, needs further research. It is recommended that future work should focus on the regionalisation of the optimal parameter sets from the monthly model presented in this research for prediction of streamflow in ungauged catchments in the Upper Blue Nile basin.

A study by Syed et al. (2014) has been published recently, aimed at providing a proper evapotranspiration variability assessment using water balance computation in the Ganga River Basin (GRB) in India for the period from 1980 until 2007. The main motivation for conducting the study was a study undertaken by Webster et al. (2011), which stated that the quantities of fresh water provided by the river will be reduced to about 50% of their current values.

The monthly Global Precipitation Climatology Project (GPCP) precipitation data available from 1979 to the present, on  $2.5^\circ \times 2.5^\circ$  latitude-longitude grids, were used in this study. Discharge data used in this study are derived from water levels measured at the gauging station on the river Ganga. The station is located in Bangladesh and is very close to the India-Bangladesh border. Upstream data from India are not available. Long-term

estimates of terrestrial water storage are derived from simulations using the Land Dynamics Model (LaD). The LaD model was developed by Milly et al. (2002) and provides monthly gridded time series of water and energy fluxes over the globe. ET estimates were obtained from LaD, General Circulation Model (GCM), and National Centre for Environmental Protection (NCEP) /Department of Energy (DOE) reanalysis (NCEPR2), a satellite-based data set using Moderate Resolution Imaging Spectroradiometer (MODIS), and Penman-Monteith model.

The terrestrial water budget used in this study is formalised as:

$$ET = P - R - \frac{\partial S}{\partial t} \quad (2-6)$$

where ET is evapotranspiration,  $\partial S/\partial t$  is the change in terrestrial water storage averaged over space, P is precipitation, and R is river basin discharge.

Analysis of predicted trend of the ET for the GRB showed an overall decline at the rate of 11 mm yr<sup>-2</sup>. However, it should be noted that, prior to trend estimation, high frequency seasonal variations were removed from the ET average time series using a 12 month moving average filter; the authors claimed that this was done in order to emphasise the inter-annual variations. Based on the correlation between ET and independent estimates of near-surface temperature and soil moisture, the authors concluded that the ET in the GRB is primarily limited by moisture availability.

There is a good opportunity to apply this approach to larger-scale water budget assessments and inter-comparison studies. That also emphasises the importance of synergistic use of multi-platform hydrologic information.

The above discussion has demonstrated that developing water balance studies for water resources is important, especially in developing countries. Integrated water balance studies help to quantify the impacts of climate change by understanding the effects of water balance and hydrological elements on the water resource. There are always

assumptions made in such studies because of the lack of prerequisite data availability. The studies discussed above have generally neglected the change in water storage. They presumed that there are no significant inter-watershed transfers via groundwater or man-made conveyance structures. In general, they rely on the assumption that the average watershed precipitation and runoff can be measured with reasonable accuracy. Despite that, all of these studies consider evaporation and evapotranspiration as separate hydrological elements that have a significant impact on the water balance; the annual evaporative losses from a watershed are estimated by empirical relationships. Observation data were generally not used, and evaporation/evapotranspiration empirical models are used to estimate mean annual or mean monthly flows in ungauged areas. Providing a poor topographical representation of the studied area, or ignoring topography altogether, also leads to failures in simulating accurate runoff. Avoiding such assumptions as much as possible and increasing the dependency on observation data can lead to the development of integrated water balance studies that produce reliable estimations.

## **2.2 Climate Change Impacts on Water Resources**

The Intergovernmental Panel on Climate Change (IPCC) reports identify the term “climate change” as any change that occurs in the climate over time. All new studies and research point to greenhouse gas emissions being the main reason for the increase in the average temperature of the Earth. In fact, the average global temperature has already increased by about 0.6°C since the late 19th century. In addition, there are indications of a further rise of the average temperature by 1.4 to 5.8°C, and sea level rises by a further 9 to 99 cm, by 2100.

Warming and precipitation changes are expected to vary considerably from region to region. Changes in climate average and the changes in frequency and intensity of extreme weather events are likely to have major impacts on natural and human systems.

Climate change can cause significant impacts on water resources due to resulting variations in the hydrological cycle elements. For instance, changes in temperature and precipitation can have a direct consequence for evapotranspiration and for the quality and quantity of runoff. Consequently, the spatial and temporal availability of water resources can be significantly affected, which in turn affects agriculture, industry and urban development. Climate change impacts, adaptations and vulnerability of different water resources are subjects that have been considered in the literature, covering a wide range of different locations with different characteristics and properties (e.g. Piao et al. (2010); Bates et al. (2008); Wilby et al. (2006), etc.). Such research shows strong evidence of the existence of a linkage between the hydrological cycle and climate change, and its impacts on the water resources in terms of quantity and quality.

Many studies show that there are significant effects of climate change on water quantities in major rivers around the world. Scientists had initially tackled the issue by concentrating on changes in total annual runoff due to climate changes. Kwadijk et al. (1994), for example, considered the Rhine River as their research case study to find the effect of climate change on the discharge of the river and concluded that both annual and seasonal discharge of this river are more sensitive to changes in precipitation than to changes in temperature.

The Rhine River flow was also investigated by Shabalova et al. (2003), who evaluated climate change impacts using data from the Hadley Centre regional climate models (HadRM2 and HadRM3) and concluded that the winter discharge increased while summer discharge decreased. The magnitude of the variation was scenario-specific.

Climate change impacts on water resources have been considered in other parts of Europe as well. A significant winter rainfall increase was reported by Pfister et al. (2000), who evaluated Luxembourg water resources to understand the impacts of climate change. That report stated that the rainfall rates increased due to airflow rate increasing from west to east since 1950. Other studies (e.g. Gebremeskel et al., 2004) suggested an increase in stream flow for the future due to increased precipitation and lower

evapotranspiration. Beckmann et al. (2002) also reported an increase in rainfall in the Netherlands and North Germany, and stated that was associated with cyclonic disturbances moving from west to east over the area.

The assessment of climate change impacts on water resource management is complicated because of the coarse spatial resolution of the data available. This issue makes evaluating hydrological variables such as evapotranspiration very difficult.

Evapotranspiration is a very sensitive hydrological element to climate change. It has been chosen to be the main focus for the study to provide better understanding of the magnitudes of climate change impacts on the water resources.

Semi-aridity is the dominant climatic characteristic of the Middle East, and that makes the water resources in that area very sensitive to climate change variations. These areas of the world, and the Tigris River Basin in particular, have rarely been considered with regard to potential impacts of climate change on its water systems.

In spite of the fact that studies on the impact of climate change have been carried out on a global scale, the type and magnitude of impacts on the catchment scale is less clear in most parts of the world. Therefore, it is necessary to study effects of climate change at this scale in order that they be taken into account by policy and decision makers when planning water resources management.

### **2.2.1 Climate Change Scenario Development**

The IPCC report identifies the term 'climate scenario' as a possible indication of what the future could be like over decades or centuries, given a specific set of assumptions. These assumptions include future trends in energy demand, emissions of greenhouse gases and land use change as well as assumptions about the behaviour of the climate system over long time scales (Myles R. Allen, 2014). The report is based on several methods that were used to gain useful information about the possible future climate and their impacts using various scenario construction methods, including:

#### **1. Temporal & Spatial Analogues:**

This is an approach to develop the required climate scenarios based on historical records of the climate behaviour of a certain region. The temporal analogues approach makes use of climatic information from the past as an analogue for possible future climate (Webb et al., 1985). These types of scenarios are not ordinarily recommended to represent the future climate in quantitative impact assessments. The reason is that climate analogues most likely occur due to changes in atmospheric circulation rather than to greenhouse gas induced climate change.

## **2. Synthetic:**

Synthetic scenarios describe a technique whereby particular climate (or related) elements are changed by arbitrary amounts. For example, adjustments of baseline temperature by +1, +2, +3, or +4°C and baseline precipitation by 5, 10, 15 or 20% could represent the magnitude of future changes (IPCC-TGICA, 2007). Such scenarios do not necessarily present a realistic set of changes that are physically plausible. They are usually adopted for exploring system sensitivity prior to the application of more credible, model-based scenario.

## **3. Model-based approaches:**

The most common method of developing climate scenarios for qualitative impact assessment is by utilizing General Circulation Models (GCMs). Analysing GCMs provides a good opportunity to monitor the climate change performance in the past, present and future. Climate scenarios based on GCMs are constructed by adjusting a baseline climate, typically based on regional observations of climate over a reference period such as 1961-1990, by the absolute or proportional change between the simulated present and future climates. GCMs have been used to study the effects of increasing concentrations of carbon dioxide and other greenhouse gases on earth's climate. Two kinds of GCMs are distinguished depending on the assumption of how the current climate may change in the future. The first kind comprises those based on equilibrium response with the assumption that the current and future climates are in equilibrium. The second type of GCM comprises those run in "transient" mode, which are more realistic in their

assumption of a gradual increase in CO<sub>2</sub> and other greenhouse gases. The Atmosphere-Ocean General Circulation Models (AOGCMs) which dynamically link ocean and atmosphere, fall in the category of transient models. Examples of AOGCMs frequently used for impact and related studies include CGCM1 of Canada, ECHAM4 of Germany, and HadCM3 of the UK.

#### **4. Emission Scenarios:**

In 1996, IPCC began the development of a new set of emission scenarios, to update and replace the well-known IS92 scenarios. The new approved set of scenarios is described in the IPCC special report on emission Scenarios (SRES). Four different narrative storylines were developed to consistently describe relationships between forces driving emission and their evolution and to add context for the scenario quantification. The resulting set of 40 scenarios cover a wide range of the main demographic, economic and technological driving forces of future greenhouse gas and sulphur emission. Each scenario represents a specific quantification of one of the four storylines. All scenarios based on the same storyline constitute a scenario “family” which briefly describes the main characteristics of the four SRES storylines and scenario families as follows:

A1. The A1 storyline and scenario family describes a future world of very rapid economic growth, global population that peaks in the mid-century and declines thereafter, and the rapid introduction of new and more efficient technologies. Major underlying themes are convergence among regions, capacity building and increased cultural and social interactions, with a substantial reduction in regional differences in per capita income. The A1 scenario family develops into three groups that describe alternative directions of technological change in the energy system. The three A1 groups are distinguished by their technological emphasis: fossil intensive (A1FI), non-fossil energy source (A1T), or a balanced across all sources (A1B) (where balanced is defined as not relying too heavily on one particular energy source, on the assumption that similar improvement rates apply to all energy supply and end-use technologies).

A2. The A2 storyline and scenario family describes a very heterogeneous world. The underlying theme is self-reliance and preservation of local identities. Fertility patterns across regions converge very slowly, which results in continuously increasing population. Economic development is primarily regionally oriented and per capita economic growth and technological change are more fragmented and slower than other storylines.

B1. The B1 storyline and scenario family describes a convergent world with the same global population, that peaks in the mid-century and declines thereafter, as in the A1 storyline, but with rapid change in economic structures towards a service and information economy, with reductions in material intensity and the introduction of clean and resource efficient technologies. The emphasis is on global solutions to economic, social and environmental sustainability, including improved equity, but without additional climate initiatives.

B2. The B2 storyline and scenario family describes a world in which the emphasis is on local solutions to economic, social and environmental sustainability. It is a world with continuously increasing global population, at a rate lower than A2, intermediate levels of economic development, and less rapid and more diverse technological change than in the A1 and B1 storylines. While the scenario is also oriented towards environmental protection and social equity, it focuses on local and regional levels.

### **2.2.2 Downscaling**

For long rivers, it is impossible to predict how much water flow or vanish precisely. Robust records of at least several past decades of hydro-metrological data sets (e.g. stream flow, rainfall, Evaporation and Transpiration, infiltration, etc.) have to be available to make the “best guess” of what the river discharge will be. Furthermore, to be able to estimate the river water losses due to evapotranspiration, it is necessary not only to know annual rainfall/run-off variations, but also seasonal, monthly and even daily peaks and troughs.



Global Climate Models (GCMs) were considered as the primary tool for understanding how the global climate may change in the future. However, these currently do not provide reliable information on scales below about 200 km (Stocker et al., 2013). The poor quality and gaps in observation data provided to this research is considered as one of the major challenges faced (Refer to chapter 3, 5 and 6).

The downscaling approach is suggested to overcome such a problematic issue in this study. This methodology has been developed and tested in other studies e.g. (Hensen et al., 2012). Downscaling is a method for obtaining high-resolution climate or climate change information from relatively coarse-resolution Global Climate Models (GCMs). The available studies indicate that downscale processes have the potential to produce finer resolution datasets from the global reanalysis records which is suitable for hydrological and meteorological applications (Srivastava et al., 2013). It can be considered as a strategy for generating locally relevant data from Global Circulation Models (GCMs). The overarching strategy is to connect global scale predictions and regional dynamics to generate regionally specific forecasts. GCMs always show an excellent description of the climate change behaviour on continental and hemispherical levels. However, Dibike et al. (2005) state that GCMs inherently cannot show local sub-grid scale features and dynamics such as local topographical features and convective cloud processes. Moreover, GCMs are not designed for climate change impact studies and do not provide a direct estimation of hydrological responses to climate change.

GCMs typically have a horizontal resolution of between 250 and 600 km and between 10 and 20 vertical layers in the atmosphere, and sometimes as many as 30 layers in the oceans (IPCC, 2007; Barrow et al., 2000). This means that their resolution is very coarse relative to the scale of the units that are required to be investigated. This coarse resolution also means that representation of the earth's surface (i.e. underlying topography) in the model is also poorly detailed in comparison to reality with obvious implications for the accuracy of the climate simulation. Consequently, output from GCMs is not generally of a sufficient resolution or reliability to be applied directly to represent

present-day climate or subsequent future climate conditions. Therefore, the need for detailed local or regional scenarios of climate change for impact studies has resulted in the development of a number of methodologies for deriving such information, generally from GCMs (Robock et al., 1993). These methodologies, termed 'downscaling', have been designed to bridge the gap between the information that the GCMs can provide and that required by modellers undertaking impact studies (Wilby et al., 1997).

Downscaling approaches are always found as either spatial or temporal. The temporal approach produces fine-scale temporal data from coarser-scale temporal information. It is mainly used in derivation of daily scenario data from monthly or seasonal scenario information. As for the spatial approach, it produces finer resolution climate information from coarser resolution GCM output. Here, the assumption is that it will be possible to determine significant relationships between local and large-scale climate and that these relationships will remain valid under future climate conditions (IPCC, 2007).

### **2.2.3 Dynamical Downscaling:**

The dynamical downscaling technique is based on the use of regional climate models (RCMs), which generate finer resolution output based on atmospheric physics over a region using GCM fields as boundary conditions (Giorgi et al., 1999). The physical uniformity between GCMs and RCMs is governed by the correspondence of their large-scale circulations (von Storch et al., 2000). As a consequence of the higher spatial resolution output, RCMs provide a better description of topographic phenomena such as orographic effects (Christensen et al., 2007), and the finer dynamical processes in RCMs produce more realistic mesoscale circulation patterns (Buonomo et al., 2007). However, RCMs are not expected to capture the observed spatial precipitation extremes at a fine cell scale (Fowler et al., 2009). Studies have found that the RCMs performance depends on the RCM resolution, on the region and the season on either end. Although RCMs may give feedback to their driving GCMs, many dynamic downscaling approaches are based

on a one-way nesting approach and have no feedback from the RCM to the driving GCM (Maraun et al., 2010).

RCMs do have a heavy legacy of biasing resulted from GCMs when trying to simulate precipitation for example on large scales (Durman et al., 2001) and the inter-model differences are related to model biases (Frei et al., 2006). Moreover, Christensen et al. (2008) suggests that GCM biases may not be linear and biases may not be cancelled out by simply taking differences between the control and future scenarios, which many studies have adopted. On the other hand, imperfect modelling and numerical stability also adversely affect RCMs (e.g. Lenderink et al., 2008; Maraun et al., 2010).

Despite their rapid development, RCMs are still ridden with problems related to parameterisation schemes due to the fact that physical processes are modelled at a scale on which they cannot be explicitly resolved (Maraun et al., 2010). The RCM precipitation outputs are still found to be sensitive to the numerical scheme and parameters (Fowler et al., 2009; Bachner et al., 2008; Murphy et al., 2009). The discrepancies between real average values and site-specific data are expected to remain a problem (Chen et al., 2008).

#### **2.2.4 Statistical Downscaling:**

Statistical downscaling is a straightforward means of obtaining high resolution climate projections (Wilby et al., 2004). It establishes particular statistical relationships between the GCMs in coarse state and good quality local scale observations.

With respect to types of statistical methods, downscaling can be categorical, continuous-valued or hybrid (Wilby et al., 1997). In categorical downscaling, classifications and clustering are the common statistical techniques to relate data to different groups according to large-scale circulation patterns and data attributes (Zorita et al., 1999). For continuous-valued downscaling, regression relationships are widely used to map large scale predictors onto local-scale predictands (Chandler et al., 2002). In hybrid downscaling, different statistical approaches are combined (Wilby et al., 2002).

Wilby et al. (2006) assessed the uncertainty of climate change, deployable water resources, and water quality dynamics for the River Kennet, using downscaled data outputs from three GCM runs. Gellens et al. (1998) applied a conceptual hydrological model to several Belgian catchments using observed data perturbed by GCM outputs. Brouyère et al. (2004) used an integrated hydrological model and outputs from three GCM runs to assess climate change impacts on groundwater resources for the Geer basin in Belgium.

Diaz-Nieto et al. (2005) explored the relative merits of using statistical downscaling and change factor methods to study low flows in the River Thames using CATCHMOD hydrological model. Although statistical downscaling can be a computationally efficient alternative to dynamic downscaling, the validity of statistical downscaling is based on an assumption that the empirical relationship identified for the current climate will hold for future climate scenarios (Wilby et al., 2004).

The statistical downscaling method examined in this thesis generates hydrological series at a catchment scale which is similar to the target scale in many dynamical downscaling models (e.g. 25x25km Hadley RCM). As the output of the developing statistical and general dynamic downscaling converge to similar scale, the results from the statistical downscaling method developed here may be useful for setting benchmarks for dynamic downscaling. In this work, weather generator type downscaling is of particular interest because weather generators are very general statistical methods allowing combinations of various downscaling techniques and can provide weather sequences for areas without long climate records (Richardson et al., 1984).

It should be noted that the statistical downscaling technique's basic assumption is not variable, i.e., that the statistical relationships developed for the present day climate also hold under the different forcing conditions of possible future climates. This limitation is also applied to the dynamical approaches; studies based on the SD largely restricted themselves to a single driving GCM. The developers of one of the most widely used statistical models (SDSM) report that such an approach is a very straightforward means

of obtaining higher spatial resolution scenarios by applying coarse-scale climate change projections to a high resolution observed climate baseline (Wilby et al., 2004). This method is often used when the Regional Climate Models' outputs are unavailable, for sensitivity studies, or whenever rapid assessments for multiple climate change scenarios (and/or Global Climate models experiments) are required.

## 2.3 Evapo[transpi]ration

The general identification of the Evapotranspiration is the summation of the water that is lost directly from open water bodies surfaces (e.g. rivers, lakes, oceans, etc.), 'evaporation', and water that can be lost from other sources which are able to hold water like soil and plants, 'transpiration'. Evapotranspiration is characterised by a high degree of ambiguity, and has been defined in many studies as the same concept but in different styles (e.g. Oxford Dictionary; Food and Agricultural Organisation (FAO); Sanford et al., 2013; Hansen et al., 1980). All of these studies and more consider different aspects of evapotranspiration in terms of its importance, estimation method tools and challenges, trends and how it may be affected by other atmospheric variables, and also analysing its components (evaporation/transpiration), etc.

The evapotranspiration constituent processes (evaporation + transpiration) take place when changes happen for one, some or all the effective variables (temperature, wind, relative humidity, etc.) seasonally or due to any other climate change issues. Due to the mass conservation law, the lost water does not disappear, but rather is retained by the atmosphere and returns back to either the same water body or other more distant water bodies via transpiration to the atmosphere. Transpiration, like direct evaporation, depends on the energy supply, vapour pressure gradient and wind. Hence, radiation, air temperature, air humidity and wind terms should be considered when assessing transpiration. The soil water content and the ability of the soil to conduct water to the roots also determine the transpiration rate, as do waterlogging and soil water salinity.

The transpiration rate is also influenced by crop characteristics, environmental aspects and cultivation practices. Different kinds of plants may have different transpiration rates. The crop development, soil and the provided water amount also should be considered when assessing transpiration (Allen R. et al., 1998).

### **2.3.1 Variables Affecting the Evapotranspiration**

As part of the hydrological cycle, there are several factors affecting evapotranspiration. The first of these is air temperature. As temperatures increase, evapotranspiration also goes up. This occurs because warmer air surrounds the water surface. Cooler temperatures cause less release of water into the atmosphere from wet surfaces. As evapotranspiration is the sum of transpiration and evaporation, when transpiration decreases, so too does evapotranspiration.

Relative humidity (the amount of water vapor in the air) is also an important consideration in evapotranspiration rates because as the air becomes more and more saturated, less water is able to evaporate and to be taken by the air. Therefore, as the relative humidity increases transpiration decreases.

The movement of wind and air across an area is the third main factor affecting evapotranspiration rates. As the movement of air increases, evaporation and transpiration increase as well because moving air is generally less saturated than stagnant air. Once saturated air moves, it is replaced by drier, less saturated air that absorbs water vapour.

The moisture available in the soil is the fourth main factor affecting evapotranspiration because when soil is lacking moisture, plants begin to transpire less water in an effort to survive. This in turn decreases evapotranspiration. The type of vegetation also affects the transpiration process. Different plants transpire water at different rates. For example, a cactus is designed to conserve water. As such, it does not transpire as much as a pine tree would because the pine does not need to conserve water. Their needles also allow

water droplets to gather on them and this water is later lost to evaporation in addition to the normal transpiration.

In addition to the main fifth factors outlined above, evapotranspiration rates are also dependent upon geography, namely, an area's latitude and its climate. Regions of the globe with the most solar radiation experience more evapotranspiration because there is more solar energy available to evaporate the water. These are generally the equatorial and subequatorial regions of the earth. Evapotranspiration rates are also highest in areas with a hot and dry climate. In the Southwest of the United States for example, evapotranspiration is about 100% of the total precipitation for the area. This is because the area experiences many warm, sunny days throughout the year paired with little precipitation. In these conditions, evaporation is at its highest. By contrast, the US Northwest's evapotranspiration is only about 40% of yearly precipitation. This is due to the much colder and wetter climate. In addition, it is at a higher latitude and experiences less direct solar radiation.

### **2.3.2 Evapotranspiration (ET) Assessment:**

Evapotranspiration can be measured directly by different methods and tools. For example, the lysimeter method which is usually utilised to measure ET by routinely measuring the change in soil moisture of a known volume of soil that is covered by vegetation (Watson et al., 1995). The disadvantage of this method is that it can be expensive economically and time consuming in terms of installing, checking, and maintaining the equipment.

ET can also be measured by determining the flux of moisture from the wetted surface to the atmosphere by using highly sensitive sensors that detect the change in meteorological variables between the surface and a fixed level above the surface. The determination of ET through these flux-related methods, while highly accurate, can be difficult and is generally used only in research settings (Allen, 2000, Atkinson, 2003). This method is also known as the energy budget method. The heating and evaporation

of water requires energy; therefore, the ET process is limited by the input of energy into the system, i.e. incoming radiation from the sun, (Allen R. et al., 1998, Atkinson, 2003). Therefore, measuring the ET can be very problematic, requiring methods that are either labour or financially intensive or that are indirect proxies of evapotranspiration. As an alternative to that, numerical models have been developed to estimate ET for use in environments that lack necessary ET measurements. Many of these models have been derived empirically through field experiments; others have been derived through theoretical approaches.

A major complication in modelling ET is the requirement for meteorological data that may not be easily available (e.g. solar radiation). This restriction at times prohibits use of more accurate models, and necessitates use of models that have less demanding data requirements.

ET is the component that links the surface energy balance to the surface water balance. If the values of the remaining components in either system are known, ET can be computed. Allen R. et al. (1998) describe the energy balance as:

$$R_n - G - \lambda ET - H = 0 \quad (2-7)$$

where  $R_n$  = Net Radiation,

$G$  = Soil Heat Flux,

$\lambda ET$  = Latent Heat Flux, and

$H$  = Sensible Heat Flux.

All the above terms are in units of  $W\ m^{-2}$  and may be positive (i.e.,  $R_n$  is received by the surface and the other fluxes are directed away from the surface) or negative (i.e.,  $R_n$  is lost from the surface and the other fluxes are directed toward the surface). In other words, a positive  $R_n$  term indicates an input of energy into the surface system (the typical daytime condition), and positive values for all other terms indicate a loss from the surface system (Dingman 1994, Allen et al. 1998, Geiger et al. 2003). The magnitude and sign of the energy balance terms depend on several factors, such as the day of the year, the



time of day, and the condition of the atmosphere.  $R_n$ ,  $G$ , and  $H$  can all be measured directly, thus permitting the computation of the latent heat flux as a residual ET.

The mass transfer method is another technique to compute ET. It examines the movement of air parcels above a generally homogenous surface (Allen et al. 1998). These parcels, also known as eddies, transport water vapour, heat, and momentum to and from an evaporating surface (Dingman 1994, Allen et al. 1998, Geiger et al. 2003). Assuming that the transport coefficients for heat and momentum are the same as those for water vapour, then ET rate can be computed by calculating the positive vertical flux of water vapour from the evaporating surface (Dingman 1994, Allen et al. 1998, Geiger et al. 2003). This assessment is typically done using the Bowen Ratio equation (Allen et al. 1998). Additional information and details about the Bowen Ratio are beyond the scope of this text and the reader should consult other texts for a complete explanation (e.g. Houghton et al., 1985, Geiger et al., 2003).

Aside from lysimeters and mass transfer techniques, several other methods exist for measuring ET directly, such as eddy covariance (Massman et al., 1995; Scott et al., 2004, Testi et al., 2004) and scintillometric techniques (Daoo et al., 2004). However, these methods require very high-resolution equipment that is generally cost-prohibitive and labor intensive. Therefore such use is typically for research only (Qiu et al., 2002; Brotzge et al., 2003).

Measuring ET using a metal evaporation pan, typically about 1 meter in diameter, is the basic approach. This method is widely used for its reasonable accuracy. The ET values obtained are a function of other considerations. Evaporation pans work under the concept of specifying the loss of a known quantity of water through evaporation using a measuring tool, e.g. Vernier calliper, to identify changes in the exact level of water. Allen R. et al. (1998) noted, these pans do not measure transpiration, and therefore they must be adjusted using calibration coefficients to represent ET. In terms of calibrating the results, pan evaporation data must be adjusted downward using a pan coefficient. Pan evaporation data typically overestimates ET due to the nature of the pan. Evaporation

pans will often still evaporate at night due to the residual heat that is stored in the water of the pan. Additionally, there are differences in temperature, atmospheric turbulence, and humidity above the water in the pan that make evaporation rates different from that over a leaf surface. Finally, the stomata of a plant control the return of loss of water back to the atmosphere and act as a regulator. The water in an evaporation pan has no such limiting factor and is free to evaporate as much as the atmospheric conditions will allow (Allen et al. 1998, Barnett et al.1998). Pan coefficients can be derived experimentally or through various equations (e.g. Eagleman, 1967 ; Doorenbos et al., 1977; Jensen et al., 1997; Barnett N. et al., 1998; Grismer et al., 2002, Irmak et al., 2002).

Some limitations of evaporation pans include the cost of the pan and equipment (approximately £600 to £1500) and the amount of water required, which can be critical in arid locations or locations where running water is not available (Hansen et al.1980). Another substantial cost in the operation of evaporation pan stations is the cost of personnel to take daily measurements at the site. Despite these costs, however, pan measurement was still more cost-effective than an automated weather station until recently, but as the costs of automated weather stations have decreased over the years, the option of computing ET based on meteorological data has become more cost effective due to the elimination of recurring costs.

### **2.3.3 Evapotranspiration Numerical Models**

As can be understood from the above, direct ET measurement can be considered as a relatively intensive task. Basic measurements of the atmosphere, such as temperature, humidity, rainfall, wind, and solar radiation tend to be relatively easy to collect and are available at many locations. To overcome all of those limitations and difficulties and also to be able to develop databases for ungauged environments, a wide range of models have been developed to estimate ET. Many of these models have been derived through empirical and experimental work by Thornthwaite (1948), Blaney and Criddle (1950), Jensen and Haise (1963). However, other studies (e.g., Penman, 1948, Hargreaves,

1974, Hargreaves and Samani, 1985) developed equations through theoretical approaches that involve a combination of the energy budget and mass transfer methods. They are normally classified into three essential types: temperature based models, radiation based models and a combination of the two (Jensen et al., 1990, Dingman, 1994, Watson and Burnett, 1995). Temperature models only require measurements of air temperature as the sole meteorological input to the model (e.g., Thornthwaite, 1948, Doorenbos and Pruitt, 1977; Jensen et al., 1990). Radiation models (e.g., Turc, 1962, Doorenbos and Pruitt, 1977, Hargreaves and Samani, 1985) are typically designed to use some component of the energy budget concept and usually require some form of radiation measurement. Finally, combination models (e.g., Penman, 1948) combine elements from both the energy budget and mass transfer models to give very accurate results (Jensen et al., 1990). The Penman family of models is by far the most commonly used combination model. (Jensen et al., 1990, Allen et al., 1998). Moreover, scientists distinguish between three different aspects of evapotranspiration: reference, potential and actual evapotranspiration.

Reference Evapotranspiration ( $ET_r$ ) is a modification out of the concept of ET that provides a standard crop (a short, clipped grass) with an unlimited water supply so that a user can calculate maximum evaporative demand from that surface for a given day. This value, adjusted for a particular crop, is the consumptive use (or demand), and deficit represents that component of the consumptive use that goes unfilled, either by precipitation or by soil-moisture use, during the given time period. This deficit value is the amount of water that must be supplied through irrigation to meet the water demand of the crop (Dingman, 1994, Allen R. et al., 1998).

Potential Evapotranspiration ( $ET_p$ ) is another term used in the study of evapotranspiration. It is the amount of water that could evaporate and transpire under conditions with adequate precipitation and soil-moisture supply (Hansen et al., 1980; Watson et al., 1995). So the amount of water supplied that is actually available is not an issue. Therefore, there is potential for one of these approaches to be used to calculate

ET. The ET is usually higher in the summer, on sunny days, and at latitudes closest to the equator due to the aforementioned reasons. Hydrologists monitor potential evapotranspiration because it is useful in predicting the evapotranspiration of an area and as it usually peaks in the summer, it is helpful in monitoring potential drought situations.  $ET_p$  is combined with examination of the factors contributing to actual evapotranspiration and gives hydrologists an understanding of what an area's water budget will be after water is lost due to this process. As droughts are a concern for many areas around the globe, evapotranspiration is an important topic in the study of both physical and human geography.

Actual Evapotranspiration is another type of ET, also known as consumptive use or actual evapotranspiration (AET) (Watson and Burnett, 1995), and is the sum of the amount of water returned to the atmosphere through the processes of evaporation and transpiration. The evaporation component of ET comprises the return of water back to the atmosphere through direct evaporative loss from the soil surface, standing water (depression storage), and water on surfaces (intercepted water) such as leaves or roofs (Hansen et al., 1980).

Studies have been conducted with the aim of comparing different ET models and evaluating their performance either against observations (lysimetric/evaporation pan values) or nominating a well-known ET assessment model (normally Penman FAO56) as a study benchmark and evaluating some other models against it. In such studies, the ET models are either of the same type, a combination of different types, or randomly assigned.

Some relatively newly developed ET models include the 3T, Bowen Ratio, Temperature Difference (Idso et al., 1977, Monteith, 1965, Hatfield, 1985), and ENWATBAL (Evet and Lascano, 1993) models. All of those models are temperature models. They were compared alongside the well-known Penman-Monteith ET to observations obtained using the lysimetric standard method. A study was conducted on the Japanese climate by Qiu et al. (2002). The initial outcomes of the study suggested that the Penman-

Monteith model compared well to the lysimetric standard with a mean bias error (MAE) of 0.42 mm day<sup>-1</sup>.

Another study has tested the performance of five well-known models, the SCS (Blaney and Criddle, 1950), Jensen-Haise (Jensen and Haise, 1963), Canada specific model, Baier-Robertson (Baier and Robertson, 1965), the Blaney-Criddle model (Doorenbos and Pruitt 1977) and (Modified Penman (Hansen et al. 1980) for in Quebec (Barnett et al., 1998). Model outputs were compared to an evaporation pan located about 20 km from the meteorological station on a monthly and seasonal scale for 1995 and 1996. Results suggest that the best-fit model on the seasonal scale was that of Baier-Haise, which was not found to differ significantly from the corrected pan value. This study also suggested that the models (including the FAO Blaney-Criddle and the Modified Penman) would perform better than the pan data if each model were properly calibrated to the local climate (Hansen et al., 1998). This suggestion has been supported by Xu and Singh (2000), who tested several models (including Priestley-Taylor, Makkink, and Turc) against pan evaporation data in Switzerland. Those suggestions might enhance the possibility that every parameter of each model may require to be appropriately tuned for any location used with, especially if the model is not composed unequivocally for that location's climate. The two studies above might suffer from at least one possible defect; when using pan evaporation data as a reliable standard of measurement for ET, especially with the known errors in converting pan evaporation to ET (see Allen et al., 1998). Therefore, the calibration of relatively simple models against a more reliable reference (such as ET) may provide a useful means of estimating ET for agricultural and environmental applications.

Thornthwaite, Penman and Linacre ET models estimated evapotranspiration rates in four different West African climates and also have been compared between each other considering monthly based data from 1931-1960 from 34 stations. All three models were compared against evaporation pan data. When compared to evaporation data and the

Penman model, the Linacre model returned a higher correlation coefficient than the Thornthwaite method (Anyadike 1987).

Other studies that use the 56PM model as the standard include Utset et al. (2004), Gavin and Agnew (2004), and Irmak et al. (2003a, 2003b).

In this study, the choice of models has been based on model complexity. Models requiring relatively few variables are compared to those requiring many more variables, to assess whether the complexity does really matter when evaluating ET over an arid/semi-arid catchment like the Tigris basin in Iraq. Further investigations and details about the selected ET models are discussed in Chapter 5.

## **2.4 Evapo[transpi]ration Impacts on Rivers**

As detailed above, Evaporation and Transpiration can be considered as major outflow processes of water budgets for river catchments. River losses assessments need to consider several factors carefully, including water surfaces (e.g., wetland, pond, etc.), vegetation, or both. In addition, this issue may require an estimation of evaporation, transpiration, or both to estimate water level changes periodically. The combined effects of water surface evaporation, soil moisture evaporation, and plant (if there is any) transpiration for this system are often significant components of annual water budgets. Evaporation tends to lower water level in a river, pond or wetland over time, and evapotranspiration acts to dry out the soil before the next season. During wet the season, however, evaporation and evapotranspiration are typically not significant compared to precipitation, discharge and infiltration, and are often not considered in water budget calculations.

As discussed earlier, Evapotranspiration is a function of meteorological conditions, such as air temperature, wind speed, relative humidity, and solar radiation; and of evaporation/transpiration surface conditions (i.e., fraction of reflected incident sunlight), water temperature, water surface roughness, and water availability. One of the major

assumptions that should be made when calculating  $ET_p$  is the complete availability of the water that covers the entire basin. Therefore, water availability in the soil is negligible and the complexity associated with water stress does not need to be determined. Water stress can be minimised by irrigation systems. Reference plant ET is used to further simplify the determination of ET. Reference plant ET is the potential ET for a standard reference plant. The two most widely used reference plants are alfalfa and grass. Reference plant ET allows the impact of meteorological variables to be assessed using relatively constant plant conditions. Complexities related to time varying vegetal cover and water stress do not need to be considered. The conversion of reference plant ET to potential ET for different plant types is done using plant or crop factors.

Equation (2.8) represents the average annual ET for a catchment as a component of the water balance. The change in storage increases and decreases during the year; for many years, however, the net change is generally small. Therefore, for average annual ET,  $\Delta S \approx 0$ , and typically  $DS \approx 0$ . Equation (2.8) can be simplified to Equation (2.9), which indicates that the average annual ET is equal to the difference between the average annual precipitation and average annual runoff depth. For example, the Minnesota Department of Natural Resources publishes maps that allow the average annual precipitation depth and average annual runoff depth to be estimated for any location in Minnesota using this equation.

$$P - ET - RO - DS = \Delta S \quad (2-8)$$

where, P = Precipitation Depth

ET = Evapotranspiration

RO = Runoff Depth Measured at Stream or River Gauging Station

DS = Deep Seepage Depth

$\Delta S$  = Change in Stored Water Depth

Estimating evapotranspiration for any watershed:

$$ET = P - RO \quad (2-9)$$

where, P = Precipitation Depth

ET = Evapotranspiration

RO = Runoff Depth Measured at Stream or River Gauging Station

ET estimates usually are indirectly obtained from measured meteorological data or other variables. Energy balances provide a useful theoretical framework for converting the indirect measurements into ET estimates. Key energy terms are net radiation, sensible heat loss, and latent heat of ET. The daily energy balance for plant canopies and water bodies can be calculated using Equation (2-10), in which all energy terms have units of energy per unit area per day.

Daily Energy Balance for Plant Canopies and Water Bodies:

$$R_n = (L)ET + H_s \quad (2-10)$$

where, ET = Evapotranspiration Depth Per Day

L = Latent Heat of Vaporisation (approximately equal to 540 cal/cm<sup>3</sup>)

H<sub>s</sub> = Sensible Heat Loss

Pan evaporation techniques are widely used to measure evaporation from water surfaces and ET from soil and plant canopies (Farnsworth and Thompson 1982, Jensen et al. 1990). With these techniques, pans are filled with water and are placed on/or near the water body or within the standard plant canopy conditions. Evaporation rates from pans are used to estimate evaporation or reference plant ET. Pan evaporation rates are typically greater than actual lake evaporation and reference plant ET rates. Therefore, an adjustment factor, called a pan coefficient, is used and typically ranges between 0.64 and 0.81, as shown in Equation (2-11).

$$E = A \times C_{pan} \times ET_{pan} \quad (2-11)$$

where, E = Average Annual Evaporation

A = Area of Water Surface

C<sub>pan</sub> = Pan Coefficient

ET<sub>pan</sub> = Evapotranspiration Values Measured by Evaporation Pan



To conclude, if the change in water in the soil is known (through soil moisture change or runoff), any loss after water gain has been accounted for through precipitation or watering is attributed to ET (Watson et al., 1995; Allen R. et al., 1998). In addition, evapotranspiration can have a significant influence on the equilibrium of the water budget component for rivers and other water bodies existing in arid and semi-arid environments, and it has to be carefully estimated. Moreover, it is clear that the potential evapotranspiration can be calculated for unlimited water supply conditions. On the basis of this analysis, the ET method (Evaporation Pan) can be used to estimate the evapotranspiration and can represent the Evaporation from the water surface in the same time. This will be further explained in chapter 5. The resulting values from this process can generate the 'Evapo[transpi]ration' term which can be used to define the river water losses caused by the evaporation in areas such as the Tigris river basin which relies on the runoff as the only source of water for the river itself and the surrounding land.

## 2.5 Hydrodynamic Models

Hydrodynamic models are developed to represent water flow within the river channel routing water along the modelled river. This section summarises a review conducted by Pattison (2010) relating to the subject of how channel flow hydraulics are represented in models of different complexity.

There are three main groups of river hydrodynamic/routing models; (1) hydrological/storage methods; (2) convection-diffusion equation based methods; and (3) methods using the St. Venant equations. The simplest river routing methods are based on basic hydrological or storage principles and take no account of flow resistance.

1D hydraulic models have been used widely for several applications and purposes (Chow, 1959; Bhallamudi et al., 1991; van Niekerk et al., 1992). In such researches, this type of model can provide river flow/flood events in a less computationally demanding

manner (e.g. propagation and diffusion of the flood wave, Moussa et al., 1996). However, they cannot represent spatially complex topography, require accurate representation of the bed slope, and channel cross sections. The representation of the channel bathymetry is limited because, due to interpolation, features between cross-sections are not included. This means that representing floodplain storage can be problematic. Another assumption of these models is that lateral and vertical variations of flow characteristics are negligible. They are suitable for modelling in-bank flows (Knight et al., 1996), but inappropriate for overbank flows involving topographically complex floodplains. They are based on calculations including the roughness parameter that represents friction, form resistance, turbulence, floodplain topography and vegetation. The parameterisation of roughness is a fundamental aspect of hydraulic modelling. This is because the roughness of the channel and floodplain differ and therefore affect the conveyance of water in different ways (Hunter et al., 2005).

The most common parameter used to represent roughness is Manning's  $n$ , which combines the effect of numerous factors that cause flow resistance, including vegetation (Mason et al., 2003), channel planform, obstructions, stage-discharge relationship and sediment interactions. One of the main problems with using Manning's  $n$  is that it is constant over time, whilst in reality roughness effects are spatially and temporally variable (Holz et al., 1982).

1D models can be used to represent the floodplain, but do so with simplistic storage and routing approaches (Mizanur et al., 1995), using either an extension of channel cross sections or by using a parallel channel. However, these approaches require some a priori knowledge of flow paths (Bradbrook, 2006, Haestad et al., 2003, Thomas et al., 2007). Furthermore, important channel features, such as meanders, are only accounted for in the lumped friction parameter. Examples of 1D hydrodynamic models include HEC-RAS, MIKE 11 and ISIS-Flow etc. These are all industry-developed hydraulic models, with user interfaces that simulate steady and unsteady flows for single and dendritic channels, as

well as whole channel networks. They can also all represent channel structures, such as bridges, culverts and weirs.

ISIS-1D is the hydraulic model which has been selected to for this study for a few reasons. Firstly, there was no strong emphasis in any of the 1D models published in literature to represent the process of water losses propagation along a river precisely, and this is the process of interest of this thesis. Secondly, the data available for model validation only consists of gauged stage and discharge records; spatially distributed evaporation loss data is not available. This type of data is more compatible with 1D hydraulic models (Horritt et al., 2002). Finally, CH2MHILL (Model Developer) offered to supply "ISIS-1D (1000 Nodes)", which facilitated incorporating a large amount of river network features and elements. It could thus act as a good starting point for model refinement.

## **2.6 River Profile Development**

Alongside the required hydrological parameters which have to be available for the modelling, river physical characteristics need to be identified including catchment boundaries, catchment area and water surface area, drainage density, channel length, channel slope, river bed surface roughness, soil type, surrounding vegetation and river cross section properties. The availability and quality of those data are crucial to the success of the simulation as they have great impacts on the modelling of overland flow due to their influence on storage capacity and conveyance, both in the channel and on the floodplain (Ghavasieh et al., 2006, Mejia et al., 2011). Due to their effect on the flow dynamics of a channel and the considerable uncertainty in observed data. Many researches (e.g. Myers, 1991, Wolff et al., 1994, Woltemade et al., 1994, Johnson, 1996, Wohl, 1998, Anderson et al., 2006, Sholtes et al., 2011) have studied the impacts on flow attributed to these parameters including the cross-section elevation data.

One of the focus areas of this research is to assess whether a novel cross section and river profile development method can be used to provide an aid to building more adequate river profiles and to represent e.g. the Tigris River in the hydraulic model as it is one of the major boundary conditions of the model.

In the following sections, some of the well-known river profile measurement techniques are presented and analysed with regards to how adequate they are for the priority of river channel parameters used in hydrodynamic modelling:

### **2.6.1 Field Measurement**

The traditional depth collection technique (rod & rope) is still the most common technique used for collecting river depth and cross-sectional depth data. This technique is highlighted widely in literature. For example, the United States Geological Survey (USGS) in the National Handbook of Recommended Methods for water data acquisition report; Texas Water Resources Institute (under the USGS) in Techniques of Water-Resources Investigations report (Buchanan et al., 2010); and United States Department of Agriculture Forest Service in Stream Channel Reference Sites: An Illustrated Guide to Field Technique (Harrelson et al., 1994). This method of physically measuring the depth of the river with a surveying rod (stadia) and a weighted rope is the most commonly used and widely accepted method. Location and distance information is determined by surveying instruments and the river width is divided into increments for multiple cross-sectional depth measurements.

This method for getting river profiles, specifically cross-sectional river profiles, is expensive, time consuming, and requires a great deal of man-power and specialist tools and training. This method requires the conversion of hand collected data to digital format, which is time consuming and can cause errors. Several people are required to collect the depths; with the process being time and labor intensive. River surveyors wade across the river, carrying a handheld survey rod to measure water depth, or negotiate the cross-section by a boat guided by a cable marked with river width increments (US Geological

Survey, 1976). River depth can be difficult to measure and several bias or errors of physically measuring depth can occur. The largest issue arises due to the fact that most researchers choose to collect data in the warmer months, rather than during flood events or annual high flows, which severely limits the validity of data.

Sonar (sound navigation and ranging) has been used in military, commercial, and civilian applications to estimate river profiles. Military use of sonar began during World Wars I and II, and was primarily used for navigation, communication, and enemy detection (Urlick, 1975). Use of sonar in the commercial and civilian sectors has mostly been for navigation, to identify deeper water where ships can travel and to produce bed maps of the sea and large rivers.

The discovery of transduction, the conversion of electricity to sound and vice versa, was an integral step in development of the sonar systems used today. Sound is a pressure wave and the pressure change caused by sound on certain types of crystal pairs will cause an electrical charge across them, which is called piezoelectricity. Devices that accomplish this are referred to as transducers. Hydrophones are transducers that convert sound into electricity and projectors are transducers that convert electricity into sound. These are the two main parts of active sonar systems (Urlick, 1975).

Passive sonar systems listen to sounds generated by the target and is used for communication, telemetry, control applications and distance finding. Active sonar systems generate a sound (pulse) that bounces off the target, and the sound returns to the system as an echo. The amount of time it takes for the echo to return can be used to calculate the distance and is called echo-ranging (Urlick, 1975).

The operating range for the sonar is usually from 0.6- 450 m with a precision of 0.1 m. The portable sonar equipment system is mounted on a boat and used to record water depths directly onto a laptop computer. The boat is positioned at specific distances from the shore via a cable to acquire positioned depth measurements and data is collected from repeated cross-sectional passes. The boat mounted sonar system is evaluated to determine its precision and the precision of the field data collection technique.

The sonar system accuracy is normally assessed by comparing to traditional survey transect data from a regularly gauged site. The procedure usually proves to be a reliable, accurate, safe, quick, and relatively economical method to record river depths for stream studies. Flug et al. (1998) show that sonar systems can be an effective means of collecting river data. The use of sonar allows for faster, more intensive large scale river depth collection in short periods of time. River depths dynamically change over time can be assessed and georeferenced. Sonar allows for more frequent and easily repeatable surveys. However, it is not cost effective and is not utilised on a large scale to collect river data.

Fiscor (2005) conducted river mapping with a canoe based underwater video mapping system (UVMS) for the Big South Fork National River and Recreation Area (BISO). Fiscor used the Lowrance LMS-350A sonar unit for depth measurement and found during simple tests that it reads 0.18 m (0.6ft) greater than the actual depth when in fresh water and is unreliable at depths less than 0.5 m (1.6 ft). Multiple river reaches were categorised by their average and maximum depth, flow characteristics, and substrate composition. Depth maps were created in GIS to assist in creating the required maps.

McConkey et al. (2011) utilised a canoe and kayak-based UVMS for that same river (BISO). The system collected georeferenced sonar-depth data that was used to calculate rugosity. The GPS and depth point-to-point data are used for the rugosity calculations and averaged over 100 data points. McConkey defines rugosity as “a measure of variations in height amplitude of a surface. It is commonly measured by the length of a chain conforming to a rough surface divided by the straight-line length between the start and ends of the chain. The rugosity was used as an indicator for identifying large boulder fields with 67% accuracy. Depth and rugosity maps were created for the BISO system.

This research uses some 14 sets of river cross section data that have been measured using one or more of the above techniques. They were measured at different locations

along the Tigris River. They can be considered a great asset for model calibration and validation.

### **2.6.2 River Stream Delineating Using DEMs**

A more recent method that is widely used to create topographical profiles for land and streams is called LiDAR. LIDAR, which stands for Light Detection and Ranging, is a remote sensing method that uses light in the form of a pulsed laser to measure ranges (variable distances) to the Earth. These light pulses, combined with other data recorded by the airborne system, generate precise, three-dimensional information about the shape of the Earth and its surface characteristics.

A LIDAR instrument principally consists of a laser, a scanner, and a specialised GPS receiver. Airplanes and helicopters are the most commonly used platforms for acquiring LIDAR data over broad areas. Two types of LIDAR are topographic and bathymetric. Topographic LIDAR typically uses a near-infrared laser to map the land, while bathymetric lidar uses water-penetrating green light to measure seafloor and riverbed elevations as well. LIDAR systems allow scientists and mapping professionals to examine both natural and manmade environments with accuracy, precision, and flexibility.

NOAA scientists use LIDAR to produce more accurate shoreline maps, make digital elevation models for use in geographic information systems, to assist in emergency response operations, and in many other applications.

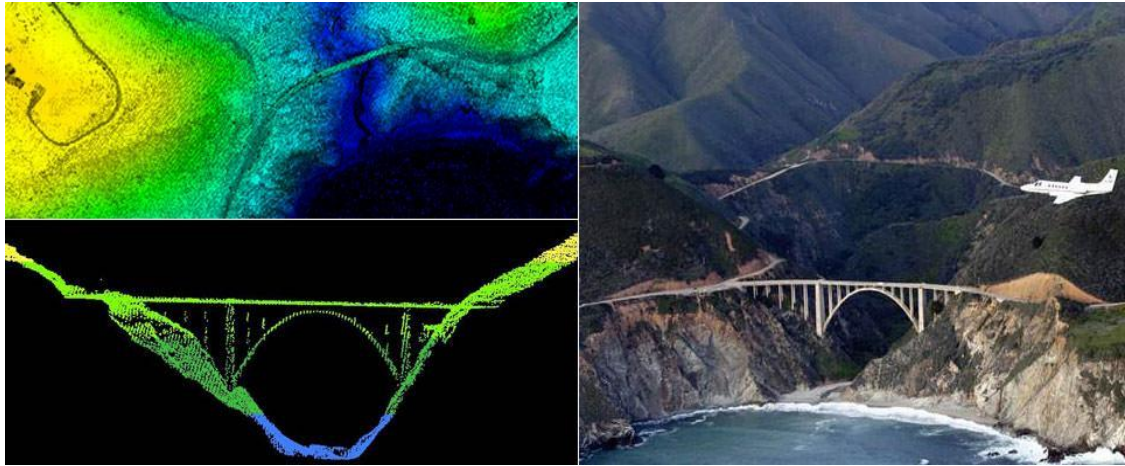


Figure 2.2: NOAA survey aircraft (top) over Bixby Bridge in Big Sur, Calif using LIDAR data. a top-down (bottom left) and profile view of Bixby Bridge.

LiDAR systems are used in many researches to determine the water depths of the river, for example, Flug et al. (1998), Marcus et al. (2003), Kinzel et al. (2007) and Charlton et al. (2003). Kinzel et al. (2007) in particular, evaluated LiDAR for the collection of shallow depths (< 1.0 m) in a braided, sand-bedded river.

Marcus and Fonstad (2008) argued that LiDAR does not measure the depth, but estimates it using several ways such as multiple regression equations or models based on physically collected data.

Marcus et al. (2003) evaluated the potential of 1-m resolution, 128-band hyperspectral imagery available for mapping depths of streams in the northern Yellowstone region (middle of USA). A stepwise multiple regression was used to determine the relationship strength between depth and spectral reflectance. Equations were developed for estimating depths throughout the stream. Depth was isolated as the primary driver of observed spectral reflectance on the images, so depth could be estimated. This technique of measuring depths generated  $R^2$  values ranging from 28% for runs and glides in third order reaches to 99% for glides in fifth order reaches (Marcus et al., 2003). The less accurate depth estimates obtained from smaller streams are attributed to the increase in a wide range of depths and surface turbulences on a single pixel. The authors of that research concluded that the high accuracies achieved indicate that high spatial



resolution hyperspectral imagery can be a powerful tool for watershed-wide mapping and modelling of streams. However, the use of this imagery for stream mapping is limited by the need for clear water, no tree cover obscuring the stream, and the availability of airborne hyperspectral sensors. The aerial imagery in the study was not georeferenced and would be an obstacle if wanting to integrate the classification maps into GIS analyses with other data layers.

The National Aeronautics and Space Administration's Experimental Advanced Airborne Research LiDAR (NASA EAARL) was tested due to its advances with water penetrating capabilities. The study was conducted on two river reaches in Nebraska in 2002 and 2005. The LiDAR measurements were computed with a terrestrial algorithm and were compared to ground-truth GPS point measurements. The root mean square errors of the depth measurements taken on submerged sand in two different areas were 0.18m and 0.24m. These measurements were deeper than the actual depth. Because the LiDAR's laser pulse travels slower in water (0.11 m/ns) than in air (0.15 m/ns), the depth has to be calculated as 0.04 m/ns deeper or 1.36 m for every 1 m of actual depth if the pulse is assumed to be through air. This is why an algorithm was developed for the bathymetric (underwater depth) data. LiDAR's ability to collect bathymetry data is limited by the visibility, clarity, and depth of the water (Kinzel et al., 2007).

The LiDAR technique requires specialised equipment that fly over the river in favourable weather, which obviously can be very expensive. Marcus and Fonstad (2007) assert that most of the studies that use these technologies are proof-of-concept at local or reach scales and the use of the technology needs to be expanded.

In general, this technique is still rarely used because of the huge financial requirements as well as data bias that can occur when individuals make a conscious or unconscious choice to not wade into deeper water to collect depth measurements. Simple errors of leaning on measuring poles for stability when collecting depth measurements can also occur. The LiDAR data are still limited by river visibility from the air and shadows. The technology has limitations in collecting deeper depths because light must penetrate to

the bottom of the stream. The accuracy of these techniques is still very variable (Marcus and Fonstad, 2008).

The majority of drought/flood prone places around the world do not have the ability to benefit from the development of state-of-the-art inundation models given that LiDAR derived terrain data and SAR images are usually prohibitively expensive (Sanyal et al., 2004). This scenario leaves most of the studies with the option of using freely available DEMs. The Shuttle Radar Topography Mission (SRTM) DEM or the Advanced Spaceborne Thermal Emission and Reflection Radiometer (ASTER) Global Digital Elevation Model (GDEM) define the model geometry and the cloud-free optical imagery of water as the primary source of distributed observed data for model calibration and validation.

Despite the fact that the potential usage of the SRTM DEM in flood and inundation modelling studies is demonstrated in several occasions (e.g. Sandra 2007; Manfreda, 2011) and its data reliability is highlighted to identify flood-prone regions with a modified topographic index, it is well known that these terrain data contain considerable noise/error (Bhang et al., 2007). A global performance assessment study of the SRTM data by Rodriguez et al. (2006) revealed an absolute height error of 6.2 m, 5.6 m and 6.2 m for Eurasia, Africa and South America respectively. Since, radars' bands used in the SRTM instrument do not penetrate the canopy the SRTM DEM captured the tree top elevation rather than the surface at any place with dense foliage.

The Advanced Spaceborne Thermal Emission and Reflection Radiometer Global Digital Elevation Model (ASTER GDEM), in spite of having a higher spatial resolution of 30 m, is reported to have significant anomalies and much higher RMSE than the SRTM DEM when compared with LiDAR derived elevation data derived from ICESat (Reuter et al., 2009). While evaluating the recently available second version of the ASTER GDEM, Slater et al. (2011) commented that the data have an effective resolution that is lower than 30 m and contain systematic bias in comparison to the other reference DEMs and ground control points. Hence, both the SRTM and GDEM products are not really suitable

for inundation modelling, at least in the forms that are available for download. Bates (2012) did in fact note that the purpose of creating these global data sets most probably did not include inundation modelling.

Due to the high cost of acquiring radar imagery, there are very few requests for data acquisition in developing nations to capture flood events on the ground. Consequently, for any river basin under study outside industrialised countries there is very limited chance of finding a flood scene in the archive of radar data providers. In the absence of radar imagery, optical imagery has been successfully used on many occasions for delineating the flood extent (Wang et al., 2002, Sanyal and Lu, 2005, Jain et al., 2005, Ip et al., 2006). The Landsat archive, which is accessible at no cost, contains numerous cloud-free scenes of inundated surface that can be quite valuable for inundation modelling in the developing world.

In spite of all the constraints mentioned above there is an increasing trend of utilising freely available terrain data for hydraulic modelling of streamflow. Due to the coarse nature of the available terrain data (e.g. SRTM DEM), the majority of these studies has been undertaken at continental scale. For example, Yamazaki et al. (2012a) applied a global river model, namely CaMa-Flood (Yamazaki et al., 2011), to model the seasonal cycles of water level elevations in the Amazon River using the SRTM DEM as the terrain input and the simulated water surface elevations compared with Envisat altimetry.

Development and application of flow routing and inundation models in data sparse regions of the world is mostly confined to very large continental river basins such as the Amazon (da Paz et al., 2011), Congo (Jung et al., 2010), Niger (Neal et al., 2012a) and Ob (Biancamaria et al., 2009). The abovementioned studies are primarily engaged in simulating seasonal or annual cycles of river discharge and water level or even water budget and flooding pattern of large wetlands of the Niger River (Zahera et al., 2011) and the Nile Basin (Petersen and Fohrer, 2010). A number of novel attempts were reported to deal with the low resolution of the freely available DEMs that were used in these investigations. Paiva et al. (2011) developed a GIS-based algorithm that includes

extraction of river cross-sections, delineation of river networks and catchments from the SRTM DEM and used geomorphic principles to estimate the river width and depth. Yamazaki et al. (2012b) proposed a pit removal strategy to reduce the anomalies in the SRTM data arising from vegetation canopy and sub-pixel structure and reported an improvement in the simulated water surface elevation. However, its DEMs needed to be adjusted in terms of agreement with the observed records. Neal et al. (2012a) demonstrated how a subgrid scale representation of a channelised portion of the flow can help to simulate streamflow in narrow channels that cannot be captured in the low resolution global DEMs. However, the authors of this research stated that model still needs measurements of channel depth and width to derive the empirical relationship for estimating channel-bed elevation from bank elevation and channel width.

Few studies have been recorded which take the SRTM in to account as a means of extracting River cross sections as an alternative when other sources are unfeasible to use such as (Woldemichael et al., 2010, Patro et al., 2009).

Virtual Globes, such as Google Earth (GE) are popular providers of desktop-based 3D virtual environments. Virtual environments are defined as a visualisation of part of the whole world based on a virtual globe technology. The development of the virtual globes of today's providers builds upon a history of visionaries and early technologies, most of which no longer exist. 3D virtual environments often consist of a digital elevation model and high-resolution imagery. Based on virtual globe technology a global reference system is provided making them suitable for the visualisation of transnational as well as local geodata sets.

GE also has DEMs imbedded within it as it is one of GE's competitive features. Those DEMs have been used in several studies with different applications. They were also used within the hydrologic sector to generate topographic data to map catchments and watersheds (Rusli; et al., 2012, McInnes et al., 2011). However, the source of its digital elevation models (DEMs) and nor its resolution are known. Others state that Google Earth uses digital elevation model (DEM) data collected by NASA's Shuttle Radar

Topography Mission (SRTM) enabling 3D view of the whole earth, but the authors of this study could not find a concrete reference for such a statement. In fact, some studies tried to investigate Google Earth's DEM resolution and justify the usage of the extracted data from it by doing a comparison analysis between it and other well-known DEM data sets (Hoffmann et al., 2010). Others went further and preferred to ask Google Help about this issue, but the response was negative.

The Google Earth Blog reported in an article titled 'Google Earth More Realistic with Better Terrain' published in June 6<sup>th</sup> 2007 that an update with high resolution 3D terrain (DEM) has been released by Google Earth with 10m world-wide resolution. An investigation carried out by the authors led to the discovery that this update was released on 2nd of June 2007. That version covers only the following parts of the earth: parts of Greenland and Antarctica – some parts of Canada (area around Toronto), Catalonia in Spain, the State of Alabama, St. Paul, Minnesota, Puerto Rico, Iran, New Zealand and parts of Russia.

In this study, it has been decided to investigate whether there is a possibility to generate reliable river cross sections at the Tigris to form a river profile. That could be another challenge for GE to face as until now this can be done either by using high-resolution Lidar data sets (no such data over the study region) or laser dataset (very expensive with health and safety limitations). Using GE DEMs to the traditional or those unfeasible methods.

GE is a promising alternative to provide good DEMs. There is a good potential for it be utilised to get more details, at least for floodplain cross sections that cannot be provided by the echo sounder data (observed). GE also presents a great opportunity to walk through the whole river to appoint critical locations, e.g. river bends, dams, bridges, etc., "on the fly". Dragging a path in a desired location, e.g. across a river within GE, that gives an elevation profile. To extract, digitalise and analyse the resulted elevation profile, a GPS location, altitude and time route editor is utilised. This method is used in the present study to provide the required Tigris river profile with reasonable accuracy.

## 2.7 Chapter Conclusion & Research Questions

Efficient water resources management helps to develop a more sustainable environment. Typical water balance studies for a basin in general include determination of the inflows or sources (rainfall and incoming streamflow) and outflows or sinks (evapotranspiration, diversion, and river discharge). Only a few studies around the world have considered evapotranspiration as one of the major sources of water losses in rivers, and to the best of our knowledge, there is no existing study that considers the impact of the climate change when assessing evapotranspiration in the Tigris River watershed in Iraq. However, there are numerous studies comparing the performance of ET models against either observations or other reputable ET model(s). Other studies have conducted comparison analysis studies in some locations within Iraq. However, in all of these studies, it was not clear how the models were selected. The methodologies followed were either complex or ambiguous; also, no published studies have examined the spatial variability of ET models across the entire Tigris watershed, a state with a great northwest to southeast gradient in temperature and precipitation.

The strengths and weaknesses of downscaling methods are discussed widely in the literature for temperature and precipitation as climate change indicators for different regions and seasons. Temperature is often used as a variable for example to assess and predict evapotranspiration. However, little attention is given to the choice of downscaling method when examining other climatic variables, e.g. Evapotranspiration, directly. Similarly, little has been done to assess the impacts of these variables on hydrological systems.

An adequate river profile representation with an accurate description of the model parameters is required to predict the flow magnitude and water levels along the reach accurately. These are essential requirements for the successful implementation of water quantities management plans and assessments. Tools are developed to extract spatial features which are useful for hydraulic models utilising different approaches. However,

obtaining detailed topographical data for a river basin is often difficult task as the process involves an expensive and time consuming survey campaign (ground or airborne) and painstaking post-processing of the survey data, and this is especially the case for developing countries. Many studies have dealt with topographical data scarcity in river modelling. Most of them rely on the integration of GIS with digital elevation models (DEM) obtained from remote sensing satellites or other globally available data sets. One of the aims for this study is to investigate the suitability of data which can be extracted from free sources that provide the required river cross section profiles along with other beneficial details such as hydraulic structures, algae/plants, island locations and other characteristics along the river. With the obtained river cross-section data, flood simulation and analysis was carried out on large parts of the Tigris River, Iraq, using the ISIS-1D modelling software package.

Based on all above, the following questions are raised:

1. Which one of the well-known ET models best represents the evapotranspiration rates for rivers located in arid and semi-arid catchments with severe lack of data? (Addressed in chapter 2 & 5).
2. Is it possible to study the past, present and future ET trends for rivers located in arid and semi-arid catchments with severe lack of data? (Addressed in chapter 2 & 5).
3. Do the available weather simulation and forecast models such as SDSM have the ability to predict future ET trends for rivers located in arid and semi-arid catchments with severe lack of data? (Addressed in chapter 2 & 5).
4. Is Google Earth capable of generating accurate river cross sections in areas with severe lack of data? (Addressed in chapter 2 & 6).
5. Is ISIS-1D able to provide accurate river losses estimation for long rivers? (Addressed in chapter 6).
6. Are any of the available water balance models capable of adequately highlighting water losses for rivers located in arid and semi-arid catchments with severe lack of data? (Addressed in chapter 2 & 7).

## Chapter Three: Area of Study and Data Availability

The main aim of this chapter is to describe the available data used to study the water quantity of the Tigris river in Iraq accurately. This chapter also identifies the difficulties experienced when the data were collected, and suggests some strategies to overcome these difficulties. The following sections describe the Tigris River catchment and provide a brief background of the physical aspects of the catchment, for example, geography, climate, hydrology, topography, and area of utilisation/spread. The data is needed to develop an overview of the hydrological processes in the catchment in order to conceptualise how the system (river network) should be modelled in sufficient detail to meet the requirements specified in the research objectives. Thus, the following points are taken into consideration: (1) the spatial and temporal detail required for the model(s), (2) the system dynamics, (3) boundary conditions, and (4) how the employed model(s) parameters can be determined from the available data.

### 3.1 Location, Topography and Climate

This study considers the part of the Tigris that is formed downstream of the Mosul Dam all the way to Basra in Iraq (Figure 3.1 and appendix 2). The river in that region flows through in hilly countryside with villages and cities up to 350m above the sea level close to Mosul. This area forms the upstream section of the area of interest to this study. There are four main tributaries draining into the Tigris, as shown in Figure 3.2, Greater Zab, which originates in Turkey and it is considered as the largest tributary supplying the Tigris River. Little Zab originates in Iran, not far from the Iraqi border. Further down the main Tigris reach, the Adhaim is an intermittent stream located entirely inside Iraq. North of Baghdad, a barrage diverts water from the Tigris to the Euphrates via the Tharthar Canal. Downstream of Baghdad, the Tigris flows through a flat landscape for 343 km, where it receives water from the shared Iranian-Iraqi Diyala River and several valleys before forming the Shatt al Arab at the confluence with the Euphrates near the city of



Qurnah (BGR, 2013). The Tigris River basin has in total about 371,000 km<sup>2</sup> shared between Turkey, Syria, Iraq and Iran, the basin riparian countries. Iraq makes up the second largest area after Iran by about 38% from the total basin area (Partow, 2001).

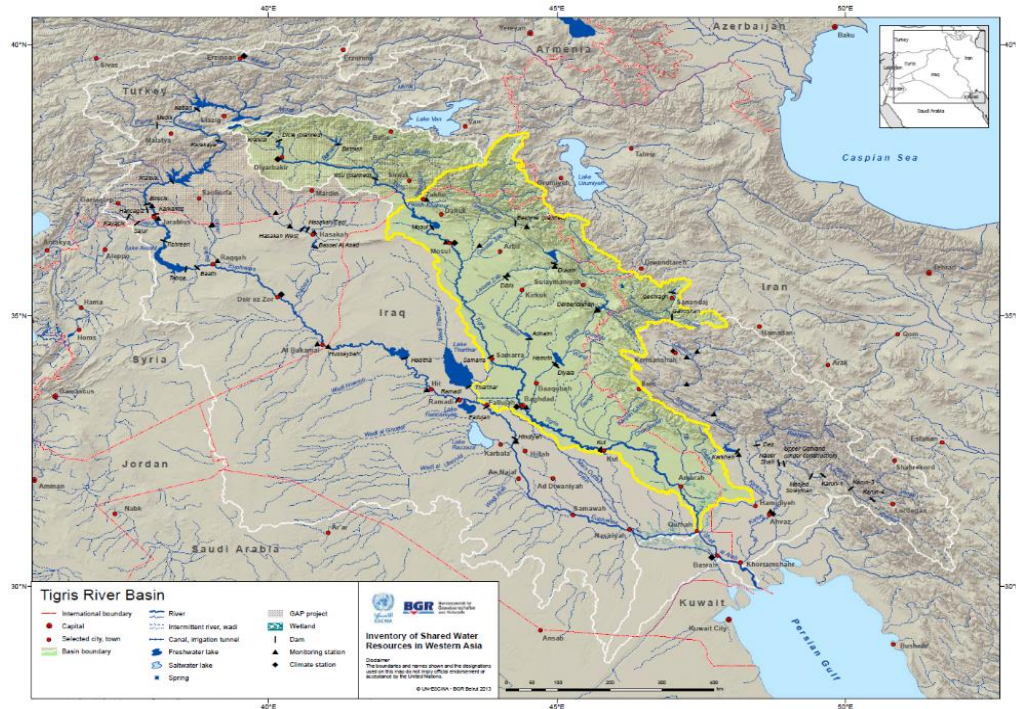


Figure 3.1: (and appendix 2) The entire Tigris-Euphrates Rivers Basin is highlighted by white line. The map shows the mean annual precipitation distribution for the Tigris River Basin only as well as this research's case study area which is highlighted in yellow. Source: (BGR, 2013) and edited by the author.

The water losses of the selected part of the basin pose a serious threat to the livelihood of the citizens living in that region. Topographically, the Tigris basin in the upstream region is characterised by the mountains of Mosul and their intervening valleys, and low-lying coastal plains further downstream before it flows into the Persian Gulf. The following table shows the names of the most important multi-purpose stations located along the river as well as their locations and their elevations above the sea level:

Table 3.1: Main Gauging Stations Locations and Elevations above the Sea in Iraq.

No.	Station	Region	Location	Elevation above the sea
1	Mosul	North	36 34 00° N, 43 13 00° E	223m
2	Baghdad	Middle	33 32 50° N, 44 42 20° E	34m
3	Basra	South	30 50 00° N, 47 81 67° E	5m

The climate in the Tigris Basin ranges from semi-humid in the headwaters of the north, to semi-arid close to the confluence with the Euphrates in southern Iraq. Mean annual basin precipitation is estimated to be approximately 335 mm (New et al., 2002). However, values of 800 and 150 mm have been registered in the upper and lower parts respectively (Kibaroglu, 2007). There is a noticeable shift from a more humid climate to an increasingly hot and dry climate from north to south. Mean precipitation in the basin mostly occurs between November and April, with snowfall in the mountains from January to March. Given the semi-arid to arid climate in the lowlands of Iraq, evapotranspiration causes considerable water loss in the Mesopotamian region. Air temperatures in the Tigris Basin range from 2°C in winter in Mosul's Highlands to 52°C in summer in Basra (New et al., 2002).

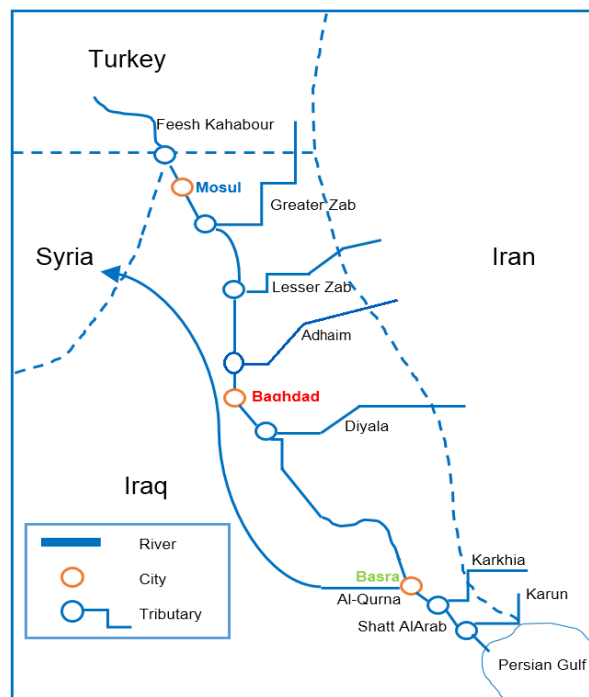


Figure 3.2.: Sketch of Tigris River System showing the main tributaries. Developed by the author.

### 3.2 Available Data for Tigris River

The following sections highlight the main sources of data that were used for this research. The validity of the data sources along with sources of uncertainty are also discussed.

### 3.2.1 Terrain Surface Representation using DEMs

Digital Elevation Models (DEMs) from different sources were identified for use in this study. It is important to select the best terrain surface representation of the studied area. The DEMs are used to identify the catchment boundary delineation and the drainage network, and therefore have significant influence on the assessment of the watershed's hydrological characteristics. DEMs as a topographical data are normally used to obtain necessary information pertaining to the elevations of points of interest, flow convergence and divergence, which are some of the important factors that influence the runoff velocity, surface roughness, and slope angle and length.

DEMs are normally derived from remote sensing technology, spot levels and/or contour maps. DEMs have been used in previous studies to substitute measured data and have been used to assess hydraulic and metrological characteristics in many parts of the world where there is a lack of necessary data (Sulebak, 2000). There is a lack of surface elevation data for the Tigris catchment, so it was decided to investigate several sources of DEMs to assess their viability and feasibility in terms of getting better terrain features. The Shuttle Radar Topography Mission (SRTM) digital elevation data, namely SRTM 90m Digital Elevation Database v4.1, was downloaded from the Consultative Group for International Agricultural Research (CGIAR) website on Oct. 2012, and The Advanced Space-borne Thermal Emission and Reflection Radiometer (ASTER) Global Digital Elevation Model (GDEM) Version 2.1 arc-second (30m) was downloaded from the USGS Earth Explorer website. Both data sets are supplied by NASA and were obtained for use in the present research study.

Google Earth was also considered as a source of terrain data. Results of preliminary tests were encouraging and suggested that it could be a viable alternative data source when there is a need to study rivers located in developing countries where there is a severe lack of information.

### 3.2.2 Observed Meteorological Data

A set of observed (climatic and meteorological) data which spans from 1959 to 1970 was obtained for this research. This data set has missing data values for the period from May-1966 until January-1969. This data set includes maximum and minimum temperature and relative humidity, surface wind speed and direction, atmospheric pressure, sunshine durations, precipitation, dew point, vapour pressure, soil temperatures for several locations in Iraq including Mosul, Baghdad and Basra. All of these data can be used as a cornerstone to provide reasonable estimates for the spatial and temporal distribution of the evapotranspiration within the basin. This data set also includes Pan Class A evaporation measurements for the period 1966 to the end of 1970, which was used to understand the evapotranspiration trends in this catchment.

The data set described above was provided early in the research program by the Ministry of Water Resources, Iraq. It was implemented by the Climatological Department in the Directorate General of Civil Aviation, Ministry of Communications, Baghdad.

As mentioned above, the obtained set of data has several gaps. Furthermore, the rest of the set is poorly documented, badly typed, poorly laid out and sometimes not even readable (Figure 3.3).

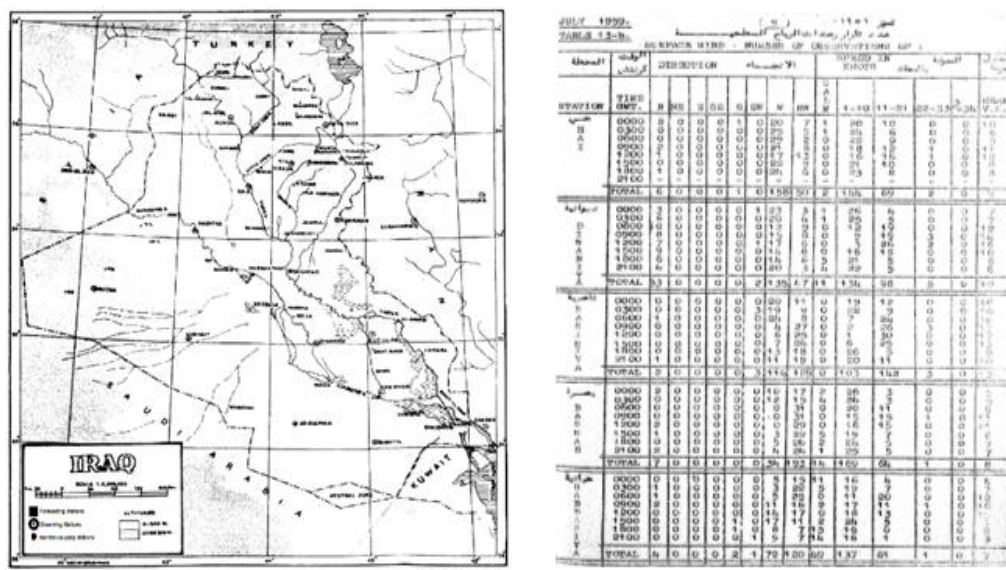


Figure 3.3: A sample of the data set available (1969-80), including a map representing Iraq and a list of surface wind speed measurements for some stations located in Tigris Basin.

The data was rearranged and digitalised during the research. Additionally, another data set was provided for this research by the Iraqi Ministry of Water Resources and the Iraqi Environmental Ministry. The new data set includes all the material necessary to develop a considerable comparison of evapotranspiration models and to implement trend analysis based on relatively comprehensive historical data. The new data set, which extends from 1970 to 2005, including some missing values caused by the Gulf War in 1991 and the most recent war in 2003, was based on monthly averages for most of the standard metrological variables. These data are well maintained, organised, and digitalised. The data sets discussed above were considered to be sufficient for model calibration and validation purposes. This section reviews the changes of the main meteorological variables used to develop ET models during the study period from 1970 until 2000. In particular, Maximum and minimum temperature, relative humidity, wind speed solar radiation, alongside with the observed ET data using Pan class (A) and precipitation are reviewed. It should be noted that, these variables are observations obtained from three gauging stations (Mosul, Baghdad and Basra) along the examined Tigris reach, provided by the Iraqi water resources ministry to fulfil this study's requirements as mentioned in chapter one and three. The purpose of establishing this section is to understand the spatial and temporal distribution of the meteorological variables and how do they (if at all) affect the ET sensitivity over the Tigris.

### 3.2.2.1 Average Annual Temperatures:

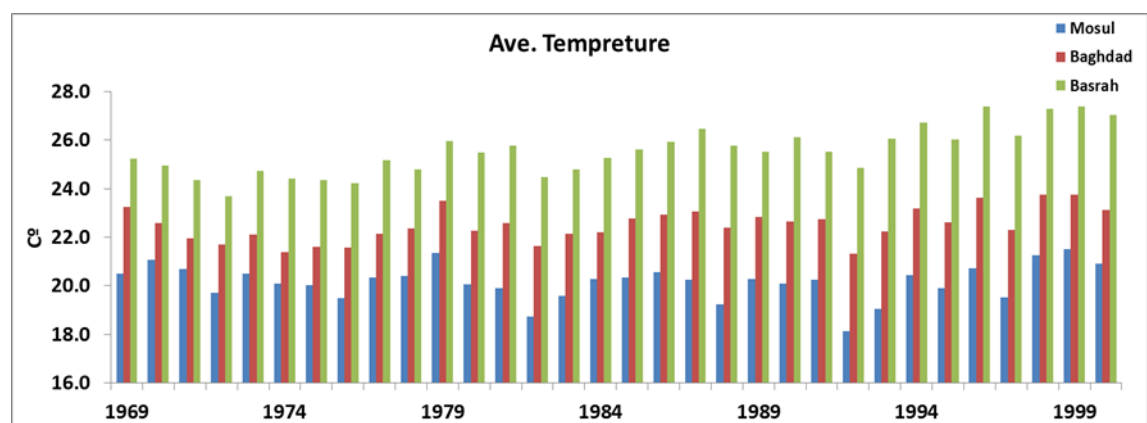


Figure 3.4: Average annual temperature recorded over The Tigris in Iraq

Figure 3.4 represents the annual averages of the temperature data sets calculated from other monthly average data sets obtained from gauging stations along the Tigris. From data distribution over the study period, Basra takes the lead because of its location in the south of Iraq, which well known of its warm climate. The mean temperatures average over the study period recorded about 26 °C and it increased about 6% over the period of study. The hottest season (August – 2000) recorded 48.9 °C. The mean monthly maximum temperature has recorded 32.2 °C. The mean temperature in Baghdad, the middle region recorded relatively lower mean temperature over the period of study, it was about 22.3 and increased by 1.5%. The northern region (Mosul gauging station) recorded the lowest mean average temperature over the time, and that could be because naturally because its location in the north. It should be noted that, the mean temperature changing rare for the northern region remain relatively constant over the time.

### 3.2.2.2 Relative Humidity:

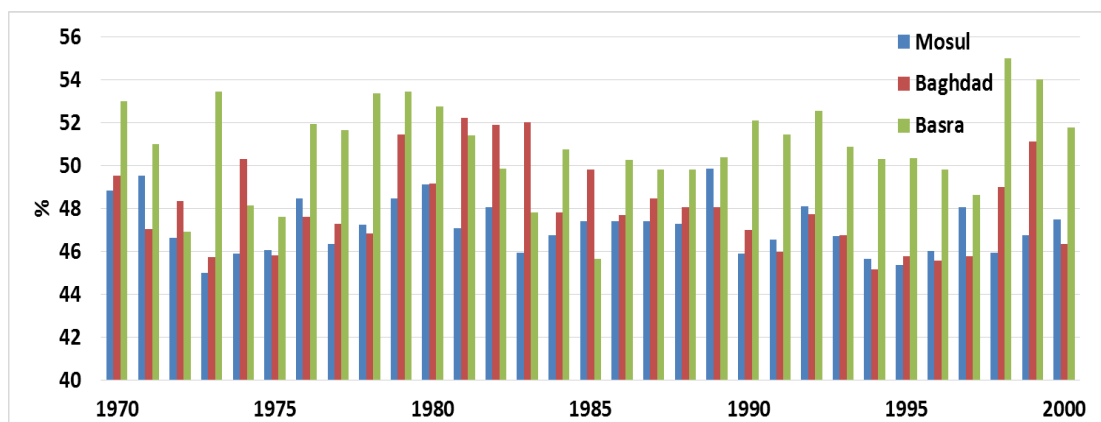


Figure 3.6: Average annual relative humidity recorded over The Tigris in Iraq

Figure 3.5 represents the annual averages of the relative humidity data sets calculated from monthly average data sets obtained from gauging stations along the Tigris. From data distribution over the study period, Basra once again recorded relatively higher relative humidity, that could be probably because of its location closer to the Persian gulf as well as the agricultural density and the wide marsh areas in this region.



The mean relative humidity recorded about 55% and it increased about 1% over the period of study. 100% relative humidity value was recorded several times, especially during wet season (e.g. February – 1991 and December 1999) The mean relative humidity in Baghdad, the middle region recorded relatively lower, compare it to the southern region, over the period of study, it was about 48%. The northern region (Mosul gauging station) recorded the lowest mean average relative humidity over the time, and that could be because naturally because its location in the north. It should be noted that, the mean relative humidity changing rare for the northern region remain relatively constant over the time.

### 3.2.2.3 Wind Speed:

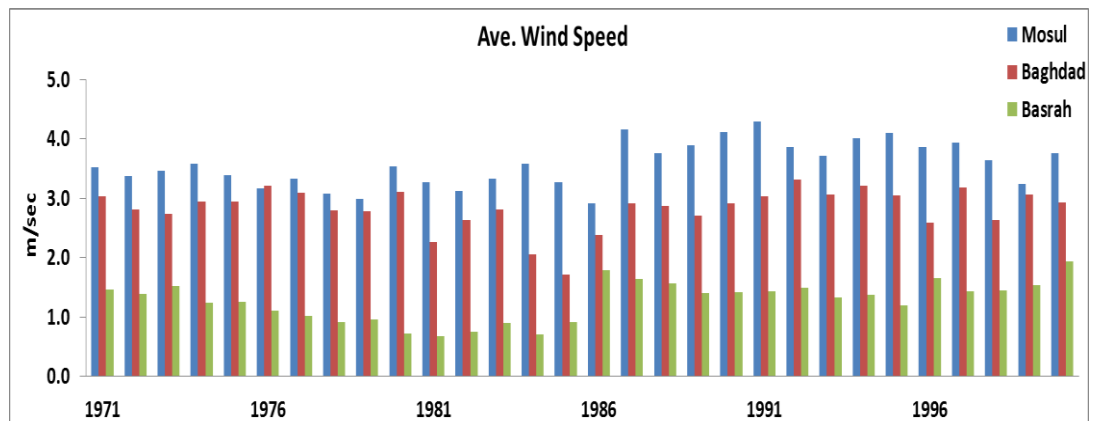


Figure 3.6: Average annual wind speed recorded over The Tigris in Iraq

Figure 3.6 represents the annual averages of the wind speed data sets calculated from monthly average data sets obtained from gauging stations along the Tigris. From data distribution over the study period, Basra now recorded the lowest wind speed rare in comparison to the other regions. The northern region is dominating now. It could probable because of it longitude/latitude and also could be because of the height above the sea (Mosul City – 260m in comparison to Basra City – 5m).

The mean wind speed recorded about 3.5 m/sec and it increased about 7.1% over the period of study. The mean wind speed in Baghdad, the middle region record was lower,

compare it to the northern region, it was about 2.8 m/sec. The southern region (Basra gauging station) recorded the lowest mean average wind speed over the time (1.6m/sec).

### 3.2.2.4 Solar Radiation:

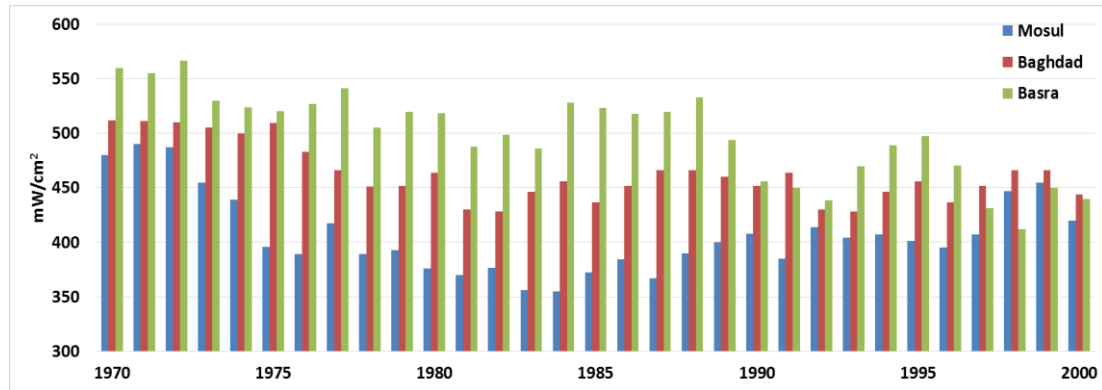


Figure 3.7: Average annual incoming solar radiation recorded over The Tigris in Iraq

Figure 3.4 represents the annual averages of the incoming solar radiation data sets calculated from monthly average data sets obtained from gauging stations along the Tigris. From data distribution over the study period, Mosul now recorded the lowest in comparison to the other regions. The mean solar radiation recorded about 512 mW/cm<sup>2</sup> and it decreased about 17.1% over the period of study.

### 3.2.2.5 Atmospheric Pressure:

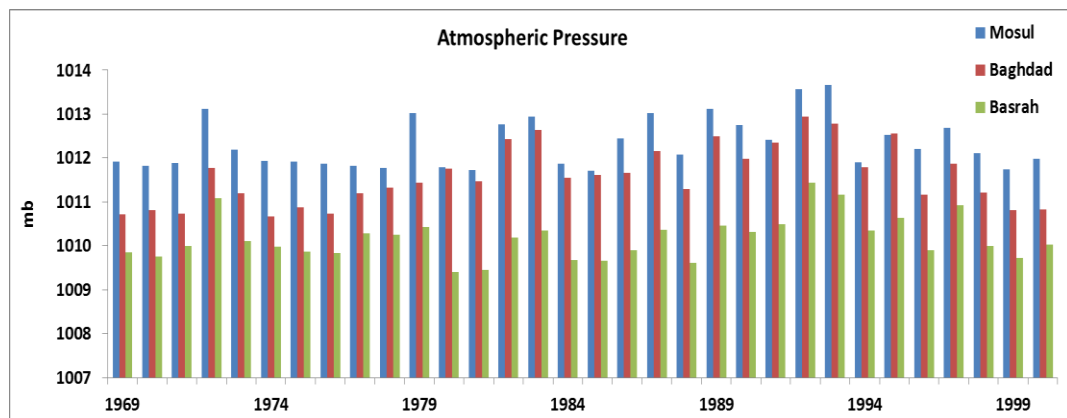


Figure 3.8: Average annual atmospheric pressure recorded over The Tigris in Iraq

Figure 3.8 represents the annual averages of the atmospheric pressure data sets calculated from monthly average data sets obtained from gauging stations along the Tigris. From data distribution over the study period, Mosul recorded the highest in



comparison to the other regions. It could probable, once again because of its longitude/latitude and also could be because of the height above the. The southern region is dominating now. The mean solar radiation recorded about 1013.8 mb and it increased about 8.3% over the period of study.

### **3.2.3 Observed Tigris River Flow and Water Level Data**

River discharge and water level measurements are needed as boundary conditions to run the hydraulic model. Considerable water level records have been provided by the Ministry of Water Resources in Iraq (MoWR) for different locations along the Tigris, most importantly the very downstream ones, as they play a multi-faceted role because they are used to run the hydraulic model as another prerequisite element, for calibration and validation purposes, and also to measure the total river losses.

Historical water flow records were obtained from Saleh's report (2010) as it provides a useful summary of stream-flow characteristics for all long-term stream-flow gauging stations in Iraq including stream-gauging stations at different locations along the Tigris River. It details each stream-flow gauging station as well as providing maximum, minimum, and mean discharge records. Historical records were found in this report from the 1930s to 2005. However, the discharge records in this report based on monthly averages and involve large sections of missing data.

### **3.2.4 Observed River Cross-Section Data**

A successful river study requires an understanding of river profile features. Achieving that depends on how much data, and how many tools, are available. In particular it is vitally important to produce a high quality a group of cross sections for the interesting features of the river. Getting hold of a good number of field-measured cross sections at critical points along the river gives a better chance of obtaining accurate discharge values and examining other features such as meanders, riffles as well as wetted parameter, hydraulic radius, river slope, etc. Field cross section measurement

data sets from nine locations along the Tigris have been provided exclusively by the Iraqi ministry of Water Resources for use in this study. The locations of these cross sections respectively are listed in the table below:

*Table 3.2: Main Cities along Tigris River. Their locations and elevations above the sea level*

No.	Name	Location	Level above the Sea level
1	Mosul	36°36'18.58"N 42°48'59.26"E	255m
2	Al-Sherqat	35°31'56.39"N 43°14'25.51"E	145m
3	Bijee	34°55'56.36"N 43°31'02.11"E	101m
4	Tekreet	34°34'44.54"N 43°42'42.09"E	76m
5	Sameera'a	34°09'09.43"N 43°52'19.98"E	52m
6	North of Baghdad	33°31'07.96"N 44°18'22.14"E	30m
7	Sweerah	32°57'29.82"N 44°44'12.82"E	25m
8	Nomaniah	32°34'37.09"N 45°24'54.67"E	19m
9	Kut	32°31'42.82"N 45°51'06.35"E	16m

These nine cross sections have been surveyed using the SonTec RiverSurveyor System. Details of three additional cross sections have been obtained from a previous study published by Al-Hafith (2012) to investigate the hydraulic characteristics of Tigris River at Mosul city. Cross section surveys were carried out using the Echo Sounder–Depth Meter. These cross sections are named in this section in the same way they were named in the previous study, S39, S46, S49, S63 and S64 and illustrated in Chapter 6. In total, observations for 14 river cross sections were available. This is not enough to build the profile for a large river profile with many changes such as the Tigris, which is well known to incorporate many meanders and changes in slopes over slow discharges: in turn, this can affect the river flow velocity and discharge estimations. Most of the obtained river cross sections are without any details about the river floodplains whatsoever. However, they are still useful when for evaluating the river profile used in this research.

### 3.2.5 Historical Reanalysed Data

Because of the severe lack of the metrological data available to this study, it was decided to utilise the "NCEP/NCAR Global Reanalysis Products, 1948-continuing", namely (NCAR\_DS090.0) after evaluating its suitability by conducting a comparison/correlation analysis against local observed data sets.

The outcomes consist of over 80 different variables including geopotential height, temperature, relative humidity, U and V wind components, and also evapotranspiration, etc. in several different coordinate systems, such as 17 pressure level stacks on 2.5x2.5 degree grids, 28 sigma level stacks on 192x94 Gaussian grids, and 11 isentropic level stacks on 2.5x2.5 degree grid. The data are available at 6 hour intervals with T62 (209km) resolution. The NCEP\_DS090.0 is archived and made freely available to access in CISL Research Data Archive website which is managed by NCAR's Data Support Section. Different file formats have been used to store such data sets (i.e. WMO GRIB and IEEE) which are makes data processing more complicated.

### 3.2.6 Hydrological Predictors

The statistical downscaling technique of the pattern scaling method was used to investigate whether the Tigris river basin will suffer from extreme events such as floods or droughts during the next 100 years. Such events would have a direct impact on the sustainability of the river basin. The Global Circulation Models (GCM) of HadCM3 were used in this study under the A2 and B2 IPCC emission scenarios to develop the necessary future atmospheric variables including Evapotranspiration. Researchers normally consider only temperature and/or precipitation scenarios for up to 2100 in the Tigris River basin by downscaling into the finest grid possible. The predictor variables are supplied on a grid basis, so that after selecting the location of the required sites on the grids, the data file is made available. Further details are discussed in chapter 4, section 4.3.3.

### 3.3 Data Management

As same as the case for many catchments located in developing countries, the investigated catchment in this study has major quality problems. Price et al. (1994) have summarised some potential significant data challenges for catchments in developing countries. Most of them are similar to the challenges faced in this research study.

The study area is data-poor and the majority of the available spatial information has been derived from satellite surveys in recent years, and is stored in relatively inaccessible places because of the political situation in Iraq. Other older hardcopy maps owned by the government were however available as well as other remotely sensed data. Furthermore, substantial data records, books, and general literature were destroyed in wars (Iraq/Iran 1980-88, the Gulf 1990 and "Iraq Liberation" until 2003). The social and economic structures of the country restrict accessibility of the data including geo-referenced information. A field visit to Iraq now is almost impossible.

To achieve the project objectives, the author has relied on some mediators for data gathering which has caused additional significant drawbacks and difficulties as some of them were not specialists. Other challenges result from communication difficulties and include documents written only in the Arabic language, bad/non-existent infrastructure, limited working hours in Iraq and limited hours of electricity supply together with difficulties dealing with bureaucratic systems. It must be noted that a huge amount of the data obtained for the present study were not digitalised. The data collected were mainly analogue (geological and contour maps) and in the form of hardcopy raw data such as rainfall records. Noteworthy is the fact that the available georeferenced and hydrologic data acquired from specific individual sources were not considered fully reliable.

## Chapter Four: Methodology

In this chapter, a logical framework is presented to highlight all the steps followed to model the Tigris River and its water losses patterns according to climate changes impacts and different entry discharges along the river system. The suggested framework is designed to overcome limitations (e.g. severe lack of necessary information and data) that were discussed in previous chapters, and which can be a hinder in achieving the main research aims. Detailed description of the utilised statistical downscaling model (SDSM) and hydraulic model (ISIS - 1D) in terms of basic calculations and development of models for the Tigris river network are presented as the main approach to understanding the nature of water losses within the river. The study was implemented by the following procedure (imbedded in Figure 4-1), in which four main phases were outlined, namely:

a) Preparation of the necessary data, b) choosing the appropriate ET model, c) develop the river profile and d) application of the hydrodynamic model.

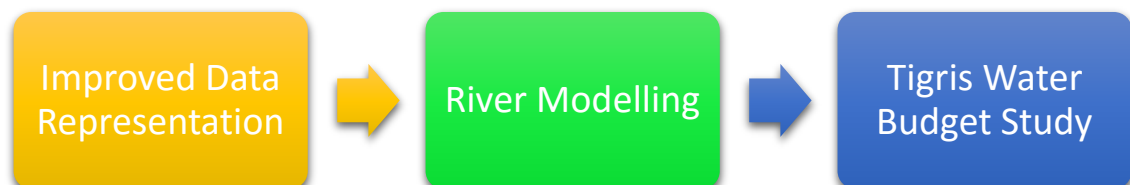


Figure 4-1: The general procedure to study the water losses of Tigris River.

First, observations including meteorological data, hydrological data, and river cross sections and topographical benchmarks were obtained and corrected in order to producing a large volume of accurate data. The observed meteorological data were used to estimate the climate change impacts on the water availability. In addition, it gives an opportunity to investigate the trend (weather increasing or decreasing) of those meteorological data individually. Hydrological data, including river flow and water level data were employed to estimate the inputs and outputs of the Tigris system. The potential of getting a set of reanalysed evapotranspiration data (1948 – continued) provided by NCEP/NCAR employed to reconstruct the original data is investigated. HadCM3A2a and

HadCM3B2a variables were employed to predict the Evapotranspiration trends for the next 100 years based on different climate change scenarios. The statistical downscaling technique used those variables as predictors for that purpose. Topographical observations including river cross sections along the river were used for calibration and validation processes as well as to calculate other river characteristics. In this process, the hydraulic roughness coefficient (Manning's  $n$ ) was estimated and compared against published values for the same area. NASA Shuttle Radar Topography Mission Global 30 arc second (SRTMGL3) raster set that covers the Tigris Basin was obtained in an aim to generate Tigris river profile. Some cross sections were generated by using the 3D analysis tool in ArcGIS. The potential of using Google Earth as a source of topographical points that can be used together to form cross sections for a river was tested in this study. The 3DRoutBuilder was employed as a tool to extract cross sections from Google Earth data sets. The hydrodynamic model ISIS – 1D was utilised as a flow/water levels simulator in both of the research phases (Data Preparation and Water Losses Pattern Modelling). The key result of this process was an ability to review water losses at any point along the Tigris River reach.

## 4.1 Evapo[transpi]ration

The meteorological variables (for example, maximum and minimum temperature, relative humidity, solar radiation, wind speed, etc.) are the parameter to quantify the impacts of the climate change over a basin.

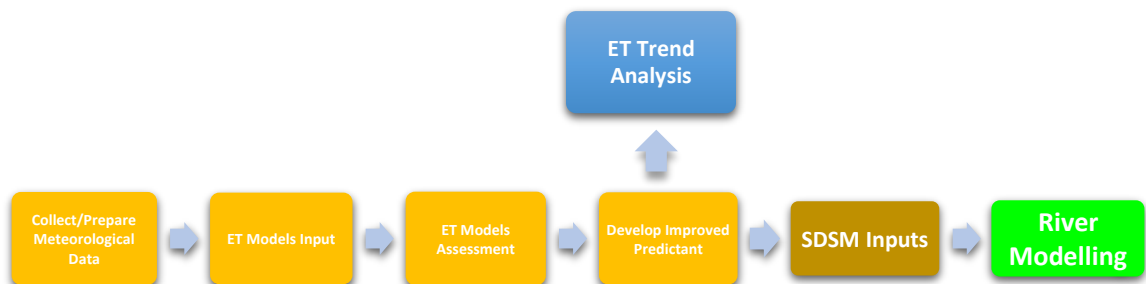


Figure 4.2: A procedure shows the stages that the meteorological data go through to prepare the ET data required for the water losses assessment.

In addition, these variables can be used to model other variables, e.g. evapotranspiration. Analysing different metrological variables as longer historical data sets can help to assess the sensitivity of the evapotranspiration due to changes in these variables. This in turn can help to analyse and model the evapotranspiration trends for the basin.

The observed data sets source and their quality are discussed in Chapter 3. The meteorological data, were provided from different sources. A large amount of data was in the form of typewritten hardcopies, of which a considerable amount was difficult to decipher. A 10 year period' worth of data (1960 – 1970) were successfully converted by the author to Excel sheets and made useable. The rest of the data employed in this research (1971 – 2010) were already digitalised. The need to digitise the first data group was because to implement ET and other variables trends analysis which in turn needs a huge amount of data sets. This is not achievable by using only the second group because the latter suffers from data discontinuity because of wars and other reasons. Several measuring stations along the Tigris River were considered, however it was decided that only the data that originated from the Iraqi main cities' stations (Mosul/North, Baghdad/Middle, and Basra/South) would be used due to a higher quality and continuity. The evapotranspiration and precipitation data sets have been through the same process as the other metrological variables above.

The meteorological variables can provide an aid to simulate evapotranspiration by incorporating them into theoretical models. There was a need to carry out such an approach because the obtained observations including the evaporation Pan Class (A) needed to be reconstructed. For that reason, five ET models were selected according to their complexity and compared against each other and against the available observations. The selected models are Shuttleworth and Wallace (S-W), Penman-Monteith –FAO56, McNaughton and Black (Mc-B), Priestly and Taylor (P-T) and Hargreaves Evaporation Mass Transfer. Each of these models is discussed in chapter 5. To the best of the author's knowledge, there are only few studies available that

compare the performance of ET models. However, the selection according to the complexity approach can be considered a new one. Moreover, there is no such study conducted over any of the Iraqi Basins.

The NCEP/NCAR Reanalysis dataset (1948–continuing) project is considered a valuable source of data for the research. It is a joint product from the National Centres for Environmental Prediction (NCEP) and the National Centre for Atmospheric Research (NCAR). This project is a continually updating gridded data set that represents the state of the Earth's atmosphere, incorporating observations and numerical weather prediction (NWP) model output from 1948 onward. It has over 80 different variables, (including geopotential height, temperature, relative humidity, U and V wind components, etc.) in several different coordinate systems, such as 17 pressure level stack on 2.5x2.5 degree grids, 28 sigma level stack on 192x94 Gaussian grids, and 11 isentropic level stack on 2.5x2.5 degree grid. Its potential evaporation data set is employed within this research. This data source was used as it has previously been widely used in other research projects and is easily accessible. Secondly, NCEP/NCAR project provides metrological data sets in 6 hourly averages stored in GRIP file format. Hence, it can easily be converted into monthly, weekly or daily average bases as required.

The PanoplyWin Data Viewer package which was found by NASA has been used to plot those 6 Hourly data sets on geo-gridded latitude-longitude, latitude-vertical, longitude-vertical, and time-latitude arrays from larger multidimensional variables. MATLAB was used to open those GRIP files and implement the averages calculation. The resulted data sets were firstly on monthly averages bases for both of the evaporation and precipitation, and that was to assess the performance of the NCEP/NCAR products against the research observations. On the other hand, daily data sets were used as predictants and have been employed to achieve the other research objectives.



## 4.2 SDSM

One of the well-recognised statistical downscaling tools which are applied widely in climate impact studies is Statistical Down-Scaling Model (SDSM). It is one of the major elements in this study and can help to reconstruct the missing data and improve their quality.

SDSM is a (windows®) based decision support tool for regional and local scale climate change impacts assessments. This model was widely utilised because it permits the spatial downscaling of daily precipitation and temperature.

The SDSM model is founded on physical linkages between climate on the large scale and weather on local scale with ensembles of high resolution climate scenarios using multiple linear regression techniques. The regression component of the model enables the formulation of empirical relationships between local-scale weather parameters (predictands, e.g. precipitation) and daily atmospheric circulation patterns and moisture variables (predictors, e.g. relative humidity) at target sites (Wilby et al., 1997). The stochastic component of SDSM is used to inflate the variance of downscaled output to better agree with the observed daily data, and enables the generation of multiple simulations with slightly different time series attributes, but the same overall statistical properties (Diaz-Nieto et al., 2005). SDSM needs predictor variables provide daily information to produce predictand variables that describe conditions at the site scale.

Because the ground observation data was only available on a monthly basis and SDSM only works at the first stages in daily bases, it was decided to rely on products from NCEP/NCAR Reanalysis Project (NNRP or R1) to substitute the monthly ground data.

The resolution of the global Reanalysis Model is T62 (209 km) with 28 vertical sigma levels stores data at 6 hour intervals. The production has gone back to 1948 and going forward continuously. There are over 80 different variables, (including geopotential height, temperature, relative humidity, U and V wind components, etc.) in several different coordinate systems, such as 17 pressure level stack on 2.5x2.5 degree grids,

28 sigma level stack on 192x94 Gaussian grids, and 11 isentropic level stack on 2.5x2.5 degree grid. Once the quality of the data is assured, the next critical step is the selection of large-scale predictor variables. The stereotypical approach to such studies is to use either temperature or precipitation, or both in some cases, as predictands alongside other variables e.g. mean sea level pressure, surface specific humidity, relative humidity etc. to perform as predictors. In this section, there is an effort to change this stereo type. Statistical relationships are established between indices of regional weather and locally observed ET (as predictand) data for the period from 1969 to 2000. Regional weather data (atmospheric and surface predictor variables) are obtained from the National Centre for Environmental Prediction (NCEP) and are processed to conform to the 2.5° latitude × 3.75° longitude grid of the Hadley Centre's coupled ocean/atmosphere climate model HadCM3. The statistical relationships established are then used to downscale ensembles of the same local variables for the future climate, using data supplied by HadCM3. Analysis of future climate change is done based on three time slices: 2020s, 2050s and 2080s, which correspond to the 30- year periods 2010-2039, 2040-2069 and 2070-2099, respectively. These data include 3 sets:

**NCEP\_1961-2001:** This directory contains 41 years of daily observed predictor data, derived from the NCEP reanalyses, normalised over the complete 1961-1990 period. These data were interpolated to the same grid as HadCM3 (2.5 latitude x 3.75 longitude) before the normalisation was implemented. **H3A2a\_1961-2099:** This directory contains 139 years of daily GCM predictor data, derived from the HadCM3 A2(a) experiment, normalised over the 1961-1990 period. **H3B2a\_1961-2099:** This directory contains 139 years of daily GCM predictor data, derived from the HadCM3 B2(a) experiment, normalised over the 1961-1990 period.

The downscaling process involves several tasks. Figure 4.3 represents the outline of the procedures for downscaling local climate scenarios using SDSM very well. The figure's details are quoted from Wilby et al. (2002) and edited by the author to be more corresponding to the research case study and purposes.

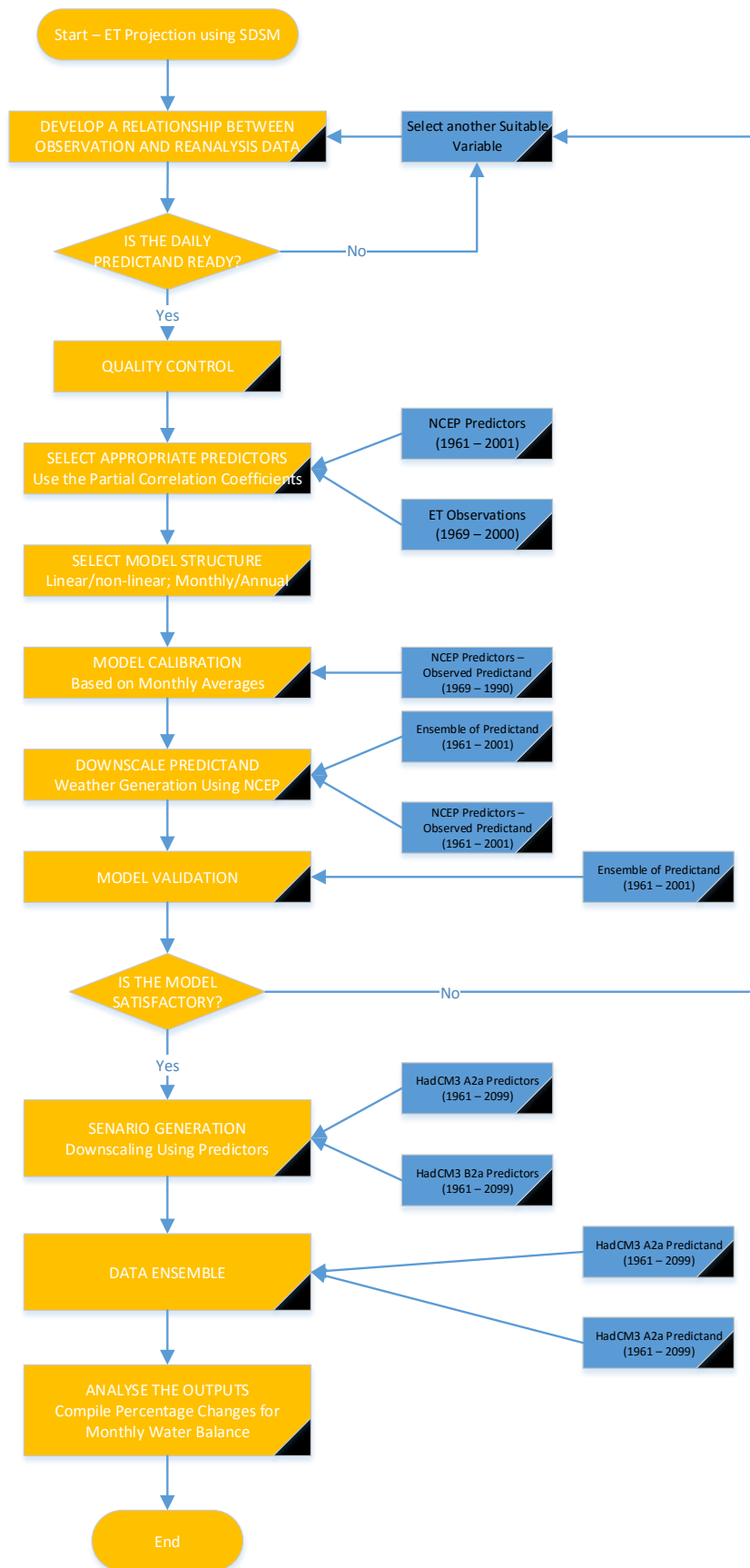


Figure 4.3: Evapotranspiration prediction process using SDSM

### 4.3 River Profile and Hydraulic Characteristics

A well-represented river profile including longitude and latitude, hydrodynamic slope along the river is an important element in assessing water losses from a river, especially when a severe lack of data is involved. A good longitudinal and latitudinal representation for points along the river will aid using the available water level data for different locations along the river to simulate the flow for these points whenever it is needed. The most significant limitation of this research is how to develop a river profile to model the Tigris along the area of study. A river profile is required to develop the hydraulic model. Data was available for only 14 observed cross sections (see explanation in chapter 6). All of these were obtained as images. To digitise those cross sections into data, the “WebPlotDigitizer” was used. WebPlotDigitizer is a free online tool that helps to upload the image of a graph and extract the data. This work was carried out because these cross sections are the only data available to calibrate and validate the simulated river profile.

According to the hydraulic model's requirements, a cross section for each 1km distance along with an additional number of cross sections is required at points along the river with critical changes (e.g. bends, hydraulic structures, river steep, etc.). About 1250 river cross sections are needed to model the research case study. Using observations at this point would be impossible. A comparative analysis of three different approaches to extract river cross sections profiles was carried out using the 14 existing observed cross sections. Two of those approaches are widely used. However, the third one, to the best of the author's knowledge, has not been used before.

The first generated cross section set which was developed using SRTMGL3 DEMs SRTMGL3 is one of NASA's LPDAAC (The Land Processes Distributed Active Archive Centre) collections. It is available to download from the website of Earth Explorer by USGS (U.S. Geological Survey) as tiles of  $1^{\circ} \times 1^{\circ}$ . The interpolate line tool from 3D Analyst Toolbox in ArcGIS was utilised in this study to help determine contour, slope,

and/or elevation of points and lines in desired locations and digitalise them in the same time. The desired locations were identified in advance. The observed cross section locations of the Tigris River were identified by an earth browser as KML files. Then those KML files were converted into GIS layers. These layers are placed automatically on the final DEM raster to represent the cross sections locations. The manifested bits of the floodplain distance and river bank slopes on both channel sides of the observed river cross sections have been considered to interpolate some cross sections including the river bed along the river as another approach to develop river profiles. The required cross sections were then compared against the observed ones.

Despite this, the source of the Google Earth DEM layer is still ambiguous; it has been employed to extract river cross section profile, as the preliminary tests were promising. In addition to the information that can be obtained immediately when the surveying is conducted along the basin, this could increase the potential of using this approach in such an application. The desired cross section locations are identified then as paths on the map.

3DRoutBuilder was used as a GPS location, altitude and time route editor for high resolution control over paths directly in Google Earth. The 3DRoutBuilder adjusts altitude and location of one or more points in centimetre increments, Views include altitude profiles against distance, correct and smooth barometric drifts. Moreover, it can also extract altitude and location data to any other suitable formats, in addition to detailing the left and right river banks. All the hydraulic characteristics including manning numbers, hydraulic radius, wetted parameters, manning numbers, etc. for the observed cross sections as well as for the generated ones were calculated using WinXSPRO which is a Windows™ software package designed to analyse stream channel cross section data for geometric, hydraulic, and other sediment transport parameters. All of the above elements have been explained thoroughly in chapter 6.

Figure 4. illustrates the procedure of river cross sections generation and comparison.

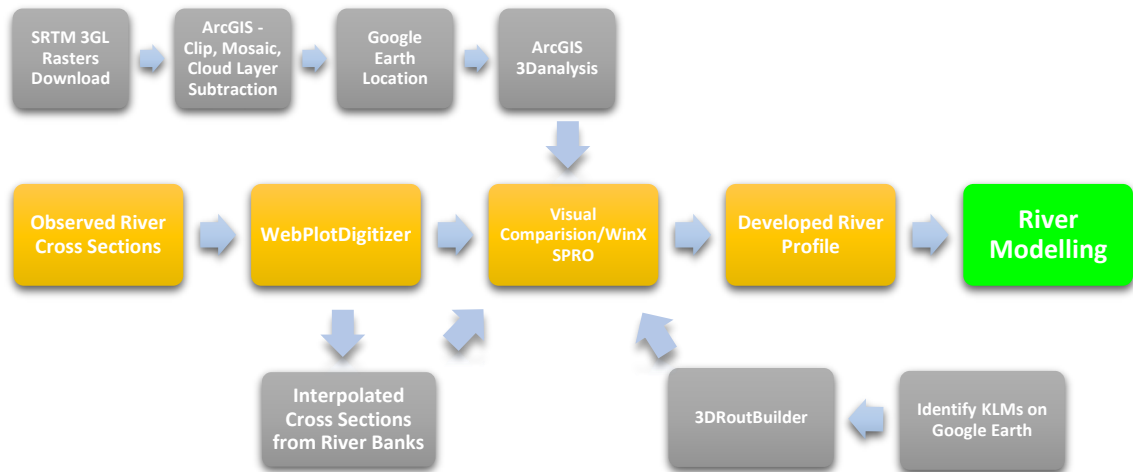


Figure 4.4: A procedure shows different river profile generation's methodologies including their steps.

The figure above shows that there are only two steps needed to get river cross section when using 3DRoutBuilder and Google Earth. That could be another merit for this methodology.

#### 4.4 Physically Based Hydrodynamic Model (ISIS – 1D)

Estimating river losses from Arid/Semi-Arid river basins is the final aim of this study. Using a widely used commercial 1D hydraulic model can help to give accurate flow and water level simulation results. These simulations can be obtained using the boundary conditions including water discharge, river profile representation, etc. A 1D hydraulic model such as ISIS-1D helps to understand the hydraulic nature of the river network, and also to assess the potential impacts of climate change on the river discharge through utilising predicated evapotranspiration.

ISIS is a hydrodynamic model used world-widely (Lin et al., 2006). It simulates flows and water levels in open channels and estuaries. It is able to model complex looped and branched networks, and also designed to provide a comprehensive range of methods for simulating floodplain flows. It works, as many hydraulic models (e.g. MIKE and HEC-RAS), by solving the 1D continuity and St. Venant momentum equations for each cross section along the modelled river system and all time-steps (Graham, 2003).

The ISIS-1D utilises partial differential equations to solve the fundamental flow processes within the modelled channel (refer to chapter 2, the manual is freely available at [www.isisuser.com](http://www.isisuser.com)). The ISIS – 1D steady state calculations were carried out for several reasons. First is to assess the developed model performance in general and also to assess its capacity to handle extreme events. Secondly and most importantly, filling the data gaps and re-constructing the available observations. ISIS – 1D has the ability to use water levels to simulate river flow and observe.

At this stage in modelling process, some assumptions were made including the flow being steady along the developed river network and the water surface slope being less than 5%. The computational procedure is undertaken based on the solution of the 1D energy and momentum equations. At this stage, it was assumed that the hydraulic nature does not change rapidly along the river network. Therefore, the energy equation was applied instead of the momentum approach. In addition, due to the lack of the measured bathymetry along the downstream river network, the momentum approach which requires very well-defined bathymetry for the centroid of each cross-section could not be applied.

The energy equation used in ISIS is the 1D St Venant equation to simulate open-channel flow. Horizontal exchange of discharge between channels and floodplains are assumed to be insignificant and the discharge is distributed according to the conveyance. The assumption is fulfilled in this study because the river network is large and therefore the discharge going beyond the banks during the flooding period (if there is any) is not significant (in a dry region such as Tigris Basin) compared to the total conveyed discharge. As for the flow data, it was very difficult to obtain good quality of data for the required period. For that reason, it has been decided to employ the “*Stream Gage Descriptions and Streamflow Statistics for Sites in the Tigris River and Euphrates River Basins, Iraq*” which has been prepared by Saleh (2010) and MoWR and published by USGS. This report contains statistical summaries of streamflow data for all long-term

streamflow-gaging stations in the Tigris River and Euphrates River Basins in Iraq as monthly averages.

In ISIS, the cross-section is subdivided into different units with uniformly distributed velocity to calculate the conveyance over a single cross-section over the floodplain (Figure 4.). In this approach, the cross-section is subdivided due to different Manning's  $n$  coefficients assigned to each subdivision. The conveyance is then summed to get the in-channel left and right overbank conveyance.

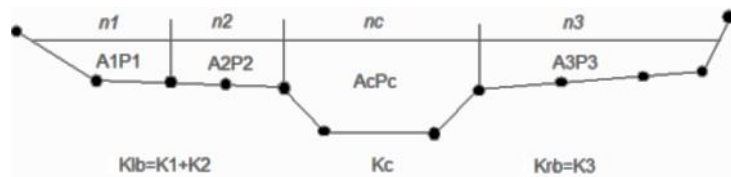


Figure 4.5: ISIS conveyance subdivision method

One of the important features of ISIS is that it is allowing the representation of the river floodplains in different ways; the easiest one is only extracting the channel cross sections. However, different roughness parameter values should be considered for the channel wetted parameter and the floodplain. Another way in which the floodplain can be represented is generating spill units at the top of the channel banks connecting the main channel to the floodplain, which can either be represented by a parallel channel or storage/reservoir units (Lin et al., 2006). This approach is a more accurate representation, but is more computationally demanding. Details and information are required as well about the roughness of the whole channel and the floodplain along the simulated river profile. The only way of getting such values is calculating the Manning number in different places along the modelled reach and then compare it to what is published in the literature. At the end, a set of rivers discharge and water level values related to time are requested to calibrate and validate the model.

In order to carry out unsteady simulations, estimates of initial conditions (flow and stage) were created by steady state run at every model node. This is most often obtained by carrying out a steady state run first at a proposed start time. The unsteady solver in ISIS



uses the so-called “box” finite difference operator. This operator is implicit, which means that long periods can be simulated as well while other processes such as regional flood events are carried out. Such operators enable the partial differential equations describing channel flow to be transformed into a set of linear algebraic equations connecting the flows and depths at discrete locations or nodes along the channel. ISIS uses a sparse matrix solver (numerical function helps to uniform and normalise random distribution of elements) to solve an ‘all-system’ matrix that includes every inserted element, e.g. branched channel networks and objects such as boundaries and embankment spills. The step by step ISIS-Tigris model development is well explained in chapter 6 alongside with proper justifications for the elements which are used to build the model.

Figure 4. illustrates the procedure of generation the required information using the physical – based hydrodynamic model as a preparation for the final water budget and water losses assessment.



Figure 4.6 Procedure for developing the required information for the water budget/water losses assessment using a hydrodynamic model.

## 4.5 Water Balance/Water Losses Assessment

Although the reviewed water balance studies achieved some successes in terms of water losses assessments in particular regions, none of them can be applied directly in this study because of the critical situation of Tigris river basin. As an arid-semi arid basin the study area is mostly depending on upstream seasonal releases rather than on precipitation or snowing. According to observations investigations and analyses, the precipitation rate is only about 10% of the surface water.

Despite the critical situation of the basin and the severe lack of necessary information, the main aim of this research is to provide as accurate water losses assessment as

possible by utilising reliable sources of data and avoid assumptions as much as possible. However, some prerequisite logical assumptions have to be made to maintain a reasonable water losses model. The change in ground water level over time is assumed to be zero in most of the previous studies. Evaporation and evapotranspiration have always been taken into account as the major water losses elements in the hydrological cycle; in this research they are assessed separately but counted as one unit called evapotranspiration. The runoff is a key element of the water budget. River profile modelling method has been developed to aid better quality of runoff simulations. Most of the current studies either ignored this issue or used unfeasible ones. In this research, there is a good chance to incorporate the population rate variations in the water balance model as one of the key elements. To the best of the author's knowledge, the impact of the population rate variations on water balance have been overlooked in other research. That could be because most of the studies that have been conducted took into account only two consecutive flow gauge stations readings to calculate the water losses. In the case of this study, the terrestrial water budget model which is already reviewed in chapter 2 will be used; however, the reviewed model will be modified to be suitable to fulfil this research study's requirements. The suggested model and procedure will be as follows (refer to figure 4.7):

$$R = Rel - Pop - ET + P \mp \frac{\partial S}{\partial t} \quad (4.1)$$

where:

*R*: River Basin Discharge

*Rel*: Upstream Seasonal Releases

*Pop*: Population Water Consumption

*ET*: Evapo[transpi]ration Rate

*P*: Precipitation

$\frac{\partial S}{\partial t}$ : Ground Water Changes which equals to (Zero) in this case.

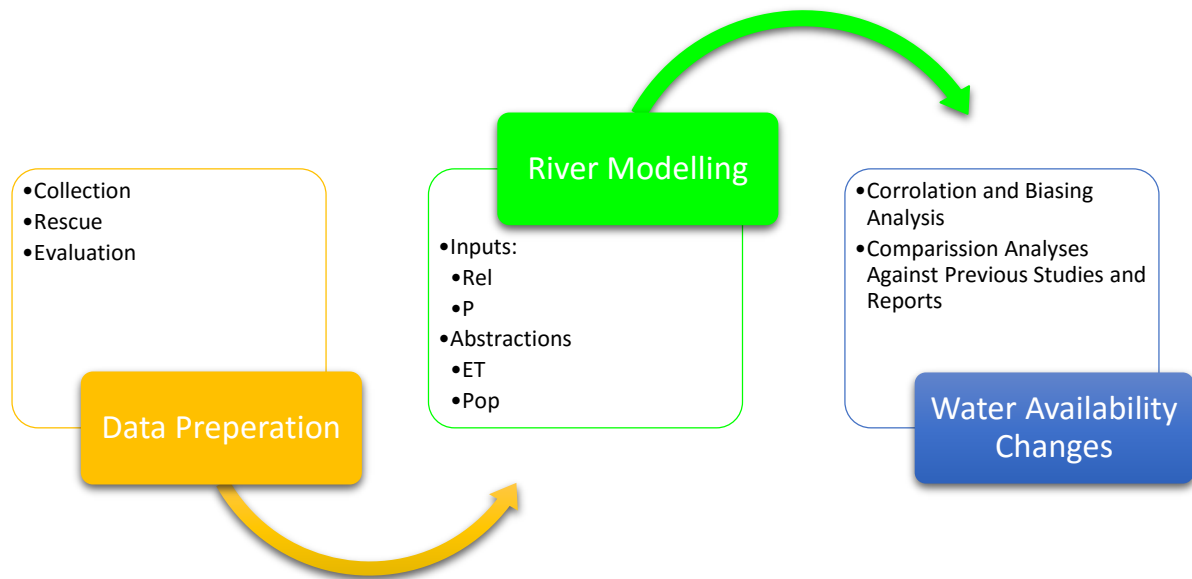


Figure 4.7: Procedure showing the hydrodynamic aiding to develop the water budget/water losses assessment

## 4.6 Summary

This chapter represents the theoretical framework of how to achieve the research objectives. It shows the importance of data modelling and investigations. It also summarises the types of data which are used and highlights its qualities and limitations. A historical data set provided by a gauging station to represent the climate and flow rate for each of the regions along the river, which will allow spatial patterns of water losses trends of magnitude and frequency to be assessed. Furthermore, ET/precipitation records are constructed for several different timescales. There were comprehensive justifications of why ISIS, for example, Google Earth and 3DRoutBuilder are considered as major pivots for this research and other tools. All the modelling tools, materials and computational equipment and resources which are used within this study were explained in detail. Moreover, in the following chapters, there will be further explanations about the elements which are used in this research which have not been covered in depth in these previous chapters.

## Chapter Five: Evapo[transpi]ration

Evapotranspiration (ET) is a term used to define the process of water surface evaporation and plant/soil transpiration from the Earth to atmosphere. It is one of the most important processes in the hydrological cycle because it is responsible for the atmosphere's water vapour as well as ruling river discharge, irrigation demand and soil moisture contents. To the extent that, Evapotranspiration might be considered in some cases as the main source of water loss in areas which suffer from a lack of rainfall such as Tigris River basin. Accurate estimation of ET is therefore essential for water budgeting and planning.

Climate change is causing a steady rise of temperature and changes in rainfall patterns as well as increases in ET rates which in turn affects the entire hydrological system. Thus, quantifying the changes in ET due to climate change is very important for the management of long-term water resources, especially in lands depending on agriculture as an important source of life alongside. It is essential to measure the possible changes in ET and probability of water losses due to climate change so as to provide better water resource management plans.

Often, studies distinguish between two different aspects of evapotranspiration, potential and actual. Potential evapotranspiration or  $ET_{pot}$  is the measurement of the atmosphere's ability to remove water from the surface through evaporation and transpiration, assuming no control on water supply, whereas the actual evapotranspiration or  $ET_{act}$  is the quantity of water that is actually removed from a surface due to evaporation and transpiration.

The calculation of the  $ET_{pot}$  depends on the intensity of solar radiation, air temperature, humidity and wind speed. Only the humidity is negatively correlated with  $ET_{pot}$  (i.e., the greater the amount of water vapour already in the atmosphere, the less that can evaporate), while the others are positively correlated.

The calculation of  $ET_{pot}$  from available meteorological data is seen to be a much simpler operation, and even works for night measurements, than the computation or

measurement of  $ET_{act}$  from a vegetated surface, because  $ET_{act}$  to be accurate the water transpiration through plant leaves is also included. However, water loss from a catchment area does not always proceed at the potential rate, since this is dependent on a continuous water supply.

When vegetation is unable to abstract water from the soil, then the actual evaporation becomes less than potential evaporation. Thus, the relationship between  $ET_{act}$  and  $ET_{pot}$  depends upon the soil moisture content. Quantifying the actual evapotranspiration losses depending on the soil moisture content, from the author's opinion, suits the research studied area because it represent a typical arid/semi-arid land, not fully covered by vegetation. Figure 5-1 represents Thornthwaite's method which is used to calculate the ratio of the  $ET_{act}$  to  $ET_{pot}$ , (Ward, 1999). This figure shows how to estimate the ratio of the actual evapotranspiration to the potential evapotranspiration depending on the moisture availability and the catchment soil type:

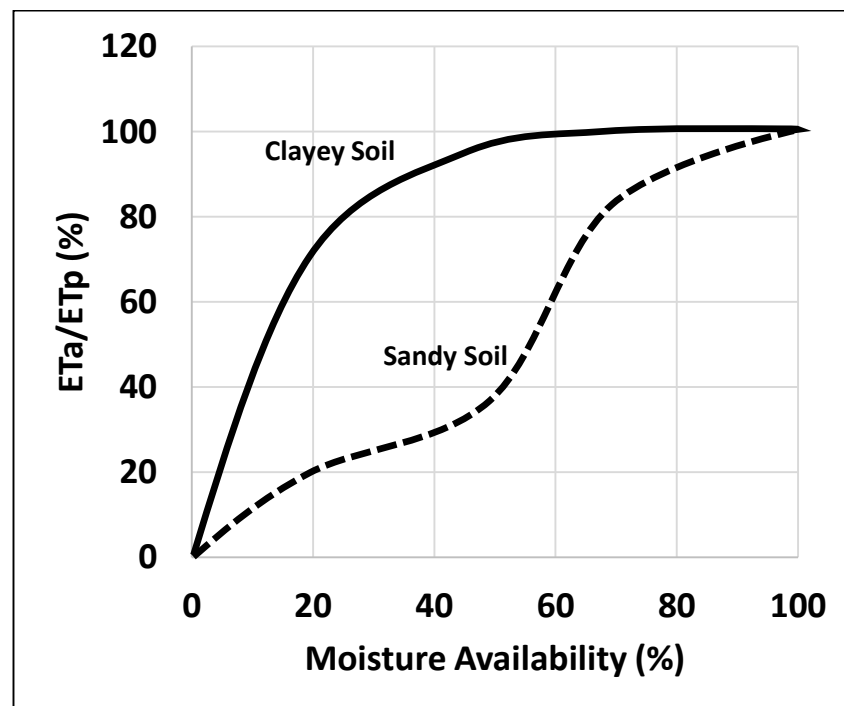


Figure 5-1: Thornthwaite relationship between soil type, moisture availability and the ratio between actual and potential evapotranspiration. The source: *LEARNING HYDROLOGY*, edited by the author.

It should be noted that, the method of collecting the field ET data for this research is the Evaporating Pans. These pans are installed either in platforms built in the middle of the

river or nearby one of the river banks (as per the source of the information provided, Figure 5-2). In this case, the  $ET_{pot}$  or the Evaporation (E) rate which comes from such approach could represent the  $ET_{act}$  so far for the river. Alternatively,  $ET_{act}$  can be derived from  $ET_{pot}$  which is obtained from the suitable evapotranspiration model multiplied by the  $ET_{act}/ET_{pot}$  (Figure 5-1). The results can be considered as the amount of the water lost from the area around the river (the remaining area of the catchment).

The resulting ET out of this process, the summation would be the actual amount of the lost water from the river, as the river itself can easily be considered as the only source of water for this area of study because of its weather conditions and the sever lack of the rainfall.

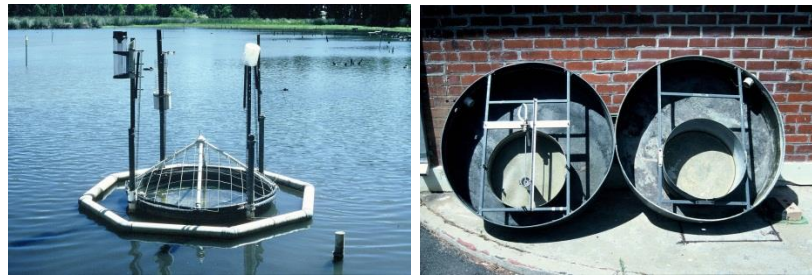


Figure 5-2: Evaporation Pans

It is important to identify the type of the soil within the basin and the moisture contain. The Food and Agriculture Organization of United Nation has cited a study was conducted to show some of the physical properties for the soil for many part in Tigris basin. The study states that Tigris basin in general is dominantly coarse-textured soils mechanical composition of the various profiles ranged from 80-95% sand, 1.5-12.8% silt, and 2.7-10.5% clay with average soil moisture between 25 – 35%.

A set of monthly time series data starts from 1970 to 2000, including all the variables that can be utilised to model evapotranspiration as well as the evaporation values were digitalised and made ready for analysis as one of this research's main objectives.

The meteorological data provided was used to calculate potential evapotranspiration for the study period (1970 – 2000). The field's pan evaporation values obtained are suffering severe missing values and discontinuity. However, they were enough for assessing the

evapotranspiration models performance and for calibrating purposes. Long term data set of evapotranspiration over the area of study was developed using the statistical downscaling model (SDSM) taking in the account different climate change scenarios.

This type of analysis is important because any major shift in seasonal or spatial  $ET_{pot}$  patterns could have negative consequences for the water availability and in turn for agricultural situation within the basin.

In the following sections, there are few aspects are discussed as follows:

1. Investigation of the impacts of the  $ET_{act}$  on the River losses by analysing its historical trends by using available ET pan class (A) records. Those records were obtained from three locations alongside the river. There were used also to assess the performance of six widely used simple  $ET_{pot}$  models, namely Penman-Monteith -FAO 56, Shuttleworth & Wallace, Priestly Taylor, McNaughton and Black and direct evaporation mass transfer against  $ET_{pot}$  Pan class A, in terms of identify which one of those models simulates the ET best ate that region.
2. Investigate whether there is a possibility to substitute the numerous numbers of reanalysed variables by only the reanalysed NCAR  $ET_{pot}$  data to fill the gaps of the missing data and to help to generate others for future ET projections (refer to Section 4.2).

## 5.1 Evapotranspiration Models

Many evapotranspiration numerical models have been developed during the last 60 years. Each method has been developed for specific climatic setup. Some of these methods are basically the modified version of other methods.

The major concern in estimating ET is the reliability and accuracy of the methods (Tukimat et al., 2012). There is a fact that these models cannot give accurate estimations each time when they are applied to in different locations. Nevertheless, there are few methods which are reliable over a broad climatic region. Reliability of these methods has been tested in different parts of the world including some parts of the Middle East (e.g.

Iran, Saudi Arabia, etc.) and they are found to estimate ET very close to field observation. The selection of the ET models in this study based on varying considerations. Some of those models are “parameter rich models”, e.g. Penman-Monteith – FAO56 and Shuttleworth and Wallace. Simple models e.g. Priestly Taylor, McNaughton - Black and Evaporation Mass Transfer were considered as well. The following subsections identify the selected ET models including their incorporated variables.

### 5.1.1 Pan Class (A)

Pan Class A: the source of the data advised that the field ET data obtained by using Evaporation Pans class (A) located in Mosul, Baghdad and Basra. These pans are also known as Sunken Colorado Pans. They are utilised to hold water during observations for the determination of the quantity of evaporation at the given locations. The used Sunken Colorado pans are normally circle, 1 m (3 ft) radius and 0.5 m (18 in) deep and made of unpainted galvanised iron (Subramanya, 1994). It is either surrounded by bigger pan and buried in the ground to within about 5 cm (2 in.) of its rim or installed directly to the water to avoid the metal over heat as appear in Figure 5-2.

One of the most common and fairly reliable techniques for estimating ET is using evaporation pan data when adjustments are made for the pan environment (Singh, 1989). The ratio of ET to Class A pan evaporation defines the pan coefficient,  $K_p$ , whose values range from 0.35 to 0.85.  $K_p$  is essentially a correction factor that depends on the prevailing upwind fetch distance, average daily wind speed, and relative humidity conditions associated with the sitting of the evaporation pan (Doorenbos et al., 1977). Reliable estimation of evapotranspiration (ET) using pan evaporation data depends on the accurate determination of pan coefficients ( $K_p$ ). Pan coefficient ( $K_p$ ), according to the type of the pan, average wind speed and the relative humidity is in this case is equal to 0.85 as per the FAO paper 24, was considered in the calculation as we are here estimating potential evapotranspiration rates.



### 5.1.2 FAO56 – PM

Penman-Monteith – FAO56 (FAO56 – PM): Penman (1948) combined the energy balance with the mass transfer and derived an equation to compute the evaporation from an open water surface in standard climatological records of sunshine, temperature, humidity and wind speed.

$$\lambda E = \frac{[\Delta(R_n - G)] + (\gamma \lambda E_a)}{(\Delta + \lambda)} \quad (5.1)$$

where

$\lambda E$  = evaporative latent heat flux ( $\text{MJ m}^{-2} \text{d}^{-1}$ ),

$\Delta$  = slope of the saturated vapor pressure curve [ $e^\circ/T$ , where  $e^\circ$  = saturated vapor pressure (kPa) and  $T_{\text{mean}}$  = daily mean temperature ( $^\circ\text{C}$ )];

$R_n$  = net radiation flux ( $\text{MJ m}^{-2} \text{d}^{-1}$ ),

$G$  = sensible heat flux into the soil ( $\text{MJ m}^{-2} \text{d}^{-1}$ ),

$\gamma$  = psychrometric constant ( $\text{kPa } ^\circ\text{C}^{-1}$ ), and

$E_a$  = vapor transport of flux ( $\text{mm d}^{-1}$ ).

This so-called combination method was further developed by many researchers and extended to cropped surfaces by introducing resistance factors. “FAO56 – PM” name comes because the food and agriculture organisation of the united nations considers this models as a standard method to estimate ET and published it in FAO paper number 56, (Allen, 2000).

$$ET_o = \frac{(0.408 * \Delta * (R_n - G) + \left(\gamma \frac{900}{T + 273}\right) * u_2(e_s - e_a))}{(\Delta + \gamma (1 + 0.34u_2))} \quad (5.2)$$

where,

$ET_o$  is the reference evapotranspiration ( $\text{mm day}^{-1}$ );

$\Delta$  is the slope vapor curve ( $\text{kPa } ^\circ\text{C}^{-1}$ ),

$R_n$  is the net radiation of the crop surface ( $\text{MJm}^{-2} \text{day}^{-1}$ ),

$G$  is the soil heat flux density ( $\text{MJm}^{-2} \text{day}^{-1}$ ),

$T$  is the air temperature at 2m height ( $^\circ\text{C}$ ),

$u_2$  is the wind speed at 2m height ( $\text{m s}^{-1}$ ),

$e_s$  is the saturation vapor (kPa),

$e_a$  is the actual vapor pressure (kPa), and

$\gamma$  is the psychrometric constant ( $\text{kPa } ^\circ\text{C}^{-1}$ ).

Zotarelli et al. (2010) from University of Florida well explained the historical development happened on (Penman, 1948) model and show step by step evapotranspiration calculation instructions.

### 5.1.3 S – W

Shuttleworth & Wallace (S – W): Shuttleworth et al. (1985) extended the Penman-Monteith 1948 ET model to be able to evaluate ET from sparse vegetation environment by considering: (i) the transpiration from vegetation and (ii) the evaporation from substrate soil. The Penman-Monteith model treats the crop canopy as a single uniform cover, or “big-leaf”, but neglects the evaporation from soil surface. Over a large basin, however, the big leaf assumption is rarely valid. There are often many vegetation types co-existent, and always some parts or periods where or when the vegetation is not “closed”. Both the soil surface and the vegetation leaves evaporate or transpire moisture to the atmosphere and their relative importance changes significantly, as the vegetation develops. The ideal approach is that applicable at all times and places and able to reflect the changes of surface conditions. The S–W model (equation 5-3) meets this criterion. It is highly complex with many parameters and demands a great deal of data on the meteorology and the land surface characteristics.

$$ET_s = \frac{\Delta(R_n - G) + \frac{[(24 * 3600)\rho c_p(e_s - e_a) - \Delta r_a^s(R_n - R_n^s)]}{(r_a^a + r_a^s)}}{\Delta + \gamma \left[ \frac{1 + r_s^s}{(r_a^a + r_a^c)} \right]} \quad (5.3)$$

where

$ET_s$  evaporation from soil,

$e_a$  actual vapour pressure,

$R_n$  and  $R_n^s$  net radiations above canopy and to soil surface respectively,

$G$  soil heat flux,

$r_a^s$  and  $r_a^a$  aerodynamic resistances from soil to canopy and from canopy to reference height respectively,

$r_s^s$  soil surface resistance,

$e_s$  is the saturation vapour pressures (kPa),

$\Delta$  is the slope of saturation vapour pressure curve (kPa °C<sup>-1</sup>),

$q$  is the mean air density at constant pressure (kg m<sup>-3</sup>),

$c_p$  is the specific heat of moist air at constant pressure (MJ kg<sup>-1</sup> °C<sup>-1</sup>),

$r_a^c$  is the psychrometric constant.

#### 5.1.4 P – T

Priestly and Taylor (PT): Priestley & Taylor (1972) found that the actual evaporation is 1.26 times greater than the potential evaporation and hence they replaced the aerodynamic terms with a constant value of 1.26. Consequently, Priestley- Taylor method needs only long-wave radiation and temperature to estimate ET. Priestley-Taylor equation for computing ET is given below:

$$ET = 1.26 * \left( \frac{\Delta}{\Delta + \gamma} \right) \frac{(R_n - G)}{\lambda} \quad (5.4)$$

where,

$\Delta$  is the slope vapor curve (kPa °C<sup>-1</sup>),

$\gamma$  is the psychrometric constant (kPa °C<sup>-1</sup>),

$R_n$  is the net radiation of the crop surface (MJm<sup>-2</sup> day<sup>-1</sup>),

$G$  is the soil heat flux density (MJm<sup>-2</sup> day<sup>-1</sup>), and

$\lambda$  is the latent heat of vapor (MJ kg<sup>-1</sup>).

### 5.1.5 Mc - B

McNaughton and Black (Mc-B): McNaughton and Black 1973, (Mc-B), adjusts the potential evaporation for the effects of the canopy that does not use a crop coefficient. It uses one or more resistances that attempt to model the ability of the plant to transport water from the soil and transpire. These resistances are a function of soil water availability, the depth of the root system, the maturity level of the plant and its condition (which implies antecedent conditions can play a role), and the existing atmospheric conditions.

$$ET = c_p \rho \frac{D}{\gamma r_s} \quad (5.5)$$

where,

$c_p$  is specific heat at constant pressure,

$\rho$  is air density,

$D$  is vapor pressure deficit, and

$r_s$  is soil surface resistance.

### 5.1.6 ETH

Hargreaves Evaporation Mass Transfer (ETH): Hargreaves and Semani (1985) proposed several improvements for the Hargreaves (1968) model (H) for estimating grass-related reference evapotranspiration. The developed model is as follows:

$$ET = 0.0023(T_{ave.} + 17.8) * (T_{max} - T_{min})^{0.5} * R_a \quad (5.6)$$

where,

$ET$  is reference evapotranspiration (mm/d),

$R_a$  is terrestrial radiation and ( $\text{MJ m}^{-2} \text{d}^{-1}$ ),

$T_{ave.}$ ,  $T_{max}$  and  $T_{min}$  are respectively the average, maximum and minimum temperatures ( $^{\circ}\text{C}$ ).

Table 5.1 below shows the complexity of each ET model used in this study by highlighting how many variables incorporated in each model.

Table 5.1: Comparison of the complexity of each model in terms of quantity of parameters required.

Variable	Variable Description	S-W	FAO56-PM	Mc-B	PT	EMH
T	Temperatures (°C)	✓	✓	✓	✓	✓
R <sub>a</sub>	Terrestrial radiation and (MJ m <sup>-2</sup> d <sup>-1</sup> )	✓	✓	✓	✓	✓
Δ	Slope Vapor Curve (kPa °C <sup>-1</sup> )	✓	✓		✓	
γ	Latent heat of vapor (MJ kg <sup>-1</sup> )	✓		✓	✓	
c <sub>p</sub>	Specific heat at constant pressure	✓	✓	✓		
ρ	Air density	✓	✓	✓		
D	Vapor pressure deficit	✓	✓	✓		
r <sub>cs</sub>	Psychometric constant	✓	✓	✓		
u <sub>2</sub>	wind speed at 2m height (m s <sup>-1</sup> )	✓	✓			
r <sub>ca</sub>	Aerodynamic resistances from soil to canopy	✓				
r <sub>sa</sub>	Aerodynamic resistances from canopy to soil	✓				
r <sub>ss</sub>	Soil surface resistance	✓				

It should be noted that, all of these variables needed and were not observed, either calculated from equations or extracted from tables well explained in Crop evapotranspiration - Guidelines for computing crop water requirements Produced by Natural Resources Management and Environment Department and published in FAO Corporate document repository, Annex 2. Meteorological tables.

## 5.2 ET Models Comparison

Many values of obtained observations from the data provider, especially the Evaporation Pan class (A) data sets are missing. This issue could be the main handicap of achieving the aim of this study for developing an accurate integrated water balance study for the Tigris. The five ET models (already discussed in the section above) utilised meteorological and weather data at Mosul, Baghdad and Basra stations to identify which of these models can fairly substitute the observations and reconstruct the available data sets.

Preliminary calculations based on a monthly average observed meteorological data for the period from 1970 to 1980 were made. This period of time was chosen in particular because it provided the best data quality in a comparison to other periods. The results

were compared against ET observations for the same period. Figure 5-3 shows a visual comparison conducted to evaluate the performance of the selected models against the observations over the study area (Tigris northern, middle and southern regions).

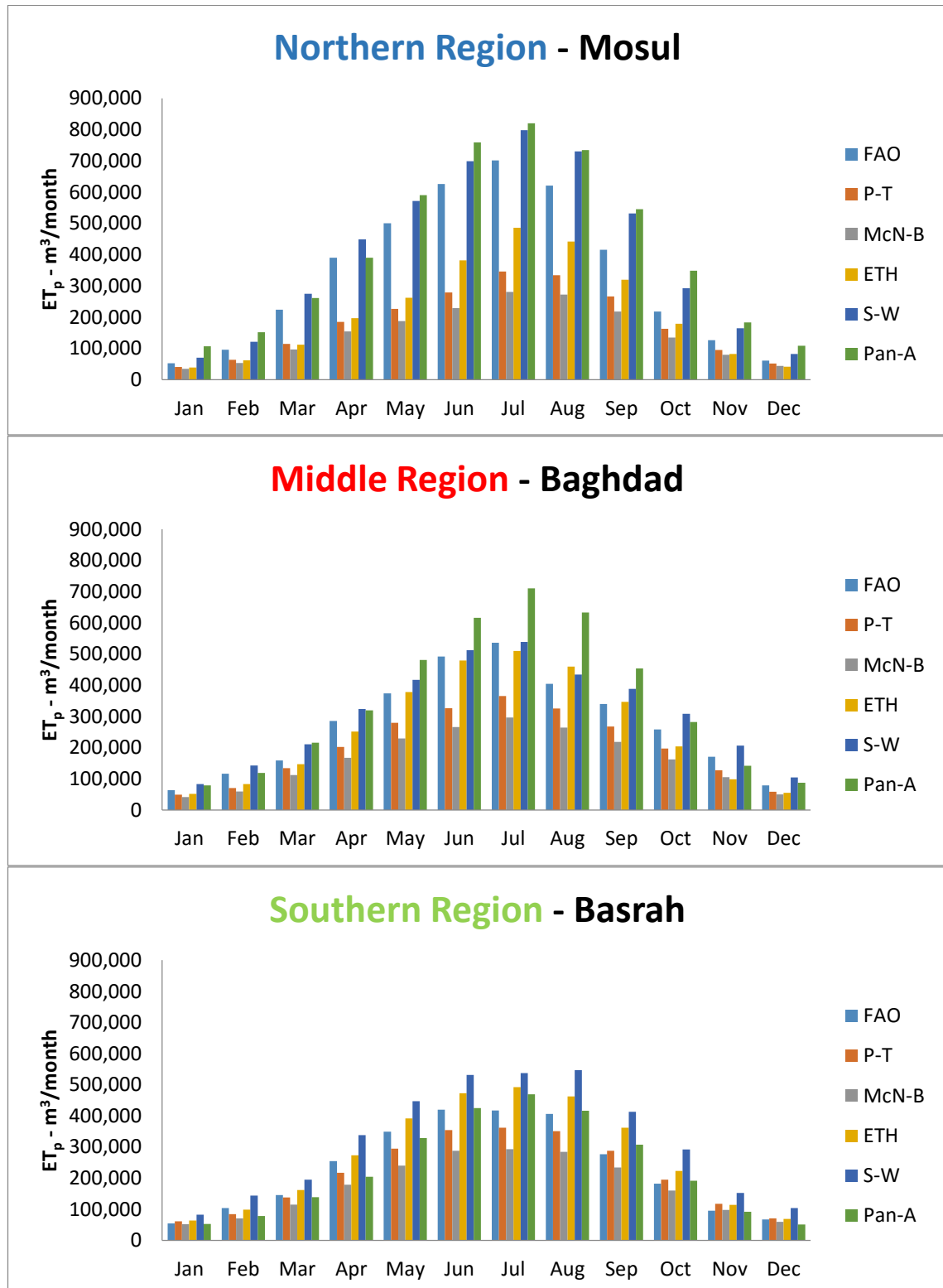


Figure 5-3: Comparison of mean monthly potential evapotranspiration based on Pan-A method and five empirical methods over the Tigris Basin – **Northern**, **Middle**, **Southern** regions.

The figure above shows a well corresponding to the results of all of the selected models against the observations. They performed very well in terms of forming the general seasonal ET production patterns. The evapotranspiration peaks during the summer months (in this studied region the summer starts normally from June and ends in September) and its minimum during the winter months as expected.

It can be well noticed that the evapotranspiration ratings which are resulted from the numerical models during the winter months are quite corresponding to each other till reach to clear variations in the summer months.

Although the southern region is well known by its dry and hot climate but it has recorded during the study period a harmonic and lower evapotranspiration rating relatively. The evapotranspiration rate went higher not even in the middle region which supposed to be the area between two different climates and give the average, but it was at the northern region which is supposed to be cooler relatively; and that conflicts with norm. In the other hand, all potential evapotranspiration models simulated ET and gave reasonably well performance against the measured evapotranspiration at the wet seasons.

Most of the models tended to under predict evapotranspiration in the dry-hot seasons (May-end of September). The reason behind this could be because the  $ET_p$  models were designed for well-watered soil conditions rather than natural summer-time Mediterranean drought conditions.

Linear relationships (Figures 5.9, 5.10 and 5.11) show to which extent the selected models are corresponding the observations along Tigris. The results show that the most complex ET model (S-W) performed better among the other models against the observations when evaluate the ET in the northern region.

S-W is followed by the second model in terms of the complexity (FAO56-PM). Surprisingly, the simplest model (ETH) comes third. However, all the models were slightly under-estimating the observations.

By considering the middle region, all the models were considerably under estimating the ET observations. Nevertheless, it should be highlighted here that S-W, FAO56-PM and

ETH very competitive results among each other. This note is important and well analysed in later discussion.

At the southern region, all the selected models were performing well generally. S-W here slightly was over predicting the observations, while ETH and FAO56-PM performed well against each other and against the observation. The ETH here was relatively better than anyone.

The Nash-Sutcliffe efficiency (NSE) is applied in this study. It is a normalised statistic that determines the relative magnitude of the residual variance ("noise") compared to the measured data variance ("information") (Nash and Sutcliffe, 1970).

NSE indicates how well the plot of observed versus simulated data fits the 1:1 line.

Nash-Sutcliffe efficiencies range from  $-\infty$  to 1. Essentially, the closer to 1, the more accurate the model is.

$$NSE = 1 - (\text{sum}(\text{obs} - \text{sim})^2) / \text{sum}(\text{obs} - \text{mean}(\text{obs}))^2 \quad (5.7)$$

- NSE = 1, corresponds to a perfect match of modelled to the observed data.

- NSE = 0, indicates that the model predictions are as accurate as the mean of the observed data,

-  $-\infty < NSE < 0$ , indicates that the observed mean is better predictor than the model.

Table 5.2: ET models efficiency calculated by NSE and  $R^2$

Region	Efficiency	ET Models				
	Coefficients	S-W	PM-FAO56	P-T	Mc-B	ETH
Northern	NES	0.86	0.84	0.39	0.43	0.79
	$R^2$	0.57	0.32	0.15	0.17	0.94
Middle	NES	0.68	0.76	0.27	0.33	0.71
	$R^2$	0.71	0.78	0.96	0.45	0.91
Southern	NES	0.85	0.67	0.49	0.52	0.92
	$R^2$	0.49	0.18	0.7	0.87	0.94



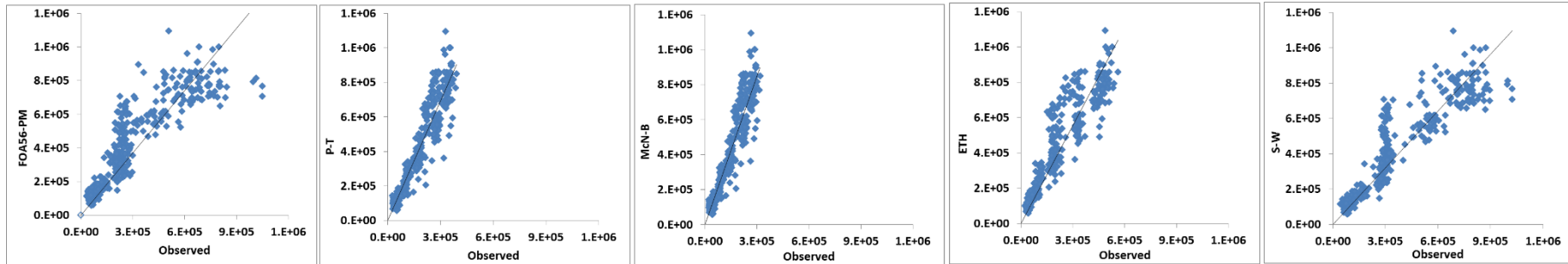


Figure 5-4: Performance of the selected ET models against ET observations over Tigris northern region.

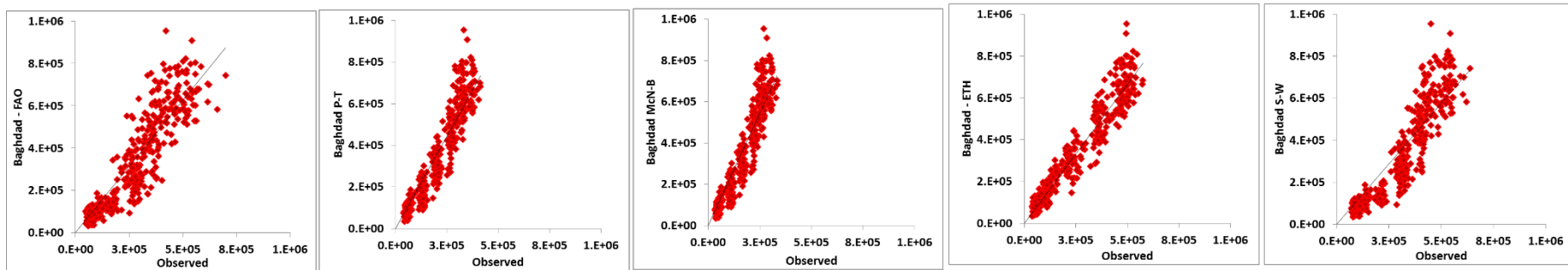


Figure 5-5: Performance of the selected ET models against ET observations over Tigris middle region

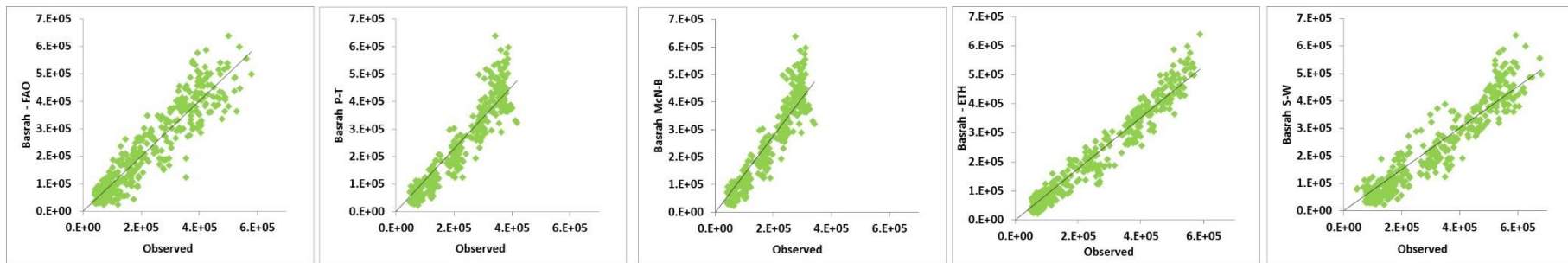


Figure 5-6: Performance of the selected ET models against ET observations over Tigris southern region

All the potential ET models had the same trends comparing to the observed ET. However, the resulting low ET rates in winter seasons and high ET rates in the summer seasons as expected. In the northern and the middle regions, the ET models were under estimating the potential evapotranspiration in general. That was because those regions were windier and with low relative humidity relatively. The selected ET models performed well in the southern region (high relative humidity). The FAO56-PM model has performed well only for the southern region and only in terms of the unity with the observed data set. However, in terms of the diffusion, the ETH has performed well not only for southern region but even performed reasonably for the others. Despite the under estimating, S-W, the model which meant to be the richest model among the selected models in terms of the parameter requirements has performed reasonably well in the upper regions. By considering the analysis above, ETH is suitable to be considered alongside with the Evaporation Pan Class A to calculate the actual losses from the river Tigris in the future. That is because S-W model is unfeasible for data scarcity reasons. In addition, the actual ET which comes from such model over such area is any way only about 0.2 of the calculated potential ET (refer to figure 5.1). Maximum and Minimum temperatures are that major variables which the ETH relies on and these variables are usually measured in basic weather and metrological collecting stations.

### **5.3 Evapo[transpi]ration Losses Representation**

On the basis of 'what happened in the past', at least an idea can be obtained of what will happen in the future, predict the future of water removal from a river caused by ET requires the implementation of a robust trend analysis uses a stock based on historical data. In this section, the aim is to exploit the trend analysis concept as a method of showing information in sequence over time over the study area of this research. This will also provide an opportunity to project the future direction to define the ET losses pattern. From the section above, estimating the actual river losses which are formed by the ET can be developed by considering the evaporation from the water surface + (the

actual evapotranspiration (which is about 0.2 of the modelled/potential evapotranspiration (refer to figure 5.1)). This relationship is illustrated as follows:

The total actual water losses from the river by Evapo[transpi]ration = reconstructed Pan (A) + 0.2 x Modelled Evapotranspiration.

The calculations show clear evidence in the differences in regional characteristics of evaporation. Those differences might be due to climate attributes diversity between the sub-basins, and also the variety of the topography as well as the longitudes and latitudes. The southern region which is hotter gives lower river losses rate in contrary to what is expected and to the upper regions that meant to be relatively cooler. As a result, the amount of the losses can be calculated (table 5.3). The Evapo[transpi]ration values were calculated from reconstructed observations for the period from 1969 – 2000 from Mosul, Baghdad and Basra and then applied to the whole Tigris River catchment by taking the total basin area.

*Table 5.3: Calculated maximum, minimum, and mean values for the Tigris water losses due to Evapo[transpi]ration.*

Region	Maximum water losses m <sup>3</sup> /month	Mean water losses m <sup>3</sup> /month	Minimum water losses m <sup>3</sup> /month
North	540,931,000	207,289,000	29,172,000
Middle	471,512,000	171,591,000	16,592,000
Southern	315,588,000	114,220,000	11,560,000

The table above shows that Tigris lost a significant amount of water due to only Evapo[transpi]ration over the studied period. The average water losses per year calculated as the summation of the average losses per month from the three regions and multiplied by 12 (number of months/year), which could reach the threshold of 15 billion cubic meter per year.

## 5.4 Evapo[transpi]ration - Future Projections

It has been decided to consider evapotranspiration to be the main element that produces evapotranspiration future predictions rather than consider other meteorological variables (i.e. traditionally - temperature).

The statistical down scaling model (SDSM) version 5.1.1 is used in this study as a tool to identify the future climate change impact on the evapotranspiration and in turn the impact of the evapotranspiration on river losses. SDSM is used in this study because it facilitates the rapid development of multiple, low-cost, single-site scenarios of daily surface weather variables under current and future regional climate forcing. Additionally, the software performs ancillary tasks of predictor variable pre-screening, model calibration, basic diagnostic testing, statistical analyses and graphing of climate data. Firstly, a comparison analysis between observed monthly evapotranspiration data against the reanalysed NCAR ET data was conducted to evaluate the suitability of NCAR data sets as an alternative to the daily observations. This process was conducted by utilising Web-based Hydrograph Analysis Tool (WHAT). WHAT provides fast computations for  $R^2$  and Nash-Sutcliffe coefficients to calibrate/validate models, (see figures 5.7 and 5.8). Through that, daily statistical relationships are established between surface and upper atmospheric circulation NCAR ET data for the period from 1961 to 1980 variables.

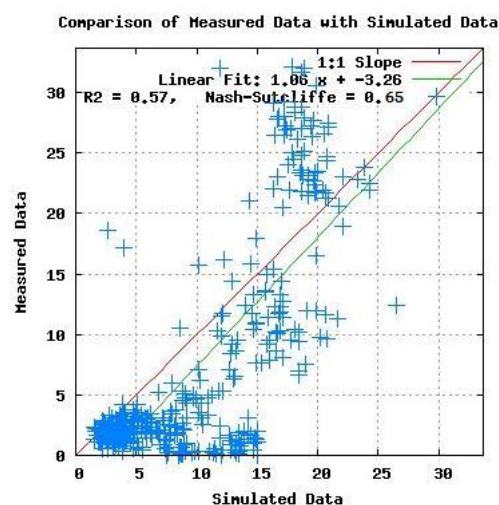


Figure 5-7: Northern Region (Mosul) measured Evapo[transpi]ration – NCAR ET relationship.

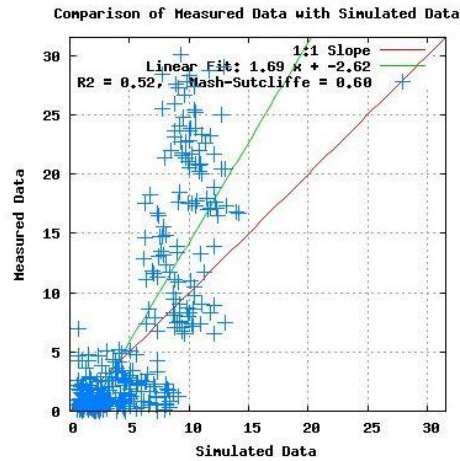


Figure 5-8: Southern Region (Basra) measured Evapo[transpi]ration – NCAR ET relationship.

At this stage, it was not possible to implement the Middle region’s measured Evapotranspiration – NCAR ET relationship because the obtained reanalysed data have huge data gaps. However, the evaluation of the northern and the southern regions reanalysed performance compared to the observation was enough to say that such type of data could be suitable when considering the whole the research circumstances. Although, the middle region suffers from a huge data missing values, SDSM still can bridge those gaps and solve the issue. Statistical downscaling now involves developing quantitative daily relationships between predictor and predictand. The predictor represents large-scale atmospheric variables as shown in Table 5.2 whereas the predictand represents local surface variables (in this case, ET).

Table 5.2: Types of Predictor Variables

No.	Predictor variable	Predictor description
1.	mslpaf	mean sea level pressure
2.	p5zhaf	500 hPa divergence
3.	p_faf	surface air flow strength
4.	p8_faf	850 hPa airflow strength
5.	p_uaf	surface zonal velocity
6.	p8_uaf	850 hPa zonal velocity
7.	p_vaf	surface meridional velocity
8.	p8_vaf	850 hPa meridional velocity
9.	p_zaf	surface vorticity

No.	Predictor variable	Predictor description
10.	p8_zaf	850 hPa vorticity
11.	p_thaf	surface wind direction
12.	p850af	850 hPa geopotential height
13.	p_zhaf	Surface divergence
14.	p8thaf	850 hPa wind direction
15.	p5_faf	500 hPa airflow strength
16.	p8zhaf	850 hPa divergence
17.	p5_uaf	500 hPa zonal velocity
18.	p500af	Relative humidity at 500 hPa
19.	p5_vaf	500 hPa meridional velocity
20.	p850af	Relative humidity at 850 hPa
21.	p5_zaf	500 hPa vorticity
22.	p500af	500 hPa geopotential height
23.	shumaf	Surface specific humidity
24.	p5thaf	500 hPa wind direction
25.	tempaf	Mean temperature at 2m
26.	rhumaf	Near surface relative humidity

Daily observed-modified Evapo[transpi]ration data from 1961 to 1990 at Mosul, Baghdad and Basra stations' locations are used for downscaling. They are grouped into two categories: the first set ranges from 1961 to 1970 and is used to establish a statistical relationship with the NCEP climate data, which will be used to calculate future climate changes; the second set of observed data ranges from 1971 to 1980 used to independently to verify the downscaled ET data before synthesising future scenarios.

The choice of predictor variables is one of the most influential steps in the development of statistical downscaling procedure. Identifying empirical relationships between gridded predictors and single site predictands is central to all statistical downscaling. The choice of appropriate downscaling predictor variables based on seasonal correlation analysis, partial correlation analysis, and scatter plots. One of the approaches is to choose all predictors available, see Table 5.2, and run the explained variance on a group of eight

or ten at a time. As an outcome of the grouping process, those predictors which have high explained variance are selected. Then partial correlation analysis is done for selected predictors to see the level of correlation with each other. There could be a predictor with a high explained variance but it might be very highly correlated with another predictor. This means that it is difficult to tell that this predictor will add information to the process and therefore it will be dropped from the list. Finally, the scatterplot indicates whether this result is due to a few outliers or it is a potentially useful downscaling relationship. The selection of predictor climate variables is affected by the influence of the variables on the climate of the study area and by the availability of predictor variables in both the NCEP and GCM data archives. Predictors are chosen on the basis of predictor predictand partial correlation, percentage of variance of predictand explained by predictors, and sensible physical predictor-predictand relationships.

Based on the results, suitable predictor variables are chosen for the ET as presented in Table 5.3.

Table 5.3: Downscaling models and large scale atmospheric predictor variable used to downscale ET for the Tigris River Catchment

Predictand	Location	Predictor abbreviation	Predictor
Evapo[transpi]ration	Mosul	mslpaf	Mean Sea Level Pressure
		p_uaf	Surface Zonal Velocity
		p5_vaf	500 hPa Meridional velocity
		p500af	Relative Humidity at 500 hPa
		p8_vaf	850 hPa Meridional Velocity
		p850af	850 hPa Geopotential height
		tempaf	Mean Temperature at 2m
	rhumaf	Near Surface Relative Humidity	
	Baghdad	mslpaf	Mean Sea Level Pressure
		p5_vaf	500 hPa Meridional velocity
		p8_vaf	850 hPa Meridional Velocity
p_uaf		surface zonal velocity	

Predictand	Location	Predictor abbreviation	Predictor
		tempaf	Mean Temperature at 2m
		rhumaf	Near Surface Relative Humidity
	Basra	mslpaf	Mean Sea Level Pressure
		p_zhaf	Surface divergence
		p_thaf	surface wind direction
		tempaf	Mean Temperature at 2m
		rhumaf	Near Surface Relative Humidity

The model calibration process constructs downscaling models based on multiple regression equations, given daily weather data (the predictand) and regional-scale, atmospheric (predictor) variables. The model type determines whether individual downscaling models will be calibrated for each calendar months, climatological season or entire year. The model is structured as a monthly model for both precipitation and temperature downscaling, in which case twelve regression equations are derived for twelve months using different regression parameters for each month equation. Finally, the data period should be set in order to specify the start and end date of the analysis. The calibration is done for a period of 20 years (1961-1980).

One of the criteria commonly used in evaluating the performance of any useful downscaling method is whether the historic (observed) condition can be replicated or not. It is therefore imperative that the methods used for transferring results of climate models to meteorological stations generate ET time series that have the same statistical properties as observed meteorological data that is used for hydrological modelling. Thus HadCM3 is downscaled for the baseline period for two emission scenarios (A2&B2) and statistical properties (mean & variance) of the downscaled data is compared to observed data. By using the selected predictor variables and observed ET from the study period, the SDSM model is calibrated. Figure 5-9: Visual Representation of how the generated daily ET values correspond the 'modified' observed ET over the Northern Region. shows



NCAR observed and downscaled mean monthly ET for Mosul station. Mosul data sets at this point in particular as it has considerably less number of daily missing data, which are only 105 missed values when it is compared against Baghdad station for example, which has missed values for about 2687.

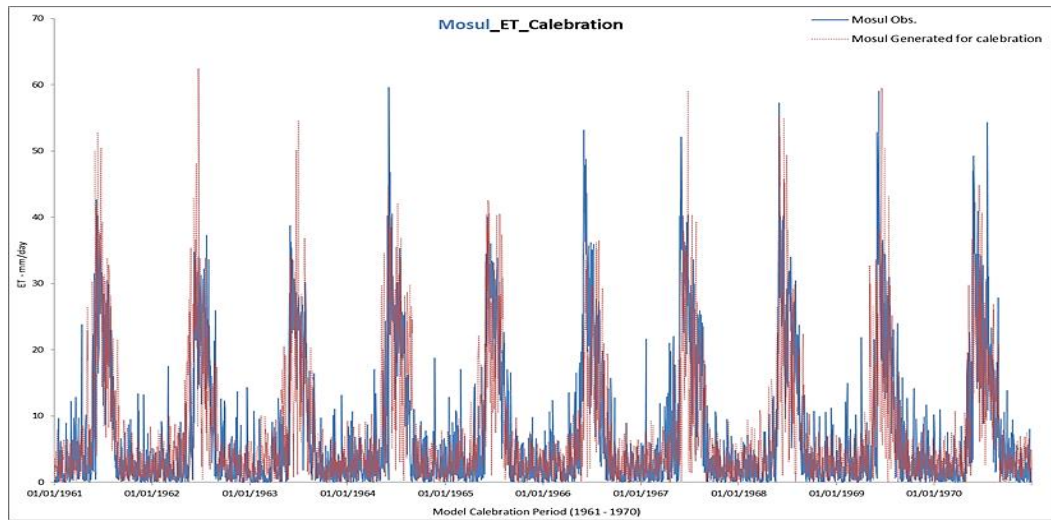


Figure 5-9: Visual Representation of how the generated daily ET values correspond the 'modified' observed ET over the Northern Region.

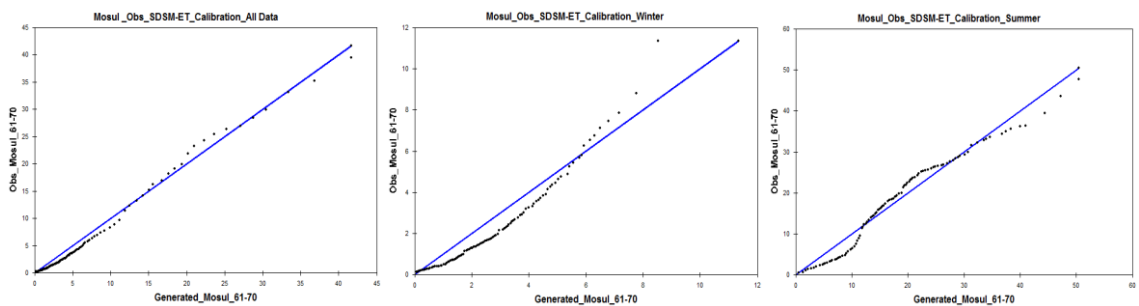


Figure 5-10: Northern downscaled ET model representation for the period 1961 to 1970 (SDSM Default)

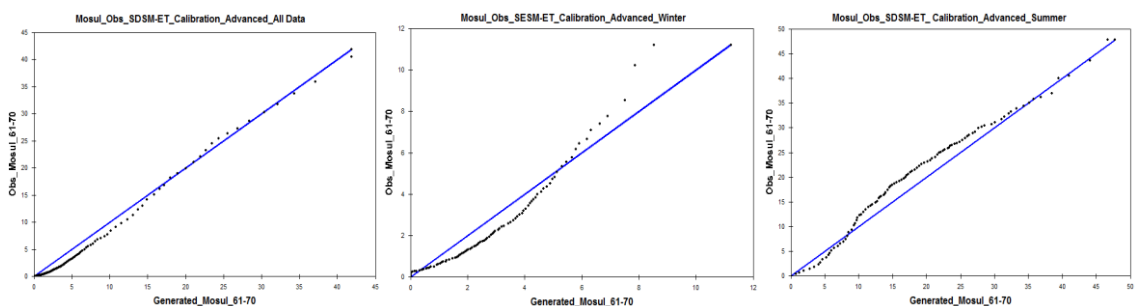


Figure 5-11: Calibration of the downscaled model for the period 1961 to 1970 (after model setting changes)

The default SDSM global settings are well selected first (Figure 5-10). Only some adjustments in the model stochastic parameters, namely variance inflation, bias correction and model transformation were made for better data fitting and comparing purposes (Figure 5-11).

After implementing the calibration utilising the observed data from the period 1961 – 1970 and the generated data set for the same period, there were only few changes have been noticed. It should be noticed that  $R^2= 0.995$  and Nash-Sutcliffe Coeff. = 0.979 for comparing the all observed vs generated, for only winter period  $R^2=0.918$  and Nash-Sutcliffe Coeff. =0.800,  $R^2 = 0.977$  and Nash-Sutcliffe Coeff. = 0.955 for summer. The mean ET ensemble scenario is synthesized with respect to the validation data. This is done by incorporating NCEP predictor variables for the period of 1971 to 1980.

Figure 5-12 shows the observed and downscaled Daily ET in Mosul station for the period of validation (1971-1980). As can be seen in this figure, ET frequency of wet days and hot days are captured quite satisfactorily.

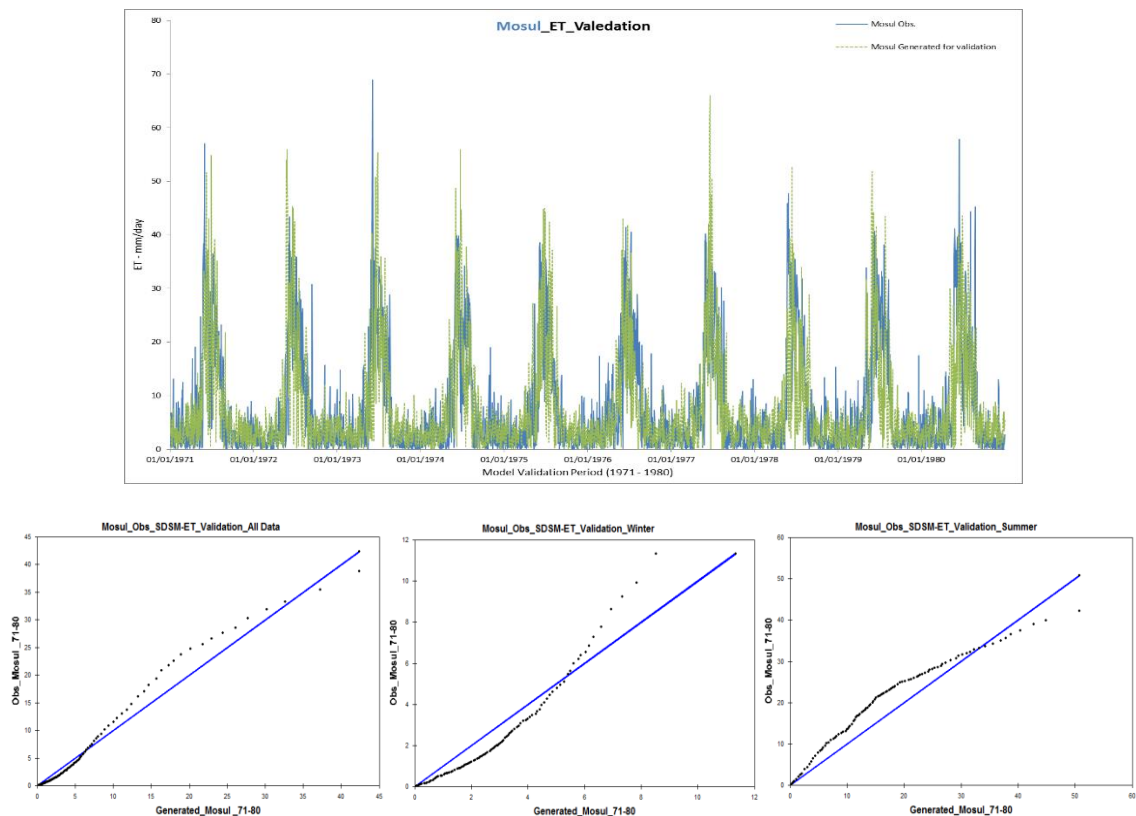


Figure 5-12: Validation of the downscaled model for the period 1971 to 1980

The SDSM model performs reasonably well in estimating the ET except for the winter season of the validation period (figure 5.12). This result, however, can still be considered as satisfactory given the fact that ET downscaling is more problematic than any other variable like for example when estimating temperature and/or precipitation, because daily ET amounts at individual sites are relatively poorly resolved by regional-scale predictors. The choice of predictor variables is one of the most influential steps in the development of statistical downscaling procedure for the ET. The ideal predictor must be strongly correlated with the target variable, physically sensible and plausible, well represented in the GCM control run, and capture multi-year variability.

Daily ET amounts at individual station continue to be the most problematic variable to downscale. The SDSM manual gives some examples about the expected variances values from the predictors: temperatures values could reach 85% and precipitation values from 10% to 15% (and in some cases below 10%). The average variance for ET is very typical, as in this study's case the ET variation was a range from 55% to 74%. This arises because of the generally good predictability of daily ET amounts at local scales by regional forcing factors. The relatively average variance for ET underlines the more stochastic nature of ET occurrence and magnitude. In the same time, it could be considered as an indicator for the difficulty to capture the characteristics of the variability of the ET regime in the downscaling process, as also suggested in other studies e.g. Wilby and Wigley (2000); Wilby et al. (2003).

The downscaling outputs ability to represent the baseline climate is a necessary condition to have reasonable confidence on the reliability of the climate change anomalies computed from the scenarios runs. Although the calculated correlation coefficients for the ET can be an indicator for high uncertainty and relatively a poor quality of downscaling, but in the case of Tigris River region. The resulted ET can be very useful for such research purposes, despising the fact that the resulted downscaled ET even after careful screening of most relevant predictors, some of the downscaled output is still significantly different from the observed values. This is especially the case for

downscaling ET and its variance for the winter season of the validation period and with such uncertainties in downscaled data for the baseline period it will be fine to have large confidence in the downscaled values for future climate scenarios and to use these for meaningful climate change impact studies. It should be noted that any uncertainty associated with ET implies high uncertainty in river losses estimation. For that, there is a need for more refined GCM results and more understanding of predictor-predictand relationships for making feasible management decisions. Baghdad data sets could be a good example for utilising the statistical downscaling model SDSM in bridging the gaps and reconstruct the historical observed data. Figure 5.13 highlights the ability of SDSM in reconstruct Baghdad's daily datasets for the period from 1961 - 1980.

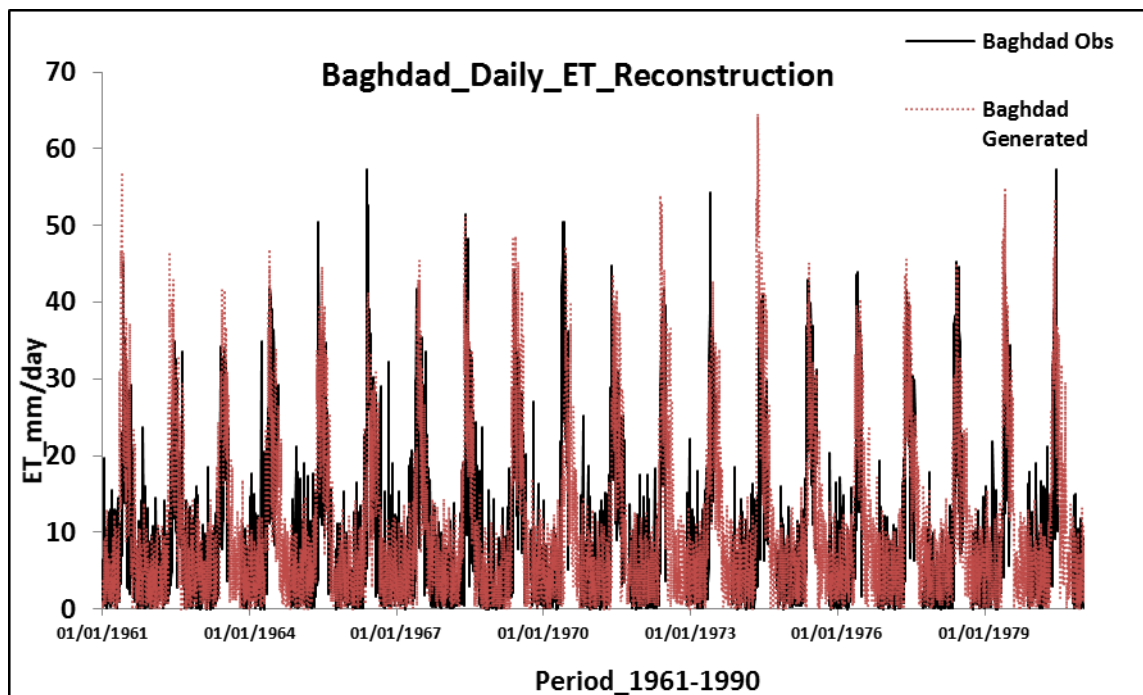


Figure 5-13: Data missing values substitution/simulation using SDSM over the middle region (Baghdad).

As a result, synthetic daily time series were produced for the two emission scenarios (HadCM3A2a and HadCMB2a) for a period of 139 years (1961 to 2099) (figures: 5.14 – 5.16). The ET downscaling process requires more attention as it is more complex than other meteorological variables to estimate (e.g. temperature) because, in general, at individual sites the amount of daily ET are relatively weakly resolved by the regional-scale predictors.

The climate scenario for future period was developed from statistical downscaling using GCM predictor variables for two emission scenarios based on the mean of one ensemble for the period from 1991 till 2099. The length of these periods is chosen to be long enough to allow drought/flood frequency analysis when considering the river water losses later. The annual changes of future ET projections with respect to the baseline period (1961-1990) are shown in figures (5.14 – 5.16). The ET results show that the future periods will dramatically increase. That makes a good chance to conclude the significance of the ET losses from the river.

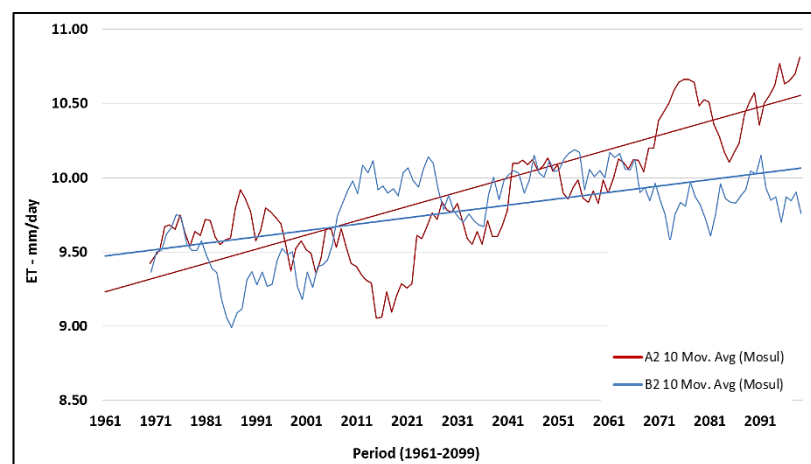


Figure 5-14: Tigris northern region annual average ET for the period from 1961 to 2099 using downscaled HadCM3 A2 and B2 models

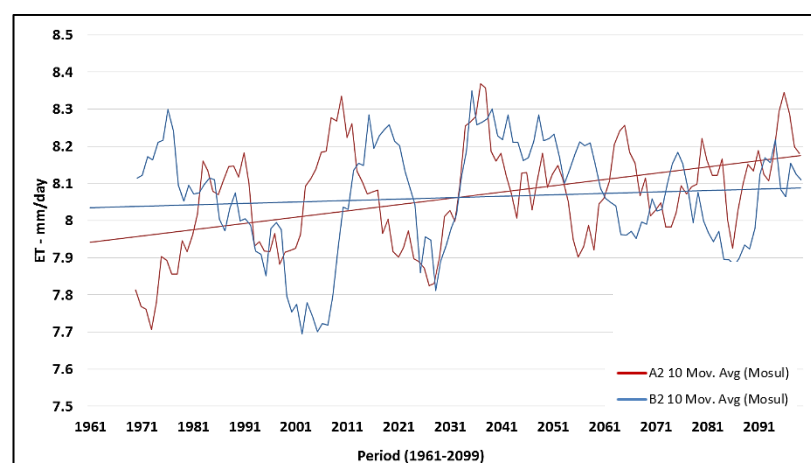


Figure 5-15: Tigris Middle region annual average ET for the period from 1961 to 2099 using downscaled HadCM3 A2 and B2 models

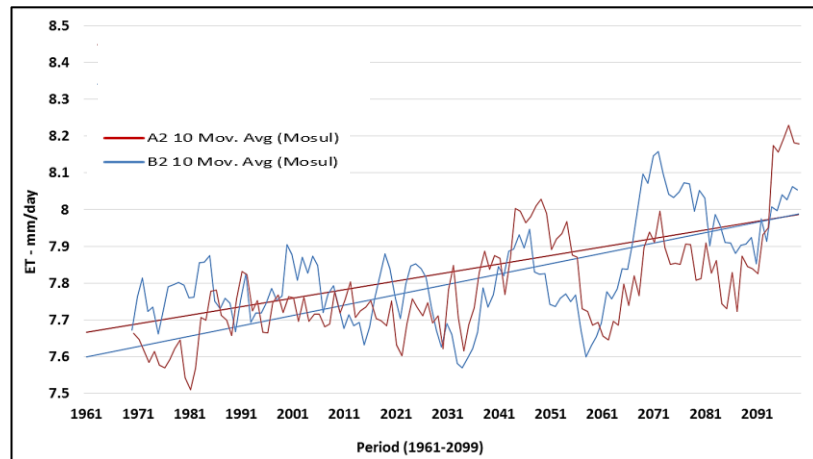


Figure 5-16: Tigris southern region annual average ET for the period from 1961 to 2099 using downscaled HadCM3 A2 and B2 models

Both of the examined climate scenarios recorded a noticeable increasing over the study period. Downscaled results show consistency between the A2 scenario and the B2 scenario over Tigris regions. The northern region ET is the highest as expected. The mean average ET losses in the northern region is about 9.7mm/day over the 140 examined period, while in the middle and the southern regions, ET records 8.3 and 7.8mm/day respectively. Compared with the B2 (5.2%, 0.6% and 5%) scenario, the A2 (6.4%, 3.8% 4.6%) and scenario shows more increase in yearly mean ET, which leads to which can be an evidence as well to increase the temperature and decrease in precipitation for example.

## 5.5 Summary

Monthly observed evapotranspiration data were collected from locations along the river Tigris alongside with other meteorological data (e.g. Max & Min Temperature, Relative Humidity, Wind Speed, Solar Radiation, etc.). These data sets were exclusively provided for this study by the Iraqi water resources ministry to develop an accurate estimation of the Tigris River losses.

Trend analysis was conducted using monthly observed ET data using Pan Class (A) method and covering the period 1969 – 2000 indicating that each region within the whole basin has recorded increases of evapotranspiration losses. In addition, each region has

recorded its own ET values because of the variance of the meteorological and topographical characteristics between each region. The southern region (Basra) gave a lower rate of ET while it is hotter when compared it to the other regions. The northern region (Mosul) has recorded the highest ET rate.

To investigate this further, it was decided to exploit the other metrological data available to model the evapotranspiration performance historically. According to the literature, there are a numerous ET models no a consistent evidence exists about which ET model could be used to give good simulation outcomes. For this reason, it was decided to conduct a comparative analysis based on the complexity of the models (the number variables are needed) for number of well-known ET models to see which one performs best to give accurate ET losses. The results for indicate that all of the nominated models were under estimating the observed data. Hargreaves Evaporation Mass Transfer (ETH) has given the most reasonable ET values compared to the models.

In this study, statistical downscaling approach is applied to synthesise future ET scenarios for the Tigris river basin, Iraq, rather than relying on downscaling other variables such as temperature, relative humidity, precipitation, solar radiation, etc. and employ them again to calculate ET. That required finding a relationship between the available monthly observed ET values with NCAR daily data. The resulted data sets were used as a baseline to predict ET for up to 2099 using SDSM. The SDSM decision support model is used to assist in constructing future regional scenarios. The model is first calibrated for period 1961 to 1970 using modified daily observed ET at Mosul station, with atmospheric and circulation predictor variables from NCEP gridded data that cover the study area. After that, the SDSM model is applied to generate future period (1981 to 1990) which was considered for verification. Future implementation is performed with predictor variables using the output from HadCM3a2A and HadCM3B2a GCM scenarios experiments. The synthesised future scenarios will be used directly are used as an input to the hydrodynamic model ISIS in the next chapter to study the future impacts of the ET on simulating future stream-flow of Tigris.

The downscaling results show that ET losses will become gradually higher in future periods. The result clearly shows that the magnitude of lost ET with a percentage of Compared with the B2 (5.2%, 0.6% and 5%) scenario, the A2 (6.4%, 3.8% 4.6%) and scenario shows more increase in yearly mean ET. Consequently, that would give a significantly increase of frequency of flow.

There are a number of limitations concerning the assessment of climate change on the water resources. Firstly, due to data availability and high computational time demand, outputs of only one GCM and two emission scenarios limits the assessment. Secondly, prediction of the future climate is based on statistical predictor-predictand relationships that exist for the present condition, but which will not necessarily remain the same in the future. The downscaling is also performed only at three points along the basin and the results were then applied to the entire study area. This is due to the lack of long time and reliable measured daily data of ET, which in the study area are only available at Mosul, Baghdad and Basra stations. Thirdly, high uncertainty associated with ET prediction implies high uncertainty in predicting river flows for future periods, indicating the need for more refined GCM results and/or a better understanding of predictor-predictand relationships for making feasible management decisions.



## Chapter Six: River Modelling

This chapter outlines the numerical modelling methodology used to analyse river water losses located in arid and semi-arid catchment in a developed country. A hydrodynamic model is built using ISIS 1D for the examined reach as described in chapter 2. The examined Tigris reach starts from Mosul Dam, taking in the account the contributing tributaries downstream and ends in Basra where the Tigris meets the Euphrates at Qarmat Ali (refer Chapter 3). The potential ability of ISIS to represent the spatial and temporal distribution of the water losses for arid and semi-arid basin is investigated.

This chapter highlights the significance of the Evapo[transpi]ration for the river (which was assessed in chapter 5) alongside with assessing other water losses' sources. That in turns provides a chance to assess possible future impact of climate change on water resource availability for this region.

It has been decided to utilise a hydrodynamic computer modelling tool to implement this objective. ISIS – 1D is a widely used hydrodynamic model for simulating flow and water levels. It requires robust data sets of historical and simulated initial and boundary conditions including river flow and water levels, and topographical data, etc., to give accurate results. A novel methodology is presented here to generate river profiles for shallow rivers using remotely sensed data. ISIS – 1D can be used to help in assessing the impact of the Evapo[transpi]ration for the outlined stream flow in the previous chapters.

This chapter describes all the available input data that was used in the ISIS – Tigris model, and investigates the quality of those data as the model's boundary conditions as well as for the model results. Understanding the changes in river flow and water level is important to develop water resources and water scarcity strategies. This is particularly important as the uncertainty of the non-linear relationship between climate and

streamflow is expected to increase as a result of the amplified climate variability under predicted climate change scenarios (Bates et al., 2008).

Integrated management of streamflow under new foreseen uncertainty is needed to balance the competing demands. Such a management study will support water supply, ecosystem protection, etc. Assessment of the effects of climate change therefore requires understanding of effects on streamflow variability, including high and low flow extremes across a wide range of time scales, from hours and days in the case of floods) to months and years for water losses.

The developed ISIS model has been used in this study to assess discharge changes in order to give a better understanding of the effects of the climate change on water losses from a river located in arid catchment in a developing country due to Evapo[transpi]ration.

## 6.1 Boundary Conditions

A large part of the Tigris River network was simulated with ISIS using a series of individual 'building blocks' known as hydraulic units. Each unit represents a particular hydraulic attribute of the modelled network, e.g. a river section, a junction, etc. Historical river flow and level data were obtained from a wide range of sources, analysed, and then used as boundary conditions. Some data have been provided by IWRM and other data have been collected from literature (as outlined in chapter 2).

Firstly, a comprehensive river profile is needed. It can represent channel dimensions (length and width(s)) and elevations (topographic data) as well as a historical record of the water discharge. Secondly, initial and boundary conditions are prerequisite; and finally, floodplain topographic data as well as channel roughness information water stage data are needed for model validation and calibration.

An in-depth understanding of the river bathymetry including 2 and 3 dimensional cross section data along the river, especially at critical points e.g. bends, hydraulic structures, waterfalls and lakes to accurately analyse the river water losses.

The spacing between channel cross sections is a critical factor to assess the errors introduced by lowering cross section resolution and survey inaccuracies (Burnham et al., 1990). Table 6.1 gives some recommended values for relationships of the required minimum cross section spacing to channel slope for slopes ranging from 0.1 to 3.3m/km for the section spacing for 75 to 1000m (Samuels, 1995).

*Table 6.1: Cross Section Spacing Recommendations in 1D Hydraulic Models*

<b>Channel Slope (m/km)</b>	<b>Section Spacing (m)</b>
3.3 – 1.0	75
1.0 – 0.3	200
0.3 – 0.1	500
< 0.1	1000

In this case, the available surveyed cross sections are spaced at 500 to 1000m for channel slopes ranging from <0.1 to 0.3.

Required initial conditions consist of flow record inputs from the upstream of the reach and any tributary inputs. A steady state flow simulation requires upstream flow data and information at the start of the period of investigation. The water flow and levels data output of this steady simulation then provides the initial conditions to an unsteady simulation.

One of the features of ISIS is allowing the representation of the river floodplains in different ways. The easiest one is simply extending or following on with the same slope of the channel cross section. However, in that case, different roughness parameter values should be considered for the channel wetted parameter and the floodplain. Another way in which the floodplain can be represented is by generating spill units at the top of the channel banks connecting the main channel to the floodplain, which can either be represented by a parallel channel or storage/reservoir units (Lin et al., 2006). This approach provides representation that is more accurate but is computationally more demanding. Details and information are required for the roughness data for the whole channel and the floodplains along the simulated river profile. The only way of getting

such data is to calculate Manning's number in different places along the modelled reach using the available discharge records, river hydraulic slope and river profile characteristics and then compare it to published data. A set of river discharge and water levels are required to calibrate and validate the model. Those data sets are identified in the following sections:

### **6.1.1 Discharge of Tigris River**

One of the most important input facilities in ISIS model is the Flow Time Boundary unit. It can be utilised to model the discharge hydrograph which is specified as a boundary condition at the upstream end of the modelled network. A discharge data set namely Mosul\_Dam was incorporated as data pairs comparing monthly averages flow and time start from January 1970 to January 1985 at this stage of the study (Figure 6-1), only because of the lack of data due the severe armed conflicts in that time.

This facility gives the opportunity to check the input data before the computational run is carried out as well as specify the time increment which is added into the model for the preceding flow vs time when new discharge data is inserted or appended. The water inflow records are important in the process of identifying and assess the potential river losses alongside water supply and demand. In this study, five discharge data sets including the Mosul Dam, (Tigris tributaries, namely, Great Zab, Lower Zab, Adheem and Diyala were introduced into the model. Initially, average monthly discharges for the period from 1970 until 1985 for those streamflow gaging stations within Tigris River basin in Iraq were used in chapter seven to help assessing the reduction in available water resources and evaluate the consequence of the increasing water demand. There is another discharge data set available that can be extend to the year 2000 but it is suffering from considerable gaps and discontinuity. It has not been represented here as it might disturb the trend projection of the river flow. However, they are still being used in later stages.

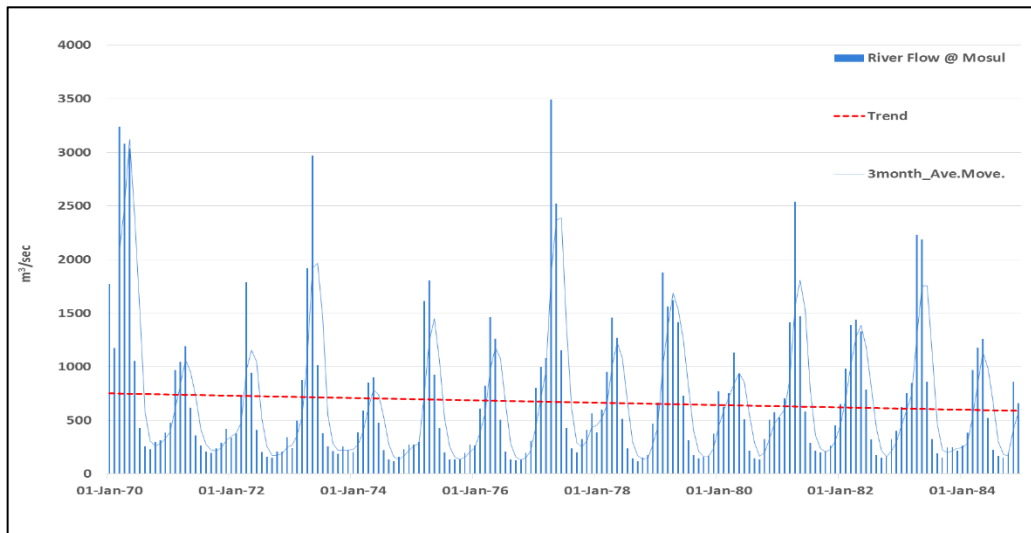


Figure 6-1: 15 years' worth of monthly mean discharges at Mosul Dam streamflow-gaging station extracted from Saleh (2010) and edited by the author.

The water discharge data were used to generate trend lines of discharge versus time. These trend lines were then applied to estimate already ongoing reduction in water quantities over the period from 1970 until 2000. Figure 6-1 highlights that about 5.45% (from 650 m<sup>3</sup>/sec to 618 m<sup>3</sup>/sec) decreasing in mean monthly average water releases over the selected 15 years (from 1970 to 1985) to the Tigris River from Mosul Dam in the upstream end.

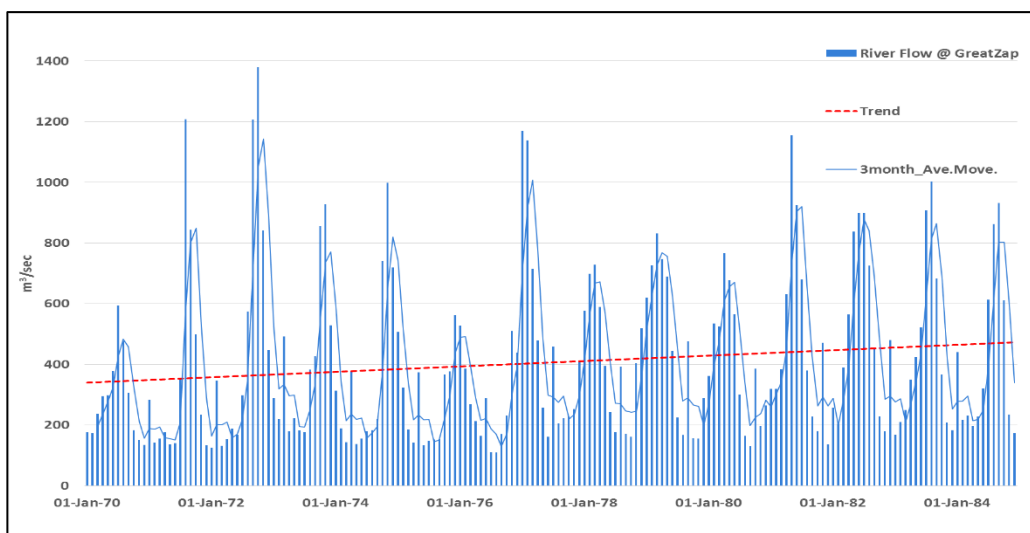


Figure 6-2: 15 years' worth of monthly mean discharges at GreatZab Tributary streamflow-gaging station extracted from Saleh (2010) and edited by the author.

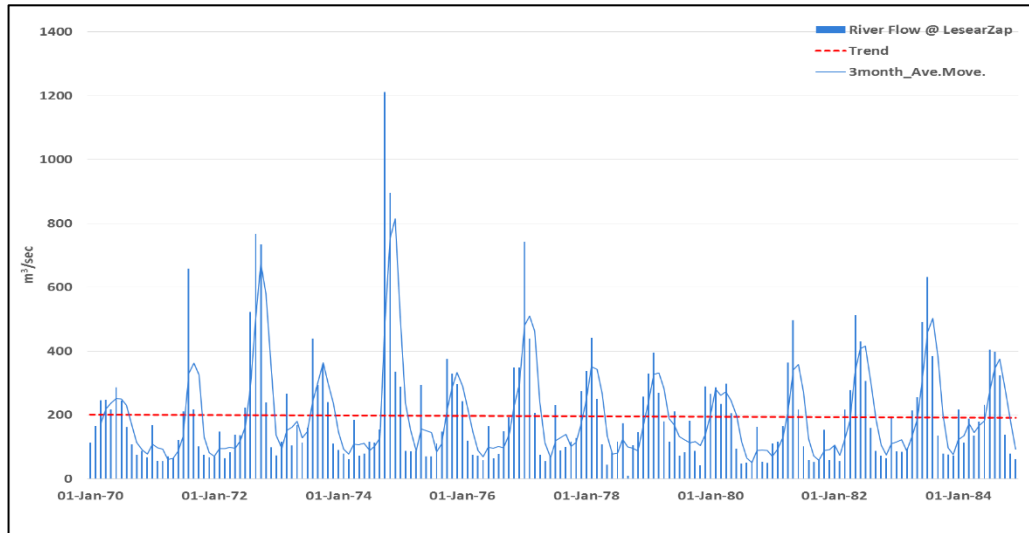


Figure 6-3: 15 years' worth of monthly mean discharges at LesearZab Tributary streamflow-gaging station extracted from Saleh (2010) and edited by the author.

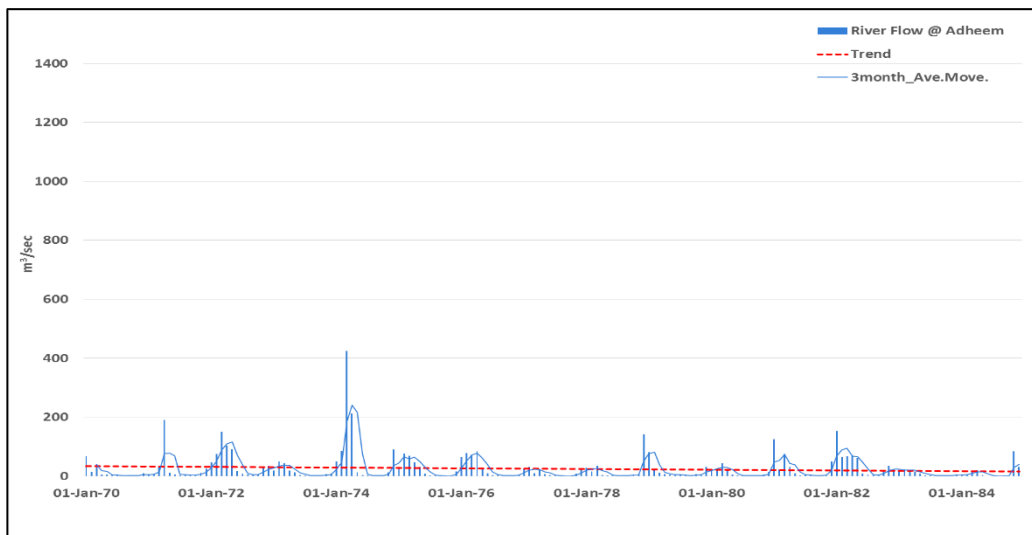


Figure 6-4: 15 years' worth of monthly mean discharges at Adheem Tributary streamflow-gaging station extracted from Saleh (2010) and edited by the author.

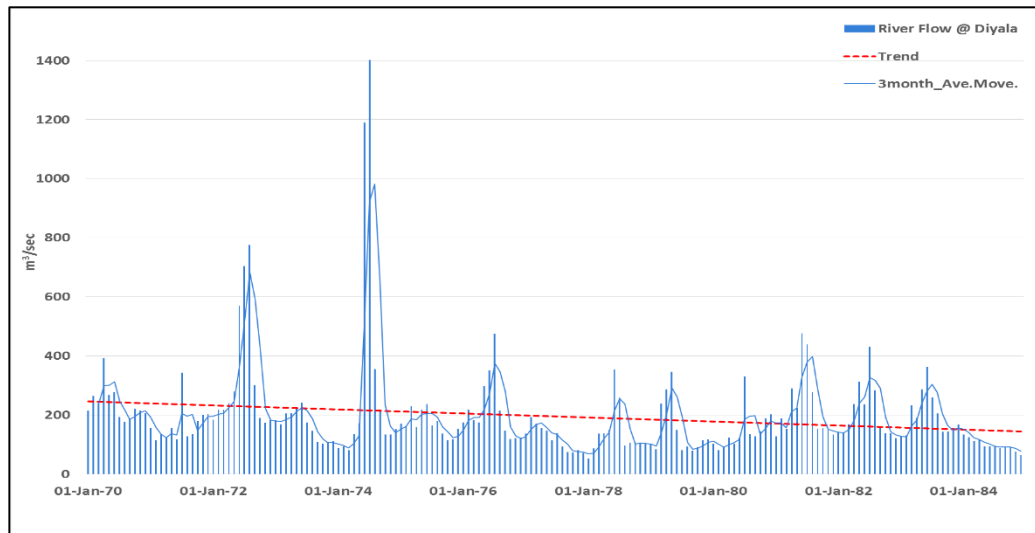


Figure 6-5: 15 years' worth of monthly mean discharge at Diyala Tributary streamflow-gaging station extracted from Saleh (2010) and edited by the author.

Figures 6.2 to 6.5 have been processed from the same source of data. They represent the monthly averages of the water discharge from tributaries flowing into Tigris downstream of Mosul Dam (refer to Chapter 3). The analysed water discharge data of these gauging stations were then used to estimate the average annual flow of the entire river network (refer to chapter seven). Most of them indicate reduction in discharge (LeaserZab – 5%, Adheem – 8.5% and Dyala – 17.8%). Only the GreatZab tributary recorded increasing by about 6.5% from its mean monthly average which is  $423\text{m}^3/\text{sec}$ . The downward recorded of the water availability over the period from 1970 to 1985 is believed to be due to the increasing demand and possibly the consequences of climate change. Over all, the discharge of the main reach of Tigris River and most of its tributaries are showing downward trends for the investigated period of 1970 – 1985.

### 6.1.2 Tigris River Profile Development

There are several definitions for the river cross sections (CSs). Some studies have defined CSs as simple as being paths across a river that lie orthogonally to the river flow direction, e.g. Harrelson et al. (1994). Other studies like Rhoads et al. (2003) identify the CSs as encompassing the geomorphological diversity of a river from detained

topographic mapping. Pavelsky et al. (2008) defines CSs as river flow widths, which are where cross sections would be measured, as the shortest cross sectional distance from the water's edge to the other, vertical to the reach channel. All of those definition are acceptable, however, any river is subjected to flood/drought events; so limiting the definition to the river water surface is not enough, and it could be extended to include the river banks and also some of the floodplains. Implementing water quantity assessments and water balance studies for any river requires a comprehensive and sufficient representation of the river channel and floodplain geometries alongside with an accurate assessment of its hydraulic characteristics (Nicholas et al., 1997). A river profile as the most important input of a hydraulic model, and the details and accuracy of the representation of the channel geometry are a very significant determinant of model performance (French et al., 2000, Pappenberger et al., 2005).

Hydrodynamic models require a continuous representation of the channel bed. In the majority of situations, a portion of the main channel remains under water and thus it is difficult to create a terrain model for the channel from LiDAR survey or photogrammetry. Linear interpolation of the available surveyed cross-sections is not straightforward due to various facts including bends in the river, existence of channel islands not captured by a sufficient number of cross-sections and failure to capture the river thalweg (Merwade et al., 2008), etc.

It should be noted that, when there is a need to survey a river and its floodplain, cross-sections can extend onto dry land some times. Depth measurements or river bed elevations are collected at specific intervals and noticeable breaks in slope along a cross-section depending on the river or defined cross-sectional width. The depth between these points is interpolated to produce a continuous cross-sectional profile. These profiles allow for the wetted perimeter of the river to be calculated. The wetted perimeter is an important river characteristic that is often utilized for estimating a river's minimum allowable flow and for predicting areas of suitable habitat (Gergel et al., 2002).



One of the most important boundary conditions for the hydraulic model used in this research is, the cross sectional data along the study area. As for this study, ideally, and accounting to Table 6.1, one cross section for each kilometre distance covers 850km along the reach. Building a river profile for such a long reach is technically demanding. As there were data available only fourteen observed cross sections were conducted by different methods for different locational along the river.

For that reason, several methods to generate river profiles have been examined and compared in this study to find the best method to aid the research case. This section investigates the viability of a method to develop a whole river profile, a river profile that contains reasonably good resolution cross sections in desired locations. A method which can be used to measure whole floodplains, river slope and other hydraulic characteristics as well as being able to define the locations and the types of any hydraulic structures or any other obstructions (lakes, marshes, algae, etc.) along the river flow. This method will help to open a new avenue for scientists who use hydraulic models (e.g ISIS and Hec-RAS) in areas with a severe lack of data. Data unavailability can be due to a number of reasons, for example, financially and or field accessibility for politically unstable countries like Iraq. These countries often are in water basins which need significant and accurate water balance studies to be carried out urgently due to the magnitude of the water losses. The examined methods are illustrated as follows:

1. Traditional methods:

Theodolite intersections, theodolite stadia, electronic distance measurement, depth-surveying bar, lead-line, handled survey and echo sounder are the main methods used for water bathymetry. Such methods provide river cross-sections data with high-resolution relief surveys. However, they are too expensive relating to many research budgets. Also sometimes, these methods are not only prone to the inaccuracy of instruments, distances, weather conditions, indivisibility and communication device, but also involved in tedious workload which leads to low efficiency. Some unfavourable factors such as the flow of the water and the nonlinear movement of the surveying ship

make measuring the depth of the water more difficult. Lack of skills and cooperation among surveyors might result in a low accuracy in the position fix of cross-section points, thus further affects the quality of cross-section survey of the river (DEC, 2006).

## 2. Software tools:

have been (and are being) developed and updated to extract spatial features that are useful for hydraulic models, from topographical data sources, both in GIS (Merwade et al., 2008); (Tesfa et al., 2011) and non-GIS environments (Schwanghart et al., 2010). However, obtaining detailed topographical data for every river basin under study is a difficult task as the process involves an expensive and time consuming survey campaign (ground or airborne) and a painstaking post-processing of the survey data (Liu, 2008); (Mandlbürger et al., 2009); (Merwade et al., 2008). Other studies have been implemented to deal with topographical data scarcity in river flood modelling. Most of those studies rely on the integration of GIS with digital elevation models (DEMs) which are obtained from remote sensing satellites for example, (Asante et al., 2008); (Herath et al., 2003); (Merwade et al., 2005); (Sanders, 2007).

## 3. Satellite Images:

Approaches which depend on satellite images only provide information used to define the topographical data for flood propagation modelling (Qi et al., 2011), but they are not only able to completely describe the river cross section in full since the sensors cannot penetrate much deeper than the water surface. This has led to work using data assimilation techniques which attempt to identify a (synthetic) cross-section that is hydraulically equivalent to the real river geometry (Honorat et al., 2006); (Roux et al., 2004). These approaches rely on linear interpolation and either hypothesising the geometry of the cross section. The characteristics of this geometry are estimated to consider the topography of the overbanks in the assimilation process. They need a high resolution of satellite imagery. Nevertheless these techniques are still subject to river

bed and other river profile features guesstimations as such techniques need a dense of observation data not only about the river cross sectional profile but even require water elevation and flow velocity detailed information which are not always available. Only five cross sections (S36, S46, S49, S63, and S64) out of 14 can be utilised to test the reliability of the cross section generation methodologies above at once, are represented in Figure 6-6. That was because only those 5 had their own floodplain slopes extended, which can be used to synthese cross sections (cross section developing method – type 3).



Figure 6-6: Shows Mosul City Centre and Tigris River. The locations of the five cross sections are illustrated as red lines crossing the river.

Alongside the remarkable presentation of the river and the topographical area features, this figure shows the ability of Google Earth to provide other details in high resolution within the river itself, for example, bridges, islands, other hydraulic structures, farms and urban areas. Details that would often not be noticed by other DEM providers. This study suggests a new method of generating river profiles for data sparse areas with improved

hydraulic characteristics, using Google Earth and 3DRouteBuilder. This method is simple and can assist hydraulic modellers who are carrying out studies in areas with a severe lack of data. The Tigris River in Iraq has been chosen as a case study site for this method, since it is a large river with very few measured cross sections.

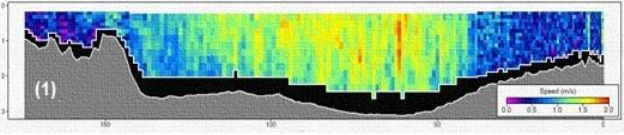
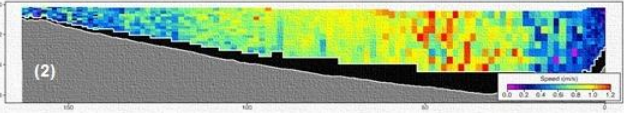
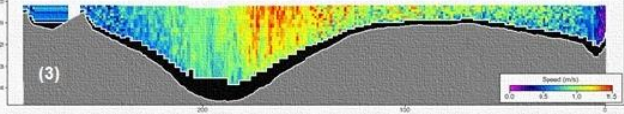
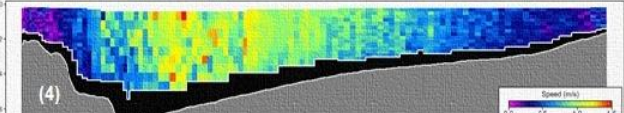
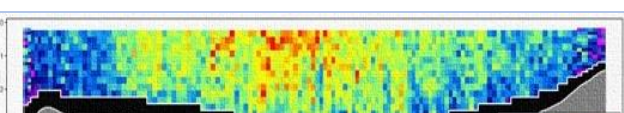
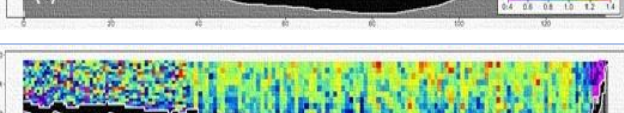
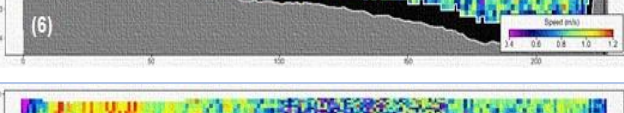
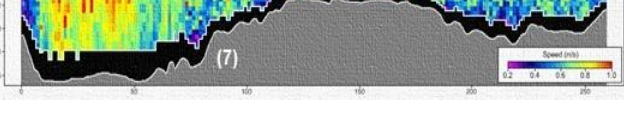
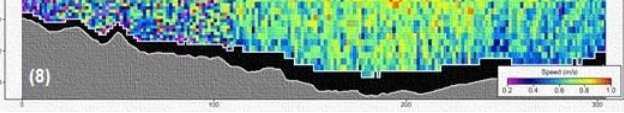
### **6.1.2.1 Observed Data Base**

In the following, a combination of pre identified river cross sections locations, most of them have been provided exclusively from the Iraqi ministry of water resources (IMWR) for this study and others have been obtained from the literature are considered as field measured data (see Table 6.2 and Table 6.3). Those observations were used to validate other approaches of extracting river cross sections. The comparative analyses include calculation and review of the simulated hydraulic characteristics against observed ones.

The first step was extracting cross-sections from the NASA SRTMGL3 and compare them to the observed ones in terms of the locations using ArcGIS Geo-processing tool. The second step was utilising the observed river banks' slopes and interpolate them to generate synthetic cross sections. The third one was extracting cross sections from the same pre identified locations by using Google Earth through a free licensed GPS editor called 3DRoutBuilder. As a result, the best obtained river cross-section data are incorporated within ISIS-1D modelling software package to carry out river losses estimation covering the whole downstream basin of Tigris River Basin, Iraq.



Table 6.2: observed cross sections' details obtained in different locations along Tigris River using the River Surveyor technique and provided exclusively to this research

Cross-section	Location	Source
	Mosul 36°36'18.58"N 42°48'59.26"E, elev. 255m	IMWR
	Al-Sherqat 35°31'56.39"N 43°14'25.51"E, elev. 145m	IMWR
	Bijee 34°55'56.36"N 43°31'02.11"E, elev. 101m	IMWR
	Tekreet 34°34'44.54"N 43°42'42.09"E, elev. 76m	IMWR
	Sameera'a 34°09'09.43"N 43°52'19.98"E, elev. 52m	IMWR
	North of Baghdad 33°31'07.96"N 44°18'22.14"E, elev. 30m	IMWR
	Sweerah 32°57'29.82" N 44°44'12.82"E, elev. 25m	IMWR
	Nomaniah 32°34'37.09" N 45°24'54. 67"E, elev. 19m	IMWR
	Kut 32°31'42.82"N 45°51'06.35"E, elev. 16m	IMWR

The 9 cross sections shown in the table above have been surveyed by using the SonTec RiverSurveyor System. In the manual of this tool, which is freely available online at ([www.sontek.com](http://www.sontek.com)), the entire system is described along with other useful information.

The SonTek RiverSurveyor system is a highly accurate Acoustic Doppler Profiler (ADP) system integrated with a compass/2-axis tilt sensor, temperature sensor, internal recorder, and a vertical acoustic beam (echo-sounder) specifically designed to measure river discharge, 3-dimensional water currents, depths, and bathymetry from a moving or stationary vessel. The RiverSurveyor measurement system is fitted to a manned powerboat where the ADP's transducer face should be fully submerged in water as shown in Figure 6-7.

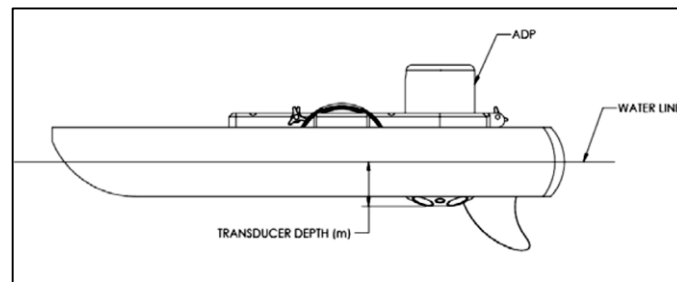


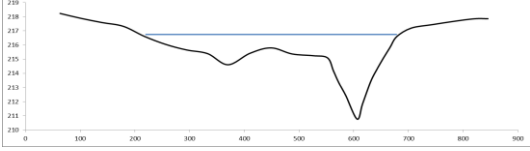
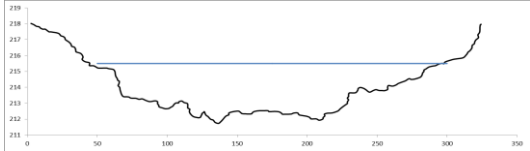
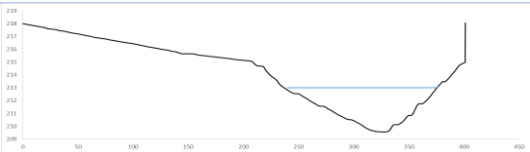

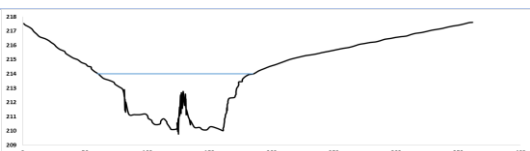
Figure 6-7: Outline of RiverSurveyor system and transducer depth

Another 5 cross sections were obtained from a previous study, (Al-Hafith, 2012), which was already published to investigate the hydraulic characteristics of Tigris River at Mosul city. Cross sections survey in this study was carried out by using the Echo Sounder – Depth Meter. The field measuring process was divided into two main stages. The first stage includes measuring river water levels above the sea level, the width of the channel as well as the channel bed dimensions. The second stage was carried out by using the same device to survey the floodplains of the river on both channel sides in addition to any islands along the river channel.

The Echo Sounder is a small portable low cost ultrasonic water depth instrument meter, which is used for measuring water depth in silting or sedimentation studies, dredging surveys in lakes, rivers, ports, sea, and inshore hydrographic surveying. It is not necessary for the device to be attached or fitted to a platform; it can be also used manually. So the accuracy of the measurement is depending on the experience of the

person who takes the measurements. It has been decided to utilise those cross sections in this study (Table 6.3).

Table 6.3: Five observed cross sections' obtained in relatively closed locations along Tigris River Reach in Mosul City using the River Surveyor technique and provided exclusively to this research

Cross-section	Location	Source
	S39_Mosul 36°21'57.72"N 43°06'35.65"E elev. 211m	(Al-Hafith, 2012)
	S46_Mosul 36°21'24.02"N 43°07'20.99"E elev. 211m	(Al-Hafith, 2012)
	S49_Mosul 36°21'12.08"N 43°07'37.93"E elev. 211m	(Al-Hafith, 2012)
	S63_Mosul 36°19'41.14"N 43°09'16.56"E elev. 211m	(Al-Hafith, 2012)
	S64_Mosul 36°19'51.99"N 43°09'19.80"E elev. 211m	(Al-Hafith, 2012)

Because of the low resolution of the cross section representations in (Al-Hafith, 2012) study, it was difficult to incorporate its figures in the format they were in. they were before digitalised in this study using "WebPoltDigitizer". Table 6.2 shows the cross sections' profiles which have been measured by SonTek River Surveyor. The water depth within the river and the river bed's width are also highlighted.

In studying the river characterises focusing on the observations, it can be noticed that, the Tigris River is a shallow and not very wide river especially in the north and the south regions. The average depth can reach 4m and the river width is typically about 180 – 250m. The width at some location can reach 800 – 1000m. The average velocity is about 1 – 1.5 m/sec as an average. Most importantly, the bed profile and depth of the water

look reasonable but the measurements do not give any details about the river banks, let alone the floodplains. Figure 6-8 has been quoted from the tool's manual as it explains that limitation very well.

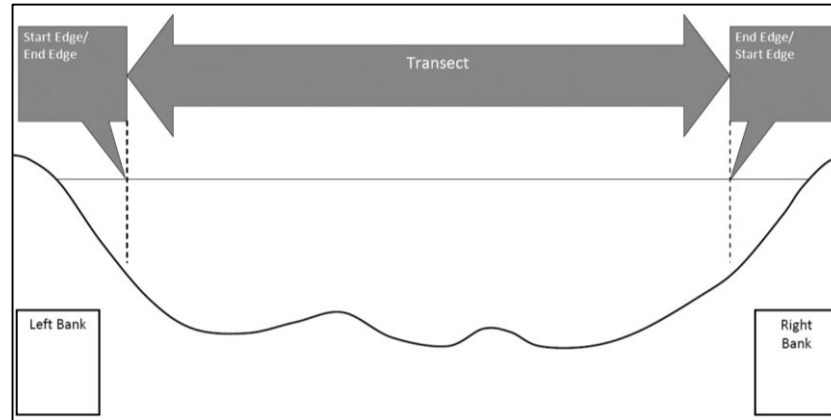


Figure 6-8: The movement range of the SonTek River survey boat (refer to Table 6.2) within the channel width represented by the double sided arrow

Table 6.3 also shows the channel width, depth(s), water level within the channel, as well as the channel elevation compared to sea level. The figure also shows the ability of this technique not only to measure the channel profile with water level including both bank sides but even for it being able to extend onto the floodplains.

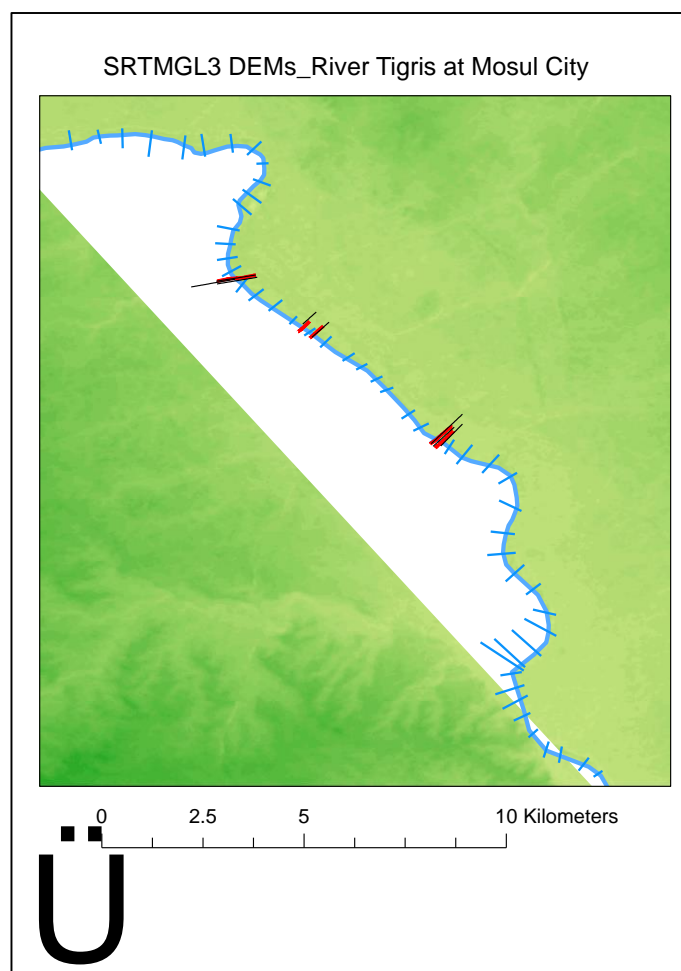
### 6.1.2.2 Shuttle Radar Topography Mission (SRTM)

The Shuttle Radar Topography Mission (SRTM) obtained elevation data on a near-global scale to generate high-resolution digital topographic database of Earth. SRTM is an international project spearheaded by the National Geospatial-Intelligence Agency (NGA) and the National Aeronautics and Space Administration (NASA). The SRTMGL3 is one of NASA LPDAAC (The Land Processes Distributed Active Archive Centre) collections. It is available to download in the website of Earth Explorer by USGS (U.S. Geological Survey) as tiles of  $1^{\circ} \times 1^{\circ}$ . It has been decided to utilise such data set because it is free accessibility. A preliminary comparison analyses has been conducted to know which digital elevation data set is better in terms of showing terrain profile. SRTM90 which is also available freely to download in the same data source above gave



insufficient output to fulfil the aim of the study, while SRTMGL3 has a finer resolution over the study area and could bring more details.

The SRTMGL3 DEMs which have been downloaded for this study are stored as tiled datasets. Those tiles are all, adjacent and have the same resolution and coordinate system. These tiles were merged together, clipped and mosaicked for the whole river stretch and processed using GIS tools to convert them into one DEM raster with one grid format. Removing the cloud layer process is also applied to improve the terrain resolution (Figure 6-9).



*Figure 6-9: A processed SRTM GL3 raster for Mosul City. Tigris River's centre line is represented in light blue line, the 5 cross sections locations are identified in red lines cross the river reach.*

The interpolate line tool from 3D Analyst Toolbox in ArcGIS was utilised in this study to determine contour, slope, and/or elevation of not just points but even lines in desired locations and digitalise them at the same time. The desired locations need to be exactly

identified. In this case, the observed cross sections' locations in were extracted using an earth browser as KML files. These KML files were converted by GIS into layers. These layers are placed automatically on the final DEM raster to represent the cross sections locations.

### **6.1.2.3 Google Earth & 3DRoutBuilder**

As an extension to Google Earth (GE) identification which is already mentioned before, GE also has DEMs imbedded within it, as it is one of GE's competitive features. Those DEMs have been used in several studies with different applications. They are also used in the hydrologic sector to generate topographic data to map catchments and watersheds (McInnes et al., 2011, Rusli; et al., 2012). However, this is controversial as the source of it being a digital elevation model (DEM) and its resolution is not being known. Some researches state that Google Earth uses digital elevation model (DEM) data collected by NASA's Shuttle Radar Topography Mission (SRTM) enabling 3D view of the whole Earth planet ([en.wikipedia.org/wiki/Google\\_Earth](http://en.wikipedia.org/wiki/Google_Earth)). The authors could not find a concrete reference for such a statement. In fact, some studies have tried to investigate what Google Earth's DEM resolution is to justify the usage of the extracted data from it by doing a comparison analysis between it and other well-known DEM data sets (Hoffmann et al., 2010). The authors of this study went even in further investigating directly with Google about it, but the response was negative.

It has been noticed that there was an announcement mentioning a high resolution 3DRoutBuilder world – wide terrain (DEMs) having been released by GE with 10m cover. An investigation was implemented by the author discovered that an update was occurred on 2nd of June 2007 which covers only the following parts of the earth: Parts of Greenland, Antarctica – some strips, Parts of Canada (area around Toronto), Catalonia part of Spain, State of Alabama, St. Paul, Minnesota, Puerto Rico, Iran, New Zealand, Parts of Russia.

Because of the lack of research found in this area, it was decided to investigate whether there is a possibility to generate reliable river cross sections to form river profile for the Tigris which can aid the modelling.

GE can be a good asset as a DEMs source according to the studies that investigated the reliability of it as an alternative to traditional unfeasible methods. It can be utilised to get more details also for floodplain cross sections that cannot be provided by the echo sounder data (observed). GE also gives great opportunity to virtually walk through the whole river and appointing critical locations, e.g. river bends, dams, bridges, etc. lively. Basically, dragging a path in a desired location, e.g. across a river within GE, that gives an elevation profile.

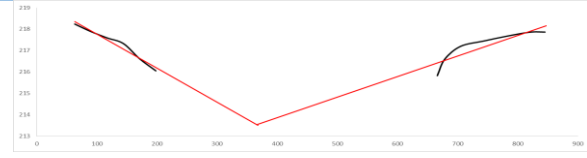
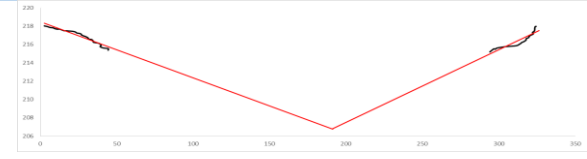
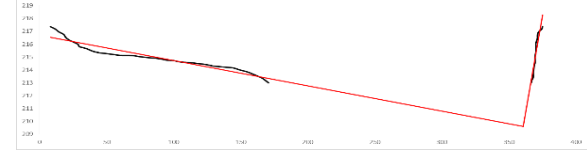
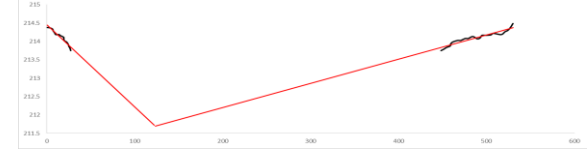
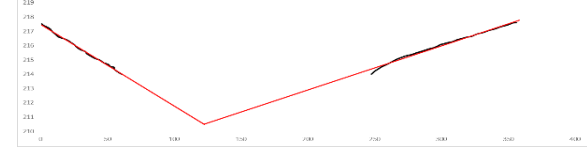
Extracting data tool is required to digitalise and analyse GE's DEMs to develop river profile elevations. The 3DRoutBuilder was tested to carry out the work and it has been approved that it has a great potential in this regard.

3DRoutBuilder is a GPS location, altitude and time route editor for high resolution control over paths directly in Google Earth or it could be for any Earth browser. After that, the extracted files can be retraced at scalable real-time speed. It adjusts altitude and location of one or more points in centimetre increments, views altitude profiles against distance, correct and smooth barometric drifts. Moreover, it also can extract altitude and location data to any other suitable formats. In addition to measuring river banks, 3DRoutBuilder was also used to measure the river beds. The resulting completed cross sections are matching the observed ones well as can be seen in the results section.

#### **6.1.2.4 Synthetic Cross Sections**

Small part of the floodplain distance and the river banks slopes on both river sides has been considered to interpolate some cross sections and including the river bed along the river. This method only works for sections (in this case only the ones in Table 6.3) that have parts of their floodplains and river banks dimensions on both river sides (Table 6.4).

*Table 6.4: River Cross Sections with interpolated River Bed*

Cross-section	Location	Source
	S39_Mosul 36°21'57.72"N 43°06'35.65"E elev. 211m	(Al-Hafith, 2012)
	S46_Mosul 36°21'24.02"N 43°07'20.99"E elev. 211m	(Al-Hafith, 2012)
	S49_Mosul 36°21'12.08"N 43°07'37.93"E elev. 211m	(Al-Hafith, 2012)
	S63_Mosul 36°19'41.14"N 43°09'16.56"E elev. 211m	(Al-Hafith, 2012)
	S64_Mosul 36°19'51.99"N 43°09'19.80"E elev. 211m	(Al-Hafith, 2012)

### 6.1.2.5 WinXSPRO

A cross section hydraulic analysis tool called WinXSPRO is also employed in this study to calculate and analyse the cross sectional hydraulic characteristics. It is Windows™ software package designed to analyse stream channel cross section data for geometric, hydraulic, and other sediment transport parameters.

Cross section input data may be from standard cross section surveys using rod and level or sag-tape procedures or even any other method to generate cross sections. WinXSPRO allows subdividing the channel cross section into multiple sub-sections and has the ability to vary water-surface slopes with discharge to reflect natural conditions. Analysis options include developing stage-discharge relationships, evaluating changes in channel cross-sectional area, and computing sediment transport rates.

The estimated stream-channel geometry cross section hydraulic characteristics and sediment transport output can be used to assist with channel design and monitoring, in-

stream flow analysis, the restoration of riparian areas, and the placement of in-stream structures. It was developed by Hardy et al. (2005) from the department of agriculture, Utah State University US. The developers of this software package provide a detailed description of the software including installation, utilisation, features and limitations of it in a manual which is available freely online. All the hydraulic characteristics, including the cross sectional area, surface water width, depth, wetted parameter, hydraulic radius and water surface slope for the extracted cross sections will be compared against the observed ones in the following sections.

The study demonstrates that hydrodynamic modelling of this river is greatly improved by generating extra river cross sections to fill in the large gaps between the small numbers of measured cross sections. Furthermore, the study demonstrates that the combination of Google Earth and 3D route builder generates more realistic cross sections than the other interpolation methods, and that this further improves the hydrodynamic modelling results.

### **6.1.2.6 Observed and Developed Cross Section Comparison**

By going back to Table 6.2, the missing river banks dimensions can be a problem in the comparative analyses whereas the google earth (GE) data extracted by 3DRoutBuilder (3DRB) is capable of capturing the complete channel width including river banks in both sides. To overcome this problem, interpolate the observed river bed data is interpolated to reach the known water surface level is suggested to get complete channel profile. At this stage, measured cross sections, cross sections extracted from GE by 3DRB (GE3DRB), and cross sections extracted from SRTMGL3 by 3Danalyst (SGL3Danalyst) are illustrated and compared in the following figures. Only the cross sections which have been generated interpolating the observed river banks were also considered. It should be noted that, identifying the cross section locations in SRTMGL3

was implemented by geo-referencing those locations from google earth also into SRTMGL3 data set. This was carried out by converting the locations KML files into layers to be shown by ArcGIS Map.

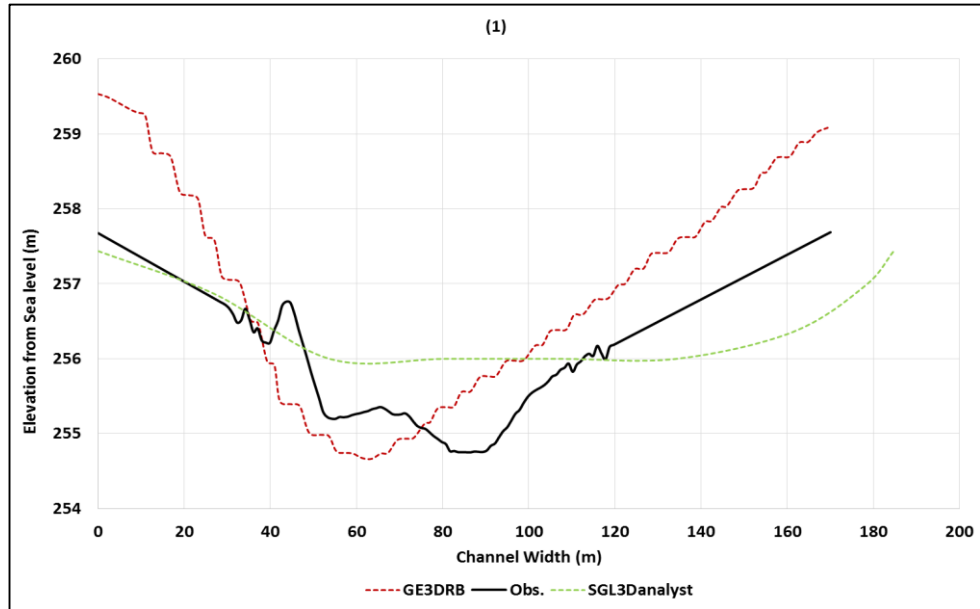


Figure 6-10: shows elevations of measured cross section (Obs.) at location – number 1 as identified in Table 6.2. This cross section is compared against one generated using SRTM GL3 raster (SGL3Danalyst) and another one generated using Google Earth DEM (GE3DRB).

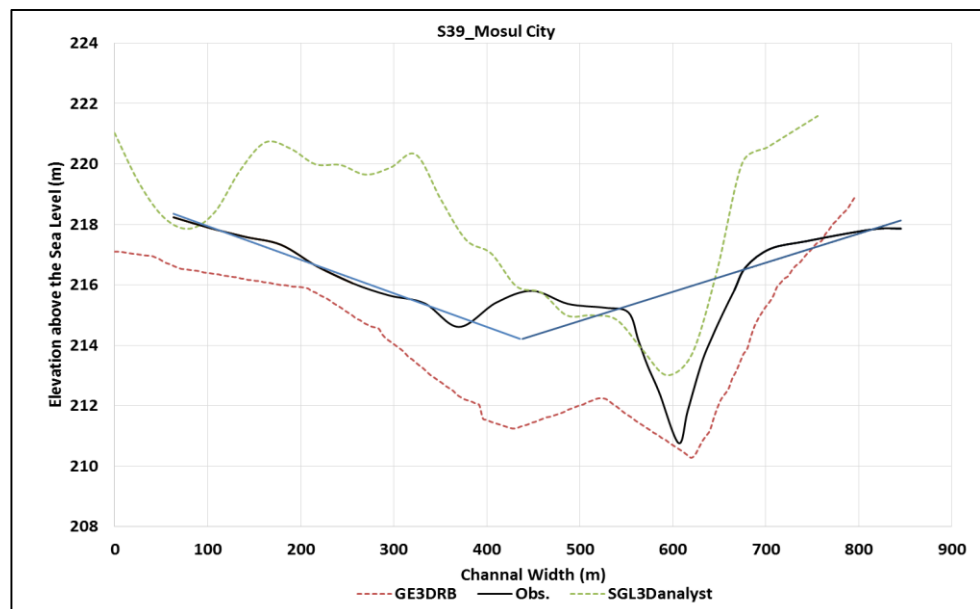


Figure 6-11: shows elevations of measured cross section (Obs.) at location – number S39 as identified in Table 6.2. This cross section is compared against one generated using SRTM GL3 raster (SGL3Danalyst) and another one generated using Google Earth DEM (GE3DRB).

Figures (6.12 – 6.23) are illustrated in appendix (1). The cross sections shapes and dimensions are matching reasonably fine. Some differences were noticed here and there, and that might be due to the capturing time. GE3DRB always performed very well in terms of the positioning (location) and elevation in contrast to SGL3Danalyst which always needed repositioning and even sometimes re-elevating. Not only that, but SGL3Danalyst also gives river bed level considerably deeper than the observed.

SRTMGL3 as any of the other SRTM datasets has considerable errors vertically and horizontally. An assessment of SRTM topographic products has been conducted by Rodriguez et al. (2005) which explains those errors. The results show that the river banks are matching well. The river bed's shape and river depths are showing a good similarity between observed data. and GE3DRB. GE3DRB provides a good number of measuring points as evidence to its high resolution. That could help to expose more geological and topographical details for the cross sections. The case study (along Tigris River) contains lots of curves and meanders especially in the middle region in addition to numerous numbers of islands with different sizes and figures. Identifying the locations of those river elements which are matching well with the observed data was achieved by using GE3DRB. A comparative analysis shows that GE3DRB synthetic cross sections and SGL3Danalyst data. The river morphological parameters (cross sectional area –  $A$ , wetted parameter –  $W$ , water surface width –  $b_s$ , average depth –  $\bar{h}$ , and flow velocity –  $V$  as well as the hydraulic radius  $R_h$ ) were calculated. Analysing these parameters is important to give a general picture of the hydraulic characteristics for the Tigris River in whole, as well as, it is a good opportunity to trade-off between the models in more details. Those calculations have been implemented by WinXSPRO (Figure 6-12). All of the calculated hydraulic characterises for the cross sections (simulated and observed) are shown in the figure 6.31 and arranged according to their locations. Table 6.5 summarises the outcomes of analysing the cross sections hydraulic characteristics.

Table 6.5: Summary of the Cross sections Hydraulic Characteristics Averages

<b>Hyd. Char.'s</b>	<b>Observed</b>	<b>GE3DRB</b>	<b>Synthetic</b>	<b>SGL3Danalyst</b>
<b>A (m<sup>2</sup>)</b>	795.71	779.89	831.70	1140.19
<b>W (m)</b>	314.33	319.12	288.00	183.35
<b>b<sub>s</sub> (m)</b>	311.24	306.63	390.49	259.72
<b>R<sub>h</sub> (m)</b>	2.66	2.59	4.27	6.80
<b>h<sup>-</sup> (m)</b>	2.88	2.87	2.56	3.75
<b>V (m/s)</b>	3.16	3.12	3.99	5.78
<b>b<sub>s</sub> / h<sup>-</sup></b>	108.07	106.84	152.54	69.26



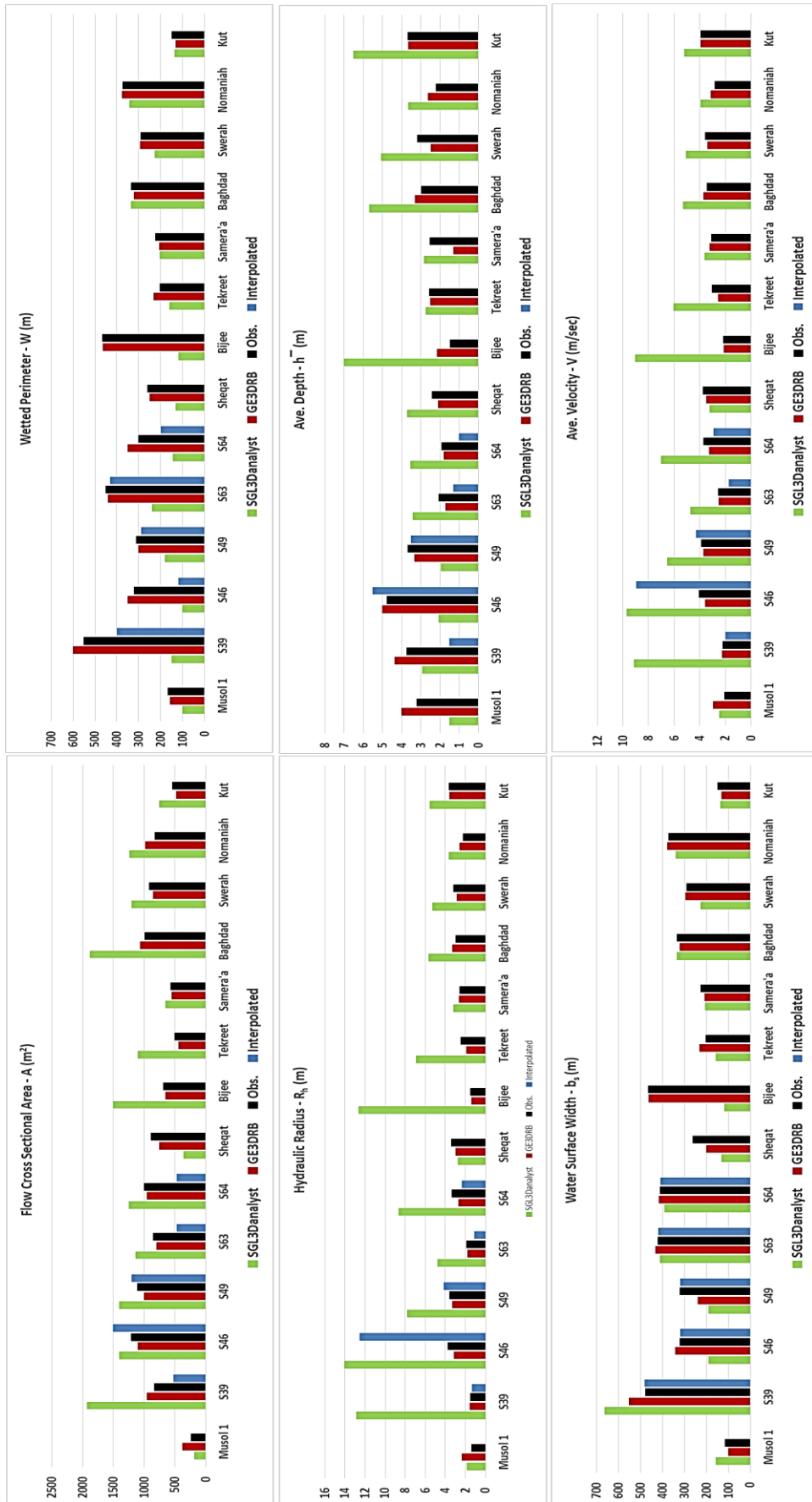


Figure 6-12: Tigris River Hydraulic Characteristics

There is variation of the cross sectional areas along the river in general. This could be due to the river long path as well as the large number of dams and other hydraulic infrastructures which have been implemented along the river itself and which would cause a considerable reduction of the flow velocity. The calculated hydraulic characteristics from GE3DRB are showing a substantial convergence at the level of all the morphological parameters in particular, while the results from SGL3Danalyst in general show over estimation of all parameters.

### **6.1.2.7 Generated Tigris River Profile**

After justifying the methodology (using GE3DRB cross sections) to generate the river profile, about 1200 cross sections including longitude, latitude and geographic location elevations above sea level have been generated and were inserted into the hydraulic model using ISIS River Section Unites to simulate the whole river profile to be one of the main boundary conditions. The River Section unit in ISIS simulates the flow of water in natural and man-made open channels. Those units have been used to insert all the cross sectional data sets that have been generated using Google Earth and the 3DRoutBuilder approach.

Figure 6-13 represents the whole Tigris River long sectional profile as an outcome of inserting the 3DRoutBuilder/Google Earth cross section data sets into ISIS by its cross section units. The figure is showing and differentiating both of the river banks and bed elevations and locations along the river. It clearly shows how the river flow slope changes from the northern region to the southern region. It should be noted that, a relatively considerable downgrading to the river steeping was recorded at section 355 in particular. This 355 node represents a point in Sammera's city, north of Baghdad. This point can be considered as a joint in the river between the steeper upstream sections. From that point onward, there was not any large gradient recorded until it reaches the last cross section in the study area downstream.

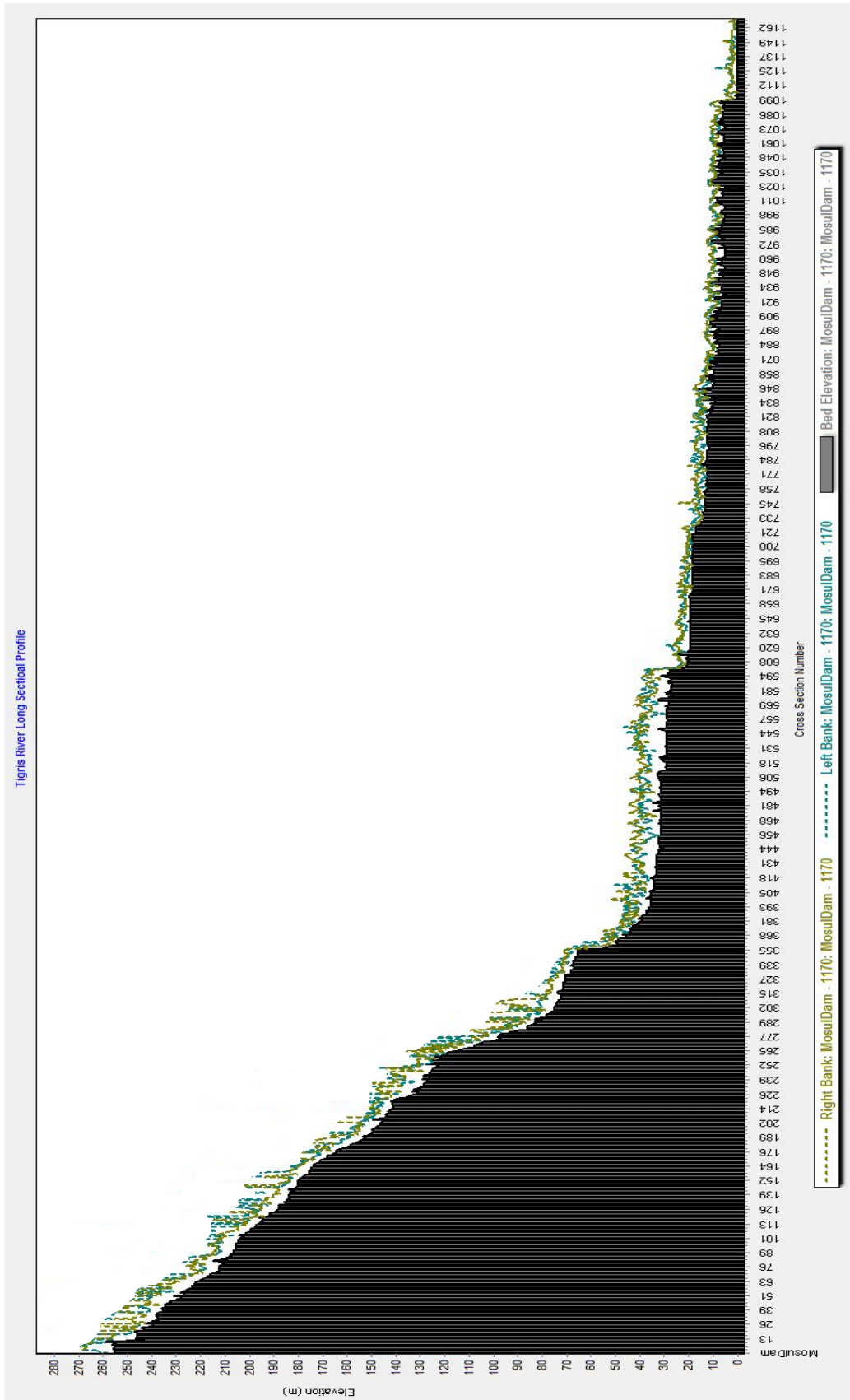


Figure 6-13: Tigris River Resulted Longitudinal Section from inserting the generated River Cross sections using 3DRoutBuilder and Google Earth

The change in the slope at Sammera's city may explain the depths of the river which becomes larger downstream of this point. This change in slope will change the river's ability to transport its sediments. When the bed slopes of the southern stream sections are assessed, it is noticed that, these are relatively shallow. That could be because the low flow of the river and the large number of the hydraulic projects along that area which could help to reduce the flow velocity and lead to more sediment accumulation in addition to the flatted nature of that area.

ISIS interpolated sections units were employed in the model for two reasons: Firstly, in the case of sparse cross sectional data, they ensure smooth gradients between channel properties thus avoiding sudden variations which can cause sensitivity in a model. Thus, they should be used when properties vary radically between sections. The other reason to use Interpolated Sections is to ensure adequate spatial resolution. In regions where there is likely to be significant water surface curvature, or in a backwater profile, interpolated sections should be inserted. The number of how much interpolated sections should be added to the model is specified in the first steady state run.

### **6.1.3 Rainfall/Evapotranspiration Boundaries**

Rainfall/Evapo[transpi]ration boundary condition data sets cover the study period from 1970 to 2000 have been incorporated in the Tigris model. This would help to identify the rainfall/Evapo[transpi]ration influences into the system, as there is a particular interest within this research to show how significant is the evapotranspiration proportion of the water volume losing from Tigris network. The Evapo[transpi]ration data sets predicted from chapter five were used in the same way that the discharge boundaries inserted. Such values can be used directly in mass equations in ISIS 1D utilising REBDY (rainfall and evaporation boundary condition data) units. The REBDY units have been connected with either a lateral inflow units to create an inflow into one or more units with a magnitude based on the water surface area of the receiving unit. A REBDY unit must either be connected to exactly one lateral inflow unit or to any number of lateral inflow

nodes of river section units. This can then divide the resultant inflow across the network accordingly. The lateral inflow unit must have its distribution method set to AREA for the REBDY unit to apply correctly.

### 6.1.4 Abstractions

Identifying the amount of water that is being extracted from a river is normally carried out by the traditional method. Traditionally, compare two conservative gauge stations readings located along the river. This methodology, however, doesn't quite fulfil the main aim of the research which is determining how the Evapo[transpi]ration affects Tigris River. That is because the results of the traditional method take all the losses in the account as river abstractions, and do not show the impact of each water balance element individually. This section suggests to consider available data show the population growth rates from seven Iraqi governorates (main cities) located along the river, Table 6.6 (provided from the Iraqi government and also made available in (Citypopulation.de, (2015)) and Figure 6-14, and 500m<sup>3</sup>/inhabitant/yr to represent the water demand with the model. The value 500m<sup>3</sup>/inhabitant/yr is the water withdrawal per capita as per a factsheet about mentioning the water situation in Iraq published by the Joint Analyses Unit – UN. That value equals to the Total water withdrawal (summed by withdrawn for agricultural, industrial and municipal purposes) divided by the Total of population.

Table 6.6: National Periodical Census for Iraqi Governorates located along the study area

Governorates	Area (km <sup>2</sup> )	Population				
		C 1977-10-17	C 1987-10-17	C 1997-10-17	P 2011-07-01	E 2014-01-01
Arbīl	14,471	541,500	770,439	1,095,992	1,612,700	1,749,900
Baghdād	734	3,189,700	3,841,268	5,423,964	7,055,200	7,665,300
Kirkūk	10,282	495,400	601,219	753,171	1,395,600	1,508,900
Al-'Amārah	16,072	372,600	487,448	637,126	971,400	1,050,600
Al-Mawşil	37,323	1,105,700	1,479,430	2,042,852	3,270,400	3,524,300
Tikrīt	24,751	363,800	726,138	904,432	1,408,200	1,509,200
Al-Kūt	17,153	415,100	564,670	783,614	1,210,600	1,303,100
		<b>6,483,800</b>	<b>8,470,612</b>	<b>11,641,151</b>	<b>16,924,100</b>	<b>18,311,300</b>

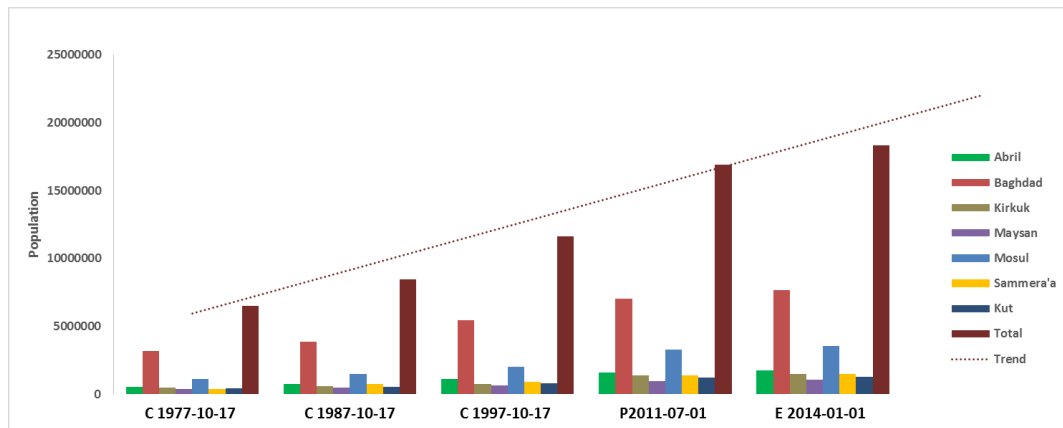


Figure 6-14: Population Growth Distribution from Seven Main Cities Located along Tigris River

The figure above clearly represents the considerable increasing in population of Iraq. A simple calculation process using the above values to get CAGR or the compound annual growth rate is conducted.

$$CAGR = ((Ending\ Value)/(Starting\ Value))^{\frac{1}{No.\ of\ Years}} - 1$$

The total population from the first census (c1977-10-17) which is equal to **6,483,800** represents the starting value, and the most recent census (E2014-01-01), 18,311,300, represents the ending value. The number of years is considered for the period between the first and the last censuses (1977 – 2014) which about 37 years. Out of that, the CAGR equals to 2.85%. It indicates that the population is in a continuous increasing.

Seven ISIS abstraction units (represent the seven major cities along the river) were employed at this stage to assess the Evapo[transpi]ration impacts on the water flow and water levels along the river.

### 6.1.5 Normal/Critical Depth Boundary

An ISIS normal/critical depth boundary (NCDBDY) unit was set after the last river section of the downstream (at the end of the system). This unit is meant to enable the users to specify a downstream boundary condition and automatically generates a flow-head relation based on the previous section data. This facility has been applied as an alternative to the flow-head boundary which cannot be supplied to the model as there is a sever lack of data about it. Through this process, the slopes (i.e. Bed and Water

Surface) were automatically generated by taking in the account several consecutive nodes (cross sections).

### **6.1.6 Tigris Model Description**

All the boundary conditions units required to run the model have been set including QT (Flow-Time) for the main reach and the other main tributaries, River section which have been developed using GE and 3DRoutBuilder, 7 abstraction units as well as ET modelling units, etc. About 1250 river section units plus the other boundary condition units meant to be utilised within the model in one go, but due to the limitation of the provided hydraulic model which has capacity to model open channels with only 1000 node. It has been decided to break down the main model into three individual models (Northern , Middle and Southern regions), this was also to over tack the problem of adding interpolated river section units (more nodes) which are recommended to be added by ISIS to facilitate the run by reducing the un-convergence modelling.

To implement the break down process successfully, initial boundary conditions were required to run the other models (the middle and the southern). To over tack this issue, it has been decided to utilise the downstream simulated outputs (flow/stage) to represent the initial boundary conditions for the following region and so on with a chance to check the model(s) performance from time to time. It has been decided to stop inserting more generated river sections when the model development reaches the last point just before Tigris inters Amarah City (Figure 6-15). Modelling Tigris River at the southern region becomes more difficult as it starts branching into several small channel (converted from a single thread channel to multiple channel with highly sinuosity) and also into some marshes.



Figure 6-15: Iraqi Marshes Map quoted from "UNEP Study Sounds Alarm about the Disappearance of the Mesopotamian Marshlands"

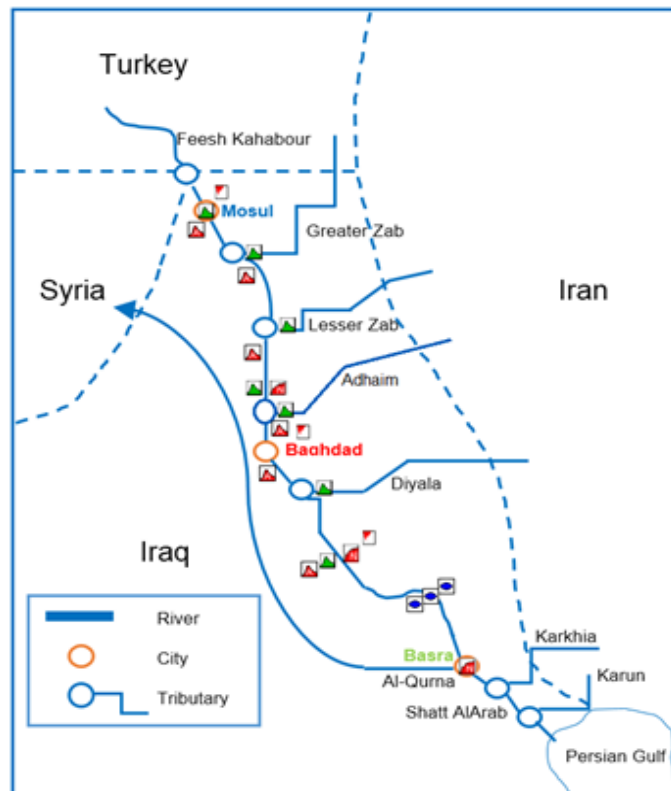


Figure 6-16: Schematic of full ISIS-Tigris structure



## 6.2 Tigris Steady State Modelling Results

Steady state is where the modelling takes a “snapshot” of the river reach at an instant in time. It therefore represents one condition of flow and cannot investigate something that happens over a period of time.

The ISIS model of the Tigris was first run in steady state mode for the highest historical discharge record. As a result, water levels were investigated over the entire reach length, with the aim being to determine the change in water level at each CS along the Tigris and also to check the developed river model and look at different options of cross-section shapes and sizes.

Both direct steady-state and Pseudo-timestepping methods to optimise run-time and enhance model stability are available in ISIS – 1D (Halcrow et al., 1999).

Results of the direct steady state solution method are only shown in this section for several reasons: (i) it is applicable to in-bank flow regimes; (ii) it is very fast and accurate and requires very little initial data. Whilst time-stepping method requires a big and accurate time step data to develop initial conditions for unsteady simulations, which could not be done due to the severe lack of data.

The historical flow record for September - 1972 has been utilised as the discharge initial boundary condition. This record is the highest recorded flow event ( $3645\text{m}^3/\text{sec}$ ) recorded during the study period of 1970 – 2000.

A 6 km reach which is outlined in section 6.1.2 - Table 6.6 was used to assess the reliability of the steady state simulations. Five of the observed CSs are located in this reach. Four models were established utilising river profiles made from (i) observations, (ii) 3DRB, (iii) interpolation; and (iv) 3DAnalysis, as outlined in section 6.1.2. The September 1972 flow event was used as well to examine the capability of each model to handle high events. The results were four water stages illustrated in Figure 6-17.

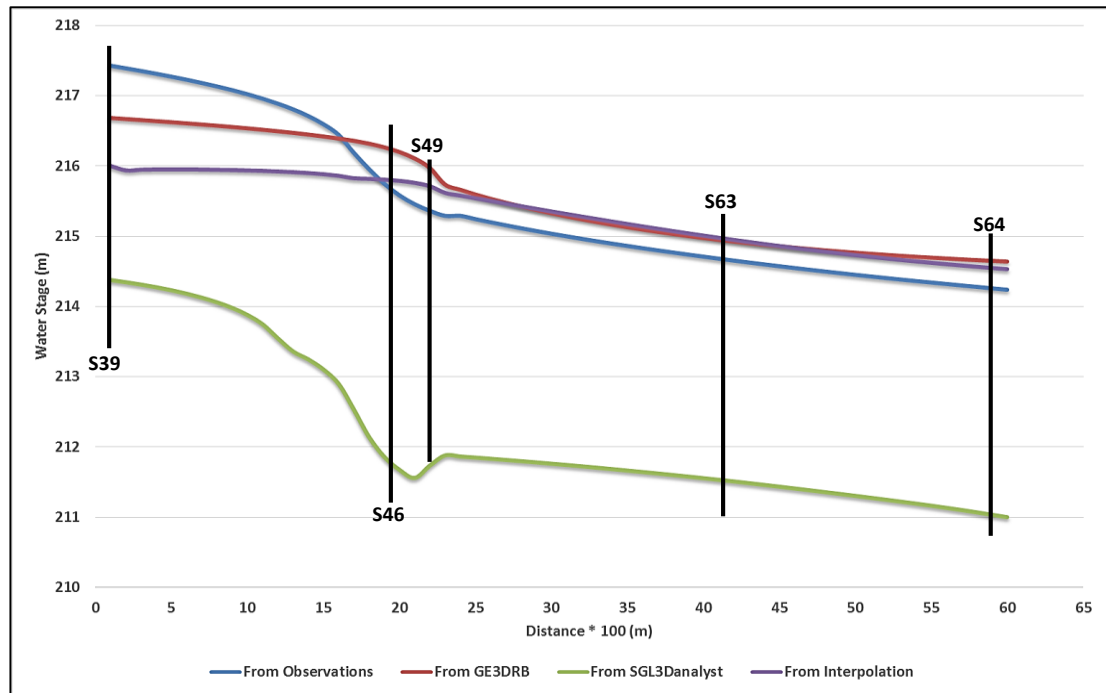


Figure 6-17: Steady state river stages for four generated river profiles.

Figure 6.31 above shows a comparison of predicted water stage resulting from incorporating observed river profile (blue curve) against others produced by incorporating river profiles generated by Google Earth and 3DRoutBuilder (in red), SRTMGL3 and 3Danalyst (in green) and interpolated river profile (in purple). All these stage profiles follow the same trend of decreasing. The assessed slope along the 6km reach is about 0.0005 for all the generated profiles. However, the 3Danalyst model noticeably underestimates water levels along the examined reach. This is another reason why the methodology has been excluded for generating river profiles.

Simulated water levels slightly underestimate the upstream water levels of the reach. This could happen because river profiles generated by GE3DRB and from river banks' interpolation are deeper and less featured. In other words, the modelled river profiles have less water-river bed friction. For the same reasons, the purple curve is almost flattened when compared to the green and blue. Correlation coefficients were calculated for the water levels, which look already closer. ( $R^2$ ) and Nash-Sutcliffe coefficients are 0.94 and 0.86 respectively for the GE3DRB model. As for the interpolated model ( $R^2$ ) and Nash-Sutcliffe coefficients are 0.84 and 0.63. The model which is

generated by incorporating interpolated river profile is limited only to this reach in particular, because it can only be generated from available river bank topographical data. And according to the correlation analysis as well, the GE3DRB model shows very well corresponding to the water levels predicted by the observed river profile model.

The latest findings give more confidence of the capacity of the developed Tigris model to produce the predictions required for the next step using the steady state simulation.

The resulted water level of the entire examined reach is illustrated in Figure 6-18:

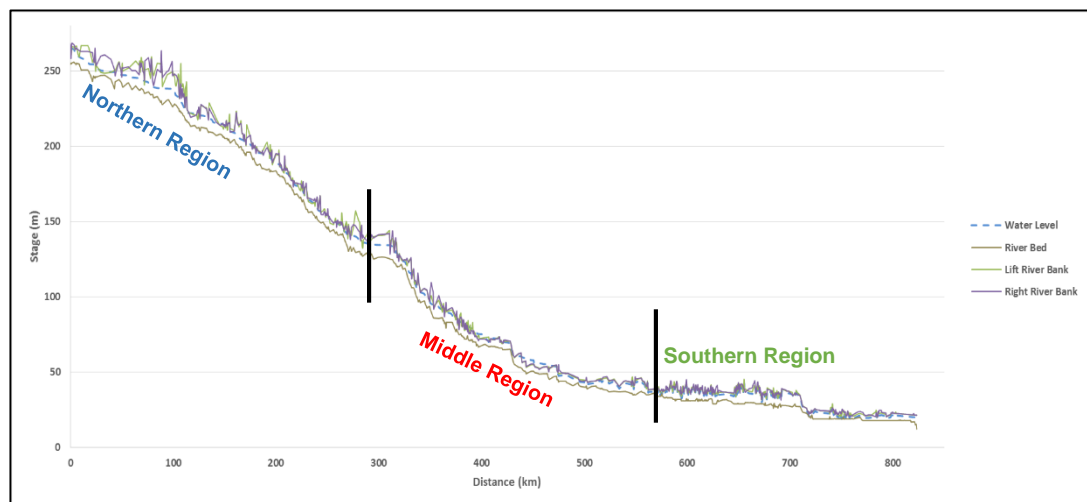


Figure 6-18: The Generated Tigris model by Incorporating September 1972 event and GE3DRB.

The steady state run results will be used as the initial flow boundary conditions the unsteady run. Moreover, the results of the steady state run showed sufficiency of the input data including node spacing, model convergences, flow, storage etc. The water level has exceeded the river bank levels only in few locations along the river, mainly in the middle region. That could be due to ignoring the water consumption at this stage or the model would require ideally more cross sections to be incorporated at higher frequency, especially during the middle region section.

### 6.3 Tigris Un-Steady-State Modelling Results

The investigated study period from 1970 to 2000 suffers from discontinuity in data availability mainly due to political instabilities especially between the year 1980 and 1988, the Iraq – Iran war, and also the gulf war in 1991. Although the Gulf war did not take

longer than 6 months, it has badly affected the country's infrastructure. This war was also followed by economic blockade until 2003 which led to the water resources issues taking a lower priority for many years. Over the time, considerable amount of data were missing. It was decided to utilise ISIS 1D unsteady state condition modelling for the periods only when discharge data were available and to predict water levels and also whenever water levels data is robust, water flow can be produced.

The unsteady state modelling requires variation of the discharge and water levels inputs over time at the upstream and downstream end of the investigated study areas respectively. Estimations of the initial conditions of flow and stage are required at every model node. Carrying out a steady state runs for the flow and water stage simulation in at the proposed start time was useful when changes in how the water is stored in the river during a period of flooding or shortage.

It was decided to set the time-step of unsteady calculation of the model for every 1hr to retain a continuous stability of along the model within the examined period (1970 – 2000). Other time-steps were tested (e.g. 2hr and 3hr), however model instability and large conveyance were recorded. The developed unsteady state model facilitated in identifying how the flow varies over a period of time from a few days to a few years, and substitute the missing flow data required as the water flow in this case the key element to be care of because the river losses need to be assessed.

Model calibration followed with the main aim being to quantify errors and improve model performance. Consistency, improved production yields, and the assurance of accuracy of predictions over all will be obtained.

The calibration of a hydrodynamic model will be completed by systematic adjustment of the channel roughness parameter to alter the modelled water level until obtain a reasonable agreement to the observed water level data. For good calibration a large amount of observed data are required as the calibration will only be as good as the observed information (Beavers, 2003). This theory is applicable when assuming that the

observed data is error free. As it was mentioned above, the intense lack of data made it impossible to build an entire model to simulate changes in a river like the Tigris impossible. It will be recognised of measured data calibration accuracy. However, it is still valid to rely on the actual located information.

The unsteady state Tigris river model was run for the entire investigated time. Because the academic ISIS model licence is limited to 1000 nodes only. The whole reach was divided into three separate models (Northern, Middle, and Southern regions) as outlined above (see section 6.2, Figure 6-18). The resulting downstream information from the upper model was fed in to the following model sequentially as upstream boundary condition for that model, and so on. This facilitated all model outputs information at any desirable time for any point along the reach for calibration and validation purposes for the assessment of the water losses.

For roughness calibration the channel roughness parameter Manning's 'n' was used. A range of Manning's numbers was obtained from different sources. The model is set by default to  $n = 0.01$ . The literature suggests a range between 0.0285 to 0.035 in the main channel and 0.04 – 0.05 for the floodplains. The software WinXSPRO which was used to evaluate the river cross sectional characteristics, it calculates Manning's number as well. It suggests that the roughness parameter when considering all the 14 observed cross sections along the reach from north to south is a range from 0.017 – 0.02. The obtained Manning's (n) numbers (from model default, Literature, and WinXSPRO) is a range vary from 0.01 – 0.05, that is presumably due to differences in measurements and considerations. Nevertheless, that gives a change to assess a wide range of manning numbers on the performance of the Tigris as it is illustrated in Figure 6-19.

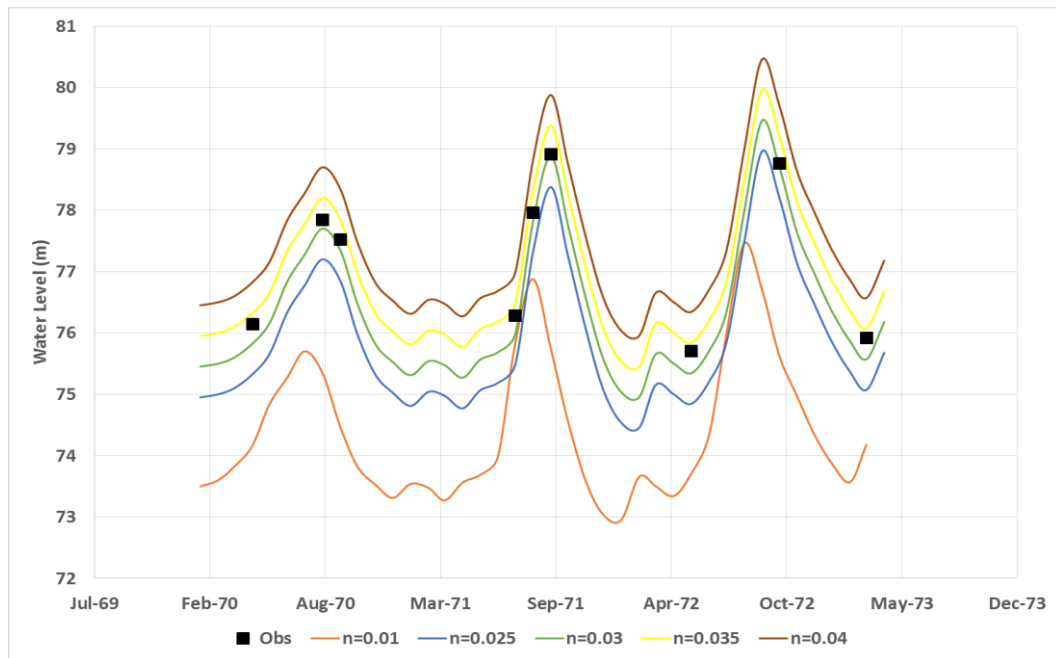


Figure 6-19: Calibration – Simulated vs Measured Water Levels at the Downstream End of the Northern Region – at Cross Section 322.

A set of water level observations was used for a gauge station located at the last point of the northern model (cross section 322) from Jan – 1970 until April 1973 and compared against sets of water levels for different roughness values ranging from  $n = 0.01$  to  $n = 0.04$ . These observations are very dispersed but still can represent the seasonal temporal distribution of the water level at that location.

The model was first run in default mode,  $n = 0.01$ . It gave a good trends corresponding, however, while the observations were set in the 15<sup>th</sup> of each month, the model takes it as in the 1<sup>st</sup> of the month. The resulting model river levels at that location recorded between 1.5 – 2m lower when compared to the observations. Consequently, a series of simulations were carried out using a range of higher Manning's numbers ranging from 0.015 to 0.05 and increases at 0.005 intervals.

As shown in Figure 6-19, the results of simulations for  $n = 0.015$  and  $0.02$  were excluded from the graph because obviously until simulation  $n = 0.025$  on ward it became closer to the observed data but still not quite there yet. Simulations for  $n = 0.045$  and  $0.05$  are excluded as well because simulation for  $n = 0.04$  is already exceeding the observations

and also from  $n = 0.04$  up is characteristic for vegetated floodplain roughness parameters, and here, the in-channel flow is being examined.

Calibration of the model for the selected period shows a reasonable correspondence between the practiced and observed data. The values which have been generated for the Tigris in low and high flows show that for  $n = 0.03$  predicted and observed water level records compare best overall ( $R^2 = 0.83$ ). However, for  $n = 0.035$  for the dry season predicted even better ( $R^2 = 0.91$ ). Roughness parameter ( $n = 0.032$ ) was applied to reduce the error for the examined period fixed to the whole model. For all of this, it is necessary now to conclude that with data available and the procedure followed, the Tigris model has been calibrated satisfactorily and to the best extent possible considering the data availability.

#### **6.4 Tigris Model: Validation**

Information extracted from the last point of the Tigris reach in the middle region model was considered for validation of the model. Cross section 640 which was the last cross section for the middle region model also represents the location of a gauging station providing flow and water level information of the river. Water level information for the study period from 1970 to 2000 was extracted from the model as shown in Figure 6-20. Following on from the calibration process, the validity of the developed hydrodynamic model performance was checked against measured data in different location for the period from January 1978 to January 1981. Those three calendar years can be considered as the driest within the study period, can be seen in Figure 6-21.

The validation results again show a good correspondence with no more than 15% difference (or  $R^2 = 0.85$ ). This validation result could be improved by not defining a single roughness coefficient for the whole channel but by differentiating the parameters along the channel and set it for all cross sections individually.

The limited amount of available field information was the biggest challenge in this study and meant that it was impossible to cover the entire selected periods (1970 – 2000). However, the available data were considered to be sufficient to estimate the performance of the developed model.

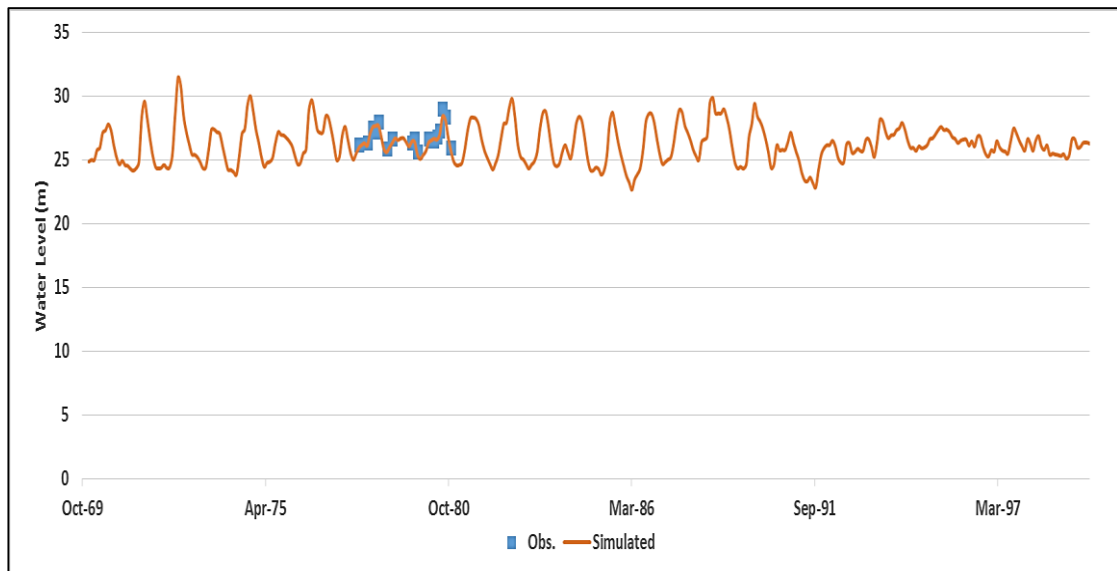


Figure 6-20: Simulated Water Level for the Study Period (1970-2000) at Cross Section 640.

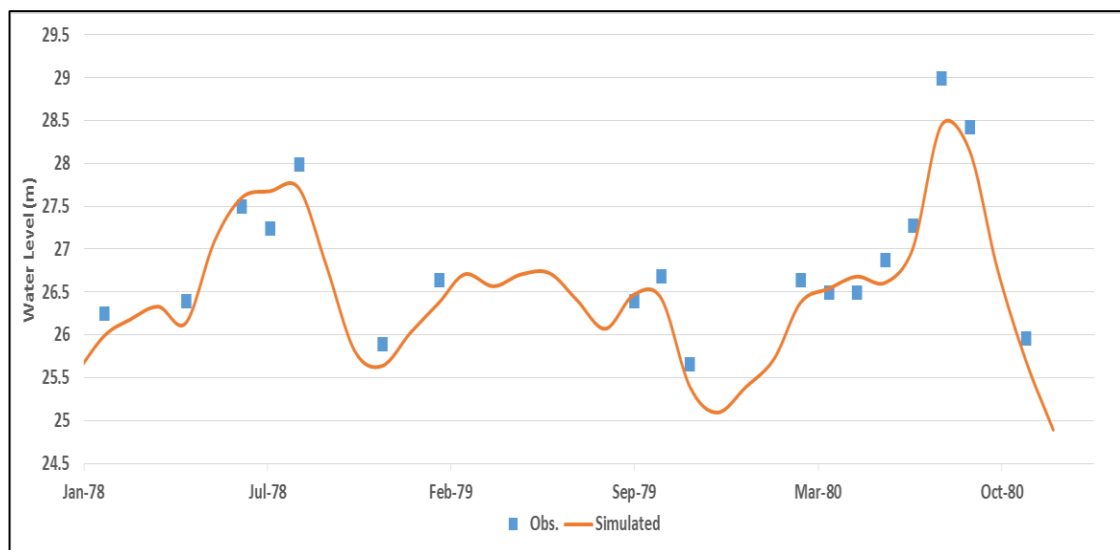


Figure 6-21: Validation of the Simulated Water Level for the Driest Period (from 1978 to 1980) of the Study at Cross Section 640.

## 6.5 Summary

This chapter showed the construction of ISIS 1D for the river Tigris. The construction of the model was completed using the data provided by the Iraqi Ministry of



Water Resources including historical data sets of river discharge and water levels including several tributaries alongside with the main water quantities which flow in the main reach. A part of the provided data was 14 surveyed river cross sections. Evapo[transpi]ration data sets developed in chapter 5 of the study period from 1970 – 2000 was incorporated in the developed model to study the impact of this variable on water quantities of the Tigris.

The water consumption rate that represents the human activities including domestic, industry and agriculture is an ambiguous issue and not clearly reported. Accordingly, this water amount had to be assessed.  $500\text{m}^3/\text{capita}/\text{year}$  is considered the water demand for the people who live in this region as per the UN. The last five censuses for the 7 cities located on the river were unitised to calculate the water demand and also the increasing/decreasing rates. A population increase of about 2.85%. This value naturally varies from city to city according to the size and the population density. All of those details and assumptions were employed to generate seven abstraction units within the model to represent the water consumptions from each city along the river.

The obtained river cross sections helped to identify the river characteristics as well as to evaluate the performance of newly employed method to generate a simple yet detailed river profile for the Tigris. 1250 river cross sections along the 850km stretch were generated using 3DRoutBuilder and Google Earth topographical layers over the Tigris Basin. The suitability of the generated cross sections was evaluated against the observations and other well-known resources. Investigations based on statistical comparisons in addition to preliminary tests were carried out, and the results confirmed that this new methodology is the best available method considering the research limitations. There was a lack of sensitivity analysis because of the lack of the observed data/cross sections.

Once the Tigris model was built, steady and unsteady state runs were executed respectively. The steady state runs were carried out to check whether the developed

model can handle extreme events and also to generate flow and water levels whenever it is needed.

After completing production of the required data sets, the model was calibrated using observed data, including discharge records, measured from January 1970 to April 1973. This set of data showed good correspondence for the simulated water levels including low and high flow events. Several runs were carried out to identify the best river bed roughness parameter for the model. Manning's numbers ranging from 0.01, the model's default, to 0.05 for vegetated floodplain were incorporated to specify the most suited 'n'. 0.03 and 0.035 Manning's numbers performed the best overall. However,  $n = 0.035$  gave only 9% difference in the predicted dry event of the calibration period (January 1970 to April 1973). Roughness parameter  $n = 0.032$  was applied to reduce the error for the examined period and fixed for the whole model. The gained model efficiency matches observations well. To obtain further confidence in these results, the model successfully produced simulations for water levels for the entire period of study (from 1970 to 2000). The simulated water levels matched well historical records from January 1978 to October 1980 obtained from a gauge station located on the last point of the modelled middle region well.

The Tigris model was calibrated and validated not only for the hydraulics but for the water losses (population consumption and ET) simulations as well. From now on, it is possible to generate all the necessary information and apply it to long-term predictions required for water balances studies and applications.

## **Chapter Seven: River Losses Assessment and Water Balance for Tigris**

To assess the Tigris water sustainability, it is important to simulate discharge changes over an extended period of time. These type of long-term simulations have been carried out using the one – dimensional hydrodynamic modelling package ISIS. The model development process is described in depth in chapter six.

Several steady state model runs have been executed to predict missing river discharge data for the study period of 1970 to 2000. After incorporating all the river's main tributaries, available river level data were used to simulate discharge values that can fill the discharge observations' gaps. Discharge output data of the northern model were used as an input for the middle region model and so on for the southern region model. The calibration and validation processes were found to be promising considering the limitations of the modelling process and existing data.

Unsteady state simulations were carried out for three scenarios for each region. The first simulation scenario only considered discharge of the main reach of the river during the period of study including tributaries. The second scenario of simulations was carried out also incorporating the population consumption rate for the cities the Tigris flows through. The third simulation scenario was carried out incorporating ET data sets for each region which were the result of simulations carried out in chapter 5.

This chapter presents the results of the long-term discharge simulations carried out for the Tigris. In the following sections, the water quantities lost from the Tigris during the period from 1970 – 2000 will be quantified and analysed. In addition, a water balance study and an initial future prediction of the water resource situation of the Tigris river basin based on the current conditions will be attempted.

## 7.1 Tigris Northern Region Model

Figure 7-1 shows a Google Earth image of the northern Tigris region. In addition, it shows a longitudinal section which was developed using 3DRoutBuilder for the Tigris river at the starting point selected for this research study, namely Mosul Dam all the way down to model cross section number 340. River cross section #340 is located in area exactly between Baiji city and Tikrit. This point (cross-section #340) also represents a gauging station location; it provides discharge and water level information about the river which was used for calibration purposes in chapter six. The longitudinal section shows the changes in topographical elevations from the upstream to the downstream of that river. Although there were only few observed river cross sections available, they correspond well with the modelled river profile elevations.

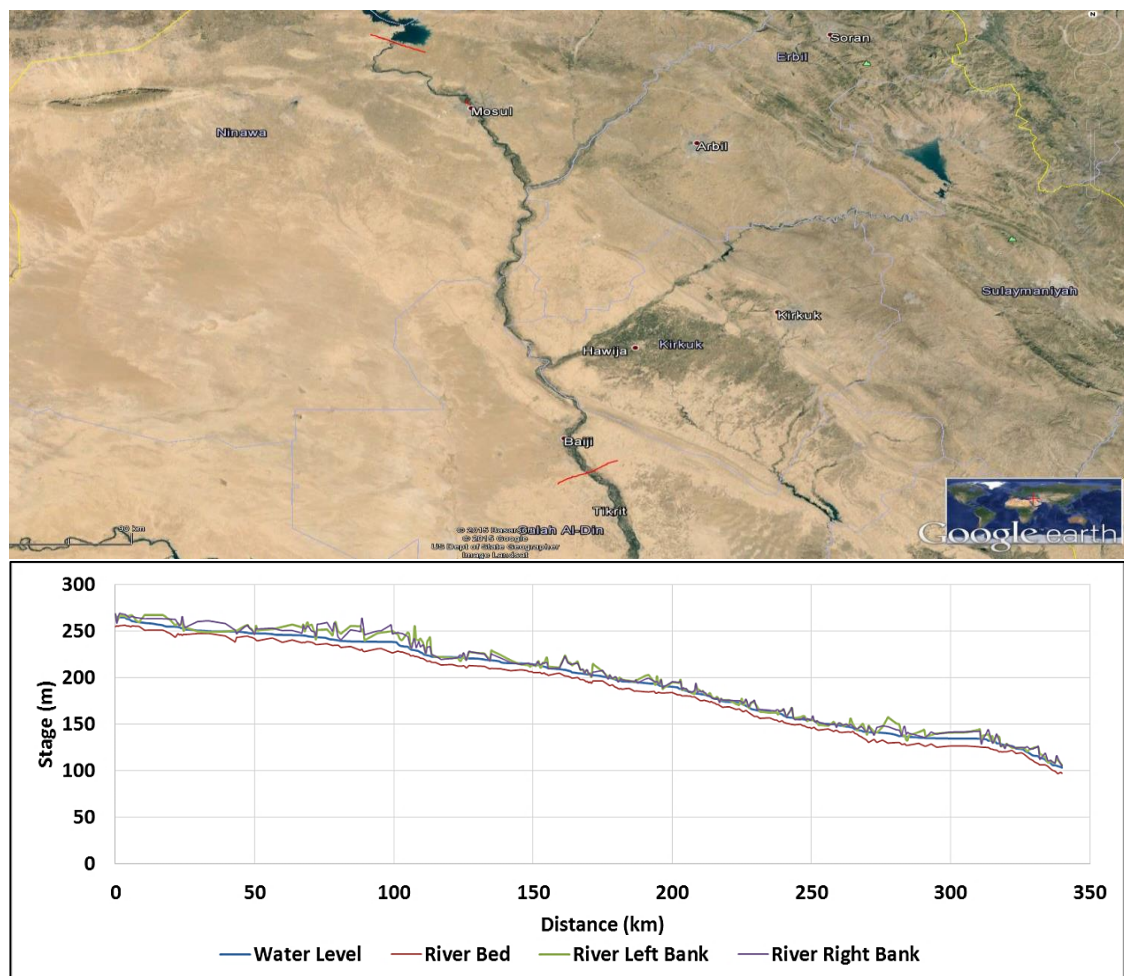


Figure 7-1: The Tigris northern model reach – an image by Google Earth and model river and water elevations

The green and purple lines within the figure represent the river left and right banks, respectively, in that region. In general, the representation of the river banks is working well. Some high river bank points were recorded reflecting the mountainous nature of that region. The main channel flow of the Tigris starting at Mosul Dam and two tributaries were modelled, namely the Great Zab and Lower Zab tributaries. The blue line in the figure represents the water elevation along the Tigris reach which is the resulting water stage of the steady state run for the model considering the Sep-1972 event (the highest recorded flow).

Accordingly, the river slope found is approximately 0.00028 downstream from Mosul Dam, the upstream boundary of the modelled domain. This value corresponds with the slope calculated using observations in chapter six.

Figure 7.2 shows the model discharge results for the investigated period of 1970 to 2000 at the most downstream cross section (# 340) and how the river is affected by the flow, abstractions and river losses including Evapo[transpi]ration.

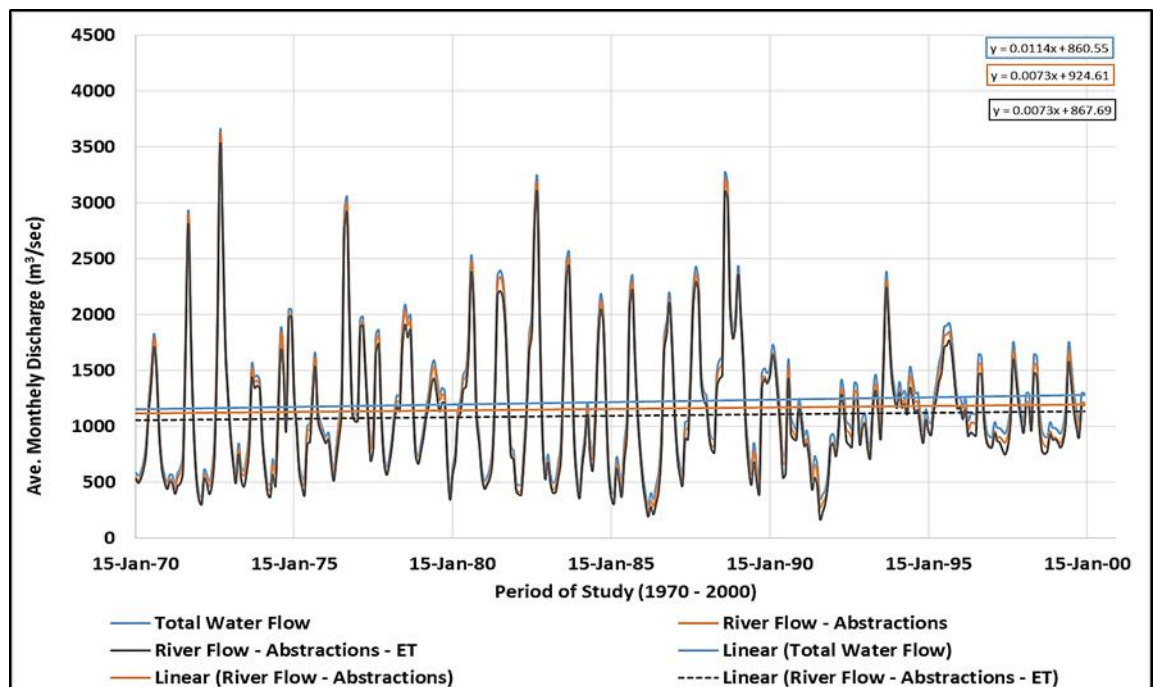


Figure 7-2: Tigris River, Water Losses\_Northern Region

There is a slight increase of %0.067 in the amount of water received into the model domain during the entire period of study from 1970 until 2000. In addition, the figure

above gives clear evidence that the upstream water releases' pattern is changing over time. These releases exceed 3000 m<sup>3</sup>/sec in the wet season and about 500 m<sup>3</sup>/sec in the dry season from the beginning of the study period until the 1990's. From the middle of the first quarter of the 1990's and towards the end of the study period, the much larger quantities (a range between 650 to 1000 m<sup>3</sup>/sec) of water were released during the dry season. However, the records showed much less water (a range between only 1500 to 1800 m<sup>3</sup>/sec) was released during the wet season than previous. The potential for changing the water releases' pattern is a direct result of the implementation of a number of hydraulic projects in the upstream countries.

The modelled discharge data shows considerable reduction over time which is thought to be a result of either abstractions or from other river losses, i.e. Evapo[transpi]ration. It should be noted that the discharge, especially in the dry season, due to abstractions and other river losses reached its lowest rate from the mid 1980's. The reason could be the limited available information about ground water exchanges/losses with/to the river channel and about the quantities of water which are being returned back to the main reach, e.g. waste water treatment, sub-basins; small rivers linked the main system, etc. Table 7.1 summarises the discharge changes due to these variables for the Tigris northern model region:

Table 7.1: Discharge values for the most downstream cross section (#340) of the Tigris northern model.

	<b>Total water received</b>	<b>Abstraction considered</b>	<b>Abstraction + ET considered</b>
<b>Changing over the period from 1970 to 2000</b>	+0.067%	-0.002%	-0.005%
<b>Max</b>	3644 m <sup>3</sup> /sec	3560 m <sup>3</sup> /sec	3475 m <sup>3</sup> /sec
<b>Average</b>	1215 m <sup>3</sup> /sec	<b>1032.2</b> m <sup>3</sup> /sec	<b>976.4</b> m <sup>3</sup> /sec
<b>Min</b>	290.4 m <sup>3</sup> /sec	27 m <sup>3</sup> /sec	8.5 m <sup>3</sup> /sec
<b>Total amount of water received over the period from 1970 to 2000</b>	437395 m <sup>3</sup> /sec	335587 m <sup>3</sup> /sec	315514 m <sup>3</sup> /sec

Even though there is the slight increase in the annual discharge received as upstream releases over the study period (about 0.067%), overall a reduction can be observed. This is believed to be caused by the increase in population rate and also by ET. The overall

water consumption in this region is about (average annual) 180 m<sup>3</sup>/sec from the total discharge of in addition to more than 65 m<sup>3</sup>/sec caused by ET. The amount of water lost by ET over the investigated period (from 1970 to 2000) is about 20100 m<sup>3</sup>/sec/region area. For the northern Tigris river region, population increase, implementation of dam structures and reservoirs along the river and also the climate change which is represented by the Evapo[transpi]ration have clearly started to have more effects in this region. The impact of the water losses on the flow is manifested especially, during the dry seasons and also increasingly towards the end of the study period and since first quarter of the 1990's in particular (0.23% reduction).

## 7.2 Tigris Middle Region Model

Discharge data set for the study period from 1970 to 2000 was extracted from the most downstream cross section in the Tigris northern model and was fed into the Tigris middle model as discharge upstream boundary conditions for the middle model. Figure 7-3 shows the location of the middle region alongside with developed a longitudinal section of the Tigris River starting from the first point selected for this research, namely cross section 340, all the way down to cross section #640 in the model. The river reach goes through Baghdad (the capital of the country). Relatively higher population rate and more hydraulic projects, industrial and agricultural areas are excited within this region. Much more water consuming is expected. River cross section #640 is located in the Kut city 170 km south-east of Baghdad. The main reach of Tigris has about 300 km length in this area. The longitudinal section shows also the changes in topographical elevations from the upstream to the downstream of that river. Although, there were only few observed river cross sections available in this case as well, they correspond well with the modelled river profile elevations. The river banks and river bed representations from the northern region were repeated for this case again. The main channel flow and two tributaries were modelled including the ongoing Tigris and water that feeds in to the river from the Adhim and Dyala tributaries. The blue line in the figure



represents the water elevation through the Tigris reach which is the resulting water stage due to the steady state run for the model considering Sep-1972 event (the highest recorded flow).

Less significant changing in river slope was recorded, about 0.00018 resampling the flatted topographical nature of the region. This value corresponds the slope calculated using observations in chapter six as well.

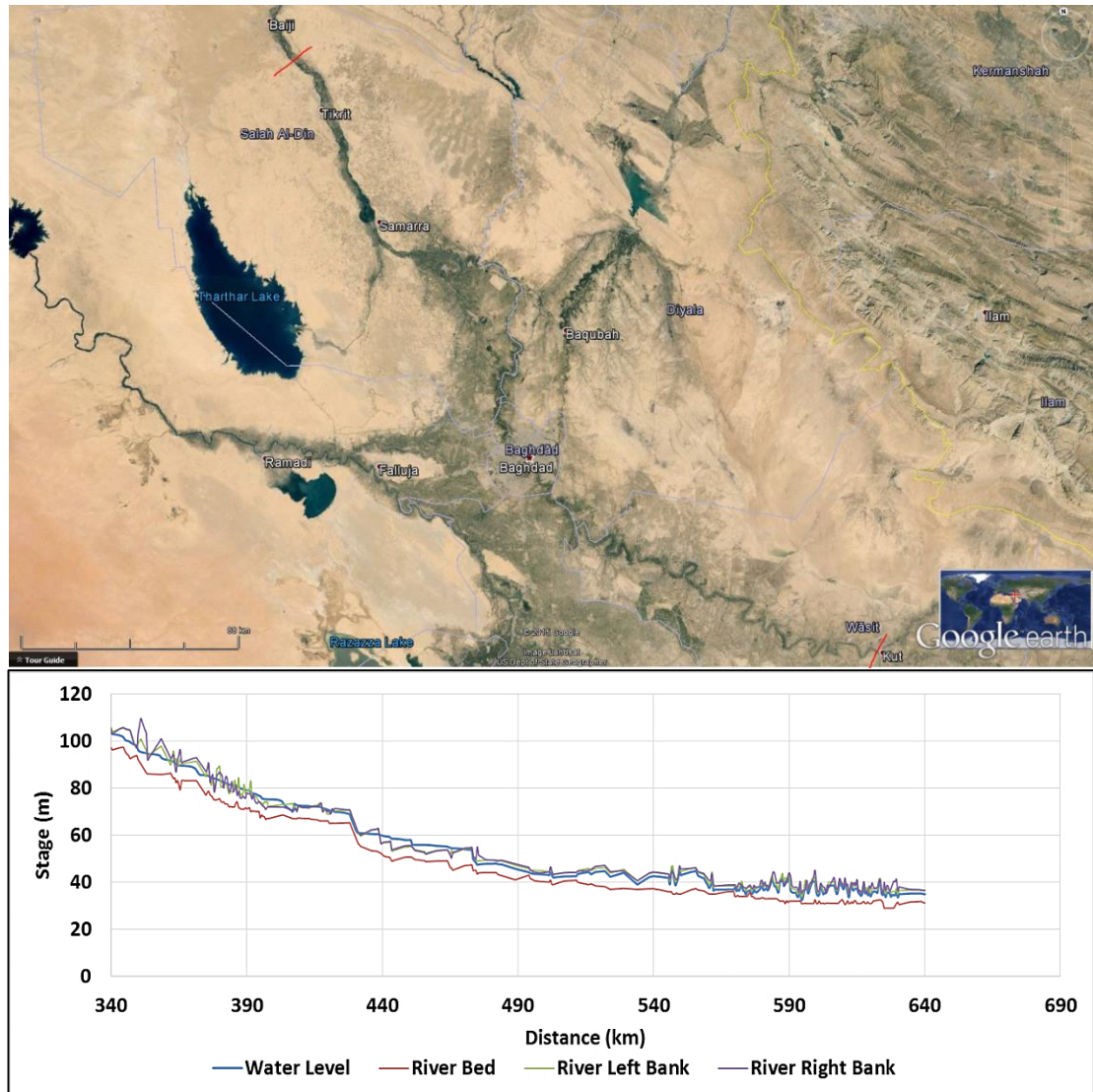


Figure 7-3: The Tigris middle model simulated by Google Earth and 3DRoutBuilder

The figure above shows that the developed river profile can handle extreme events very well. The water level has exceeded the river bank levels in a short distance with the



reach. It could be due to the limitation of the suggested methodology in generating the river cross sections, as it could not measure deeper cross sections.

Figure 7-4 shows the model discharge results for the period from 1970 to 2000 at the most downstream cross section #640 and how the river is affected by the flow, abstractions and river losses including Evapo[transpi]ration in the middle region.

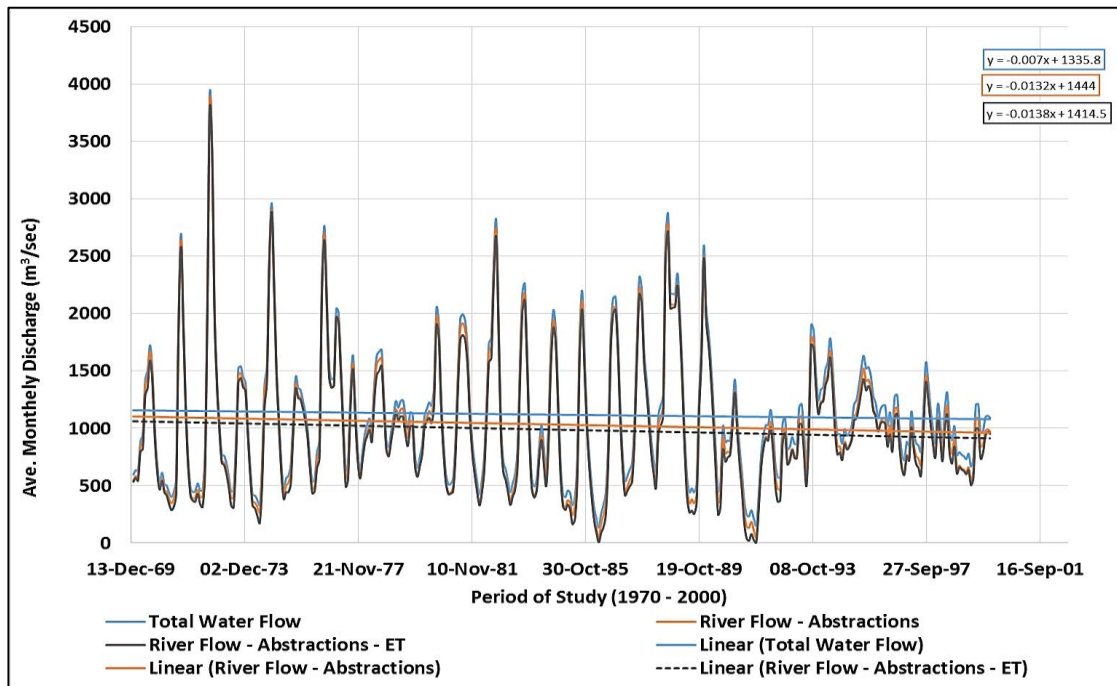


Figure 7-4: Tigris River, Water Losses\_Middle Region

Additional quantities of water came from the tributaries in this region helped to cause an unnoticeable increasing in the trend of the discharge which flow through the river reach in this region. The discharge seasonal changes over the time in this region dramatically followed the previous region releases pattern. The monthly average discharge values over the time were noticeably increased as well. However, a slight decreasing in water quantities inherited from the northern model was recorded.

The trend of the modelled discharge values in this part of the reach was showing considerable reductions in water quantities over time either from abstraction only or from river losses. It should be noted that the modelled discharge due to abstractions and river losses reached its lost rates more often compare it to the previous model. This situation happened especially in the dry seasons over the studied period. The reason behind this

could be again because of the research limitation to access further information about the water ground changes and the quantities of water back to the main reach from other water resources (e.g. waste water treatment, sub-basins, small rivers linked the main system, etc.). In the following, Table 7.2 summarises what was happening due to the considered variables for the middle region flow:

Table 7.2: Statistics obtained from the most downstream cross section (640) of the Tigris middle model.

	<b>Total water received</b>	<b>Abstraction considered</b>	<b>Abstraction + ET considered</b>
<b>Changing over the period from 1970 to 2000</b>	-0.005%	-0.18%	-0.205%
<b>Max</b>	3910 m <sup>3</sup> /sec	3820 m <sup>3</sup> /sec	3747.4 m <sup>3</sup> /sec
<b>Average</b>	1119 m <sup>3</sup> /sec	850.4 m <sup>3</sup> /sec	804.2 m <sup>3</sup> /sec
<b>Min</b>	134.3 m <sup>3</sup> /sec	15 m <sup>3</sup> /sec	2.4 m <sup>3</sup> /sec
<b>Total amount of water received over the period from 1970 to 2000</b>	40400 m <sup>3</sup> /sec	335587 m <sup>3</sup> /sec	318514 m <sup>3</sup> /sec

As shown above, there is a relatively slight downward inherited trend in the received water quantities over the period of study, which is almost unnoticeable recorded (about 0.005%). there is also a sever reduction recorded caused by the increasing in population rate and also by ET. There is more than 270 m<sup>3</sup>/sec difference by considering the average water quantity in addition to more than 46 m<sup>3</sup>/sec caused by ET. The total amount of water lost by ET over the time is about 17000 m<sup>3</sup>/sec/region area only from the middle region.

The developed hydraulic structure along the river (e.g. dams, reservoirs, etc.) and also the climate change which is represented by the Evapo[transpi]ration also show more effects over time in this region, especially, during the dry seasons and also towards the end of the study period. Noticeably, the water consumption is relatively more in this region because the number of people live in this region is relatively bigger. Moreover, the ET losses is less in this region when compare it the previous model because the ET rate is relatively less according to the findings in chapter five.

### 7.3 Tigris Southern Region Model

Discharge data set for the study period from 1970 to 2000 was extracted from the most downstream cross section in the Tigris middle model and was fed into the Tigris southern model as discharge upstream boundary. Figure 7.5 shows the location of the southern region alongside with developed a longitudinal section of the Tigris river starting from the first point selected for this research, cross section #640, all the way down to cross section #1170 in the model. The river reach goes through Kut city. It is considered as a relatively less population rate and industrial area but more agricultural land covered. River cross section #1170 is located in the Amarah city, 200 km south-east of Kut. The main reach of Tigris has about 345 km length in this area. The longitudinal section shows also the changes in topographical elevations from the upstream to the downstream of that river. There were few observed river cross sections available correspond well with the modelled river profile elevations. The river banks and river bed representations from the previous models were repeated for this case again. The main channel was modelled only (not tributaries involved). The blue line in the figure represents the water elevation through the Tigris reach which is the resulting water stage due to the steady state run for the model considering September 1972 event (the highest recorded flow). Relatively, much less significant changing in river slope was recorded, only 0.000075 resampling the flatted topographical nature of the region. This value corresponds the slope calculated using observations in chapter six as well, Figure 7-5.

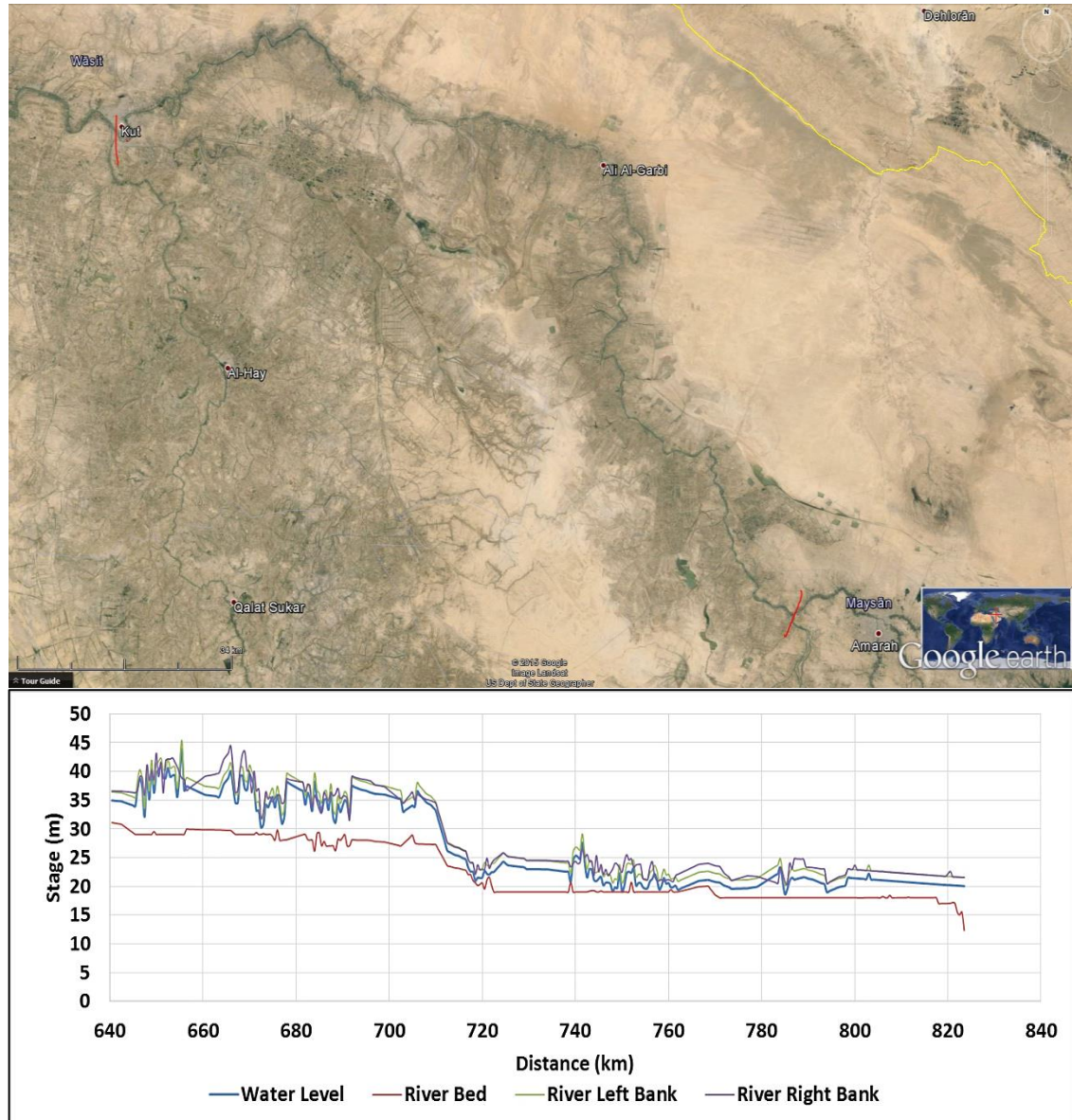


Figure 7-5: The Tigris southern model simulated by Google Earth and 3DRoutBuilder

The figure above shows that the developed river profile can handle extreme events very well. It has not been recorded that the water level exceeded the river bank levels. It could be because the reach depth is relatively shallow and the water quantity is relatively much less. Figure 7-6 shows the model discharge results for the period from 1970 to 2000 at the most downstream cross section #1170 and how the river is affected by the flow, abstractions and river losses including Evapo[transpi]ration in the middle region.

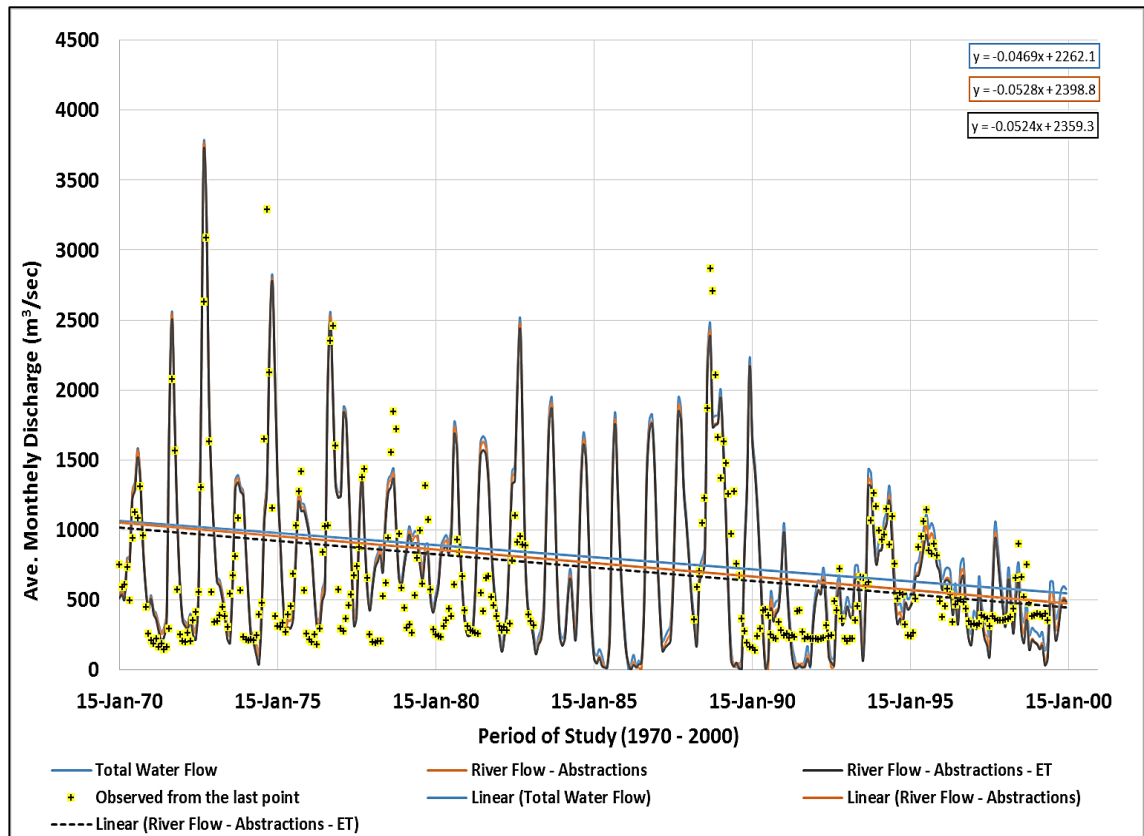


Figure 7-6: Tigris River, Water Losses\_Southern Region

Purely inherited water quantities reduction was recorded in this model based only on flow information from the previous model (about -0.205%). The discharge seasonal changes over the time in this region dramatically followed the previous regions releases pattern as well. In addition, the trend of the modelled discharge values in this part of the reach was showing considerable reduction in water quantities over time from abstraction and river losses. It should be noted that the modelled discharge due to abstractions and ET and river losses reached its lowest rates even more frequent in comparison to the previous models. The reason behind this could be because of the research limitation to access further information about the water ground changes and the quantities of water back to the main reach from other water resources (e.g. waste water treatment, sub-basins, small rivers linked the main system, etc.). In the following, Table 7.3 summarises what was happening due to the considered variables for the southern region flow:

Table 7.3: Statistics obtained from the most downstream point, cross section #1170 of the Tigris southern region model.

	<b>Total water received</b>	<b>Abstraction considered</b>	<b>Abstraction + ET considered</b>
<b>Changing over the period from 1970 to 2000</b>	-0.205%	-0.09%	-0.075%
<b>Max</b>	3747.4 m <sup>3</sup> /sec	3722 m <sup>3</sup> /sec	3684 m <sup>3</sup> /sec
<b>Average</b>	804.2 m <sup>3</sup> /sec	728 m <sup>3</sup> /sec	698 m <sup>3</sup> /sec
<b>Min</b>	134.3 m <sup>3</sup> /sec	0.7 m <sup>3</sup> /sec	0.25 m <sup>3</sup> /sec
<b>Total amount of water received over the period from 1970 to 2000</b>	<b>318514 m<sup>3</sup>/sec</b>	<b>262891 m<sup>3</sup>/sec</b>	<b>252064 m<sup>3</sup>/sec</b>

There is a sever reduction in modelled water quantities recorded in this case caused by relatively increasing in population rate and also by ET. There is more than 80 m<sup>3</sup>/sec difference by considering the average water quantity in addition to more than 30 m<sup>3</sup>/sec caused by ET. The total amount of water lost by ET over the time is about 11000 m<sup>3</sup>/sec only from the southern region.

It should be noticed that, the water consumption is relatively less in this region because the number of people live in this region is relatively less. Moreover, the ET losses is less in this region when compare it the previous model because the ET rate is relatively less according to the findings in chapter five.

There was a great chance to validate the developed models and the produced information using flow date set available for the most downstream point in the southern model. Although, the available observation for that point has lots of information and values missing but it still a great correspondence for the developed results. No more 19% difference was recorded using Nash-Sutcliff coefficient. This result can be considered as a very good achievement to the research considered the overall circumstances and limitations. And for that, the resulting flow values can be considered for reasonable water balance study.



## 7.4 Tigris River – Water Balance

The Tigris is one of the two great rivers that form the Mesopotamia, the other being the Euphrates. The Tigris flows south from the mountains of south-eastern Turkey through Iraq (Figure 7-7).

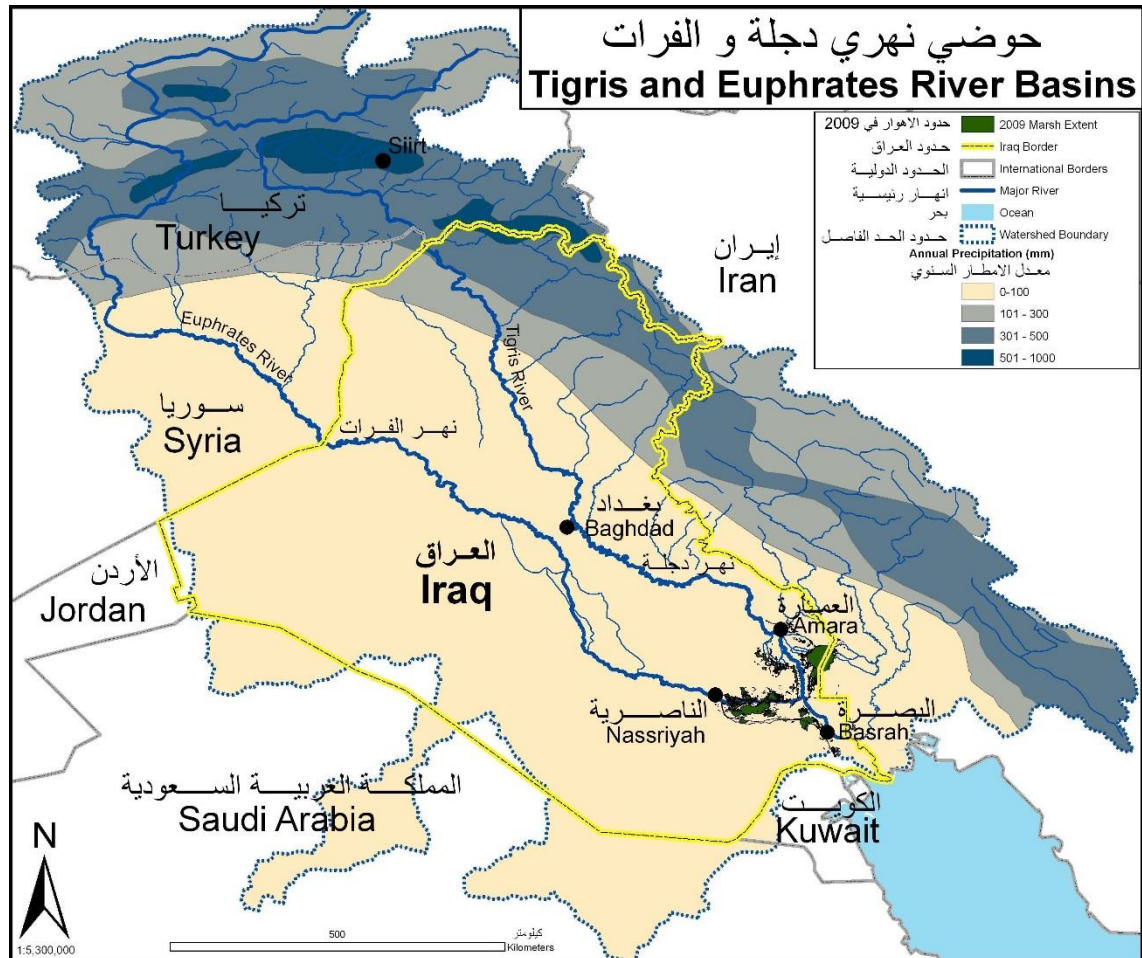


Figure 7-7: Tigris and Euphrates river basin and the annual average precipitation. Source: UVicSpace, edited by the author

The Tigris is 1,850 km long, rising in the Taurus Mountains of eastern Turkey. The river then flows for 400 km through Turkish territory before becoming the border between Syria and Turkey. This stretch of 44 km is the only part of the river that is located in Syria. The main channel continues southward and drains into the Hawizeh Marshes. Finally, the Tigris joins the Euphrates near al-Qurnah to form the Shatt-al-Arab.

Water quantities of the Tigris are believed to be affected both by climate change impacts and human activities. Understanding these influences is vital to manage water resources

in the basin. Carrying out such work requires information about the basin hydrology, especially characterisation of long-term and seasonal streamflow, including both flood and drought.

The flow of the Tigris in the upstream (as shown in the figure above – Turkey and Iran) is maintained by runoff of rainfall and snowmelt. Naturally, not all rainfall or snowmelt runs off. Some infiltrates the soil and is transpired into the atmosphere by plants or evaporates directly into the atmosphere or recharges the groundwater.

The part of the Tigris reach investigated in this study starts at Mosul Dam in the north of Iraq, and stretches all the way to Amara city in the far south of the country. This reach was selected because the majority of the people in this basin are located along this river stretch. Moreover, the amount of water flowing through this part of the reach is believed to be subjected by severe climate change impacts and dependency of upstream releases. The total annual precipitation in the overall basin is considerably less than the Evapo[transpi]ration itself over this basin (Figures 7.7 and 7.8).

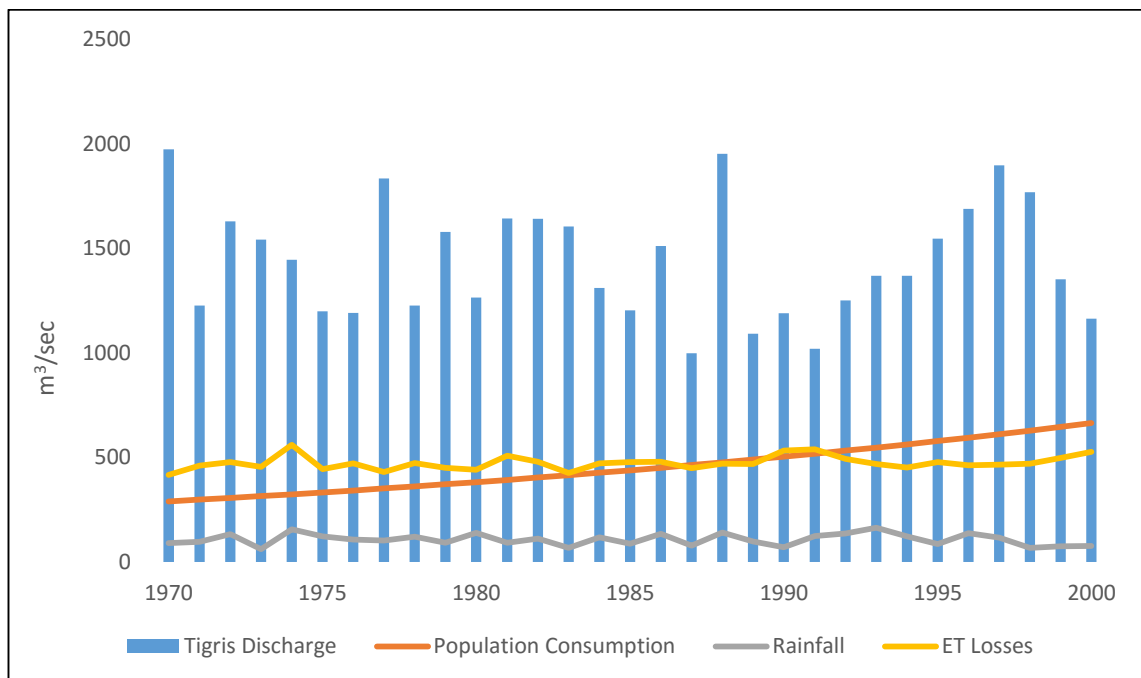


Figure 7-8: Annual precipitation, Population Consumption rate, ET and the remaining river flow at the downstream point of Tigris Model



The balance between evapotranspiration and runoff is mainly influenced by the climate. Abstractions for irrigation, which is widely practiced within the Tigris basin, are known to have a significant impact on the Tigris discharge, especially in its downstream area and during and at the end of the dry season. The net effect of temperature rise, for example is conversion of water from runoff into evapotranspiration. Across the whole investigated reach, the water flow with about 1440 m<sup>3</sup>/sec, an average of 470 m<sup>3</sup>/sec equivalent to flow of Evapo[transpi]ration with about 1.2 percent increase is converted from the Tigris as a direct result of climate change every year (Table 7.4), alongside with no more than 107 m<sup>3</sup>/sec equivalent to flow of precipitation.

*Table 7.4: Major terms in the water balance of the Tigris, 1970 - 2000. All flows are expressed as volumes of water of the basin per year.*

<b>Process</b>	<b>Mean m<sup>3</sup>/sec/yr</b>	<b>Rate of Charge %</b>
Rainfall	107	-1.73
Total Evapotranspiration	471	1.19
Net removal of ground water	-	-
Population consumption	300	2.85
Tigris Discharge	1440	-0.96

The aridity is a major attribute of this part of the basin and causes very little water being left to run off and recharge the Tigris after evapotranspiration extracts its share; most of the river's discharge is from upstream releases. It varies accordingly and with time corresponding to variability in precipitation and evapotranspiration.

Towards the end of the 20th century, the rate of noticeable increase of water losses and associated human-induced changes in evapotranspiration has constantly been going up (the total change in rate is about 3.2% over the study period from 1970 until 2000). Even if water losses were to stabilise in the future as it been assumed in this study, then further urgent increases in runoff would be needed in order to maintain the rate of discharge within the Tigris. "Water in Iraq fact sheet" report published in March 2011 by the IAU (UN Inter-Agency Information and Analysis Unit) stated that Iraq needs about 52 billion

cubic meter to meet the water demand in Tigris Basin by 2015, while this study concludes that the water amount flows along Tigris is only 44.8 billion cubic meter per year.

It was impossible to accurately predict river discharge data sets until 2100, because the main boundary condition needed, the rainfall quantities are not enough across the whole basin to represent the discharge. However, figure 7.9 shows a linear extrapolation of the discharge based on the modified - modelled discharge values at the most downstream point of the entire Tigris model (river cross section # 1170).

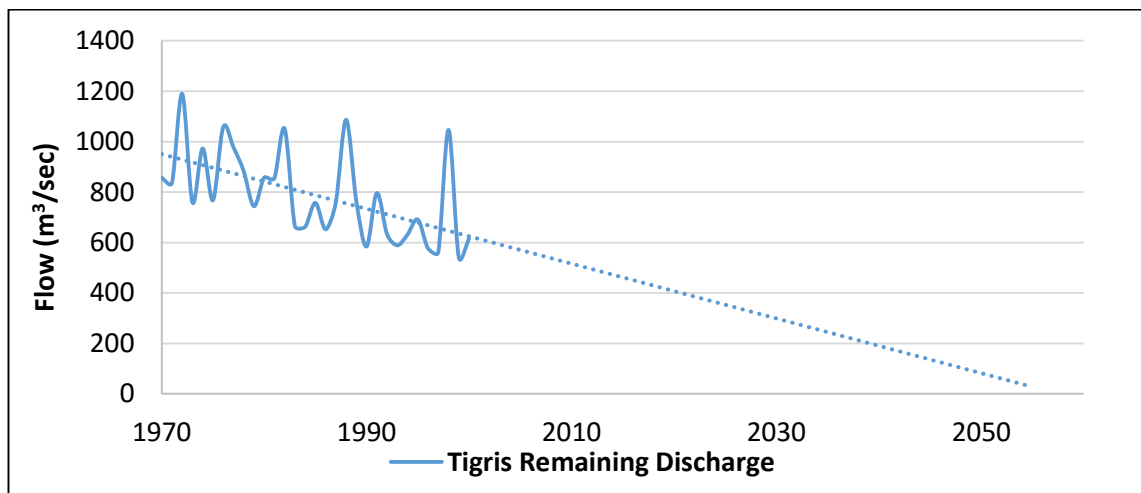


Figure 7-9: Statistical discharge prediction for the future of available water resources in Tigris.

This relationship confirms the main message of an UN report from 22<sup>nd</sup> of March 2011 warning that the Tigris could completely dry up but by the 2060. The decreasing rate of precipitation helped to make the water substitution much difficult and supported the increase in evapotranspiration losses. Absence of accurate assessment of ground water changes rate has made it difficult to assess the sustainability of water resources.

## 7.5 Summary

In this chapter, the water sustainability of the river Tigris in Iraq was assessed by carrying out a water balance study based on the findings of the previous chapters. River discharge data sets for the period from 1970 to 2000 were successfully used in computer simulations of the Tigris downstream from Mosul Dam.

Three individual models were set up for the 850km long reach of the Tigris and two major tributaries. Due to limitations of the hydrodynamic model the reach was divided into three regions (northern, middle and southern regions). Available precipitation data alongside modelled discharge and Evapo[transpi]ration information have been considered as the main elements of the water balance equation. Groundwater recharge (from the river channel) has not been included as a source of water losses in the modelling process because of lack of information of ground water levels and river bed permeability.

Precipitation across the Tigris basin downstream from Mosul dam and which only contributes up to 10% of the total river discharge was included in conducting the water balance study. The analysis of the precipitation identified a reduction in the rainfall rate by 1.73% over the time from 1970 to 2000. The Evapo[transpi]ration which forms more than 29% of the water losses has been found to be increasing by 1.2%. In addition, the water demand will be increasing proportional to the increase in population which is at 2.28% over the same time period.

As per the Iraqi Water Resource Ministry, the Tigris needs about 52 million cubic meters a year to fulfil the overall water demand. However, the water balance conducted in this study shows that the Tigris received only about 44.8 million cubic meters a year on average during the examined period as releases from the upstream countries. Moreover, a simple prediction based on water availability shows that the water flows in Tigris could be completely dried out by 2060.

## **Chapter Eight: Conclusions, Limitations and Recommendations for Further Study**

### **8.1 Research Conclusions**

The aim of this research is to give a better understanding of the impact of climate change on arid and semi-arid basins located in a developing country. Evapotranspiration (ET) is considered to represent the climate change impacts on these areas. The potential usage of Google Earth as a source of geometrical to obtain river profiles for rivers located in area with severe lack of data, was investigated in this study to aid research in developing countries.

With not many details and further explanations available, the media picked up the news that the UN announced on 22<sup>nd</sup> March 2011 (the International World Water Day) that the large rivers (Tigris and Euphrates) will become completely dry in the close future. Despite the severe lack of background information regarding this announcement, it was the main motivation of this study. Accordingly:

- A thorough investigation based on literature was made to identify the state-of-the-art technologies used to establish river losses and water balance studies for rivers located in arid and semi-arid regions.
- Based on critical literature review, large amounts of different data sets, including hydro-meteorological and high resolution topographical information are required.

Complex political situation and the fact that this region is considered as a developing country make obtaining and accessing the necessary data sets very difficult. The Iraqi water resources ministry thankfully collaborated by providing prerequisite information including some exclusive data sets to aid the objectives of this research. However, the provided information needed reformatting and editing works to make them more user-friendly.

- Some data rescue actives including digitalisation were carried out by the author.

A reasonable amount of information including meteorological, river flow, water level and some river cross section data were obtained. The main attribute of the obtained data sets was discontinuity and gaps over the investigated time period from 1970 to 2000 considered usable to calibrate and validate purposes.

- The source of the flowing water in the examined part of the reach originates mainly from upstream releases.

In fact, one of the main conclusions of this research is that runoff river recharge as a result of precipitation forms less than 10% of the total amount of water flowing within the river Tigris from its main tributaries and Mosul Dam in the north of Iraq. By presuming that the upstream releases are the main source of water to meet the water demands, the quantities of water which are removed from the river surface (evaporation) and the surrounding soil (transpiration) are considered as the river losses. Because of that, the meteorological data available, including maximum and minimum temperature, maximum and minimum humidity, wind speed, solar radiation and atmospheric pressure for the period from 1970 to 2000 (from three gauging stations along Tigris – Mosul, Baghdad and Basra) were used to model evapotranspiration data sets over the selected area.

- A comparative analysis of five well known potential evapotranspiration models was carried out.

The performance of those models (Shuttleworth and Wallace, Penman-Monteith -FAO 56, Priestly Taylor, McNaughton and Black and Hargreaves and Semani) (selected respectively according to their complexity in terms of the number of variables used) was assessed against the available Evaporation Pan class A data sets. The Hargreaves and Semani model was selected not only because of its performance (NSE = 0.79, 0.71 and 0.92 for the northern, middle and southern regions respectively), but also because it is the simplest among the others.

- Hargreaves and Semani model was used to reconstruct the available Evaporation Pan class (A) data sets over the study period.

The analysis of the results shows that the southern region which is known to be the hottest of the three has a lower river losses rate in contrast to what was expected when compared to the upper regions which are meant to be relatively cooler. However, the produced data sets do not represent the actual river losses yet, as all of the used methods including evaporation pan class (A) produce potential losses. A relationship was built to calculate the actual river losses, which is summarised as follows:

$0.85 \times \text{reconstructed Evaporation Pan class A values over time} + 0.2 \times \text{modelled potential evapotranspiration} = \text{actual water losses from the river} = \text{Evapo[transpi]ration}$ . The resulting average Evapo[transpi]ration losses are about 24 mm/day. The losses could reach about 61 mm/day across the river basin in hot seasons.

- The statistical down scaling model (SDSM) version 5.1.1 was used in this study to identify the future climate change impact on the evapotranspiration and in turn the impact of the evapotranspiration on river losses.

NCAR reanalysed daily surface evaporation data sets were found suitable to be used instead of ET observations (NES = 0.65). It was found in this study that the process of predicting the future changing rates of the evapotranspiration directly is more feasible compared to the traditional methods where temperatures and precipitation data is needed. The IPCC A2 and B2 climate change scenarios were considered in the evapotranspiration future projection. The results showed no evidence that the evapotranspiration rate will stop increasing even after 2100. In considering the selected climate change scenarios (IPCC A2 and B2), the increases recorded were 1.95 mm and 1.1 mm respectively on average across the river basin.

- The impact of the resulting Evapo[transpi]ration losses on the river flow over the studied time scale was assessed using a hydrodynamic model.

The capacity of ISIS – 1D, as a well known hydrodynamic flow and water level simulator, to model 850 km of Tigris River in Iraq was tested in this research. The construction and running of the model was facilitated by using the data provided by the Iraqi Ministry of

Water Resources including historical data sets of river discharge and water levels for several tributaries alongside with the main water quantities of the main reach.

- The main challenge was obtaining a profile for a river located in a developing country such as Iraq with no high resolution Lidar or airborne data set available.

The in-channel profile of the river had to be reasonably represented for the assessment of the shortage of water in the river. One of the major findings of this research was the use of Google Earth as reliable source of generating river cross section for a river like the Tigris with a wide and shallow channel and severe water shortage. This process was carried out using 3DRoutBuilder. This method showed to be a good avenue for those who are interested in modelling rivers which are smaller than the Tigris, in particular.

The resulting river cross sections correspond well with observations obtained from different locations along the river. Once the Tigris model was built, steady and unsteady state runs were executed.

- Steady state runs were carried out to check whether the developed model can handle extreme events and also to generate flow and water levels to fill the gaps in data sets (either flow or water level information).

The Tigris model was calibrated and validated for the hydraulics and also for the water losses (population consumption and ET) simulations, to generate all the necessary information for and carry out the long-term predictions needed for the water balance study.

- Water balance analysis was carried out over the examined reach. It shows that the recharge from precipitation along the investigated Tigris stretch only contributes to less than 10% (equivalent only 107 m<sup>3</sup>/sec flow) to the total discharge over the studied period, which is about 1440 m<sup>3</sup>/sec across the river basin.
- The amount of precipitation received during the period of study was not enough to represent flow in future predictions processes.

The analysis of the precipitation carried out in this study identified a reduction in the rainfall rate by 1.73% over the time of study. The Evapo[transpi]ration which forms more than 29% (equivalent only 470 m<sup>3</sup>/sec flow) of the water flowing within the Tigris reach was found to be increasing by 1.2%. Further, an increase in water demand equivalent to the population growth rate of 2.28% is also predicted with the population being the biggest water consumer already, which in turns; put an additional pressure by increasing the irrigation demand consequently.

According to the Iraqi water resources ministry, Tigris basin needs about 52 billion m<sup>3</sup> a year to fulfil the water demands including agriculture, marshland maintenance, civil use, industry and power generation. However, the water balance conducted in this study shows that the Tigris received only about 44.8 billion m<sup>3</sup> a year on average during the examined period as releases from the upstream countries. A simple prediction based on water availability carried out in this study shows that the water flows in Tigris could be completely dried out by 2060, taking in the account the water releases history, Evapo[transpi]ration losses and population growth rates.

Concluding it can be said; this research project has demonstrated the importance of Evapo[transpi]ration on the water balance of the Tigris in Iraq and how climate change predictions will make this an even more important factor which needs to be considered in catchment management. Also, a novel usage of Google Earth and 3DRoutBuilder is presented to generate river profiles which can provide aid for studies of ungauged catchments in developing countries or where no data exists. This is particularly relevant, owing to recent developments in remote sensing technologies and the increasing availability of datasets from data providers and the global scientific community at little or no cost.



Finally, the need for high quality data measurement and analysis becomes more vital during times such as these with rapid changes to socio-economic activity, population, and the global climate system.

## **8.2 Research Limitations**

The main challenge encountered in this research study was the lack of data (e.g. field data, historic hydro-meteorological series and their corresponding discharge) required for the modelling process. Despite the few gauging stations that exist along the Tigris, still a wide area of its catchment is characterised by ungauged stream flow and lack of other prerequisite information.

The use of only two emissions scenarios represents another limitation to the project. The use of medium high (A2) and medium-low (B2) emissions scenarios omits two other families of emissions scenarios (A1 and B1) considering the time of the research. The A1 family represents more “extreme” emissions. However, the A2 and B2 scenarios are the ones recommended for use by the IPCC and cover 90% of the total emission scenario range (Nakicenovic et al., 2000).

Another issue to be considered is the DEM resolution used to develop the river cross sections. Although it was found to be adequate for the hydrologic model at the catchment scale, the ISIS-1D hydrodynamic model ideally requires better resolution terrain data and bathymetric data of the river. Finer resolution data are required to produce cross-sections that are more accurate and produce more accurate surface water elevations especially for deeper middle region of the Tigris.

Multitude of models, processes and steps undertaken in this thesis helped to rise uncertainty in the resulting information. Reducing uncertainties in the construction of the models used and enhancing their performance would help build a more reliable river

losses assessment system. However, the scope of this topic is huge and could not be fully addressed by a single PhD study, and in reality, this PhD work contains many limitations. Nevertheless, this research has produced some interesting findings from which several directions for future work are proposed below.

### **8.3 Recommendations for Further Research**

Addressing the research questions has resulted in some worthwhile insights and additional challenges remain. Some of these are described as follows:

- Only one type of downscaling was used in the project. Future climate impact assessments should include both statistically downscaled data and dynamically downscaled data in order to take into account uncertainty due to the downscaling methodology.
- The modelling on the Tigris in Iraq illustrated the importance of Evapo[transpi]ration in influencing future catchment water balances and water losses assessment. Rainfall-runoff modelling considering no boundaries between the riparian countries and covering all the Tigris River Basin will be interesting to evaluate how the river flow will be influenced by the changes of predicted rainfall/snowfall in the future resulting from different climate change scenarios.
- The ISIS -1D hydraulic model can be a valuable tool in simulating a large number of scenarios in the catchment, typically implementing structures, levees, ponds, reservoirs, changing river bed material and any other required scenario for investigating resulting surface water elevations and discharge. In order to do so, additional field survey data are required for the area of interest.
- The accuracy of the model inputs, derived from terrain models, can be improved with the use of additional, more recent data sources producing higher resolution DEMs. Additional advances in remote sensing technology with more data/information like GloVis, LIDAR images, BRDF's, Hyperion images from EO-

1 satellite as well as field measurements using instruments such as GPS for more accurate supervised classification outputs will provide a great aid in river profile representation whenever they will be available for Tigris.

- The role of the groundwater on the discharge of the Tigris needs to be further investigated and explored to enable a more holistic investigation into the analysis of water management in this basin. Water losses to the groundwater and water recharge from the groundwater need to be quantified.
- It is also clear that the selected catchment is very vulnerable to drought situations. Therefore, there is an urgent need to investigate how to increase the collaboration between the riparian countries to establish bigger storage projects in the upstream regions that will be necessary to guarantee water releases into the future and which will provide sufficient water for all (e.g. are more dams and weirs required to be constructed along the Tigris to improve water availability in the lower catchment zones).
- The problems associated with climate change may even be exacerbated by other anthropogenic impacts on the environment such as land use change. Provision of a better understanding of local feedback mechanisms resulting from land use changes of the Tigris River Basin is also required.

## List of Publications

### Journal Papers:

- (Helu A. Under Review) Evapotranspiration of Tigris River basin: Modelling, Data Reconstruction and Trend analysis
- (Helu A. Under Review) Investigate the Possibility of Using a Freely Accessed Earth Browser Application in Generating River Profiles.
- (Helu A. Under Review) River Losses Estimation: investigate the impacts of Evapo[transpi]ration and Population increase in Tigris River Basin.

### Articles:

- (Helu A. 2013) Evapotranspiration Modelling of Tigris River – Iraq. CH2MHILL - Cardiff University collaboration Newsletter, Volume 5, Issue 3, July 2013

### Presentations and Posters:

- Poster: Zero Cost River Profile Data Generating Tool. Climate Change Consortium of Wales (C3W) Workshop held in Cardiff University December 2011. **Best Poster Award**
- Poster: Comparison of Six Evapotranspiration Models' Simulations over Arid/Semi-Arid Regains. British Hydrological Society, Imperial College London Annual Meeting, October – 2012.
- Presentation: Tigris River Losses Assessment. British Hydrological Society Annual Meeting, Imperial College London, October – 2013.
- Presentation: Evapo[transpi]ration Impacts on Tigris River. The Iraqi Day, Cardiff University, August – 2014. **Best Presentation Award**
- Presentation: River Losses: Climate Change and Population Increase Impacts in Arid Catchments. The Chartered Institution of Water and Environmental Management (CIWEM) Meeting, September – 2014. **Best micro Presentation Award**

## References

- AERTS, J. C. J. H., KRIEK, M. & SCHEPEL, M. 1999. Stream (Spatial Tools for River Basins and Environment and Analysis of Management Options): 'Set Up and Requirements'. *Physics and Chemistry of the Earth, Part B: Hydrology, Oceans and Atmosphere*, 24, 591-595.
- AL-HAFITH, I. A. I. C., T. A.; OTHMAN, KH. I. 2012. The Hydraulic Characteristics of Tigris River at Mosul City. *Al-Rafadain Engineering Journal*, 20, 48.
- ALLEN R., LUIS S. PEREIRA & DIRK RAES 1998. Crop evapotranspiration - Guidelines for computing crop water requirements - FAO Irrigation and drainage paper 56. Food and Agriculture Organization of the United Nations, Rome, <http://www.fao.org/docrep/x0490e/x0490e00.htm#Contents>.
- ALLEN, R. G. 2000. Using the FAO-56 dual crop coefficient method over an irrigated region as part of an evapotranspiration intercomparison study. *Journal of Hydrology*, Volume 229, 27-41.
- ALMAAROFI, S., ALI DOUABUL & AL-SAAD, H. 2012. Mesopotamian Marshlands: Salinization Problem. *Journal of Environmental Protection*, Vol.3 No.10(2012), Paper ID 23837, , 7 pages.
- ANDERSON, B. G., RUTHERFURD, I. D. & WESTERN, A. W. 2006. An analysis of the influence of riparian vegetation on the propagation of flood waves. *Environmental Modelling & Software*, 21, 1290-1296.
- ANDERSON, M. G. & BATES, P. D. 2001. *Model validation: perspectives in hydrological science*, John Wiley & Sons Ltd.
- ARNELL, N. W. 1992. Factors controlling the effects of climate change on river flow regimes in a humid temperate environment. *Journal of hydrology*, 132, 321-342.
- ARNELL, N. W. 1996. *Global warming, river flows and water resources*, John Wiley & Sons Ltd.
- ASANTE, K. O., ARLAN, G. A., PERVEZ, S. & ROWLAND, J. 2008. A linear geospatial streamflow modeling system for data sparse environments. *International Journal of River Basin Management*, 6, 233-241 [http://www.tandfonline.com/doi/abs/10.1080/15715124.2008.9635351#.U\\_7cue6Orng](http://www.tandfonline.com/doi/abs/10.1080/15715124.2008.9635351#.U_7cue6Orng).
- ATKINSON, B. W. 2003. *The climate near the ground*, sixth edition, R. Geiger, R. H. Aron and P. Todhunter, Rowman and Littlefield Publishers, Lanham, MD, USA, 2003. No. of pages xviii +584. ISBN 0-7425-1857-4. *International Journal of Climatology*, 23, 1797-1798.
- AVILA, A., NEAL, C. & TERRADAS, J. 1996. Climate change implications for streamflow and streamwater chemistry in a Mediterranean catchment. *Journal of Hydrology*, 177, 99-116.
- BACHNER, S., KAPALA, A. & SIMMER, C. 2008. Evaluation of daily precipitation characteristics in the CLM and their sensitivity to parameterizations. *Meteorologische Zeitschrift*, 17, 407-419.
- BAHATI, C. J. 2008. Hydrological modeling of the Congo River basin: Asoil-water balance approach. University of Botswana - Masters of Sciences (M.Sc.), [http://www.memoireonline.com/09/09/2734/m\\_Hydrological-modeling-of-the-Congo-River-basin-Asoil-water-balance-approach0.html](http://www.memoireonline.com/09/09/2734/m_Hydrological-modeling-of-the-Congo-River-basin-Asoil-water-balance-approach0.html).
- BARNETT N., MADRAMOOTOO C.A. & J., P. 1998. Performance of some Evapotranspiration Equations at a site in Quebec. *Canadian Agricultural Engineering*. 40(2): 89-103, II- E, [http://csbecscgab.ca/docs/journal/40/40\\_2\\_89\\_raw.pdf](http://csbecscgab.ca/docs/journal/40/40_2_89_raw.pdf).
- BARROW, E., LEE, R. J., & AGENCY, C. E. A. 2000. Climate change and environmental assessment Part 2, Climate change guidance for environmental assessments. Climate change and environmental assessment. [Ottawa]: Canadian Environmental Assessment Agency.
- BATES, B., KUNDZEWICZ, Z. W., WU, S. & PALUTIKOF, J. 2008. Climate change and water, Intergovernmental Panel on Climate Change (IPCC).
- BECKMANN, B.-R. & ADRI BUIHAND, T. 2002. Statistical downscaling relationships for precipitation in the Netherlands and North Germany. *International Journal of Climatology*, 22, 15-32.

- BEEVERS, L. C. 2003. Morphological sustainability of barrage impoundments. University of Glasgow, PhD thesis, [http://encore.lib.gla.ac.uk/iii/encore/record/C\\_\\_Rb2191041](http://encore.lib.gla.ac.uk/iii/encore/record/C__Rb2191041).
- BGR, U. E. A. 2013. INVENTORY OF SHARED WATER RESOURCES IN WESTERN ASIA (ONLINE VERSION). United Nations Economic and Social Commission for Western Asia; Bundesanstalt für Geowissenschaften und Rohstoffe, Chapter 3 - Tigris River Basin.
- BHALLAMUDI, S. M. & CHAUDHRY, M. H. 1991. Numerical modeling of aggradation and degradation in alluvial channels. *Journal of Hydraulic Engineering*, 117, 1145-1164.
- BRADBROOK, K. 2006. JFLOW: a multiscale two-dimensional dynamic flood model. *Water and Environment Journal*, 20, 79-86.
- BROTZGE, J. A. & CRAWFORD, K. C. 2003. Examination of the Surface Energy Budget: A Comparison of Eddy Correlation and Bowen Ratio Measurement Systems. *Journal of Hydrometeorology*, 4, 160-178.
- BROUYÈRE, S., CARABIN, G. & DASSARGUES, A. 2004. Climate change impacts on groundwater resources: modelled deficits in a chalky aquifer, Geer basin, Belgium. *Hydrogeology Journal*, 12, 123-134.
- BUCHANAN, T. J., AND & SOMERS, W. P. 2010. Discharge measurements at gaging stations. 1969 U.S. Geological Survey Techniques of Water-Resources Investigations, book 3, chap A8, 65 p. (Also available at <http://pubs.usgs.gov/twri/twri3a8/>.)
- BUDYKO 1974. *Climate and life*, Elsevier Science.
- BULTOT, F., COPPENS, A., DUPRIEZ, G. L., GELLENS, D. & MEULENBERGHS, F. 1988. Repercussions of a CO<sub>2</sub> doubling on the water cycle and on the water balance — A case study for Belgium. *Journal of Hydrology*, 99, 319-347.
- BUONOMO, E., JONES, R., HUNTINGFORD, C. & HANNAFORD, J. 2007. On the robustness of changes in extreme precipitation over Europe from two high resolution climate change simulations. *Quarterly Journal of the Royal Meteorological Society*, 133, 65-81.
- BURNHAM, M. & DAVIS, D. 1990. Effects of Data Errors on Computed Steady-Flow Profiles. *Journal of Hydraulic Engineering*, 116, 914-929.
- CHANDLER, R. E. & WHEATER, H. S. 2002. Analysis of rainfall variability using generalized linear models: A case study from the west of Ireland. *Water Resources Research*, 38, 1192.
- CHEN, Z. Q., OHARA, N., ANDERSON, M. L. & YOON, J. A regional hydroclimate model for water resources management of the Tigris-Euphrates watershed. 2008.
- CHIEW, F., WHETTON, P., MCMAHON, T. & PITTOCK, A. 1995. Simulation of the impacts of climate change on runoff and soil moisture in Australian catchments. *Journal of Hydrology*, 167, 121-147.
- CHOW, V. T. 1959. *Open-channel hydraulics*, New York, McGraw-Hill.
- CHRISTENSEN, J. & CHRISTENSEN, O. 2007. A summary of the PRUDENCE model projections of changes in European climate by the end of this century. *Climatic Change*, 81, 7-30.
- CHRISTENSEN, J. H., BOBERG, F., CHRISTENSEN, O. B. & LUCAS-PICHER, P. 2008. On the need for bias correction of regional climate change projections of temperature and precipitation. *Geophysical Research Letters*, 35, L20709.
- COHEN, M. J., HENGES-JECK, C. & CASTILLO-MORENO, G. 2001. A preliminary water balance for the Colorado River delta, 1992–1998. *Journal of Arid Environments*, 49, 35-48.
- COVEY, C. 1995. Using paleoclimates to predict future climate: how far can analogy go? *Climatic Change*, 29, 403-407.
- CROWLEY, T. J. 1990. Are There Any Satisfactory Geologic Analogs for a Future Greenhouse Warming? *Journal of Climate*, 3, 1282-1292.

CUNGE, J. A. 1969. On The Subject Of A Flood Propagation Computation Method (Muskingum Method). *Journal of Hydraulic Research*, 7, 205-230.

DEC 2006. River cross-section surveying using RTK Technology. The Yangtze River project case study, <http://mycoordinates.org/river-cross-section-surveying-using-rtk-technology/all/1/>.

DIAZ-NIETO, J. & WILBY, R. L. 2005. A comparison of statistical downscaling and climate change factor methods: impacts on low flows in the River Thames, United Kingdom. *Climatic Change*, 69, 245-268.

DIBIKE, Y. B. & COULIBALY, P. 2005. Hydrologic impact of climate change in the Saguenay watershed: comparison of downscaling methods and hydrologic models. *Journal of hydrology*, 307, 145-163.

DOORENBOS, J. & PRUITT, W. O. 1977. Guidelines for Predicting Crop Water Requirements, Food and Agriculture Organization of the United Nations.

DOORENBOS, J. & PRUITT, W. O. 1977. Guidelines for Predicting Crop Water Requirements, Food and Agriculture Organization of the United Nations.

DURMAN, C. F., GREGORY, J. M., HASSELL, D. C., JONES, R. G. & MURPHY, J. M. 2001. A comparison of extreme European daily precipitation simulated by a global and a regional climate model for present and future climates. *Quarterly Journal of the Royal Meteorological Society*, 127, 1005-1015.

EAGLEMAN, J. R. 1967. Pan evaporation, potential and actual evapotranspiration. *Journal of Applied Meteorology*, 6, 482-488.

ERVINE, A. & MACLEOD, A. B. 1999. MODELLING A RIVER CHANNEL WITH DISTANT FLOODBANKS. *Proceedings of the ICE - Water Maritime and Energy* [Online], 136. Available: <http://www.icevirtuallibrary.com/content/article/10.1680/iwtme.1999.31265>.

FISCOR, A. J. 2005. Mussel Habitat Mapping in the Big South Fork National River and Recreation Area (BISO). Thesis, Master of Science, University of Tennessee - Knoxville, [http://trace.tennessee.edu/utk\\_gradthes/1884/](http://trace.tennessee.edu/utk_gradthes/1884/).

FLUG, M., SEITZ, H. & SCOTT, J. 1998. Measurement of stream channel habitat using sonar. *Regulated Rivers: Research & Management*, 14, 511-517.

FOWLER, H. & EKSTRÖM, M. 2009. Multi-model ensemble estimates of climate change impacts on UK seasonal precipitation extremes. *International Journal of Climatology*, 29, 385-416.

FREAD, D. L. 1984. DAMBRK: The NWS Dam-Break Flood Forecasting Model.

FREI, C., SCHÖLL, R., FUKUTOME, S., SCHMIDLI, J. & VIDALE, P. L. 2006. Future change of precipitation extremes in Europe: Intercomparison of scenarios from regional climate models. *Journal of Geophysical Research: Atmospheres* (1984–2012), 111.

FRENCH, J. & CLIFFORD, N. 2000. Hydrodynamic modelling as a basis for explaining estuarine environmental dynamics: some computational and methodological issues. *Hydrological Processes*, 14, 2089-2108.

FUJIHARA, Y., TANAKA, K., WATANABE, T., NAGANO, T. & KOJIRI, T. 2008. Assessing the impacts of climate change on the water resources of the Seyhan River Basin in Turkey: Use of dynamically downscaled data for hydrologic simulations. *Journal of Hydrology*, 353, 33-48.

GEBREMESKEL, S., LIU, Y. B., DE SMEDT, F., HOFFMANN, L. & PFISTER, L. 2004. Analysing the effect of climate changes on streamflow using statistically downscaled GCM scenarios. *International Journal of River Basin Management*, 2, 271-280.

GELLENS, D. & ROULIN, E. 1998. Streamflow response of Belgian catchments to IPCC climate change scenarios. *Journal of Hydrology*, 210, 242-258.

GERGEL, S. E., TURNER, M. G., MILLER, J. R., MELACK, J. M. & STANLEY, E. H. 2002. Landscape indicators of human impacts to riverine systems. *Aquatic Sciences*, 64, 118-128.

GHAVASIEH, A.-R., POULARD, C. & PAQUIER, A. 2006. Effect of roughened strips on flood propagation: Assessment on representative virtual cases and validation. *Journal of Hydrology*, 318, 121-137.

GIORGI, F. & MEARNES, L. O. 1999. Introduction to special section: Regional climate modeling revisited. *Journal of Geophysical Research: Atmospheres* (1984–2012), 104, 6335-6352.

GLEICK, P. H. 1987. Regional hydrologic consequences of increases in atmospheric CO<sub>2</sub> and other trace gases. *Climatic Change*, 10, 137-160.

GLEICK, P. H. 1993. *Water and Conflict: Fresh Water Resources and International Security*. *International Security*, 18, 79-112.

GRAHAM, R. 2003. 12D Model Course Notes. 4D Solutions Pty Limited, <http://www.12d.co.uk/downloads/v8/Rivers%20design%20course.pdf>.

GRISMER, M., ORANG, M., SNYDER, R. & MATYAC, R. 2002. Pan Evaporation to Reference Evapotranspiration Conversion Methods. *Journal of Irrigation and Drainage Engineering*, 128, 180-184.

HAESTAD & DYHOUSE, G. D. 2003. *Floodplain modeling using HEC-RAS*, Waterbury, CT, Haestad Press.

HALCROW & WALLINGFORD, H. 1999. {ISIS} Flow User Manual. Halcrow/ HR Wallingford.

HANSEN, V. E., ISRAELSON, O. & STRINGHAM, G. E. 1980. *Irrigation principles and practices*. Irrigation principles and practices. 4th edition.

HARDY, T., AND, P. P. & MATHIAS, D. 2005. WinXSPRO, A Channel Cross Section Analyzer, User's Manual, Version 3.0. Fort Collins, CO: U.S. Department of Agriculture, Forest Service, Rocky Mountain Research Station., Gen. Tech. Rep. RMRS-GTR-147., 94.

HARRELSON, C. C., POTYONDY, J. P., RAWLINS, C. L., ROCKY MOUNTAIN, F. & RANGE EXPERIMENT, S. 1994. *Stream channel reference sites: an illustrated guide to field technique*, Fort Collins, Colo., U.S. Dept. of Agriculture, Forest Service, Rocky Mountain Forest and Range Experiment Station.

HARVEY, F. 2013. Water crisis widening: 4.5 billion people live near 'impaired water sources'. *The Guardian* <http://news.mongabay.com/2013/0528-gen-water-scarcity.html>.

HENSEN, J. L. & LAMBERTS, R. 2012. *Building performance simulation for design and operation*, Routledge.

HERATH, S., DUTTA, D. & WIJESSEKERA, S. 2003. A Coupled River and Inundation Modeling Scheme for Efficient Flood Forecasting. *情報地質*, 14, 37-41  
[https://www.jstage.jst.go.jp/article/geoinformatics/14/1/14\\_1\\_37/\\_article](https://www.jstage.jst.go.jp/article/geoinformatics/14/1/14_1_37/_article).

HOFFMANN, E. & WINDE, F. 2010. Generating high-resolution digital elevation models for wetland research using Google Earth™ imagery - An example from South Africa. *Water SA*, 36, 53-68.

HOLZ, K.-P. & NITSCHKE, G. 1982. Tidal wave analysis for estuaries with intertidal flats. *Advances in Water Resources*, 5, 142-148.

HONNORAT, M., LAI, X., MONNIER, J. & LE DIMET, F.-X. Variational data assimilation for 2d fluvial hydraulics simulations. CMWR XVI-Computational Methods for Water Ressources. Copenhagen, june 2006., 2006. <https://hal.inria.fr/hal-00908191/PDF/HonnoratLaiMonnierLeDimet-CMWR06.pdf>.

HORRITT, M. S. & BATES, P. D. 2002. Evaluation of 1D and 2D numerical models for predicting river flood inundation. *Journal of Hydrology*, 268, 87-99.

HOUGHTON & D., D. 1985. *Handbook of Applied Meteorology*. New York: Wiley,

HUNTER, N. M., HORRITT, M. S., BATES, P. D., WILSON, M. D. & WERNER, M. G. F. 2005. An adaptive time step solution for raster-based storage cell modelling of floodplain inundation. *Advances in Water Resources*, 28, 975-991.



- HURKMANS, R. T. W. L., DE MOEL, H., AERTS, J. C. J. H. & TROCH, P. A. 2008. Water balance versus land surface model in the simulation of Rhine river discharges. *Water Resources Research*, 44, n/a-n/a.
- IRMAK, S., HAMAN, D. Z. & JONES, J. W. 2002. Evaluation of Class A Pan Coefficients for Estimating Reference Evapotranspiration in Humid Location. *Journal of Irrigation and Drainage Engineering-ASCE*, 128.
- JENSEN, D., HARGREAVES, G., TEMESGEN, B. & ALLEN, R. 1997. Computation of ETo under Nonideal Conditions. *Journal of Irrigation and Drainage Engineering*, 123, 394-400.
- JOHNSON, P. 1996. Uncertainty of Hydraulic Parameters. *Journal of Hydraulic Engineering*, 122, 112-114.
- KIBAROĞLU, A. 2007. Socioeconomic Development and Benefit Sharing in the Euphrates-Tigris River Basin. In: SHUVAL, H. & DWEIK, H. (eds.) *Water Resources in the Middle East*. Springer Berlin Heidelberg.
- KNIGHT, D. & SHIONO, K. 1996. River channel and floodplain hydraulics. *Floodplain processes*, 5, 139-181.
- KOTSIANTIS, S., KOSTOULAS, A., LYKOUDIS, S., ARGIRIOU, A. & MENAGIAS, K. Filling missing temperature values in weather data banks. IET Conference Publications, 2006. 327-334.
- KWADIJK, J. & MIDDELKOOP, H. 1994. Estimation of impact of climate change on the peak discharge probability of the river Rhine. *Climatic Change*, 27, 199-224.
- LANE, S. N. 1998. Hydraulic modelling in hydrology and geomorphology: a review of high resolution approaches. *Hydrological Processes*, 12, 1131-1150.
- LENDERINK, G. & VAN MEIJGAARD, E. 2008. Increase in hourly precipitation extremes beyond expectations from temperature changes. *Nature Geoscience*, 1, 511-514.
- LIANG, X., LETTENMAIER, D. P., WOOD, E. F. & BURGESS, S. J. 1994. A simple hydrologically based model of land surface water and energy fluxes for general circulation models. *JOURNAL OF GEOPHYSICAL RESEARCH-ALL SERIES-*, 99, 14,415-14,415.
- LIGHTHILL, M. J. & WHITHAM, G. B. 1955. On Kinematic Waves. I. Flood Movement in Long Rivers.
- LIN, B., WICKS, J. M., FALCONER, R. A. & ADAMS, K. 2006. Integrating 1D and 2D hydrodynamic models for flood simulation. *Proceedings of the Institution of Civil Engineers: Water Management*, 159, 19-25.
- LIU, X. 2008. Airborne LiDAR for DEM generation: some critical issues. *Progress in Physical Geography*, 32, 31-49 <http://ppg.sagepub.com/content/32/1/31.short>.
- LOHMANN, D., NOLTE-HOLUBE, R. & RASCHKE, E. 1996. A large-scale horizontal routing model to be coupled to land surface parametrization schemes. *Tellus A*, 48, 708-721.
- LUNDMARK, K. W., POHLL, G. M., CARROLL, R. W. & THOMAS, J. M. 2006. Regional Water Budget Accounting and Uncertainty Analysis Using a Deuterium-Calibrated Discrete State Compartment Model: White Pine County, Nevada, and Adjacent Areas in Nevada and Utah. American Geophysical Union, Fall Meeting 2006, abstract #H41E-0456.
- MANDLBURGER, G., HAUER, C., HÖFLE, B., HABERSACK, H. & PFEIFER, N. 2009. Optimisation of LiDAR derived terrain models for river flow modelling. *Hydrology & Earth System Sciences*, 13, 1453-1466 <http://www.cabdirect.org/abstracts/20093259301.html;jsessionid=0C06A2EC5D3CC0CA0A0B4301A9B9B639>.
- MARAUN, D., WETTERHALL, F., IRESON, A. M., CHANDLER, R. E., KENDON, E. J., WIDMANN, M., BRIENEN, S., RUST, H. W., SAUTER, T., THEMEßL, M., VENEMA, V. K. C., CHUN, K. P., GOODESS, C. M., JONES, R. G., ONOF, C., VRAC, M. & THIELE-EICH, I. 2010. Precipitation downscaling under climate change: Recent developments to bridge the gap between dynamical models and the end user. *Reviews of Geophysics*, 48, RG3003.
- MASON, D. C., COBBY, D. M., HORRITT, M. S. & BATES, P. D. 2003. Floodplain friction parameterization in two-dimensional river flood models using vegetation heights derived from airborne scanning laser altimetry. *Hydrological Processes*, 17, 1711-1732.

- MASSMAN, W. J. & GRANTZ, D. A. 1995. Estimating canopy conductance to ozone uptake from observations of evapotranspiration at the canopy scale and at the leaf scale\*. *Global Change Biology*, 1, 183-198.
- MCCABE JR, G. J. & HAY, L. E. 1995. Hydrological effects of hypothetical climate change in the East River basin, Colorado, USA. *Hydrological sciences journal*, 40, 303-318.
- MCCARTHY, G. T., UNITED, S., ARMY, CORPS OF, E. & PROVIDENCE, D. 1939. *The unit hydrograph and flood routing*, Providence, R.I., Army Engineer District, Providence.
- MCCONKEY, R. & MARIGA, L. 2011. Building social capital for inclusive education: insights from Zanzibar. *Journal of Research in Special Educational Needs*, 11, 12-19.
- MCGUFFIE, K. & HENDERSON-SELLERS, A. 2005. *Practical Climate Modelling. A Climate Modelling Primer*. John Wiley & Sons, Ltd.
- MCINNES, J., VIGIAK, O. & ROBERTS, A. 2011. Using Google Earth to map gully extent in the West Gippsland region (Victoria, Australia). 19th International Congress on Modelling and Simulation, Perth, Australia, 12–16 December 2011 <http://mssanz.org.au/modsim2011> <http://www.mssanz.org.au/modsim2011/12/mcinnis.pdf>.
- MEJIA, A. I. & REED, S. M. 2011. Role of channel and floodplain cross-section geometry in the basin response. *Water Resources Research*, 47, W09518.
- MERWADE, V. M., MAIDMENT, D. R. & HODGES, B. R. 2005. Geospatial representation of river channels. *Journal of Hydrologic Engineering*, 10, 243-251 [http://ascelibrary.org/doi/abs/10.1061/\(ASCE\)1084-0699\(2005\)10:3\(243\)](http://ascelibrary.org/doi/abs/10.1061/(ASCE)1084-0699(2005)10:3(243)).
- MERWADE, V., COOK, A. & COONROD, J. 2008. GIS techniques for creating river terrain models for hydrodynamic modeling and flood inundation mapping. *Environmental Modelling & Software*, 23, 1300-1311 <http://www.sciencedirect.com/science/article/pii/S1364815208000455>.
- MIDDELKOOP, H., DAAMEN, K., GELLENS, D., GRABS, W., KWADIJK, J. C., LANG, H., PARMET, B. W., SCHÄDLER, B., SCHULLA, J. & WILKE, K. 2001. Impact of climate change on hydrological regimes and water resources management in the Rhine basin. *Climatic change*, 49, 105-128.
- MILLER, N. L., BASHFORD, K. E. & STREM, E. 2003. *Potential impacts of climate change on california hydrology1*. Wiley Online Library.
- MILLY, P. C. D. & SHMAKIN, A. B. 2002. Global Modeling of land water and energy balances. Part II: Land-characteristic contributions to spatial variability. *Journal of Hydrometeorology*, 3, 301-310.
- MIZANUR, R. R. & HANIF CHAUDHRY, M. 1995. Flood routing in channels with flood plains. *Journal of Hydrology*, 171, 75-91.
- MORGAN, M. G., MAX, H. & MITCHELL, S. 1990. *Uncertainty : a guide to dealing with uncertainty in quantitative risk and policy analysis*.
- MOUSSA, R. & BOCQUILLON, C. 1996. Criteria for the choice of flood-routing methods in natural channels. *Journal of Hydrology*, 186, 1-30.
- MÜLLER-WOHLFEIL, D.-I., BÜRGER, G. & LAHMER, W. 2000. Response of a River Catchment to Climatic Change: Application of Expanded Downscaling to Northern Germany. *Climatic Change*, 47, 61-89.
- MURPHY, J. M., SEXTON, D. M. H., JENKINS, G. J., BOORMAN, P. M., BOOTH, B. B. B. & BROWN, C. C., CLARK, R.T., COLLINS, M., HARRIS, G.R., KENDON, E.J., BETTS, R.A., BROWN, S.J., HOWARD, T. P., HUMPHREY, K. A., MCCARTHY, M. P., MCDONALD, R. E., STEPHENS, A., WALLACE, C., WARREN, R., WILBY, R., WOOD, R. A. 2009. *Projections Science Report: Climate change projections*. Met Office Hadley Centre, Exeter. <http://ukclimateprojections.defra.gov.uk>.
- MYERS, W. R. C. 1991. Influence of geometry on discharge capacity of open channels. *Journal of Hydraulic Engineering*, 117, 676-680.

- NAKICENOVIC, N. & SWART, R. 2000. Special report on emissions scenarios. Special Report on Emissions Scenarios, Edited by Nebojsa Nakicenovic and Robert Swart, pp. 612. ISBN 0521804930. Cambridge, UK: Cambridge University Press, July 2000., 1.
- NEW, M., LISTER, D., HULME, M. & MAKIN, I. 2002. A high-resolution data set of surface climate over global land areas. *Climate research*, 21, 1-25.
- NICHOLAS, A. & WALLING, D. 1997. Modelling flood hydraulics and overbank deposition on river floodplains. *Earth surface processes and landforms*, 22, 59-77.
- OWEN-JOYCE, S. J. & RAYMOND, L. H. 1996. An accounting system for water and consumptive use along the Colorado River, Hoover Dam to Mexico. *Water Supply Paper*. - ed.
- PALMER, R. N. & LUNDBERG, K. V. 2004. Integrated water resource planning. University of Washington, Seattle, Washington.
- PAPPENBERGER, F., BEVEN, K., HORRITT, M. & BLAZKOVA, S. 2005. Uncertainty in the calibration of effective roughness parameters in HEC-RAS using inundation and downstream level observations. *Journal of Hydrology*, 302, 46-69.
- PARTOW, H. 2001. The Mesopotamian marshlands : demise of an ecosystem, Nairobi : UNEP, 2001.
- PATRO, S., CHATTERJEE, C., SINGH, R. & RAGHUWANSHI, N. S. 2009. Hydrodynamic modelling of a large flood-prone river system in India with limited data. *Hydrological Processes*, 23, 2774-2791.
- PATTISON, I. 2010. Rural land management impacts on catchment scale flood risk. Durham University.
- PAVELSKY, T. M. & SMITH, L. C. 2008. RivWidth: A software tool for the calculation of river widths from remotely sensed imagery. *Geoscience and Remote Sensing Letters, IEEE*, 5, 70-73.
- PENMAN, H. L. 1948. Natural Evaporation from Open Water, Bare Soil and Grass. *Journal: Proceedings of The Royal Society A: Mathematical, Physical and Engineering Sciences*, vol. 193, no. 1032, pp. 120-145, 1948.
- PFISTER, L., HUMBERT, J. & HOFFMANN, L. 2000. Recent trends in rainfall-runoff characteristics in the Alzette river basin, Luxembourg. *Climatic Change*, 45, 323-337.
- PIAO, S., CIAIS, P., HUANG, Y., SHEN, Z., PENG, S., LI, J., ZHOU, L., LIU, H., MA, Y. & DING, Y. 2010. The impacts of climate change on water resources and agriculture in China. *Nature*, 467, 43-51.
- PRICE, E. M. F. & HEYWOOD, D. I. 1994. Mountain environments and geographic information systems. *Mountain environments and geographic information systems*.
- QI, H. & ALTINAKAR, M. S. 2011. A GIS-based decision support system for integrated flood management under uncertainty with two dimensional numerical simulations. *Environmental Modelling & Software*, 26, 817-821 <http://www.sciencedirect.com/science/article/pii/S1364815210003105>.
- QIU, G. Y., MIYAMOTO, K., SASE, S., GAO, Y., SHI, P. & YANO, T. 2002. Comparison of the three-temperature model and conventional models for estimating transpiration. *Japan Agricultural Research Quarterly*, 36, 73-82.
- REGGIANI, P., SIVAPALAN, M. & HASSANIZADEH, S. M. 2000. Conservation equations governing hillslope responses: Exploring the physical basis of water balance. *Water Resources Research*, 36, 1845-1863.
- RHOADS, B. L., SCHWARTZ, J. S. & PORTER, S. 2003. Stream geomorphology, bank vegetation, and three-dimensional habitat hydraulics for fish in midwestern agricultural streams. *Water Resources Research*, 39.
- RICHARDSON, C. W. & WRIGHT, D. A. 1984. WGEN: A Model for Generating Daily Weather Variables.
- RIJSBERMAN, F. R. 2000. Summary report of the 2nd World Water Forum: from vision to action. *Water Policy*, 2, 387-395.

ROBOCK, A., TURCO, R. P., HARWELL, M. A., ACKERMAN, T. P., ANDRESSEN, R., CHANG, H.-S. & SIVAKUMAR, M. 1993. Use of general circulation model output in the creation of climate change scenarios for impact analysis. *Climatic Change*, 23, 293-335.

RODRIGUEZ, E., MORRIS, C. S., BELZ, J. E., CHAPIN, E. C., MARTIN, J. M., DAFFER, W. & HENSLEY, S. 2005. An assessment of the SRTM topographic products, Pasadena, California, Jet Propulsion Laboratory.

ROSGEN, D. L. 1994. A classification of natural rivers. *CATENA*, 22, 169-199.

ROUX, H., DARTUS, D., WEBB, B., ARNELL, N., ONOF, C., MACINTYRE, N., GURNEY, R. & KIRBY, C. Data assimilation applied to hydraulic parameter identification. *Hydrology: science and practice for the 21st century. Proceedings of the British Hydrological Society International Conference, Imperial College, London, July 2004.*, 2004. British Hydrological Society, 354-361  
<http://www.cabdirect.org/abstracts/20053056790.html;jsessionid=E735CE1462893931F8C637E1AA17060A>.

RUSLI, N. & RAFEE, M. M. 2012. Digital Elevation Model (DEM) Extraction From Google Earth: A Study in Sungai Muar Watershed. *Geoinformatics for Society and Environment 2012 (AGSE2012)*. , , <http://www.epublication.fab.utm.my/id/eprint/364>.

SAGLAM, Y. 2010. Water scarcity and optimal pricing of water.

SALEH, D. K. 2010. Stream Gage Descriptions and Streamflow Statistics for Sites in the Tigris River and Euphrates River Basins, Iraq.

SAMUELS, P. G. 1995. Uncertainty in flood level prediction. *International Association for Hydraulic Research, Vol 1; Integration of research approaches and applications Congress; 26th, Vol 1; Integration of research approaches and applications PROCEEDINGS OF THE CONGRESS- INTERNATIONAL ASSOCIATION FOR HYDRAULIC RESEARCH; 1; 567-572 6 Pages.*

SANDERS, B. F. 2007. Evaluation of on-line DEMs for flood inundation modeling. *Advances in Water Resources*, 30, 1831-1843 <http://www.sciencedirect.com/science/article/pii/S0309170807000279>.

SANFORD, W. E. & SELNICK, D. L. 2013. Estimation of Evapotranspiration Across the Conterminous United States Using a Regression With Climate and Land-Cover Data1. *JAWRA Journal of the American Water Resources Association*, 49, 217-230.

SCHWANGHART, W. & KUHN, N. J. 2010. TopoToolbox: A set of Matlab functions for topographic analysis. *Environmental Modelling & Software*, 25, 770-781  
<http://www.sciencedirect.com/science/article/pii/S1364815209003053>.

SCOTT, R. L., EDWARDS, E. A., SHUTTLEWORTH, W. J., HUXMAN, T. E., WATTS, C. & GOODRICH, D. C. 2004. Interannual and seasonal variation in fluxes of water and carbon dioxide from a riparian woodland ecosystem. *Agricultural and Forest Meteorology*, 122, 65-84.

SHABALOVA, M., VAN DEURSEN, W. & BUIHAND, T. 2003. Assessing future discharge of the river Rhine using regional climate model integrations and a hydrological model. *Climate Research*, 23, 233-246.

SHOLTES, J. & DOYLE, M. 2011. Effect of Channel Restoration on Flood Wave Attenuation. *Journal of Hydraulic Engineering*, 137, 196-208.

SHUTTLEWORTH, W. J. & WALLACE, J. S. 1985. Evaporation from sparse crops-an energy combination theory. *Quarterly Journal of the Royal Meteorological Society*, 111: 839-855.

SINGH, P. & KUMAR, N. 1997. Impact assessment of climate change on the hydrological response of a snow and glacier melt runoff dominated Himalayan river. *Journal of Hydrology*, 193, 316-350.

SINGH, V. P. 1989. *Hydrologic Systems: Watershed modelling*, Prentice Hall.

SRIVASTAVA, P. K., HAN, D., RICO RAMIREZ, M. A. & ISLAM, T. 2013. Comparative assessment of evapotranspiration derived from NCEP and ECMWF global datasets through Weather Research and Forecasting model. *Atmospheric Science Letters*, 14, 118-125.

- STOCKER, T. F., QIN, D., PLATTNER, G.-K., TIGNOR, M., ALLEN, S. K., BOSCHUNG, J., NAUELS, A., XIA, Y., BEX, V. & MIDGLEY, P. M. 2013. Climate Change 2013. The Physical Science Basis. Working Group I Contribution to the Fifth Assessment Report of the Intergovernmental Panel on Climate Change-
- SUBRAMANYA, K. 1994. Engineering Hydrology, Tata McGraw-Hill.
- SULEBAK, J. 2000. Applications of digital elevation models. DYNAMAP Project Oslo.
- SYED, T. H., WEBSTER, P. J. & FAMIGLIETTI, J. S. 2014. Assessing variability of evapotranspiration over the Ganga river basin using water balance computations. *Water Resources Research*, 50, 2551-2565.
- TEKLEAB, S., UHLENBROOK, S., MOHAMED, Y., SAVENIJE, H. H. G., TEMESGEN, M. & WENNINGER, J. 2011. Water balance modeling of Upper Blue Nile catchments using a top-down approach. *Hydrol. Earth Syst. Sci.*, 15, 2179-2193.
- TESFA, T. K., TARBOTON, D. G., WATSON, D. W., SCHREUDERS, K. A. T., BAKER, M. E. & WALLACE, R. M. 2011. Extraction of hydrological proximity measures from DEMs using parallel processing. *Environmental Modelling & Software*, 26, 1696-1709  
<http://www.sciencedirect.com/science/article/pii/S1364815211001794>.
- TESTI, L., VILLALOBOS, F. J. & ORGAZ, F. 2004. Evapotranspiration of a young irrigated olive orchard in southern Spain. *Agricultural and Forest Meteorology*, 121, 1-18.
- THOMAS, H. & NISBET, T. R. 2007. An assessment of the impact of floodplain woodland on flood flows. *Water and Environment Journal*, 21, 114-126.
- THORNTHWAITE, C. W. & MATHER, J. R. 1957. Instructions and tables for computing potential evapotranspiration and the water balance, Laboratory of Climatology.
- TUKIMAT, N. N. A., HARUN, S. & SHAHID, S. 2012. Comparison of different methods in estimating potential evapotranspiration at Muda Irrigation Scheme of Malaysia. *Journal of Agriculture and Rural Development in the Tropics and Subtropics (JARTS)*, 113, 77-85.
- UNESCO 2009. DRINKING WATER AND SANITATION : COMMON PROCESSES OF PURIFICATION AND TREATMENT , POLICY-WATER POLICY AND WATER MANAGEMENT. UNESCO-IHP ISARM  
<http://www.isarm.net/publications/322>.
- VAN DEURSEN, W. & KWADIJK, J. 1993. RHINEFLOW: an integrated GIS water balance model for the river Rhine. IAHS PUBLICATION, 507-507.
- VAN NIEKERK, A., VOGEL, K. R., SLINGERLAND, R. L. & BRIDGE, J. S. 1992. Routing of heterogeneous sediments over movable bed: model development. *Journal of Hydraulic Engineering*, 118, 246-262.
- VON STORCH, H., LANGENBERG, H. & FESER, F. 2000. A spectral nudging technique for dynamical downscaling purposes. *Monthly weather review*, 128, 3664-3673.
- WATSON, I. & BURNETT, A. 1995. Hydrology an environmental approach, Boca Raton, CRC.
- WEBB, T. & WIGLEY 1985. What past climates can tell us about a warmer world. Projecting the Climatic Effects of Increasing Carbon Dioxide (Eds. M.C. MacCracken and F.M. Luther), pp.237-257 Carbon Dioxide Research Division Report No. DOE/ER-0235, United States Department of Energy, Washington, D.C.
- WEBSTER, P. J. & JIAN, J. 2011. Environmental prediction, risk assessment and extreme events: adaptation strategies for the developing world.
- WIGLEY, T. M. L., JONES, P. D. & KELLY, P. M. 1980. Scenario for a warm, high-CO2 world. *Nature*, 283, 17-21.
- WILBY, R. L. & WIGLEY, T. 1997. Downscaling general circulation model output: a review of methods and limitations. *Progress in Physical Geography*, 21, 530-548.
- WILBY, R. L. & WIGLEY, T. 2000. Precipitation predictors for downscaling: observed and general circulation model relationships. *International Journal of Climatology*, 20, 641-661.

- WILBY, R. L., DAWSON, C. W. & BARROW, E. M. 2002. sdsms — a decision support tool for the assessment of regional climate change impacts. *Environmental Modelling & Software*, 17, 145-157.
- WILBY, R., CHARLES, S., ZORITA, E., TIMBAL, B., WHETTON, P. & MEARNS, L. 2004. Guidelines for use of climate scenarios developed from statistical downscaling methods.
- WILBY, R., WHITEHEAD, P., WADE, A., BUTTERFIELD, D., DAVIS, R. & WATTS, G. 2006. Integrated modelling of climate change impacts on water resources and quality in a lowland catchment: River Kennet, UK. *Journal of Hydrology*, 330, 204-220.
- WMO 2009. WMO statement on the status of the global climate. World Meteorological Organization, <http://www.wmo.int/pages/prog/wcp/wcdmp/documents/WMOStatement2009.pdf>.
- WOHL, E. 1998. Uncertainty in Flood Estimates Associated with Roughness Coefficient. *Journal of Hydraulic Engineering*, 124, 219-223.
- WOLDEMICHAEL, A. T., DEGU, A. M., SIDDIQUE-E-AKBOR, A. H. M. & HOSSAIN, F. 2010. Role of Land&#x2013;Water Classification and Manning's Roughness Parameter in Space-Borne Estimation of Discharge for Braided Rivers: A Case Study of the Brahmaputra River in Bangladesh. *Selected Topics in Applied Earth Observations and Remote Sensing*, IEEE Journal of, 3, 395-403.
- WOLF, A. T., NATHARIUS, J. A., DANIELSON, J. J., WARD, B. S. & FENDER, J. K. 1999. International River basins of the world. *International Journal of Water Resources Development*, 15, 387-427.
- WOLFF, C. G. & BURGESS, S. J. 1994. An analysis of the influence of river channel properties on flood frequency. *Journal of Hydrology*, 153, 317-337.
- WOLTEMADE, C. J. & POTTER, K. W. 1994. A watershed modeling analysis of fluvial geomorphologic influences on flood peak attenuation. *Water Resources Research*, 30, 1933-1942.
- XU, C.-Y., WIDÉN, E. & HALLDIN, S. 2005. Modelling hydrological consequences of climate change—Progress and challenges. *Advances in Atmospheric Sciences*, 22, 789-797.
- ZORITA, E. & VON STORCH, H. 1999. The analog method as a simple statistical downscaling technique: Comparison with more complicated methods. *Journal of Climate*, 12, 2474-2489.
- ZOTARELLI, L., DUKES, M. D., ROMERO, C. C., MIGLIACCIO, K. W. & MORGAN, K. T. 2010. Step by step calculation of the Penman-Monteith Evapotranspiration (FAO-56 Method). Institute of Food and Agricultural Sciences. University of Florida.
- AIMaarofi, S., Douabul, A. and Al-Saad, H. (2012). Mesopotamian Marshlands: Salinization Problem. *Journal of Environmental Protection*, 03(10), pp.1295-1301. [http://file.scirp.org/Html/3-6701625\\_23837.htm](http://file.scirp.org/Html/3-6701625_23837.htm)
- Citypopulation.de, (2015). City Population - Population Statistics in Maps and Charts for Cities, Agglomerations and Administrative Divisions of all Countries of the World. [online] Available at: <http://www.citypopulation.de> [Accessed 11 July. 2015].
- Dimov, B. (2013). Everything about energy, types of energy exploatations: May 2013. [online] Thermalenergetic.blogspot.co.uk. Available at: [http://thermalenergetic.blogspot.co.uk/2013\\_05\\_01\\_archive.html](http://thermalenergetic.blogspot.co.uk/2013_05_01_archive.html) [Accessed 28 Oct. 2012].
- Myles R. Allen, Vicente R. Barros, John Broome, Wolfgang Cramer, IPCC Fifth Assessment Synthesis Report - Climate Change 2014 Synthesis Report. Intergovernmental Panel on Climate Change (IPCC), November 2014.

# Appendixes

## Appendix 1:

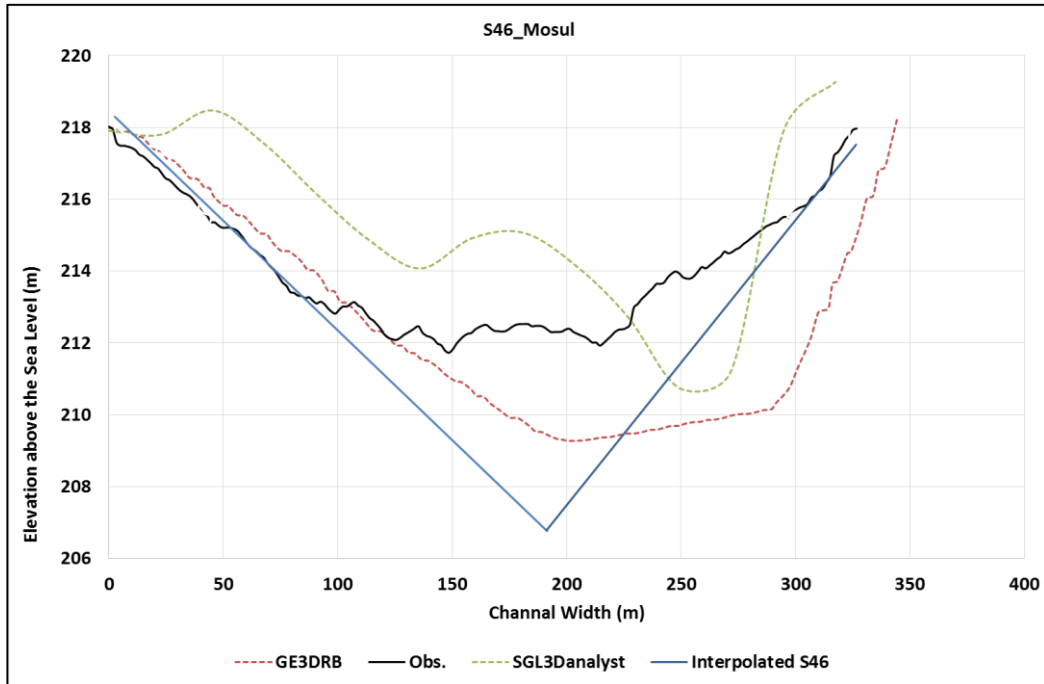


Figure 0-1: shows elevation measured cross section (Obs.) compared against one generated using SRTM GL3 raster (SGL3Danalyst); one generated using Synthetic technique (Interpolated S) and another one generated using Google Earth DEM (GE3DRB). Its location is identified in Table 6.2.

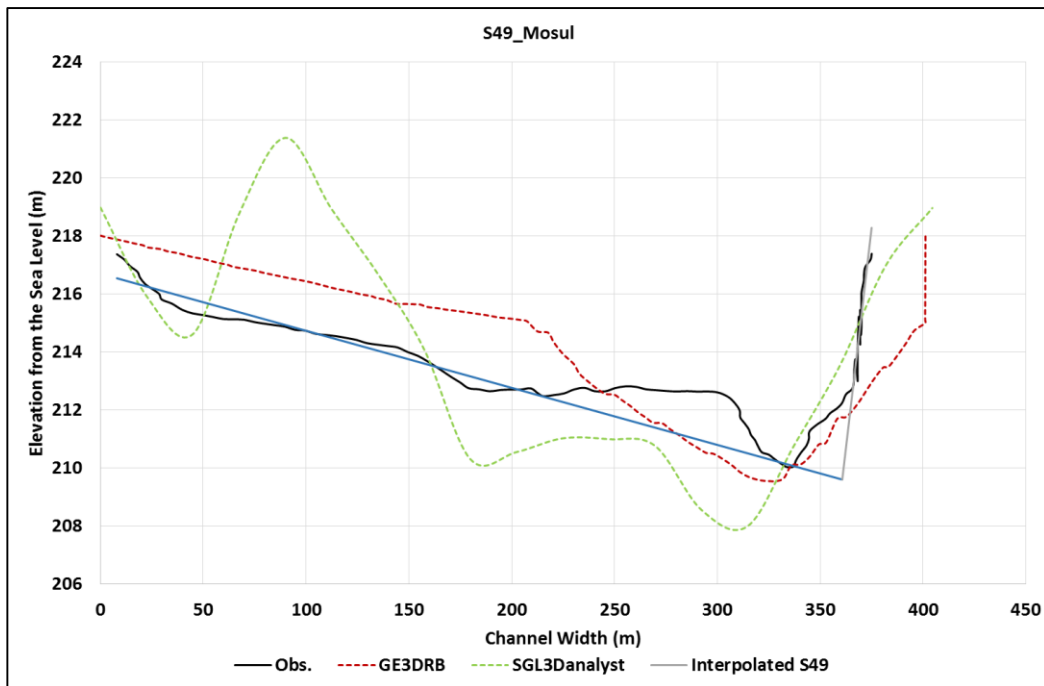


Figure 0-2: shows elevation measured cross section (Obs.) compared against one generated using SRTM GL3 raster (SGL3Danalyst); one generated using Synthetic technique (Interpolated S) and another one generated using Google Earth DEM (GE3DRB). Its location is identified in Table 6.2.

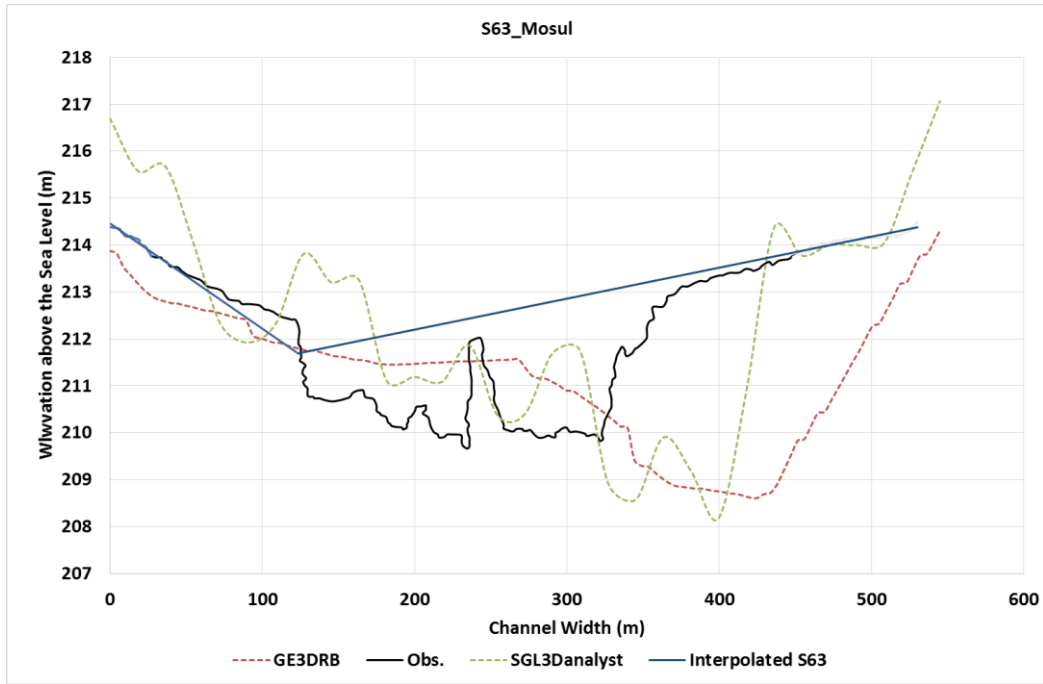


Figure 0-3: shows elevation measured cross section (Obs.) compared against one generated using SRTM GL3 raster (SGL3Danalyst); one generated using Synthetic technique (Interpolated S) and another one generated using Google Earth DEM (GE3DRB). Its location is identified in Table 6.2.

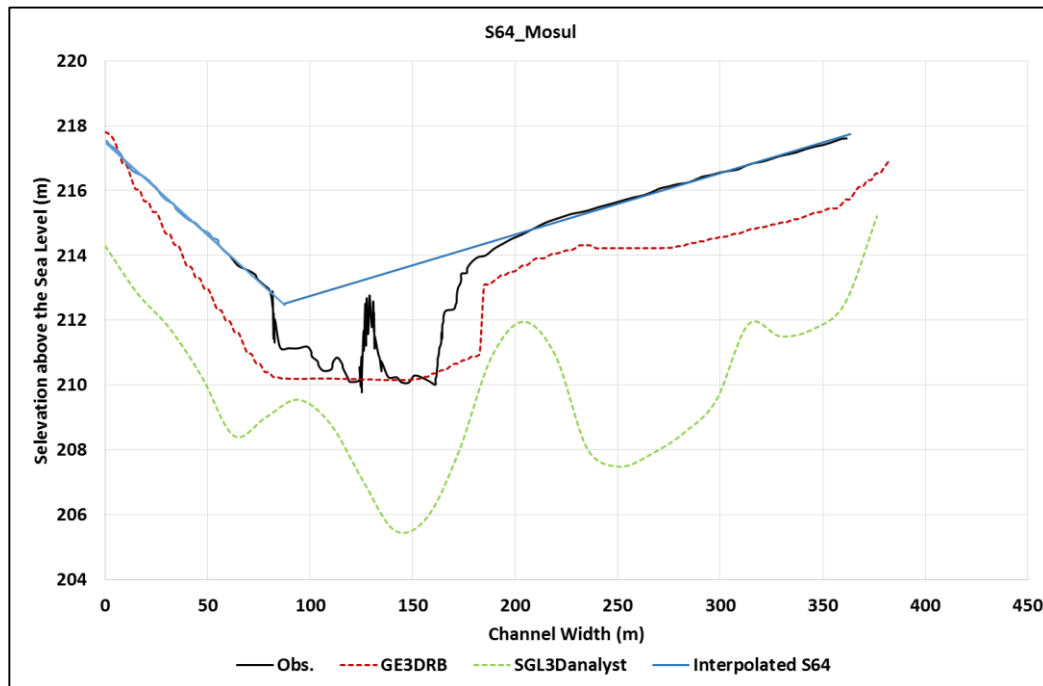


Figure 0-4: shows elevation measured cross section (Obs.) compared against one generated using SRTM GL3 raster (SGL3Danalyst); one generated using Synthetic technique (Interpolated S) and another one generated using Google Earth DEM (GE3DRB). Its location is identified in Table 6.2.



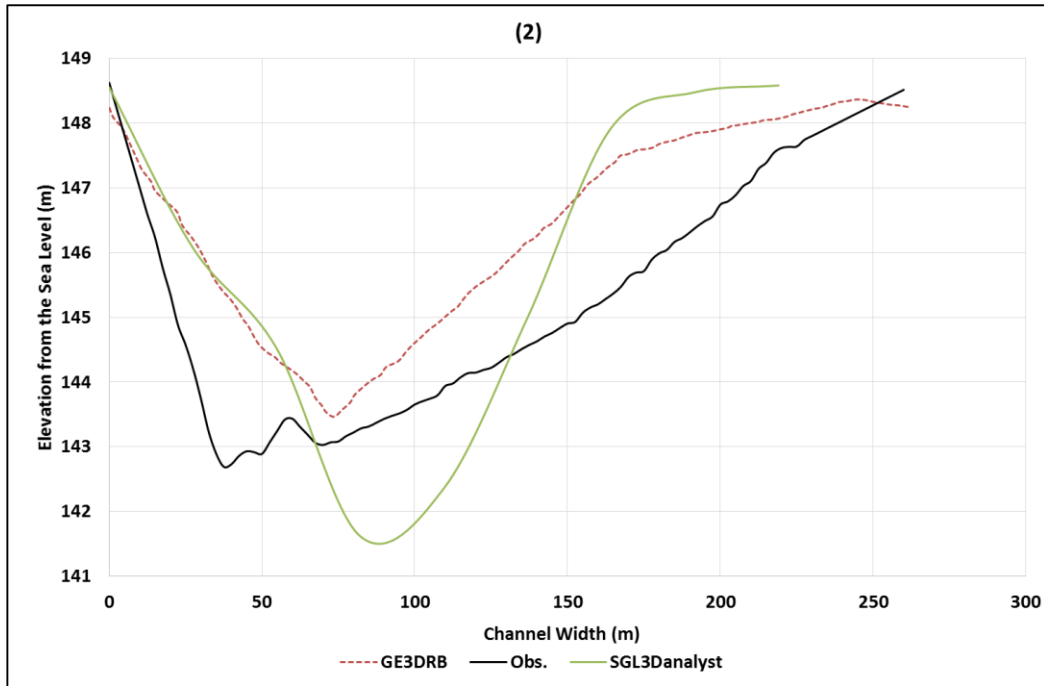


Figure 0-5: shows elevations of measured cross section (Obs.) at location – number 2 as identified in Table 6.2. This cross section is compared against one generated using SRTM GL3 raster (SGL3Danalyst) and another one generated using Google Earth DEM (GE3DRB).

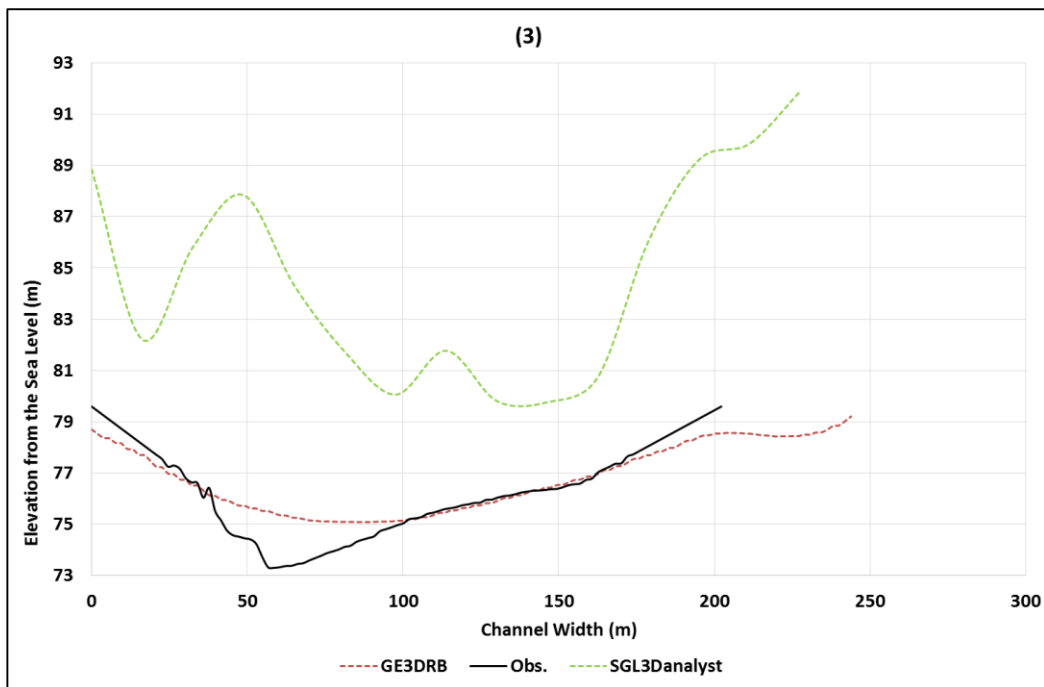


Figure 0-6: shows elevations of measured cross section (Obs.) at location – number 3 as identified in Table 6.2. This cross section is compared against one generated using SRTM GL3 raster (SGL3Danalyst) and another one generated using Google Earth DEM (GE3DRB).

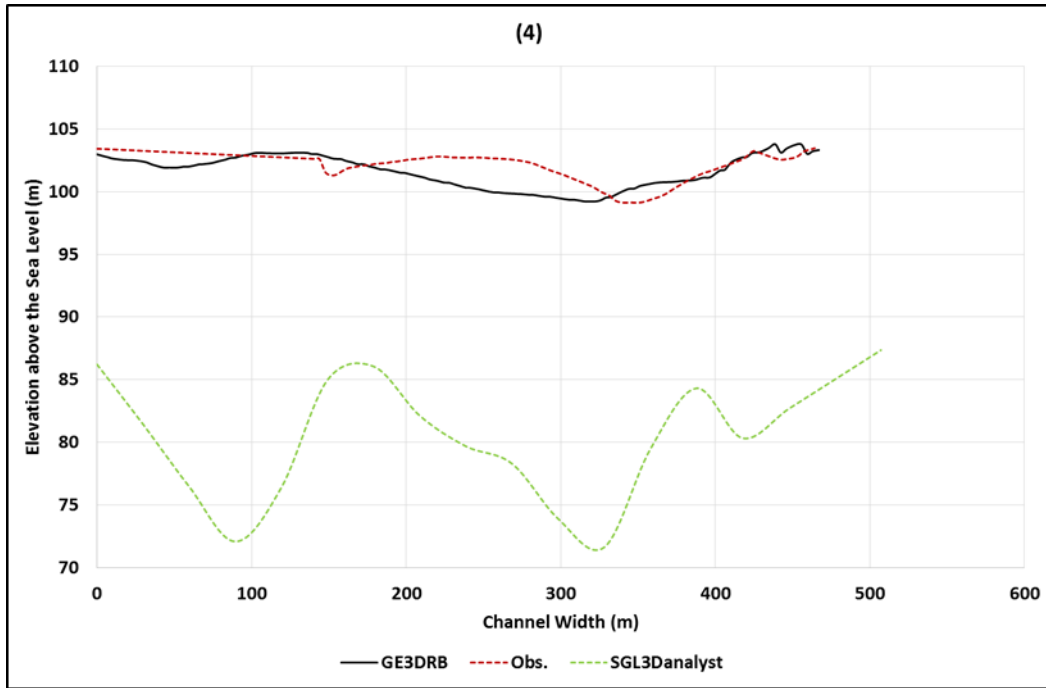


Figure 0-7: shows elevations of measured cross section (Obs.) at location – number 4 as identified in Table 6.2. This cross section is compared against one generated using SRTM GL3 raster (SGL3Danalyst) and another one generated using Google Earth DEM (GE3DRB).

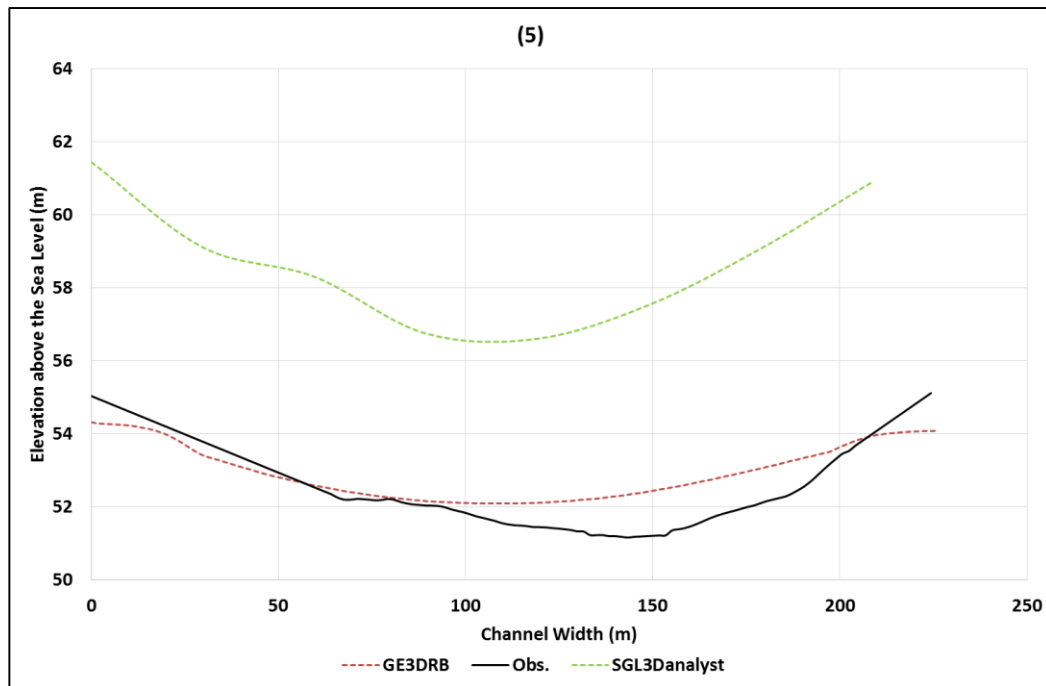


Figure 0-8: shows elevations of measured cross section (Obs.) at location – number 5 as identified in Table 6.2. This cross section is compared against one generated using SRTM GL3 raster (SGL3Danalyst) and another one generated using Google Earth DEM (GE3DRB).

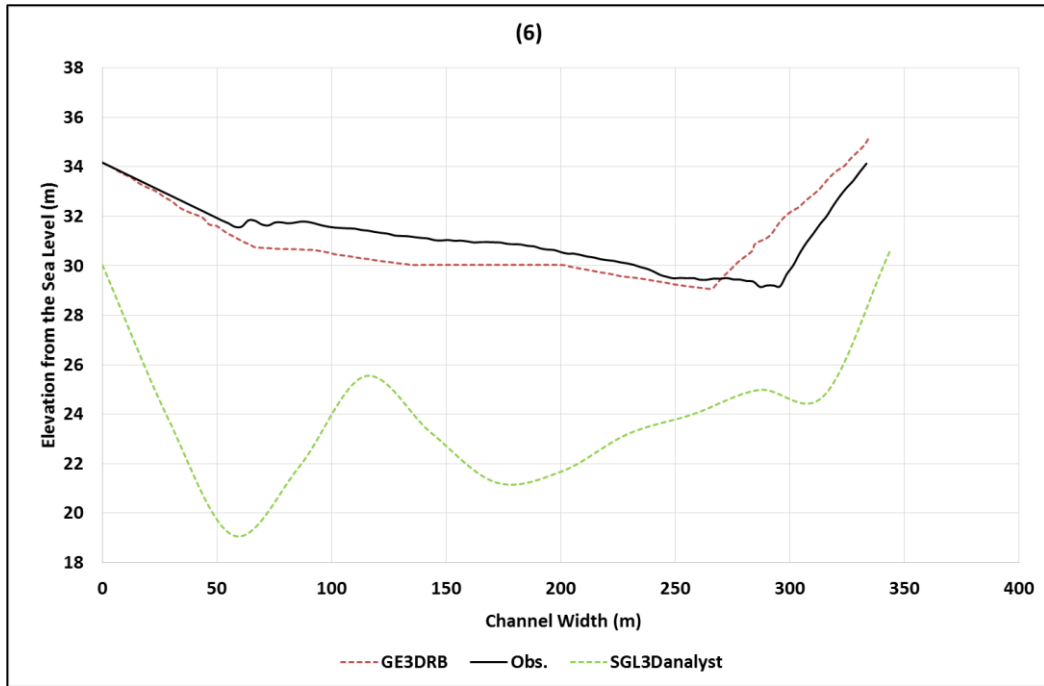


Figure 0-9: shows elevations of measured cross section (Obs.) at location – number 6 as identified in Table 6.2. This cross section is compared against one generated using SRTM GL3 raster (SGL3Danalyst) and another one generated using Google Earth DEM (GE3DRB).

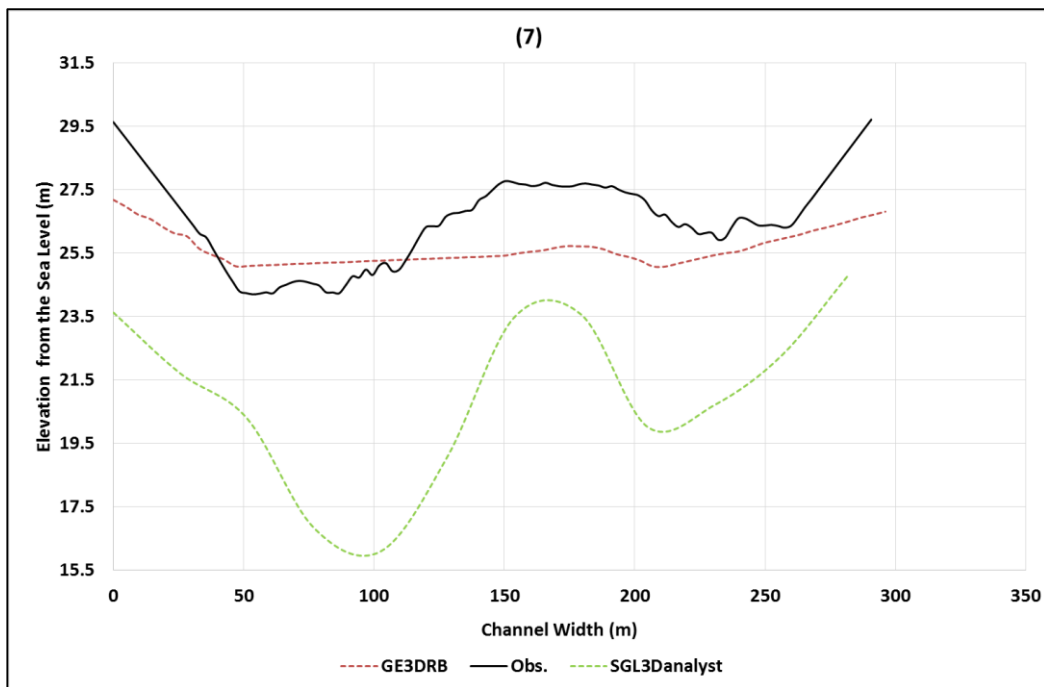


Figure 0-10: shows elevations of measured cross section (Obs.) at location – number 7 as identified in Table 6.2. This cross section is compared against one generated using SRTM GL3 raster (SGL3Danalyst) and another one generated using Google Earth DEM (GE3DRB).

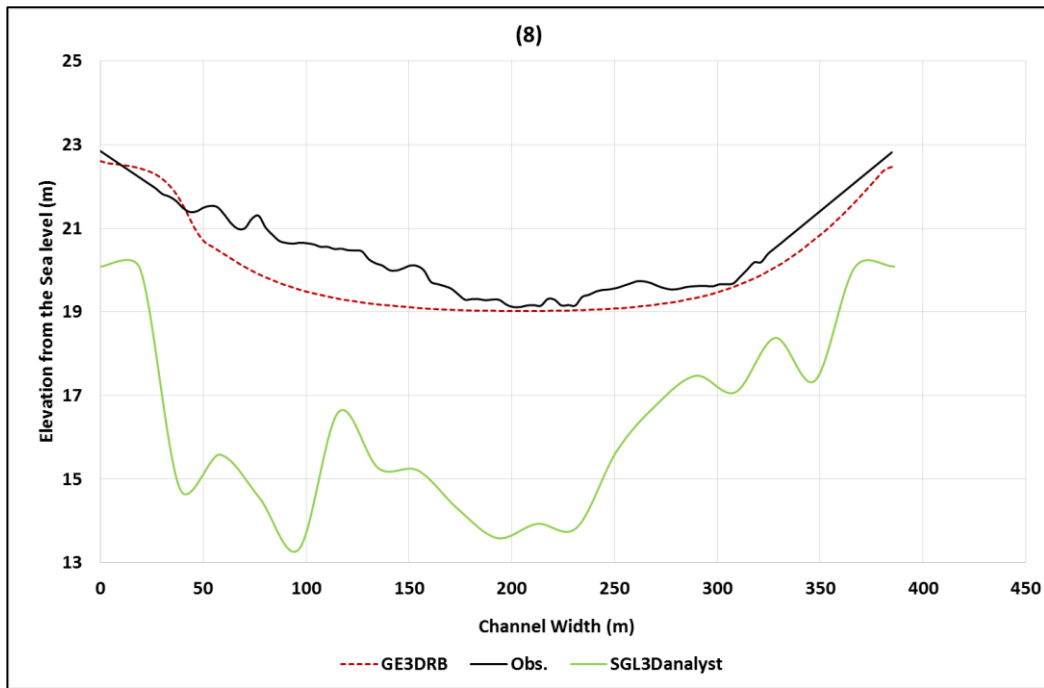


Figure 0-11: shows elevations of measured cross section (Obs.) at location – number 8 as identified in Table 6.2. This cross section is compared against one generated using SRTM GL3 raster (SGL3Danalyst) and another one generated using Google Earth DEM (GE3DRB).

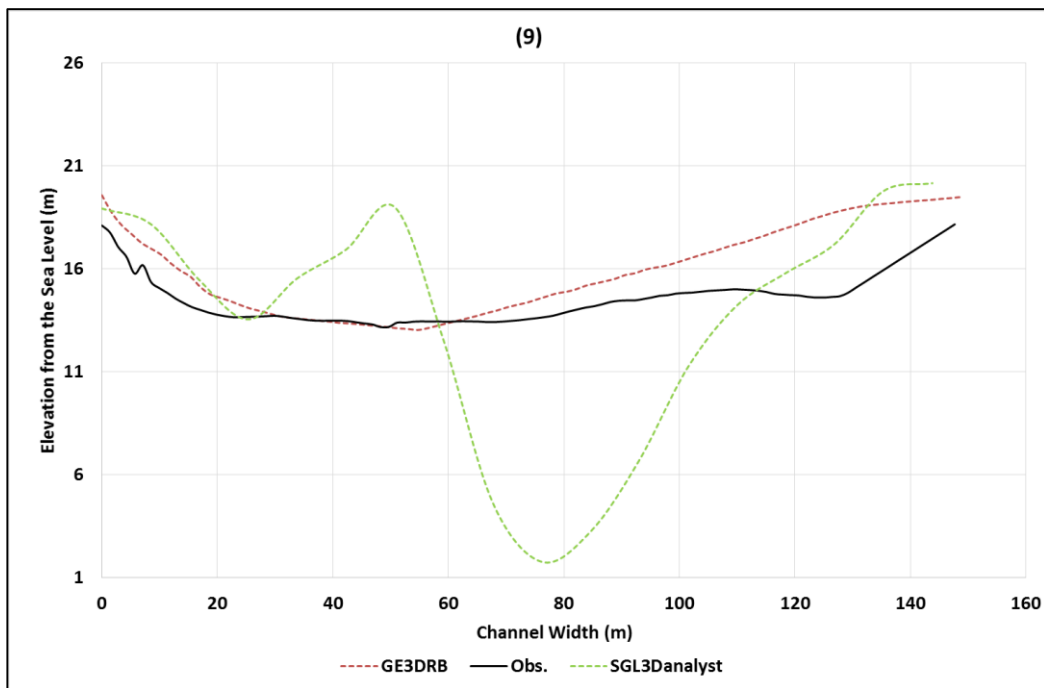


Figure 0-12: shows elevations of measured cross section (Obs.) at location – number 9 as identified in Table 6.2. This cross section is compared against one generated using SRTM GL3 raster (SGL3Danalyst) and another one generated using Google Earth DEM (GE3DRB).



Appendix 2: Tigris River Basin

